Hashemite Kingdom of Jordan

Jordan Journal of Biological Sciences

An International Peer-Reviewed Scientific Journal

Financed by the Scientific Research and Innovation Support Fund

This title is indexed in Scopus

http://jjbs.hu.edu.jo/

المجلة الأردنية للعلوم الحياتية
Jordan Journal of Biological Sciences (JJBS)
http://jjbs.hu.edu.jo

Jordan Journal of Biological Sciences (JJBS) (ISSN: 1995–6673 (Print); 2307-7166 (Online)): An International Peer- Reviewed Open Access Research Journal financed by the Scientific Research and Innovation Support Fund, Ministry of Higher Education and Scientific Research, Jordan and published quarterly by the Deanship of Scientific Research , The Hashemite University, Jordan.

Submission Address

Professor Wedyan, Mohammed A.
The Hashemite Universit y
P.O. Box 330127, Zarqa, 13115, Jordan
Phone: +962-5-3903333 ext.4147
E-Mail: jjbs@hu.edu.jo

المجلة الاردنية للعلوم الحياتية
Jordan Journal of Biological Sciences (JJBS)
http://jjbs.hu.edu.jo

International Advisory Board (Arranged alphabetically)

Instructions to Authors

Scopes

Study areas include cell biology, genomics, microbiology, immunology, molecular biology, biochemistry, embryology, immunogenetics, cell and tissue culture, molecular ecology, genetic engineering and biological engineering, bioremediation and biodegradation, bioinformatics, biotechnology regulations, gene therapy, organismal biology, microbial and environmental biotechnology, marine sciences. The JJBS welcomes the submission of manuscript that meets the general criteria of significance and academic excellence. All articles published in JJBS are peer-reviewed. Papers will be published approximately one to two months after acceptance.

Type of Papers

The journal publishes high-quality original scientific papers, short communications, correspondence and case studies. Review articles are usually by invitation only. However, Review articles of current interest and high standard will be considered.

Submission of Manuscript

Manuscript, or the essence of their content, must be previously unpublished and should not be under simultaneous consideration by another journal. The authors should also declare if any similar work has been submitted to or published by another journal. They should also declare that it has not been submitted/ published elsewhere in the same form, in English or in any other language, without the written consent of the Publisher. The authors should also declare that the paper is the original work of the author(s) and not copied (in whole or in part) from any other work. All papers will be automatically checked for duplicate publication and plagiarism. If detected, appropriate action will be taken in accordance with International Ethical Guideline. By virtue of the submitted manuscript, the corresponding author acknowledges that all the co-authors have seen and approved the final version of the manuscript. The corresponding author should provide all co-authors with information regarding the manuscript, and obtain their approval before submitting any revisions. Electronic submission of manuscripts is strongly recommended, provided that the text, tables and figures are included in a single Microsoft Word file. Submit manuscript as e-mail attachment to the Editorial Office at: JJBS@hu.edu.jo. After submission, a manuscript number will be communicated to the corresponding author within 48 hours.

Peer-review Process

It is requested to submit, with the manuscript, the names, addresses and e-mail addresses of at least 4 potential reviewers. It is the sole right of the editor to decide whether or not the suggested reviewers to be used. The reviewers' comments will be sent to authors within 6-8 weeks after submission.
Manuscripts and figures for review will not be returned to authors whether the editorial decision is to accept, revise, or reject. All Case Reports and Short Communication must include at least one table and/ or one figure.

Preparation of Manuscript

The manuscript should be written in English with simple lay out. The text should be prepared in single column format. Bold face, italics, subscripts, superscripts etc. can be used. Pages should be numbered consecutively, beginning with the title page and continuing through the last page of typewritten material.

The text can be divided into numbered sections with brief headings. Starting from introduction with section 1. Subsections should be numbered (for example 2.1 (then 2.1.1, 2.1.2, 2.2, etc.), up to three levels. Manuscripts in general should be organized in the following manner:

Title Page

The title page should contain a brief title, correct first name, middle initial and family name of each author and name and address of the department(s) and institution(s) from where the research was carried out for each author. The title should be without any abbreviations and it should enlighten the contents of the paper. All affiliations should be provided with a lower-case superscript number just after the author's name and in front of the appropriate address.
The name of the corresponding author should be indicated along with telephone and fax numbers (with country and area code) along with full postal address and e-mail address.

Abstract

The abstract should be concise and informative. It should not exceed **350 words** in length for full manuscript and Review article and **150 words** in case of Case Report and/ or Short Communication. It should briefly describe the purpose of the work, techniques and methods used, major findings with important data and conclusions. No references should be cited in this part. Generally non-standard abbreviations should not be used, if necessary they should be clearly defined in the abstract, at first use.

Keywords

Immediately after the abstract, **about 4-8 keywords** should be given. Use of abbreviations should be avoided, only standard abbreviations, well known in the established area may be used, if appropriate. These keywords will be used for indexing.

Abbreviations

Non-standard abbreviations should be listed and full form of each abbreviation should be given in parentheses at first use in the text.

Introduction

Provide a factual background, clearly defined problem, proposed solution, a brief literature survey and the scope and justification of the work done.

Materials and Methods

Give adequate information to allow the experiment to be reproduced. Already published methods should be mentioned with references. Significant modifications of published methods and new methods should be described in detail. Capitalize trade names and include the manufacturer's name and address. Subheading should be used.

Results

Results should be clearly described in a concise manner. Results for different parameters should be described under subheadings or in separate paragraph. Results should be explained, but largely without referring to the literature. Table or figure numbers should be mentioned in parentheses for better understanding.

Discussion

The discussion should not repeat the results, but provide detailed interpretation of data. This should interpret the significance of the findings of the work. Citations should be given in support of the findings. The results and discussion part can also be described as separate, if appropriate. The Results and Discussion sections can include subheadings, and when appropriate, both sections can be combined

Conclusions

This should briefly state the major findings of the study.

Acknowledgment

A brief acknowledgment section may be given after the conclusion section just before the references. The acknowledgment of people who provided assistance in manuscript preparation, funding for research, etc. should be listed in this section.

Tables and Figures

Tables and figures should be presented as per their appearance in the text. It is suggested that the discussion about the tables and figures should appear in the text before the appearance of the respective tables and figures. No tables or figures should be given without discussion or reference inside the text.

Tables should be explanatory enough to be understandable without any text reference. Double spacing should be maintained throughout the table, including table headings and footnotes. Table headings should be placed above the table. Footnotes should be placed below the table with superscript lowercase letters. Each table should be on a separate page, numbered consecutively in Arabic numerals.

Each figure should have a caption. The caption should be concise and typed separately, not on the figure area. Figures should be self-explanatory. Information presented in the figure should not be repeated in the table. All symbols and abbreviations used in the illustrations should be defined clearly. Figure legends should be given below the figures.

References

References should be listed alphabetically at the end of the manuscript. Every reference referred in the text must be also present in the reference list and vice versa. In the text, a reference identified by means of an author's name should be followed by the year of publication in parentheses (e.g.(Brown,2009)). For two authors, both authors' names followed by the year of publication (e.g.(Nelson and Brown, 2007)). When there are more than two authors, only the first author's name followed by "*et al*." and the year of publication (e.g. (Abu-Elteen *et al*., 2010)). When two or more works of an author has been published during the same year, the reference should be identified by the letters "a", "b", "c", etc., placed after the year of publication. This should be followed both in the text and reference list. e.g., Hilly, (2002a, 2002b); Hilly, and Nelson, (2004). Articles in preparation or submitted for publication, unpublished observations, personal communications, etc. should not be included in the reference list but should only be mentioned in the article text (e.g., Shtyawy,A., University of Jordan, personal communication). Journal titles should be abbreviated according to the system adopted in Biological Abstract and Index Medicus, if not included in Biological Abstract or Index Medicus journal title should be given in full. The author is responsible for the sccuracy and completeness of the references and for their correct textual citation. Failure to do so may result in the paper being withdraw from the evaluation process. Example of correct reference form is given as follows:-

Reference to a journal publication:

Bloch BK. 2002. Econazole nitrate in the treatment of *Candida vaginitis*. *S Afr Med J.* , **58**:314-323.

Ogunseitan OA and Ndoye IL. 2006. Protein method for investigating mercuric reductase gene expression in aquatic environments. *Appl Environ Microbiol.*, **64**: 695-702.

Hilly MO, Adams MN and Nelson SC. 2009. Potential fly-ash utilization in agriculture. *Progress in Natural Sci.*, **19**: 1173-1186.

Reference to a book:

Brown WY and White SR.1985. **The Elements of Style**, third ed. MacMillan, New York.

Reference to a chapter in an edited book:

Mettam GR and Adams LB. 2010. How to prepare an electronic version of your article. In: Jones BS and Smith RZ (Eds.), **Introduction to the Electronic Age**. Kluwer Academic Publishers, Netherlands, pp. 281–304.

Conferences and Meetings:

Embabi NS. 1990. Environmental aspects of distribution of mangrove in the United Arab Emirates. Proceedings of the First ASWAS Conference. University of the United Arab Emirates. Al-Ain, United Arab Emirates.

Theses and Dissertations:

El-Labadi SN. 2002. Intestinal digenetic trematodes of some marine fishes from the Gulf of Aqaba. MSc dissertation, The Hashemite University, Zarqa, Jordan.

Nomenclature and Units

Internationally accepted rules and the international system of units (SI) should be used. If other units are mentioned, please give their equivalent in SI.

For biological nomenclature, the conventions of the *International Code of Botanical Nomenclature, the International Code of Nomenclature of Bacteria,* and the *International Code of Zoological Nomenclature* should be followed.

Scientific names of all biological creatures (crops, plants, insects, birds, mammals, etc.) should be mentioned in parentheses at first use of their English term.

Chemical nomenclature, as laid down in the *International Union of Pure and Applied Chemistry* and the official recommendations of the *IUPAC-IUB Combined Commission on Biochemical Nomenclature* should be followed. All biocides and other organic compounds must be identified by their Geneva names when first used in the text. Active ingredients of all formulations should be likewise identified.

Math formulae

All equations referred to in the text should be numbered serially at the right-hand side in parentheses. Meaning of all symbols should be given immediately after the equation at first use. Instead of root signs fractional powers should be used. Subscripts and superscripts should be presented clearly. Variables should be presented in italics. Greek letters and non-Roman symbols should be described in the margin at their first use.

To avoid any misunderstanding zero (0) and the letter O, and one (1) and the letter l should be clearly differentiated. For simple fractions use of the solidus (/) instead of a horizontal line is recommended. Levels of statistical significance such as: $^{*}P < 0.05$, $^{**}P < 0.01$ and $^{***}P < 0.001$ do not require any further explanation.

Copyright

Submission of a manuscript clearly indicates that: the study has not been published before or is not under consideration for publication elsewhere (except as an abstract or as part of a published lecture or academic thesis); its publication is permitted by all authors and after accepted for publication it will not be submitted for publication anywhere else, in English or in any other language, without the written approval of the copyright-holder. The journal may consider manuscripts that are translations of articles originally published in another language. In this case, the consent of the journal in which the article was originally published must be obtained and the fact that the article has already been published must be made clear on submission and stated in the abstract. It is compulsory for the authors to ensure that no material submitted as part of a manuscript infringes existing copyrights, or the rights of a third party.

Ethical Consent

All manuscripts reporting the results of experimental investigation involving human subjects should include a statement confirming that each subject or subject's guardian obtains an informed consent, after the approval of the experimental protocol by a local human ethics committee or IRB. When reporting experiments on animals, authors should indicate whether the institutional and national guide for the care and use of laboratory animals was followed.

Plagiarism

The JJBS hold no responsibility for plagiarism. If a published paper is found later to be extensively plagiarized and is found to be a duplicate or redundant publication, a note of retraction will be published, and copies of the correspondence will be sent to the authors' head of institute.

Galley Proofs

The Editorial Office will send proofs of the manuscript to the corresponding author as an e-mail attachment for final proof reading and it will be the responsibility of the corresponding author to return the galley proof materials appropriately corrected within the stipulated time. Authors will be asked to check any typographical or minor clerical errors in the manuscript at this stage. No other major alteration in the manuscript is allowed. After publication authors can freely access the full text of the article as well as can download and print the PDF file.

Publication Charges

There are no page charges for publication in Jordan Journal of Biological Sciences, except for color illustrations,

Reprints

Ten (10) reprints are provided to corresponding author free of charge within two weeks after the printed journal date. For orders of more reprints, a reprint order form and prices will be sent with article proofs, which should be returned directly to the Editor for processing.

Disclaimer

Articles, communication, or editorials published by JJBS represent the sole opinions of the authors. The publisher shoulders no responsibility or liability what so ever for the use or misuse of the information published by JJBS.

Indexing

JJBS is indexed and abstracted by:

DOAJ (Directory of Open Access Journals)	CABI
Google Scholar	EBSCO
Journal Seek	CAS (Chemical Abstract Service)
HINARI	ETH- Citations
Index Copernicus	Open J-Gat
NDL Japanese Periodicals Index	SCImago
SCIRUS	Clarivate Analytics (Zoological Abstract)
OAJSE	Scopus
ISC (Islamic World Science Citation Center)	AGORA (United Nation's FAO database)
Directory of Research Journal Indexing (DRJI)	SHERPA/RoMEO (UK)
Ulrich's	

المجلة الأردنية للعلوم الحياتية
Jordan Journal of Biological Sciences (JJBS)
ISSN 1995- 6673 (Print), 2307- 7166 (Online)
http://jjbs.hu.edu.jo

The Hashemite University

Deanship of Scientific Research

TRANSFER OF COPYRIGHT AGREEMENT

Journal publishers and authors share a common interest in the protection of copyright: authors principally because they want their creative works to be protected from plagiarism and other unlawful uses, publishers because they need to protect their work and investment in the production, marketing and distribution of the published version of the article. In order to do so effectively, publishers request a formal written transfer of copyright from the author(s) for each article published. Publishers and authors are also concerned that the integrity of the official record of publication of an article (once refereed and published) be maintained, and in order to protect that reference value and validation process, we ask that authors recognize that distribution (including through the Internet/WWW or other on-line means) of the authoritative version of the article as published is best administered by the Publisher.

To avoid any delay in the publication of your article, please read the terms of this agreement, sign in the space provided and return the complete form to us at the address below as quickly as possible.

Article entitled:----------

Corresponding author: ----------

To be published in the journal: Jordan Journal of Biological Sciences (JJBS)

I hereby assign to the Hashemite University the copyright in the manuscript identified above and any supplemental tables, illustrations or other information submitted therewith (the "article") in all forms and media (whether now known or hereafter developed), throughout the world, in all languages, for the full term of copyright and all extensions and renewals thereof, effective when and if the article is accepted for publication. This transfer includes the right to adapt the presentation of the article for use in conjunction with computer systems and programs, including reproduction or publication in machine-readable form and incorporation in electronic retrieval systems.
Authors retain or are hereby granted (without the need to obtain further permission) rights to use the article for traditional scholarship communications, for teaching, and for distribution within their institution.

☐ **I am the sole author of the manuscript**

☐ **I am signing on behalf of all co-authors of the manuscript**

☐ **The article is a 'work made for hire' and I am signing as an authorized representative of the employing company/institution**

Please mark one or more of the above boxes (as appropriate) and then sign and date the document in black ink.

Signed:_____ **Name printed:** _____
Title and Company (if employer representative) : _____
Date: _____

Data Protection: By submitting this form you are consenting that the personal information provided herein may be used by the Hashemite University and its affiliated institutions worldwide to contact you concerning the publishing of your article.

Please return the completed and signed original of this form by mail or fax, or a scanned copy of the signed original by e-mail, retaining a copy for your files, to:

Hashemite University
Jordan Journal of Biological Sciences
Zarqa 13115 Jordan
Fax: +962 5 3903338
Email: jjbs@hu.edu.jo

Editorial Preface

Jordan Journal of Biological Sciences (JJBS) is a refereed, quarterly international journal financed by the Scientific Research and Innovation Support Fund, Ministry of Higher Education and Scientific Research in cooperation with the Hashemite University, Jordan. JJBS celebrated its 12th commencement this past January, 2020. JJBS was founded in 2008 to create a peer-reviewed journal that publishes high-quality research articles, reviews and short communications on novel and innovative aspects of a wide variety of biological sciences such as cell biology, developmental biology, structural biology, microbiology, entomology, molecular biology, biochemistry, medical biotechnology, biodiversity, ecology, marine biology, plant and animal biology, plant and animal physiology, genomics and bioinformatics.

We have watched the growth and success of JJBS over the years. JJBS has published 14 volumes, 60 issues and 800 articles. JJBS has been indexed by SCOPUS, CABI's Full-Text Repository, EBSCO, Clarivate Analytics- Zoological Record and recently has been included in the UGC India approved journals. JJBS Cite Score has improved from 0.7 in 2019 to 1.4 in 2021 (Last updated on 6 March, 2022) and with Scimago Institution Ranking (SJR) 0.22 (Q3) in 2021.

A group of highly valuable scholars have agreed to serve on the editorial board and this places JJBS in a position of most authoritative on biological sciences. I am honored to have six eminent associate editors from various countries. I am also delighted with our group of international advisory board members coming from 15 countries worldwide for their continuous support of JJBS. With our editorial board's cumulative experience in various fields of biological sciences, this journal brings a substantial representation of biological sciences in different disciplines. Without the service and dedication of our editorial; associate editorial and international advisory board members, JJBS would have never existed.

In the coming year, we hope that JJBS will be indexed in Clarivate Analytics and MEDLINE (the U.S. National Library of Medicine database) and others. As you read throughout this volume of JJBS, I would like to remind you that the success of our journal depends on the number of quality articles submitted for review. Accordingly, I would like to request your participation and colleagues by submitting quality manuscripts for review. One of the great benefits we can provide to our prospective authors, regardless of acceptance of their manuscripts or not, is the feedback of our review process. JJBS provides authors with high quality, helpful reviews to improve their manuscripts.

Finally, JJBS would not have succeeded without the collaboration of authors and referees. Their work is greatly appreciated. Furthermore, my thanks are also extended to The Hashemite University and the Scientific Research and Innovation Support Fund, Ministry of Higher Education and Scientific Research for their continuous financial and administrative support to JJBS.

Professor Wedyan ,Mohammed A.
March, 2024

JJBS

Volume 17, Number 4, December 2024
ISSN 1995-6673

Jordan Journal of Biological Sciences

CONTENTS

Original Articles

JJBS

Volume 17, Number 4,December 2024
ISSN 1995-6673
Pages 583 – 591
https://doi.org/10.54319/jjbs/170401

Jordan Journal of Biological Sciences

Synergistic Effect of *Coriander Sativum* Essential Oil and Gentamicin against Biofilm Formation of Some Pathogenic Bacteria

Eliza Hasen[1], Mohammad AA Al-Najjar[1,*], Shaymaa B Abdulrazzaq[1], Amin Omar[1], Wamidh H. Talib[1], Fatma U Afifi[1,2], Jehad almaliti[2,3], Asma Ismail Mahmod[1], Lujain F Alzaghari[1], Muna Barakat[1,*]

[1]*Faculty of Pharmacy, Applied Science Private University, Amman, Jordan;* [2]*Faculty of Pharmacy, University of Jordan, Amman, Jordan;* [3]*Skaggs School of Pharmacy and Pharmaceutical Sciences, University of California San Diego, La Jolla, San Diego, CA 92093, USA*

Received: January 5, 2024; Revised: March 24, 2024; Accepted: April 25, 2024

Abstract

Background: Essential oils extracted from aromatic plants and spices find diverse applications in food preservation, pharmaceuticals, and natural alternatives in healthcare and therapies. This study aimed to evaluate the antibacterial and antibiofilm of *Coriander sativum* essential oil (CEO) with/without the antibiotic Gentamicin against four bacterial strains: *Staphylococcus aureus, Escherichia coli, Staphylococcus epidermidis,* and *Pseudomonas aeruginosa*.

Methods: The Jordanian CEO was isolated using hydrodistillation and then analyzed using gas chromatography-mass spectrophotometry. Antibacterial and antibiofilm activities were assessed using a minimum biofilm eradication concentration assay (MBEC Assay®).

Results: The inhibitory and bactericidal effects of the CEO on all bacterial strains exhibited a concentration-dependent pattern. Among the strains, *P. aeruginosa* demonstrated the least susceptibility to CEO, with the highest minimum inhibitory concentration (MIC) recorded at 25 mg/mL. In contrast, the MIC values for *E. coli, S. aureus,* and *S. epidermidis* were 3.125, 3.125, and 6.25 mg/mL, respectively. Complete eradication was achieved for all tested bacterial strains at concentrations exceeding 50 mg/mL of CEO, except for *P. aeruginosa*. Achieving ~ 3 log reduction for *P. aeruginosa* necessitated a higher concentration of 200 mg/mL of CEO. Notably, the combination of Gentamicin with CEO resulted in either additive or synergistic activity, allowing for the use of lower concentrations of CEO to achieve antibacterial and antibiofilm effects.

Conclusion: The CEO extracted from Jordanian coriander seeds exhibited significant *in vitro* antibacterial and antibiofilm properties against *P. aeruginosa, S. aureus, S. epidermidis*, and *E. coli.* Notably, CEO demonstrated synergistic or additive effects when combined with Gentamicin, suggesting a potential strategy to alleviate antibiotic-associated side effects and enhance their antibacterial efficacy. These findings underscore the promising potential of CEO for future clinical applications, particularly in addressing challenges associated with chronic wounds.

Keywords: Antibacterial, antibiofilm, *Coriander sativum*, essential oil.

1. Introduction

Nowadays, the utilization of essential oils (EO) derived from aromatic plants and spices spans various domains, encompassing applications in food preservation, the pharmaceutical industry, and natural alternatives in medicine and therapies aimed at enhancing healthcare quality (Sulieman *et al.,* 2023). In response to an escalating demand for ingredients sourced from natural origins, essential oils are gaining prevalence in drinks, cosmetics, and toiletries (Cimino *et al.,* 2021). This shift is driven by concerns over the safety of synthetic additives, which have become progressively dubious over time (Aguiar Campolina *et al.,* 2023). Meeting the public need for natural extracts with pleasing sensory attributes and preservative efficacy is essential to thwart lipid deterioration, oxidation, and microbial spoilage. As essential oils primarily revolve around their impact on bacterial cell walls, alternate mechanisms such as disrupting enzymes, membrane proteins, or releasing cellular content subsequent to cytoplasmic membrane breakage are also under exploration (Langeveld *et al.* 2014; Zygadlo *et al.* 2017; Bueno *et al.* 2017; Delaquis *et al.* 2002; Baratta *et al.* 1998; Kačániová *et al.* 2020; Özkinali *et al.* 2017). The study of essential oils was historically dominated by considerations of flavor and fragrance (Fisher *et al.* 2008; Preedy, 2015). This interest is fueled by their perceived safety, consumer acceptance, and multifunctional potential (Ormancey, 2001).

Among plant-derived compounds, EOs from aromatic plants are one of the plant-based secondary metabolites

* Corresponding author. e-mail: moh_alnajjar@asu.edu.jo; m_barakat@asu.edu.jo

that are used as the basis of many modern pharmaceuticals to treat different illnesses (Kabera *et al.*, 2014). The effects of EOs and aroma principles on different body systems, including the respiratory system, gastrointestinal, nervous, and immune systems, as well as their anti-microbial, antifungal, and anticancer activities, have recently been the focus of interest for researchers (Amiri *et al.*, 2016). It is essential to underline that the nature and content of secondary metabolites in medicinal and aromatic plants are widely dependent on environmental factors. The geographic location, seasonal variation, temperature, rainfall, altitude, soil characteristics, the collection time and even the extraction method are known to affect EO's yield and chemical composition (Diao *et al.*, 2014).

Coriandrum sativum L., commonly known as coriander, is a noteworthy medicinal plant rich in essential oils distributed across its flowers, stems, leaves, and fruits/seeds (Klapper *et al.* 2010; Mandal *et al.* 2015). Renowned for its medicinal applications, coriander seeds have been traditionally employed to address a spectrum of health issues, including joint pain, gastrointestinal problems, flatulence, indigestion, insomnia, anxiety, convulsions, and loss of appetite.

Noteworthy, most of the studies focused on several prevalent bacterial pathogens that are known to form persistent biofilm, such as *Staphylococcus aureus, Escherichia coli, Staphylococcus epidermidis,* and *Pseudomonas aeruginosa* (Abdallah *et al.,* 2014). These pathogens are still the vast majority of research interests looking for potential agents with complete eradication processes. Moreover, the dramatic increase in anti-microbial resistance (AMR) for pathogenic bacteria represents a serious problem for human health (ECDC, 2009). In agriculture and veterinary fields, it is crucial to reduce the usage of antibiotics. Instead, it would be more relevant to exploit synergistic interactions with natural products such as essential oil (Carlone *et al.*, 2018). A limited number of studies have investigated the synergistic effects between antibiotics and EOs like coriander essential oil against bacteria (Aljaafari *et al.,* 2019). Accordingly, this study aimed to evaluate the antibacterial and antibiofilm of the seed coriander seed EO with/out the antibiotic Gentamicin against four bacterial strains: *Staphylococcus aureus, Escherichia coli, Staphylococcus epidermidis,* and *Pseudomonas aeruginosa*.

2. Materials and Methods

2.1. Plant materials

Coriander seeds were purchased from a farm located in North Jordan. This batch of seeds were harvested in May of 2021. Identification of *C. sativum* species was achieved by the Phytochemistry team, led by Prof. Fatima Afifi, the University of Jordan. The seeds were stored in a dry place, at room temperature in the Faculty of Pharmacy, Applied Science Private University. After which, the essential oil was obtained from the Coriander seeds by hydrodistillation (HD).

2.2. Isolation of the essential oil by hydrodistillation

Half a kilo of Coriander seeds was ground in 1.5L of filtered water using a mixer for 30 seconds and transferred to a round bottom flask of the Clevenger-type apparatus (Borosil, India). HD was conducted for 3 hours using a heating mantle (Electrothermal, UK). The extraction was repeated six times, and the obtained Coriander essential oil was pooled and dried over anhydrous sodium sulphate (Na_2SO_4) (Al-Shuneigat *et al.,* 2015). After dehydration, the 100% stock solution of CEO was stored at 4^o C in amber glass vials prior analysis (Afifi *et al.,* 2015).

2.3. Gas chromatography-mass spectrometry (GC-MS) analysis

A sample of the CEO was sent to the University of California- San Diego - USA to be analyzed using Agilent 5977B Gas Chromatograph-Mass Selective Detector (GC-MSD) instrument. This device has electron impact sources coupled with an Agilent 7820A GC system, enabling sample mixtures to be analyzed. This device is particularly useful for routine examination of non-polar small organic compounds with a mass between 50 and 1000 amu. Hits were analyzed against the NIST (National Institute of Standards and Technology) library (> 1 million compounds). Approximately 1 µL aliquot of CEO sample, was diluted in 10 µL of GC grade n-hexane and was then subjected to GC analysis. The analysis was performed using Varian Chrompack CP-3800 GC-MS/MS- 200 (Saturn, Netherlands) equipped with DB-5 (5 % diphenyl, 95 % dimethyl polysiloxane) GC capillary column (30 m × 0.25 mm i.d., 0.25 µm film thicknesses), with helium as a carrier gas (flow rate 0.9 mL/min). The compounds were identified by comparing them to built-in libraries (NIST and Wiley Co. USA).

2.4. Evaluation of the antibacterial and antibiofilm activities

2.4.1. Bacterial strains and growth conditions

All bacterial strains were purchased from the American Type Culture Collection (ATCC). These strains include *Pseudomonas aeruginosa* (ATCC 27853), *Escherichia coli* (ATCC 14169), *Staphylococcus aureus* (ATCC 25923), *and Staphylococcus epidermidis* (ATCC 12228). All bacterial strains were stored at –20±2^o C in cryovials before they were resuspended and then sub-cultured in nutrient broth (NB) (Oxoid, UK) overnight at 37±2^o C. The inoculum of each bacterial strain was assessed in triplicate by measuring optical density (OD). Similarly, the growth of each bacteria was calculated from the measured OD as explained below.

2.4.2. Biofilm formation on the MBEC Assay® plate

Biofilm formation and measurement of antimicrobial sensitivity of the bacterial biofilms were performed using the Minimum Biofilm Eradication Concentration Assay (MBEC Assay®) (ASTM, 2017). Each microtiter plate lid has 96 polystyrene pegs or projections distributed on the lid. Each peg provided the surface for bacteria to adhere to, colonize, and form a uniform mature biofilm (Ceri, 1999). The pegs fit precisely into the wells of a standard 96-well microtiter flat bottom plate that can grow bacterial biofilm, rinsing, anti-microbial challenge and microbial recovery.

Briefly, bacteria were cultured in nutrient broth (NB) test tubes (10 mL) overnight at 37±2^o C where they reached approximately 10^8 CFU/mL. The bacterial suspensions were adjusted to achieve an approximate bacterial density of 10^5 – 10^6 CFU/mL using the optical density where 600 nm was used to measure the planktonic growth (Al-Shuneigat *et al.*. 2014). An inoculum of 150

µL of bacterial culture was dispensed into each well of MBEC bottom plates (except for the sterility control wells) before placing the 96-peg lid back into the inoculated 96 well bottom plate. The inoculated MBEC Assay® plate was incubated for 24 ±2 hours at 37^{o} C on an orbital incubator (Lab Companion SI-600R, Korea) at 110 rpm to allow bacterial biofilm formation on the pegs. The lid with the pegs was transferred to a new sterile 96-well plate (SPL, Korea) containing 200 µL of sterile PBS for rinsing for 30 seconds. Optimizing the growth conditions for biofilm formation was determined in preliminary studies to achieve approximately 10^4 -10^6 CFU/peg.

Following the biofilm formation and the rinse steps, the 96 peg-lid was transferred to the 96-well challenge plate. The challenge plate consisted of different CEO concentrations dissolved in NB with 0.5 % of Dimethyl Sulfoxide (DMSO, AZ Chem for chemicals, Canada). DMSO was used in the untreated growth control wells that were used to calculate the log10 reduction later on. A wide range of concentrations of CEO were used; 300, 200, 100, 50, 25, 6.25, 1.6 and 0.4 mg/mL. All test dilutions were run in triplicates. Gentamicin antibiotic MIC results were obtained from earlier experiments to present as the positive control in this study (0.6, 1.22, 0.15, 0.3 µg/mL) for *P. aeruginosa, S. epidermidis, S. aureus, and E. coli* respectively. The MIC was determined as the least concentration of the antibiotic required to inhibit bacterial growth (Talib *et al.* 2010; Al-Shuneigat *et al.*. 2020). The peg-lid was then removed, rinsed in PBS, then placed over another 96-well microtiter plate containing fresh, sterile broth recovery medium (NB with 0.1% Tween-80). This recovery plate was sonicated using ultrasonic cleaner (ULTRAsonik 104x, USA) for 30±1 minutes. The recovered colony forming unit per 1 milliliter (CFU/mL) of the adhered biomass for all treatment concentrations was determined after serial dilution and spot plating of each well on Nutrient agar plates that were incubated for 24±2 hours. The adhered biomass recovery plates were topped with 100µL of sterile recovery media in each well then incubated for another 24 hours to determine the MBEC breakpoints, which is defined as the lowest concentration of antibiotic or antimicrobial capable of killing biofilm producer bacteria (Al-Ouqaili *et al.*, 2011).

2.5. Combination of Coriander essential oil with Gentamicin concentrations and determination of minimum inhibitory concentration (MIC)

Two-fold serial dilutions of CEO plus Gentamicin were prepared. Gentamicin antibiotic MIC results were calculated using microdilution method (Aboalhaija *et al.* 2021). Concentrations of CEO:Gentamicin studied on *S. aureus*, *S. epidermidis*, and *E. coli* ranged (0.39: 0.094 - 12.5: 3 µl/mL), whereas for *P. aeruginosa*, CEO:Gentamicn concentrations ranged (3.13: 0.047 - 200: 3 µl/mL). The MIC, which represents the concentration of CEO required to inhibit the growth of planktonic bacterial population, was determined using the MBEC Assay®. The MIC was determined by the bacteria shed from biofilms attached to the pegs of the MBEC Assay® plate during the anti-microbial challenge step. The MIC plate wells were spot plated instead of using turbidity reading as the CEO interfered with the absorbance and visual reading at higher concentrations (Ceri, 1999).

2.6. Bacterial Cell Count

Serial dilutions of samples exposed to treatments were prepared in sterile 0.85% (w/v) NaCl solution and plated according to the method described previously (Chen *et al.*2003). The plates were incubated at 37±2 °C for 24±2 hours and the number of colonies was determined. To measure growth inhibition, viability logarithmic reduction was calculated comparing to the untreated growth control sample with 0.5% DMSO (Bouhdid *et al.* 2009). Bacterial inoculums of 5 µL were spot plated on nutrient agar plates, then incubated overnight at 37±2 °C. After 24 ±2 hours.

Equations (1-4) used for the calculations are shown below (Centre 2010):

$$A = \#\ of\ colonies \times Dilution\ factor \quad (1)$$

$$B = CFU/Peg = (A/5mL) \times 200mL \quad (2)$$

$$C = log_{10}(CFU/Peg) = log_{10}(B+1) \quad (3)$$

$$log_{10} Reduction = C - Average\ Growth\ Control \quad (4)$$

2.7. Combination index calculation

The mode of interaction between CEO and Gentamicin antibiotic was determined using the bolographic approach. The combination index (CI) was calculated (equation 5) for combinations of the two treatments against bacterial growth (planktonic/biofilm) (Ichite *et al.*, 2009):

$$CI = (D)1/(Dx)1 + (D)2/(Dx)2 \quad (5)$$

where (Dx) 1 = dose of CEO to produce 3 log reductions (99.9% reduction) in planktonic bacteria and 2 log reduction (99% reduction) in biofilm bacteria; (D) 1 = dose of CEO to produce 99.9% planktonic or 99% biofilm bacterial inhibition in combination with Gentamicin; (Dx) 2 = dose of Gentamicin to produce 99.9% planktonic or 99% biofilm bacteria inhibition alone; (D) 2 = dose of Gentamicin to produce 99.9% planktonic or 99% biofilm bacteria inhibition in combination with CEO. Interpreted as: CI >1.3 antagonism; CI 1.1 to 1.3 moderate antagonism; CI 0.9 to 1.1 additive effect; CI 0.8 to 0.9 slight synergism; CI 0.6 to 0.8 moderate synergism; CI 0.4 to 0.6 synergism; CI <0.4 strong synergism.

In this study, two-fold serial dilutions of CEO, Gentamicin, and CEO + Gentamicin combination were prepared, with final concentration ranging from 0.78 - 25 mg/mL of CEO, 0.18 - 6 µg/mL of Gentamicin, and 0.39:0.094 - 12.5:3 of CEO + Gentamicin (mg/mL:µl/mL) for *S. aureus*, *S. epidermidis* and *E.coli*, and from 3.13 - 200 mg/mL of CEO, 0.09 - 6 µg/mL of Gentamicin, and 3.13:0.047 - 200:3 of CEO + Gentamicin (mg/mL:µl/mL) for *P. aeruginosa*.

2.8. Statistical Analysis

All results are expressed as mean ± SD (n = 4). GraphPad Prism 9 software (GraphPad Software, San Diego, CA, USA) was used to perform statistical analyses. Pertaining samples that passed the Shapiro-Wilk normality test, an unpaired t-test was used to compare means in two independent groups, while Mann-Whitney tests were used for samples that did not show normal distribution. One-way analysis of variance (ANOVA) was used to compare means of three groups or more and Tukey's multiple comparison test was used as a post hoc test. A p-value of ≤0.05 was considered a significant difference.

3. Results

3.1. Qualitative analysis of the Coriander essential oil

The amount of the CEO obtained from each 100 g coriander seeds was 0.313 (±0.01) mL, (n=3). GC analysis (Supplementary material: S1) of the hydro-distilled oil from the Coriander seeds revealed 6 major volatile compounds: α-pinene (terpene), limonene (aliphatic hydrocarbon), linalool (terpene alcohol), camphor (terpene ketone), o-cymene and γ-terpinene (hydrocarbons).

3.2. Antibacterial activity of the Coriander essential oil

In general, CEO inhibition and killing effects on the tested bacterial strains in this study were concentration dependent. Table 1 shows the quality control and numeration of average growth of bacteria during study conduction as a negative control.

Table 1. The tested bacteria numeration of average CFU/well of planktonic bacteria and CFU/peg sessile (biofilm).

Test organism	Planktonic concentrations (CFU/well)[a]	Biofilm concentrations (CFU/peg)[b]
Pseudomonas aeruginosa (ATCC 27853)	3.00×10^7	6.30×10^7
Staphylococcus epidermidis (ATCC 12228)	2.95×10^6	5.40×10^6
Staphylococcus aureus (ATCC 25923)	2.00×10^7	9.90×10^6
Escherichia coli (ATCC 14169)	1.45×10^7	3.38×10^7

[a] This column represents the mean number of planktonic bacteria growing in the wells of the MBEC Assay® plate at the same time the peg was sampled.

[b] This column represents the mean number of sessile bacteria on each peg of the MBEC Assay® plate.

3.3. Antibacterial activity of Coriander essential oil

The effect of CEO was tested using different concentrations and observed onto each bacterial strain as planktonic and biofilm phenotypes, exhibiting different susceptibility effects as shown in Figure 2 and Figure 3. It was shown in Figure 1 that *P. aeruginosa* had the least susceptible tendency to the CEO, as it possessed the highest MIC concentration of CEO (25 mg/mL), whereas the MIC of *E. coli*, *S. epidermidis* and *S. aureus* were 3.125, 6.25 and 3.125mg/mL, respectively. Complete eradication was detected on all tested bacterial strains at 50 mg/mL of CEO, except for *P. aeruginosa*, which needed 200 mg/mL of CEO to reach 2.97 log reductions. CEO showed a comparable antibacterial activity with the MIC of Gentamicin (positive control) against both *P. aeruginosa (*200 mg/mL) *and S. epidermidis*, (12.5 mg/mL). Furthermore, at concentration ≥25 mg/mL CEO, *S. epidermidis, S. aureus and E. coli the* antibacterial activity was significantly higher than MIC-Gentamicin.

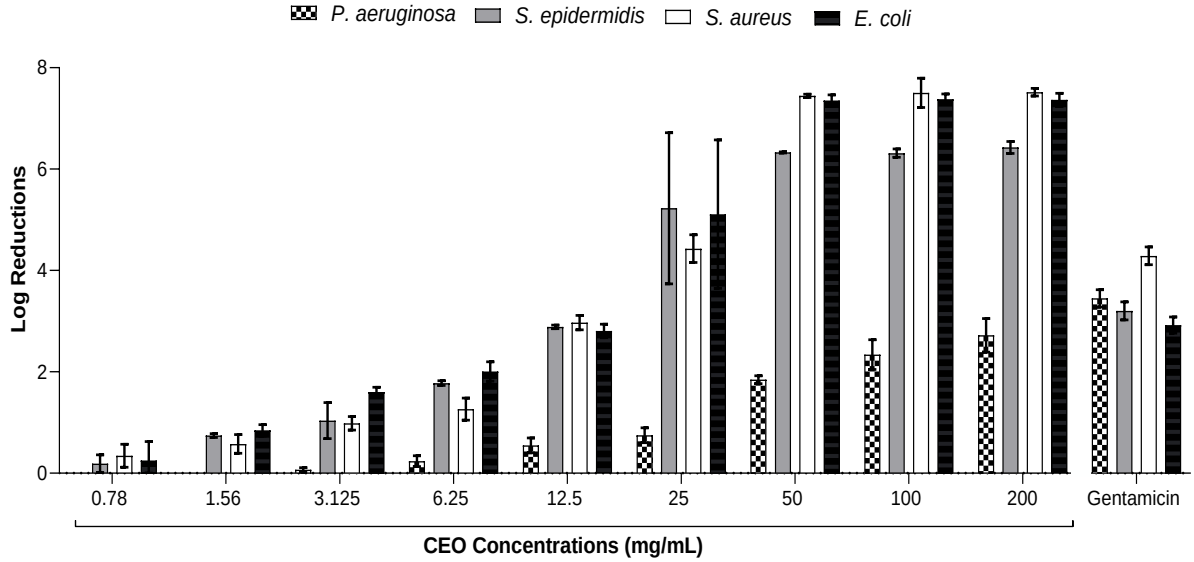

Figure 1. The effect of CEO in mg/mL on planktonic bacteria. Results represented as mean ±SD (n=4). Positive control Gentamicin MIC = 0.75 µL/mL (E. coli), 0.375 µL/mL (P. aeruginosa), 0.188 µL/mL (S. aureus) and 1.5 µL/mL (S. epidermidis).

3.4. Antibiofilm activity of Coriander essential oil (CEO)

The *P. aeruginosa* biofilm was the most resistant among the tested bacterial biofilms. The antibiofilm activity of CEO for *P. aeruginosa* was observed at 200 mg/mL, with 2.18 log reduction (Figure 3). This effect was not significantly different from the positive control-Gentamicin. For the other bacteria, antibiofilm activity of CEO on *S. epidermidis*, *S aureus* and *E. coli* was significantly observed at concentration of >25 mg/mL of CEO, which was associated with more than four log reduction, as shown in Figure 2.

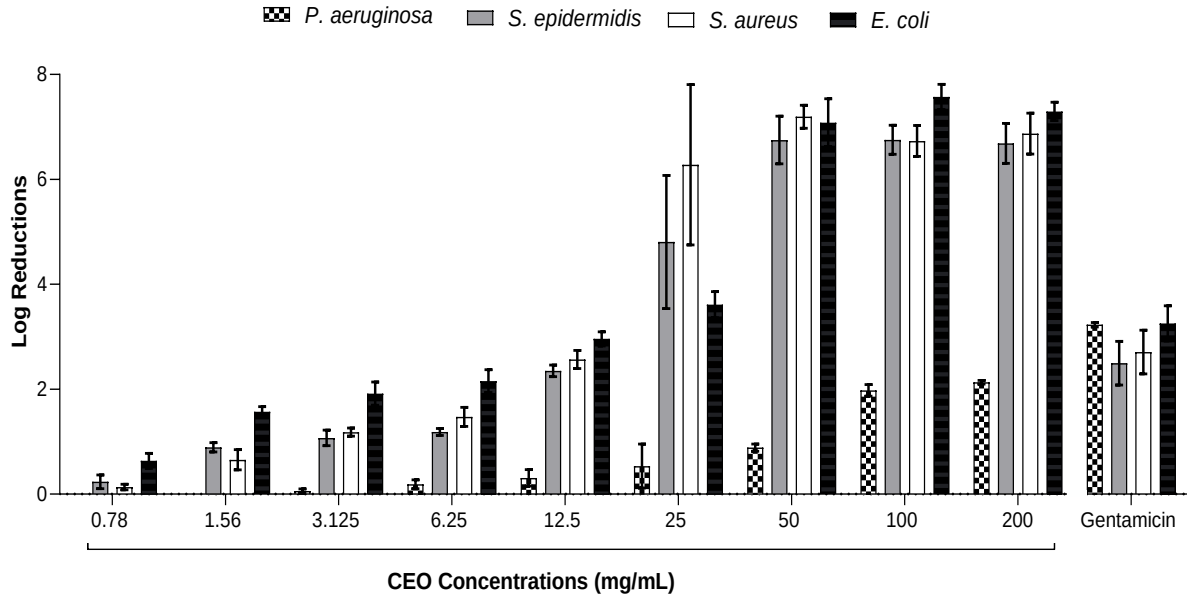

Figure 2. The effect of Coriander essential oil (CEO) in mg/mL on biofilm bacteria. Results represented as mean ±SD (n=4). Positive control Gentamicin MBEC = 6 µL/mL (*E. coli*), >6 µL/mL (*P. aeruginosa*), 3 µL/mL (*S. aureus*) and 3 µL/mL (*S. epidermidis*).

In general, similar antibacterial activities were observed for the combination of both CEO and Gentamicin, but at smaller concentrations of CEO. It was seen that the most resistant bacteria studied was *P. aeruginosa*; hence, 100mg/mL of CEO and 1.5 µg/mL Gentamicin exhibited 3 log reductions with combination index (CI)= 1 revealing that the effect was an additive effect. Similar additive effect was observed on *E. coli*, at 6.25mg/mL CEO and 1.5 µg/mL Gentamicin. Substantial synergistic effect was observed upon using this combination on *S. aureus*, as CI=0.5. at 3.123 mg/mL CEO and 0.375µg/mL Gentamicin. In between, a moderate synergism for the combination was reported for *S. epidermidis* at 3.125 mg/mL CEO and 0.75 µg/mL Gentamicin.

Table 2. The concentration values with 3 log reductions effect (99.9% reduce in bacteria), and the combination index for CEO (mg/mL) and Gentamicin (µg/mL) antibiotic against different planktonic bacteria strains.

Tested bacteria (planktonic)	CEO concentrationmg/mL	Gentamicin Concentration µg/mL	CEO concentration in combination mg/mL	Gentamicin concentration in combination µg/mL	Combination Index (CI)	Type of effect
P. aeruginosa	200	3	100	1.5	1	Additive effect
S. epidermidis	12.5	1.5	3.125	0.75	0.75	Moderate synergism
S. aureus	12.5	1.5	3.125	0.375	0.5	Synergism
E. coli	12.5	3	6.25	1.5	1	Additive effect

Furthermore, the combination of CEO-Gentamicin on biofilm of the studied bacteria had a positive effect exhibiting 2 log reductions on all bacteria except for *E. coli*, which had a CI >1.3 and is considered antagonism effect. A strong synergism was observed when using the combination on *S. epidermidis*, as CEO concentration dropped by 8 times and Gentamicin by 4 times. Even the most resistant biofilm of *P. aeruginosa* had a positive effect of the combination. To reach 2 log reductions on *P. aeruginosa* biofilm, a concentration of CEO was 12.5 mg/mL and 0.189 µg/mL of Gentamicin. Moderate synergism was observed when using the combination of CEO and Gentamicin on *S. aureus* biofilm to exhibit 2 log reductions.

Table 3 The concentration values with 2 log reductions effect (99% reduce in bacteria), and the combination index for CEO (mg/mL) and Gentamicin (µg/mL) antibiotic against different biofilm bacteria strains.

Tested bacteria (planktonic)	CEO concentration mg/mL	Gentamicin Concentration µg/mL	CEO concentration in combination mg/mL	Gentamicin Concentration in combination µg/mL	Combination Index (CI)	Type of effect
P. aeruginosa	100	0.75	12.5	0.189	0.502	Synergism
S. epidermidis	12.5	1.5	1.56	0.375	0.3748	Strong synergism
S. aureus	12.5	0.75	3.125	0.375	0.75	Moderate
E. coli	3.125	1.5	3.125	0.75	1.5	Antagonism

4. Discussion

There is a worldwide interest in discovering new and safe antibacterial agents from natural sources. Essential oils (EOs) from natural products are being extensively studied and experimented for their potential as a source of biologically active compounds (Kabera *et al.* 2014; Amiri *et al.* 2016; Diao *et al.* 2014). Most of the studies carried out by researchers of different countries showed that the raw coriander seeds consisted mainly of linalool (72.7%) followed by γ-terpinene (8.8%), α -pinene (5.5%), camphor (3.7%), limonene (2.3%), geranyl acetate (1.9%) and o-cymene (1.5%). Coriander plant exhibits diverse biological activities beyond its medicinal uses, including anti-microbial and food preservative properties (Mandal *et al.,* 2015). It was reported that leaves-coriander essential oil expressed a strong antibacterial activity against Bacillus subtilis followed by *Stenotrophomonas maltophilia* and *Penicillium expansum* (Özkinali *et al.* 2017, Kačániová *et al.* 2020). In this study, CEO's major constituents were linalool, α -pinene, γ-terpinene, camphor, o-Cymene, and Limonene. Compared with other studies in other countries, the same compounds were identified in stage three coriander seed's essential oil. Variations in the concentrations of the constituents will probably be seen when compared to other studies due to different factors, including time of harvest and seasonal conditions (Mandal *et al.,* 2015). Moreover, Linalool also represents the highest peak in the GC-MS in our study, matching the literature; this monoterpene alcohol poses antibacterial properties (Zengin *et al.,* 2014) and anti-inflammatory ones (Peana *et al.* 2002). Therefore, the detected antimicrobial activity in our work could be caused by the presence of linalool in the Jordanian CEO, which is a similar speculation to a study of CEO from Hanus, a.s. (Slovakia) (Kačániová *et al.,* 2020). However, the exact model of inhibitory action of monoterpenes remains unknown and requires further studies. Furthermore, the studies showed that the combination of linalool with α -pinene resulted in an additive antimicrobial effect (Tserennadmid *et al.,* 2011). According to literature, the antimicrobial activity of CEO was higher than that of its main constituent, linalool, suggesting synergistic effect due to the combination of more than one component (Silva *et al.,* 2011). Moreover, fractional distillation of coriander essential oil showed that the fraction that presented as less potent but more effective against tested microorganisms was the one containing a superior concentration of linalool (Delaquis *et al.,* 2002). These findings suggest that the anti-microbial activity is due to complex interactions between individual components that lead to the overall activity and not only to the effects of linalool, as could be expected.

A study observed that alcohols and aldehydes constituents of CEO predominantly inhibited Gram-positive bacteria, while linalool exhibited activity against Gram-negative strains (Delaquis *et al.,* 2002). Another study highlighted the medium to strong anti-microbial activity of aromatic volatiles and essential oils against Gram-positive bacteria such as *S. aureus* and Gram-negative bacteria like *E. coli*, with comparatively weaker effects against *P. aeruginosa* (Prabuseenivasan *et al.,* 2006). The antibacterial prowess of CEO is potentially attributed to its constituents, particularly linalool, which is known to enhance membrane permeability. Thus, it induces structural changes in both Gram-positive and Gram-negative bacteria through interactions with membrane phospholipids, membrane proteins, and specific intracellular targets (Zengin *et al.,* 2014). Additional CEO constituents, including α-pinene, camphor, γ-terpinene, geranyl acetate, and D-limonene, may also contribute to antibacterial effects by disrupting membrane structures, increasing permeability, damaging membrane proteins, and altering respiration and ion transport (Abdi-Moghadam *et al.* 2023; Bunse *et al.* 2022). Furthermore, it was demonstrated that CEO induces membrane damage, permeabilization, loss of membrane potential, and disruption of efflux pump and respiratory activities in both Gram-positive and Gram-negative species (Taiwo *et al.,* 2017).

In biofilms, bacterial cells exhibit increased resistance to antimicrobial agents compared to planktonic cells. Inhibiting biofilm growth poses a greater challenge than impeding cell attachment, a phenomenon consistent with prior findings (Sharma *et al.,* 2023). In this study, the effect of 200 mg/mL CEO on the biofilms of *E. coli, S. aureus, S. epidermidis,* and *P. aeruginosa* yielded log reductions of 7.32, 6.92, 6.68, and 2.13, respectively. A study investigated the anti-biofilm activity of Iranian *C. sativum* on *S. aureus* and *E. coli.* They demonstrated CEO's substantial anti-biofilm activity against both bacteria, with the lowest MIC values recorded at 0.8 µl/mL and 1.6 µl/mL for *S. aureus* and *E. coli*, respectively (Bazargani *et al.,* 2016). Research identified the potential of the CEO as antibacterial against the biofilm produced by Acinetobacter baumannii at 4 µL/mL for MIC and MBC. In our study, we determined the antimicrobial activity with the MBEC® method (Duarte *et al.,* 2012). In a study done in 2016, antiadhesion tests for the evaluation of the reduction in the cell attachments using the crystal violet assay were accomplished for the CEO. They found a variety of effects of the CEO on the development and growth of the biofilm with

at least 50% reduction in cell attachment with a complete inhibition of *S. aureus*. According to this study, the CEO induced the decrease of biofilm formation against *S. aureus* up to 91% (Bazargani *et al.,* 2016). In parallel, Gentamicin possesses bactericidal efficacy specifically targeting aerobic Gram-negative bacteria, making it a valuable treatment option for various common infections and serving as a positive control in our study (Turner *et al.,* 2022). The mechanism of action involves oxygen-dependent active transport through the Gram-negative bacterial membrane. Aminoglycosides, including Gentamicin, are ineffective against anaerobic bacteria due to the oxygen requirement in this process. Upon reaching the cytoplasm, Gentamicin and other aminoglycosides bind to the 16S rRNA at the 30S ribosomal subunit, disrupting mRNA translation and resulting in the generation of truncated or non-functional proteins (Chaves BJ, 2023). A study done in 2018 has explored the combination of Gentamicin with essential oils. Caraway EO, for instance, exhibited synergy with Gentamicin against strains resistant to extended-spectrum beta-lactamases (ESBL) and gentamicin-resistant strains. Similar additive effects were observed when Gentamicin was combined with thyme, fennel, basil, and clary sage (Kwiatkowski *et al.,* 2018). It is noteworthy that the combination of CEOs and antibiotics can impact multiple targets concurrently, as highlighted by a study, confirming that the mode of action of combination differs significantly than that of the same drugs acting individually (Hemaiswarya *et al.,* 2008). In a study, the combination of Gentamicin and coriander essential oil was explored, revealing that CEO can potentially enhance the effectiveness of antibiotics against *Acinto baumannii* (Duarte *et al.,* 2012). This bacterium, characterized as a Gram-negative, nonmotile, non-fermentative, and oxidase-negative bacillus, poses a challenge in treatment (Duarte *et al.,* 2012). The synergistic effect observed between CEO and antibiotics suggests promising avenues for addressing *A. baumannii* infections (Duarte *et al.,* 2012). In our study, similar effects were noted using CEO against both planktonic and biofilm bacteria, aligning with the potential for essential oils to augment antibiotic efficacy.

The broad spectrum of CEO's anti-microbial effects, as reported in the literature, may not be entirely mirrored in the context of our study, potentially limiting the generalizability of our findings. Despite these considerations, our investigation contributes valuable insights into the potential synergy between CEO and antibiotics, offering a basis for further exploration and refinement of anti-microbial strategies. Additionally, the study's focus on planktonic and biofilm bacteria provides valuable insights into the potential applications of CEO. However, the diverse nature of biofilms and their resistance mechanisms may not be fully captured by our experimental design. Biofilm formation is a complex process influenced by numerous factors, and the efficacy of CEO against biofilm-associated bacteria may be subject to variations that require further investigation. Finally, while our study sheds light on the potential synergistic effects of CEO with Gentamicin, acknowledging the limitations related to the choice of positive control, variations in essential oil compositions, and the specificity of interactions with different antibiotics and bacterial forms is crucial for a comprehensive interpretation of our findings. These limitations should be considered in the context of future research endeavors to refine our understanding of the potential applications of CEO in combination with antibiotics.

5. Conclusion

This study presents compelling evidence of the potent antibacterial activity of coriander seed essential oil (CEO) against a range of clinically relevant bacteria, including *Pseudomonas aeruginosa*, *Staphylococcus aureus*, *Staphylococcus epidermidis*, and *Escherichia coli.* Notably, CEO exhibits synergistic effects when combined with the antibiotic Gentamicin, suggesting a promising avenue for combination therapy. Moreover, CEO demonstrates remarkable efficacy in eradicating biofilms formed by *S. aureus*, *S. epidermidis*, and *E. coli*, with significant impact on pseudomonal biofilm.

The present research is the first to establish CEO action against biofilm in Jordan. The findings hold substantial implications for the management of chronic wounds, where biofilm formation poses a significant challenge. Furthermore, this study sheds light on the potential of CEO as a novel therapeutic approach in the field of infectious diseases, particularly for combating biofilm-associated infections that often exhibit resistance to traditional treatments.

Author contributions

All authors contributed equally to this work.

Funding

This research was generously supported by Applied Science Private University-Amman-Jordan.

Acknowledgement

Authors would like to thank Smart Lab and The University of Jordan - Jordan, and California-San Francisco University-USA for their cooperation and support.

Declaration of Competing Interest

The authors declare that they have no known competing financial interests or personal relationships that could have appeared to influence the work reported in this paper.

References

Abdallah, M, Corinne B, Djamel D, Pascal D, and Nour-Eddine Ch. 2014. Biofilm formation and persistence on abiotic surfaces in the context of food and medical environments. *Arch Microbiol* , **196**: 453-72.

Abdi-Moghadam Z, Yeganeh M, Alieh RS, Maryam M, Mansour S, Mahnaz M, Samira SH, Ahmad G, Farshid N, and Majid D. 2023. The significance of essential oils and their antifungal properties in the food industry: A systematic review. *Heliyon*, 29; **9**:e21386.

Aboalhaija N, Afifi, FU , Al-Hussaini M, Al-Najjar M, Abu-Dahab R, Hasen E, Rashed M, Abdel-Haq S, and Khalil E.2021. *In vitro and in vivo* evaluation of the wound healing potential of the extracts of Schinus molle L.(Anacardiaceae) grown in Jordan. *Indian J. Pharmaceut. Sci.,* **83**: 261-70.

Afifi, FU, Kasabri V, and Abaza IM. 2015. GC-MS composition and antiproliferative activity of Inula graveolens (L.) Desf. essential oil. *AJMAP* , **1**: 57-66.

Aguiar Campolina G., das Graças Cardoso M., Rodrigues-Silva-Caetano A., Lee Nelson D. and Mendes Ramos E. 2023. Essential oil and plant extracts as preservatives and natural antioxidants applied to meat and meat products: a review. *Food Technol Biotechnol* , **61**: 212-25.

Al-Ouqaili MT, AL-Quhli SQ, and Al-Izzy MY. 2011. The Role of milleri Streptococci in the Formation of Cariogenic Biofilm: Bacteriological Aspects. *Jordan J Biol Sci*, **4:**165-172.

Al-Shuneigat J, Al-Sarayreh S, Al-Saraireh Y, and Al-Qudah M. 2020. Effect of Achillea santolina essential oil on bacterial biofilm and its mode of action. *Curr. Issues Pharm. Med. Sci*, **33**: 83-89.

Al-Shuneigat J, Al-Sarayreh S, Al-Saraireh Y, Al-Qudah M, Al-Tarawneh I, and Al Bataineh E. 2014. Effects of wild Thymus vulgaris essential oil on clinical isolates biofilm-forming bacteria. *IOSR J. Dent. Med. Sci*, **13**: 62-66.

Al-Shuneigat, J, Al-Tarawneh I, Al-Qudah M, Al-Sarayreh S, Al-Saraireh Y, and Alsharafa KH. 2015. The chemical composition and the antibacterial properties of Ruta graveolens L. essential oil grown in Northern Jordan. *Jordan J Biol Sci*, **8**: 139-43.

Aljaafari M, Alhosani MS, Abushelaibi A, Lai KS, and Erin Lim SH. 2019. Essential oils: Partnering with antibiotics. **Essential Oils-Oils of Nature.** IntechOpen Publisher, United Kingdom.

Amiri SH, and Joharchi MR. 2016. Ethnobotanical knowledge of Apiaceae family in Iran: A review. *Avicenna J Phytomed* , **6**: 621.

ASTM. 2017. Standard Test Method for Testing Disinfectant Efficacy against Pseudomonas aeruginosa Biofilm using the MBEC Assay. **E2799-12.** Available from URL: https://www.astm.org/e2799-12.html

Baratta M. Tiziana H J, Dorman D, Deans SG, Biondi DM, and Ruberto G. 1998. Chemical Composition, Antimicrobial and Antioxidative Activity of Laurel, Sage, Rosemary, Oregano and Coriander Essential Oils. *J. Essent. Oil Res.* , **10**: 618-27.

Bazargani MM, and Rohloff J. 2016. Antibiofilm activity of essential oils and plant extracts against Staphylococcus aureus and Escherichia coli biofilms. *Food control*, **61**: 156-64.

Bouhdid S, Abrini, A Zhiri, MJ Espuny, and An Manresa. 2009. Investigation of functional and morphological changes in Pseudomonas aeruginosa and Staphylococcus aureus cells induced by Origanum compactum essential oil. *J Appl Microbiol* , **106**: 1558-68.

Bueno J, Demirci F, and Can Baser KH. 2017. Essential oils against microbial resistance mechanisms, challenges and applications in drug discovery. **Essential oils and nanotechnology for treatment of microbial diseases**, 1ST ed, CRC press, United kingdom 143-58.

B Bunse M, Daniels R, Gründemann C, Heilmann J, Kammerer DR, Keusgen M, Lindequist U, Melzig MF, Morlock GE, Schulz H, Schweiggert R, Simon M, Stintzing FC, and Wink M. 2022. Essential oils as multicomponent mixtures and their potential for human health and well-being.*Front Pharmacol* , **13**: 956541.

Carlone N, Tullio VC, and Cuffini A. 2018. Farmaci antibatterici inMicrobiologia generale e applicata,*Società Editrice Esculapio*. Available from: https://scuolamedicina.unich.it/sites/sc01/files/5_inferm_ass_antibiotici.pdf

The National Science foundation Engineering research Center (NSFERC). 2010. The log reduction (LR) measure of disinfectant efficacy. *MSU Cen for Biofilm Eng*, Monatana State Univeristy, **4**. Available from URL: https://biofilm.montana.edu/documents/KSA-SM-07.pdf

Ceri, H. 1999. The Calgary Biofilm Device: Measurement of antimicrobial sensitivity of bacterial biofilms. *J. Clin. Microbiol.*, **37**: 1771-76.

Chaves BJ, Tadi P. 2023. Gentamicin. **StatPearls [e-Book].** Available from:

https://www.ncbi.nlm.nih.gov/books/NBK557550/.

Chen CY, Nace GW, and Irwin PL. 2003. A 6× 6 drop plate method for simultaneous colony counting and MPN enumeration of Campylobacter jejuni, Listeria monocytogenes, and Escherichia coli. *J Microbiol Methods* , **55**: 475-79.

Cimino C, Maurel OM, Musumeci T, Bonaccorso A, Drago F, Souto EMB, Pignatello R, and Carbone C. 2021. Essential oils: Pharmaceutical and encapsulation strategies into lipid based delivery systems. *Pharmaceutics*, **13**: 327.

de Souza CC, de Souza LZM, Yılmaz M, de Oliveira MA, da Silva Bezerra AC, da Silva EF, Dumont MR and Machado ART. 2022. Activated carbon of Coriandrum sativum for adsorption of methylene blue: Equilibrium and kinetic modeling. *Cleaner Materials*, **3**: 100052.

Delaquis PJ, Stanich K, Girard B, and Mazza G.. 2002. Antimicrobial activity of individual and mixed fractions of dill, cilantro, coriander and eucalyptus essential oils. *Int J Food Microbiol* , **74**: 101-09.

Diao WR, Hu QP, Zhang H, and Xu JG. 2014. Chemical composition, antibacterial activity and mechanism of action of essential oil from seeds of fennel (Foeniculum vulgare Mill.). *Food control*, **35**: 109-16.

Duarte A, Ferreira S, Silva F, and Domingues FC. 2012. Synergistic activity of coriander oil and conventional antibiotics against Acinetobacter baumannii. *Phytomedicine*, **19**: 236-38.

European center for disease prevention and control (ECDC). 2009. The bacterial challenge–time to react a call to narrow the gap between multidrug-resistant bacteria in the eu and development of new antibacterial agents. *Solna: ECDC & EMEA Joint Press Release*. avaioable from : https://www.ecdc.europa.eu/sites/default/files/media/en/publications/Publications/0909_TER_The_Bacterial_Challenge_Time_to_React.pdf

Fisher K and Phillips C. 2008. Potential antimicrobial uses of essential oils in food: is citrus the answer?. *Trends Food Sci Technol* , **19**: 156-64.

Hemaiswarya SH, Kruthiventi AK, and Doble M. 2008. Synergism between natural products and antibiotics against infectious diseases. *Phytomedicine*, **15**: 639-52.

Ichite N, Chougule MB, Jackson T, Fulzele S, Safe S, and Singh M. 2009. Enhancement of docetaxel anticancer activity by a novel diindolylmethane compound in human non–small cell lung cancer. *Clin Cancer Res*, 15: 543-52.

Kabera JS, Semana E, Mussa AR, and He X. 2014. Plant secondary metabolites: biosynthesis, classification, function and pharmacological properties. *J. Pharm. Pharmacol*, **2**: 377-92.

Kačániová M, Galovičová L, Ivanišová E, Vukovic NL, Štefániková J, Valková V, Borotová P, Žiarovská J, Terentjeva M, Felšöciová S, and Tvrdá E. 2020. Antioxidant, Antimicrobial and Antibiofilm Activity of Coriander (Coriandrum sativum L.) Essential Oil for Its Application in Foods. *Foods*, **9**: 282.

Klapper I and Dockery J. 2010. Mathematical description of microbial biofilms. *SIAM review*, **52**: 221-65.

Kwiatkowski P, Pruss A, Grygorcewicz B, Wojciuk B, Dołęgowska B, Giedrys-Kalemba S, Kochan E, and Sienkiewicz M. 2018. Preliminary study on the antibacterial activity of essential oils alone and in combination with gentamicin against extended-spectrum β-lactamase-producing and New Delhi

metallo-β-lactamase-1-producing Klebsiella pneumoniae isolates. *Microb Drug Resist* , **24**: 1368-75.

Langeveld W, Veldhuizen E, and Burt S. 2014. Synergy between essential oil components and antibiotics: a review. *Crit Rev Microbiol* , **40**: 76-94.

Mandal S and Mandal M. 2015. Coriander (Coriandrum sativum L.) essential oil: Chemistry and biological activity. *Asian Pac J Trop Biomed* , **5**: 421-28.

Ormancey X. 2001. Formulation of essential oils in functional perfumery. *PCA*, **157**: 30-40.

Özkinali S, Şener N, Gür M, Güney K, and Olgun Ç. 2017. Antimicrobial activity and chemical composition of coriander & galangal essential oil. *Indian J. Pharm. Educ. Res*, **51**: 221-24.

Peana T, Panin F, Serra G, Pippia P, and Moretti MD. 2002. Anti-inflammatory activity of linalool and linalyl acetate constituents of essential oils. *Phytomedicine*, **9**: 721-26.

Prabuseenivasan S, Jayakumar M, and Ignacimuthu S. 2006. In vitro antibacterial activity of some plant essential oils. *BMC Complement Altern Med* , **6**: 1-8.

Preedy VR. 2015. **Essential oils in food preservation, flavor and safety**, Academic press, United Kingdom.

Said, Hakim Mohammad, and Aftab Saeed. 1996. **Medicinal herbal: a textbook for medical students and doctors**, Hamdard Foundation, Pakistan.

Shahrajabian MH . 2021. Medicinal herbs with anti-inflammatory activities for natural and organic healing. *Curr Org Chem* **25**: 2885-901.

Shahrajabian MH, Sun W, and Cheng Q. 2022. The importance of flavonoids and phytochemicals of medicinal plants with antiviral activities. *Mini Rev Org Chem*, **19**: 293-318.

Sharma S, Mohler J, Mahajan SD, Schwartz S, Bruggemann L, and Aalinkeel R. 2023. Microbial Biofilm: A Review on Formation, Infection, Antibiotic Resistance, Control Measures, and Innovative Treatment. *Microorganisms*, **11**: 1614.

Silva F, Ferreira S, Queiroz JA, and Domingues FC. 2011. Coriander (Coriandrum sativum L.) essential oil: its antibacterial activity and mode of action evaluated by flow cytometry. *J. Med. Microbiol.* , **60**: 1479-86.

Sulieman A, Abdallah E, Alanazi N, Ed-Dra A, Jamal A, Idriss H, Alshammari AS, and Shommo S. 2023. Spices as Sustainable Food Preservatives: A Comprehensive Review of Their Antimicrobial Potential.*Pharmaceuticals*, **16**: 1451.

Taiwo MO and Adebayo OS. 2017. Plant essential oil: an alternative to emerging multidrug resistant pathogens. *J Microbiol Exp*, **5**: 00163.

Talib W H, and Mahasneh A. 2010. Antimicrobial, cytotoxicity and phytochemical screening of Jordanian plants used in traditional medicine.*Molecules*, **15**: 1811-24.

Tserennadmid R , Takó M, Galgóczy L, Papp T, Pesti M, Vágvölgyi C, Almássy K, and Krisch J. 2011. Anti yeast activities of some essential oils in growth medium, fruit juices and milk. *Int J Food Microbiol* , **144**: 480-86.

Turner J, Muraoka A, Bedenbaugh M, Childress B, Pernot L, Wiencek M, and Peterson YK. 2022. The chemical relationship among beta-lactam antibiotics and potential impacts on reactivity and decomposition. *Front Microbiol* **13**: 807955.

Wei S, Lyu J, Wei L, Xie B, Wei J, Zhang G, Li J, Gao CH, Xiao X, and Yu J. 2022. Chemometric approaches for the optimization of headspace-solid phase microextraction to analyze volatile compounds in coriander (Coriandrum sativum L.). *LWT*, **167**: 113842.

Zengin H and Baysal A. 2014. Antibacterial and antioxidant activity of essential oil terpenes against pathogenic and spoilage-forming bacteria and cell structure-activity relationships evaluated by SEM microscopy. *Molecules*, **19**: 17773-98.

Zygadlo J, Zunino M, Pizzolitto R, Merlo C, Omarini A, and Dambolena J. 2017. Antibacterial and anti-biofilm activities of essential oils and their components including modes of action.' in, **Essential oils and nanotechnology for treatment of microbial diseases,** CRC Press, United Kingdom.

JJBS

Volume 17, Number 4,December 2024
ISSN 1995-6673
Pages 593 – 599
https://doi.org/10.54319/jjbs/170402

Jordan Journal of Biological Sciences

Role of MicroRNA in Obesity and Its Hypertension Complication

Weaam Gouda[1,*], Soad M. Eweida[1], Habeba Magdy[2], Hatem A. El-Mezayen[2], Elsayed Mahdy[2], Mie Afify[1], W. I. Hamimy[3], Mohamed D. E. Abdelmaksoud[1]

[1]*Biochemistry Department, Biotechnology Research Institute, National Research Centre, Egypt;*[2]*Chemistry Department, Faculty of Science, Helwan University, Egyp;*[3]*Anesthesia Department, Obesity Surgery Unit, Faculty of Medicine, Cairo University, Egypt.*

Received: October 5, 2023; Revised: March 16, 2024; Accepted: May 1, 2024

Abstract

Background: Obesity is a major problem for world health and a leading factor in morbidity and mortality. Investigating microRNA (miRNA) profiling may aid in advancing research on obesity and related diseases. The aim of this study was to investigate the expression levels of miRNA-344 and miRNA-365 in obese patients with and without hypertension compared to normal weight healthy controls to assess the potential use of these miRNAs as early and effective diagnostic markers for obesity and could be used as predictive markers for hypertension-related obesity. We also determined the relationship between the above-mentioned miRNAs and different biochemical parameters.

Subjects and methods: We studied the expression of miRNA-344 and miRNA-365 in serum samples of 63 obese patients (29 obese patients with hypertension and 34 without hypertension) and 35 non-obese healthy individuals using quantitative real-time PCR.

Results: The expression of miRNA-365 was down-regulated in the sera of obese patients with or without hypertension compared to controls. Also, the present study found that miRNA-344 expression levels were related to obesity and its related hypertension. Furthermore, the correlation analysis showed that the lipid profile was related to miRNA 365 and 344 expression levels in hypertensive and obese patients.

Conclusion: The expressions of miRNA-365 and miRNA-344 were related to obesity and its hypertension complications, suggesting that those miRNAs and their target genes might be involved in the development of obesity and hypertension.

Keywords: microRNA (miRNA), miRNA-365, miRNA-344, obesity, hypertension complications.

1. Introduction

Obesity has received widespread recognition as the cause of an elevated risk for disease, which raises all-cause mortality and shortens life expectancy by between 3.3 and 18.7 years (Hu *et al*., 2004; Leung *et al*., 2015; GBD Risk Factors Collaborators, 2016; D'Agati *et al*., 2016; GBD Obesity Collaborators, 2017). In fact, obesity is becoming more and more prominent everywhere, and this trend represents a critical health concern because it is related to a number of comorbidities, such as the metabolic syndrome, which comprises dyslipidemia, hypertension, insulin resistance, and glucose intolerance (Ng *et al*., 2014). Consequently, obesity enhances the probability of developing type 2 diabetes, heart disease, chronic kidney disease, non-alcoholic fatty liver disease, and several cancers (D'Agati *et al*., 2016; Ghaben and Scherer, 2019). If the trend continues, overweight and obesity in the Irish population will affect 89% of men and 85% of women by 2030. This will raise the prevalence of diabetes by 21%, malignancies by 61%, and coronary heart disease and stroke by 97%, all of which are directly associated with obesity (Keaver *et al*., 2013). The adverse consequences of obesity are partially mediated by the elevated total cholesterol and blood pressure, which have been linked with it (Lim *et al*., 2012).

For optimal disease management and keeping obesity-related comorbidities under control, early detection of alterations associated with obesity is essential. More research is currently being done on microRNAs (miRNAs), a type of small non-coding RNA molecules with 20–25 nucleotides that regulate gene expression by binding to mRNA and inducing transcript splicing or translation suppression (Bartel, 2004). In particular, mature miRNAs, known as circulating miRNA that are produced inside cells and released from the cytoplasm into the circulation, are extremely stable and resistant to storage handling. The noninvasive availability of body fluids (serum, plasma, and urine) and the existence of disease-specific circulating miRNA patterns provide the diagnostic and prognostic value of circulating miRNAs (Cortez *et al*., 2011). It is interesting to note that patients with metabolic diseases and healthy individuals have different circulating miRNA profiles (Guay and Regazzi, 2013; Pescador *et al*., 2013; Ortega *et al*., 2014; Iacomino *et al*., 2016; Ji and Guo, 2019). Since metabolic syndrome can be acquired by a small percentage of obese people, abnormal miRNA expression may play a role in the development of metabolic disease. Furthermore, alterations in miRNA expression have been observed in obese phenotypes, and some miRNAs have been linked to metabolic diseases such as hypertension and insulin resistance (Huang *et al*., 2018; Suksangrat *et al*., 2019;

* Corresponding author. e-mail: weaamgoudaali@gmail.com.

Lischka *et al*., 2021). As a result, miRNA may have an added benefit in identifying patients at risk for developing future diseases. In this regard, literature records that some miRNAs are confirmedly dysregulated in human obesity, so further investigation is required to fully understand how these miRNAs are related to metabolic disorders and how they can be used to diagnose, prevent, and treat obesity (Ortiz-Dosal *et al*., 2019; Vonhögen *et al*., 2020; Wang *et al*., 2021).

It has been illustrated that the miRNAs 344 and 365 influence adipocyte differentiation and stimulate adipogenesis via diverse pathways (Cho *et al*., 2019). Based on previous research, the regulation of adipocyte differentiation may be impacted by miRNA-344, although its exact role is unidentified (Qin *et al*., 2010). Subsequently, a prior study has suggested the fundamental role and mechanism of miRNA-344 in the suppression of adipocyte differentiation by activating the transcription of the Wnt/β-catenin signaling pathway downstream genes that decrease the expression of adipogenic genes (Chen *et al*., 2014). MiRNA-365 is located on chromosome 16p13.12 and plays a role in a number of physiological functions (Zhu *et al*., 2018); thus, its expression and distribution vary throughout tissues and organs (Wu *et al*., 2021). MiRNA-365, a mechano-responsive miRNA, has been identified to possess an intense ability to induce inflammatory symptoms (Zhao *et al*., 2021) and to develop different obesity grades (Gouda *et al*., 2023). Furthermore, patients with left ventricular hypertrophy-associated hypertension had considerably higher serum expression of miRNA-365, and there was a strong correlation between its expression differences and blood pressure (Wu *et al*., 2021).

As a result, we aimed to evaluate circulating miRNAs 344 and 365 as biomarkers for the prediction and early detection of obesity and its related hypertension. Their prediction could explain the progress of obesity and its comorbidities. Also, our study aimed to correlate miRNA-344 and miRNA-365 expression levels in obese, hypertensive, and obese patients with lipid profiles.

2. Subjects and Methods

2.1. Subjects

A total of 63 obese patients with a BMI ≥ 30 kg/m^2 (34 without hypertension and 29 with hypertension) who underwent bariatric surgery for obesity from the Surgery Unit at Kasr Al Aini Hospital, Cairo, Egypt, were recruited in this study; their ages ranged between 25 and 60 years. Besides, 35 age- and sex-matched healthy adult volunteers with no medical history of obesity or its complications were included as controls. Prior to participating in the study, all subjects provided written informed consent. We excluded patients who met at least one of the following criteria: (1) patients with cardiovascular disease or cerebrovascular disease; (2) participants with secondary hypertension (HTN) or taking blood pressure-raising drugs; and (3) participants with diabetes, liver disease, kidney disease, and a past history of cancer.

2.2. Sampling

After a 12-hour fast, 5 mL of peripheral venous blood was obtained from all participants. After allowing blood to clot at room temperature (25 °C), sera were separated into two portions: the first for biochemical analysis and the second for adding to QIAZol in specially marked, sterile tubes for each individual subject and storing at − 80 °C until miRNA expression levels were determined.

2.3. Anthropometric measures

Body mass index (BMI) was assessed as weight in kilogrammes (kg) divided by height in metres squared (m^2). A standardised electronic sphygmomanometer (OMRON, model HEM-7130) was used to measure each participant's blood pressure on the right arm while they were seated. Before the measurements, the participants rested for at least five minutes in a seated position with their arms resting at the level of their hearts. To reduce random error and give a more reliable basis for blood pressure calculation, we measured each subject's blood pressure three times, each one separated by a 10-minute delay. We then calculated the mean value of these three measurements.

2.4. Biochemical analysis

Stanbio Laboratory, USA, provided the lipid profile kits (total cholesterol (TC), triglycerides (TG), and high-density lipoprotein cholesterol (HDL-c). According to Allain *et al*. (1974) and Fredrickson *et al*. (1967), serum TC and TG were measured using an enzymatic colorimetric method, HDL-c was determined using Finley *et al.'s* (1978) methodology, and low-density lipoprotein cholesterol (LDL-c) was calculated using Friedewald's *et al*. (1972) formula as TC-HDL-c-TG/5. According to Heinz and Beushausen (1981), a fasting plasma glucose test was conducted immediately using the Stanbio Laboratory (USA) kit. With the use of a kit purchased from Human Company (Germany), the serum's AST and ALT activities were assessed in accordance with Bermeyer and Horder (1980). Serum urea level was estimated using the Modified Urease-Berthlot Method (Kaplan, 1984). Creatinine serum level was determined by using Jaffe Colorimetric-Kinetic, according to Murray (1984).

2.5. MiRNA expression

According to the manufacturer's instructions, total RNA was extracted using the miRNeasy Mini isolation kit from QIAgen, Germany. The MicroRNA reverse transcription (RT) Kit (Applied Biosystems) and particular miRNA RT primers were used to reverse-transcribe miRNA-344 and miRNA-365 in accordance with the manufacturer's instructions. MiRNA-344 primers were (F): ACACTCCAGCTGGGTGATCTAGCCAAAGCCT; (R): GTGCGTGTCGTGGAGTCG; and miR-365 primers were (F): ATAGGATCCTGAGGTCCCTTTCGTG; (R): GCGAAGCTTAAAAACAGCGGAAGAGTTTGG.

Thermo Fisher Scientific Inc.'s NanoDrop 2000c spectrophotometer was used to measure the quantity and quality of RNA. All RNA samples were determined to be of sufficient quality for qPCR analysis (1.93-2.10) based on measurement of the A260/A280 ratios. A final volume of 20 μL was created by mixing 2 μL of RT products with 10 μL of SYBR green PCR master mix, 1 μL of miRNA assays, and additional nuclease-free water. On a real-time system (Applied Biosystems), all reactions were carried out under the following conditions: 95 °C for 10 min, then 40 cycles of 95 °C for 15 s and 60 °C for 60 s. Target miRNA relative expression was normalised to U6. Using

the equation $2^{-\Delta\Delta Ct}$, fold changes in candidate miRNA expression were calculated (Livak and Schmittgen, 2001).

2.6. Statistical analysis

The statistical package for the social sciences, SPSS, version 20 (SPSS Inc., Chicago, IL, USA), was used to analyse the data. Means and standard error were used to characterise quantitative variables. To compare groups, an analysis of variance (ANOVA) test was used. For skewed and normally distributed data, respectively, Spearman ranks and Pearson correlation coefficients were used to determine correlations between miRNA expression levels and biochemical parameters. Significant expression levels were graphically represented by boxplot graphs. When the difference between the groups was less than 0.05, it was considered statistically significant, and when it was < 0.01, it was highly significant.

3. Results

3.1. Anthropometric and clinical characteristics of the studied subjects

In the current study, 63 obese patients were enrolled: 23 males and 40 females, with a mean age of 43.15 ± 1.5 years. A control group consists of 35 healthy individuals, 20 males and 15 females, with a mean age of 40.3 ± 0.94 years (Table 1). BMI, total cholesterol, triglycerides, HDL-cholesterol, and LDL-cholesterol displayed a significant rise in obese groups with and without hypertension compared to controls (*P*-values <0.05).

3.2. The expressions of miRNAs 344 and 365 in obese patients with and without hypertension and controls

Calculated expression levels of miRNAs 344 and 365 revealed that miRNA-344 expression was significantly elevated in the sera of obese patients without hypertension compared to obese patients with hypertension and compared to controls, as its expression increased in the obese non-hypertensive group compared to the control group and then decreased again in the obese hypertensive group, while serum expression values of miRNA-365 were significantly decreased among both obese patients with and without hypertension compared to controls (Table 2 and Figure 1).

3.3. The correlations of circulating miRNAs 344 and 365 with BMI and lipid profile in obese subjects with or without hypertension

A correlation analysis was done to address the correlated variables to miRNA expression levels. The results showed that serum values of miRNA-344 were negatively correlated with TG in obese patients with and without hypertension (*r*=-0.835, *P*=0.000, and *r*=-0.352, *P*=0.026, respectively), but positively correlated to HDL-C in obese patients without hypertension (*r*=0.315, *P*=0.048), and also positively correlated to BMI, cholesterol, and LDL-C in obese patients with hypertension (*P*<0.05). On the other hand, miRNA-365 was positively correlated with BMI and TG in obese and obese hypertensive patients with *P* values less than 0.05, more so negatively correlated with LDL-C in obese patients without hypertension (*r=-0.312*, *P*=0.013), and positively correlated with HDL-C (*P*=0.038) in obese patients with hypertension (Tables 3 and 4).

Table 1. Anthropometric measurements and clinical data of obese hypertensive, obese patients and controls

Parameter	Obese Hypertensive (n=29)	Obese (n=34)	Control (n = 35)	*P-value*
Age (Years)	45.31±2	41.0±1.6	40.31±0.94	0.057
Sex, n (%)				
Male	13 (44%)	10 (29%)	20 (57%)	0.105
Female	16 (56%)	24 (71%)	15 (43%)	
Body mass index (kg/m^2)	37.56±2.2	37.27±0.98	21.15±0.43	<0.001
Fasting Glucose (mg/dL)	90±1.7	85.79±1.8	84.56±2.5	0.115
Total cholesterol (mg/dL)	175.38±6.7	180.21±9.4	145.71±1.9	<0.001
Triglycerides (mg/dL)	135.69±8.7	125.75±10.5	87.86±2.46	<0.001
HDL-cholesterol (mg/dL)	55.38±1.1	57.75±1.6	50.43±0.72	0.030
LDL- cholesterol (mg/dL)	92.86±7.7	97.31±9	77.71±0.73	<0.001
Urea (mg/dL)	22.875±0.76	23.51±0.64	24.03±0.45	0.418
Creatinine (mg/dL)	0.93±0.016	0.92±0.026	0.87±0.022	0.164
AST (IU/L)	25±0.55	23.71±0.85	23.17±0.53	0.2
ALT (IU/L)	24.25±0.68	23.92±0.65	24±0.55	0.945

Numeric variables are presented as mean ± SE.
P value for comparison between obese and control groups.
P values <0.05 are represented in bold font and considered statistically significant.
HDL: High density lipoprotein LDL: Low density lipoprotein
AST: Aspartate aminotransferase ALT: Alanine aminotransferase

Table 2. The expression of circulating miRNA 344 & miRNA 365 in obese with and without hypertension and control groups

MicroRNA	Obese Hypertensive (n=29)	Obese (n=34)	Control (n = 35)	*P-value*
	Mean ± SE	Mean ± SE	Mean ± SE	
miRNA 344	0.254±0.05[b]	0.695±0.14[a]	0.35±0.04	0.003
miRNA 365	0.53±0.3[a]	0.57±0.18[a]	1.18±0.1	0.019

P value <0.05 are represented in bold font and considered as statistically significant.
[a] Considered statistically significant from the control group.
[b] Considered statistically significant from the obese group.

Table 3. Correlation analysis of the circulating miRNAs 344 and 365 with BMI and lipid profile in obese patients without hypertension

		BMI	TC	TG	LDL-c	HDL-c
miRNA-344	*r*	0.169	-0.020	-0.352*	-0.172	0.315*
	P	0.430	0.349	0.026	0.422	0.048
miRNA-365	*r*	0.297*	0.364	0.297*	-0.312*	0.152
	P	0.018	0.080	0.018	0.013	0.479

Spearman rank correlation coefficients and Pearson correlation coefficients for skewed and normally distributed values, respectively.
The bold format represents the significant p values (*$P \leq 0.05$).
r: correlation coefficient; BMI: body mass index; TC: total cholesterol; TG: triglycerides; HDL-c: high density lipoprotein cholesterol; LDL-c: low density lipoprotein cholesterol.

Table 4.0Correlation analysis of the circulating miRNA-344 and miRNA-365 with BMI and lipid profile in obese patients with hypertension

		BMI	TC	TG	LDL-c	HDL-c
miRNA-344	*r*	0.627**	0.529*	-0.835**	0.676**	-0.129
	P	0.009	0.035	0.000	0.004	0.635
miRNA-365	*r*	0.663**	-0.263	0.585*	-0.025	0.522*
	P	0.005	0.325	0.017	0.927	0.038

The bold format represents the significant p values
Significant levels: *$P \leq 0.05$, ** $P \leq 0.01$. *r*: correlation coefficient

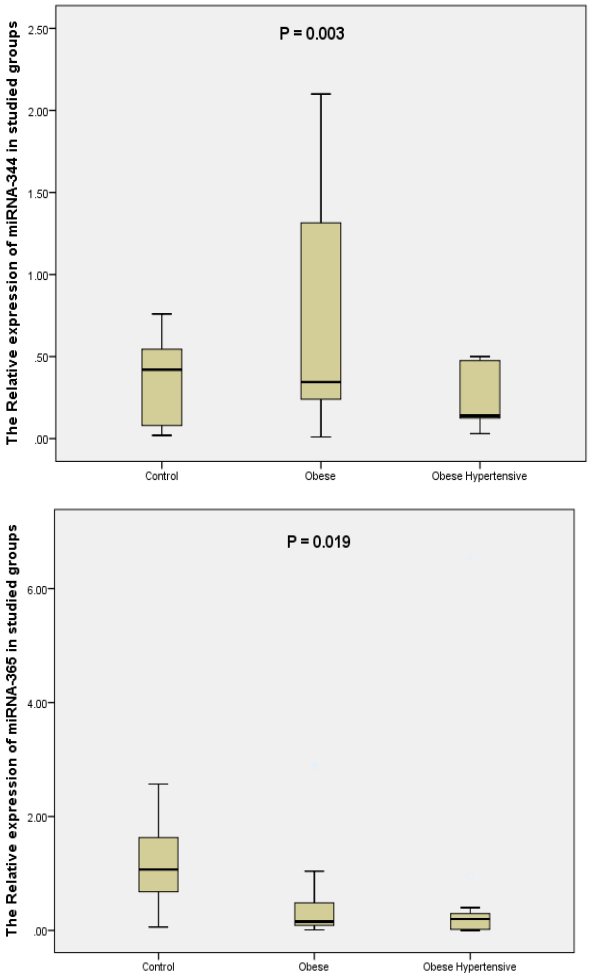

Figure 1. The relative miRNA-344 and miRNA-365 expressions in control, obese, and obese-hypertensive groups

Control group: healthy subjects with normal weight; Obese group: obese patients without hypertension; Obese Hypertensive group: obese patients with hypertension as an obesity complication.

4. Discussion

Over the last 20 years, obesity and obesity-related disorders have rapidly become a global public health concern. Recently, numerous miRNAs have been demonstrated to be important regulators of adipogenesis, more so miRNAs which are induced during adipogenesis and are down-regulated in blood samples from obese patients (Sun *et al*., 2011). MiRNA-344 and miRNA-365 have been reported to impair adipocyte differentiation (Price and Fernández-Hernando, 2016). Furthermore, Almeida and Calin (2016) have demonstrated that these miRNAs play a role in metabolic diseases and adipocyte differentiation. Based on the metabolic anomalies seen in obesity, the dysregulation of microRNA patterns, intracellular and/or extracellular, may be taken into consideration. More specifically, extracellular vesicles' altered miRNA patterns in obese patients have been thoroughly characterised, which raises the possibility that other miRNAs carried by extracellular vesicles may contribute to the development of cardiovascular problems (La Sala *et al*., 2021).

Our study investigated the expression levels of miRNA-344 and miRNA-365 in obese patients with and without hypertension and healthy controls to assess the potential of using these miRNAs as early and effective diagnostic markers for obesity and obesity-related hypertension and also to correlate these miRNAs with the lipid profiles of obese patients with and without hypertension. We found that miRNA-344 was differently expressed in the sera of obese patients compared to obese hypertensive patients and controls. Our results are in line with a recent study that revealed that miRNA-344 was up-regulated, even though not substantially, in the various obese categories based on BMI (Gouda *et al*., 2023). Moreover, the previous study by Qin *et al*. (2010) implicated that miRNA-344 had an elevated level during the process of adipogenesis as it might be involved in regulating adipocyte differentiation via the Wnt signalling pathway in a cell model. Conversely, Chen *et al.* (2014) demonstrated that miRNA 344 was significantly reduced in established culture conditions during adipogenesis and could inhibit pre-adipocyte differentiation. This could be explained by the phosphorylation of β-catenin in rats tissues, which allows it to accumulate in the cytoplasm and enter the nucleus, where it stimulates the transcription of β-catenin-dependent genes and activates the Wnt/-catenin signalling pathway by downregulating the expression of glycogen synthase kinase 3 beta (GSK3β), which results in a decrease in the expression of adipogenic genes, suggesting that miR-344 controls the process of adipocyte differentiation (Qin *et al*., 2010; Guo *et al*., 2020).

Our study showed that the expression of miRNA-365 was down-regulated in obese patients with or without hypertension compared to controls. However, till now, no research has examined the relationship between miRNA-365 and blood pressure in patients who are considered obese. Consistent with our finding regarding the expression levels of the above-mentioned miRNA in obese individuals, Gouda *et al*. (2023) showed that there was a notable decline in miRNA-365 expressions between obese patients of classes I and II compared to normal weight controls, while its expression was elevated in obese class III. Conversely to the current results concerning hypertension, according to the study of Wu *et al.* (2021), miRNA-365 serum expression was up-regulated in patients with left ventricular hypertrophy (LVH) accompanied by hypertension by targeting the S-phase kinase-associated protein 2, suggesting a clear correlation of miRNA-365 with hypertension and LVH-related blood pressure. More so, miRNA-365 has been reported to regulate the progression of the atherosclerosis process (Lin *et al*., 2016; *Surma et al*., 2020). Regarding the molecular biological assessment of the pathogenesis of hypertension, several studies have demonstrated a close relationship between the onset and progression of hypertension and miRNAs (Wu *et al*., 2017; Leimena and Qiu, 2018). According to findings from a 5-year longitudinal study, miRNAs in circulating blood vessels are linked to hypertension, suggesting that reduced serum expression levels of specific miRNAs are attributed to elevated blood pressure and new cases of hypertension (Nakamura and Sadoshima, 2018). Additionally, further investigation revealed notable differences in the expression levels of some miRNAs between healthy controls and patients with severe hypertension. Therefore, significant changes in the target genes independently regulated by these miRNAs were revealed, sparking more interest in the mechanisms expanding the variation in the expressions of circulating miRNAs (Shi *et al*., 2020), implying that miRNA expression could contribute an alternative perspective to the diagnosis and prognosis of hypertension and could be further investigated as a possible biomarker for the prediction of hypertension (Wu *et al*., 2021). Significant correlations with BMI further support the link between miR-365 and obesity and show that the biomarker is valid in obese patients without high blood pressure, which was not the case with miRNA-344. This is consistent with findings from other research looking for biomarkers associated with obesity. On the other hand, our results showed BMI correlations with miRNAs 344 and 365 in obese hypertensive patients. MiRNAs regulate lipid metabolism and also contribute to the occurrence of obesity and its complications (Kadamkode and Banerjee, 2014; Plaisance *et al*., 2014). In this regard, the correlation analysis in our study showed that miRNA-344 and miRNA-365 were correlated with lipid profiles in obese patients with and without hypertension. We demonstrate that in obese patients, miRNA-344 was positively connected with HDL, negatively associated with triglycerides, and also positively correlated with total cholesterol and LDL in obese hypertensive patients. However, miRNA-365 was associated with triglycerides and LDL, which are interconnected risk factors for metabolic illness. Excessive lipids, a low-grade systemic chronic inflammatory condition, and the accumulation of excessive visceral fat are all characteristics of obesity (Mirhafez *et al*., 2016). So, these mechanisms set off a chain of events that leads to salt retention, endothelial dysfunction, increased RAAS and sympathetic nervous system stimulation, poor control of barometric and chemoreflexes, and high blood pressure (Seravalle and Grassi, 2017; Vonhogen *et al*., 2020).

This is because the levels of many miRNAs are different in obese people compared to healthy controls, making them possible for non-invasive metabolic biomarkers (Heneghan *et al*., 2011; Ortega *et al*., 2013; Prats-Puig *et al*., 2013; Cui *et al*., 2018; Al-Rawaf, 2019; Ji and Guo, 2019). However, the first validation of circulating miRNA-344 and miRNA-365 as significantly expressed circulating serum miRNAs in obesity and its related hypertension added a novel marker to obesity miRNA signatures. The present study concludes that the expressions of miRNA-344 and miRNA-365 were altered in the sera of obese patients with or without hypertension compared to controls, suggesting that circulating miRNAs 344 and 365 have additive values as predictive markers for obesity and related hypertension. Future research can be directed towards extracting and validating their target genes that might be linked to the pathological development of obesity and hypertension complications.

5. Author Contributions

- Conceived and designed the study: Elsayed Mahdy, Mie Afify
- Diagnosis and selection of all participants in the study: Waleed Hamimy

- Contributed reagents, materials, and analysis tools: Mohamed D.E. Abdelmaksoud, Hatem A. El-Mezayen and Habeba Magdy
- Weaam Gouda contributed to the analysis of the results.
- Weaam Gouda and Soad M. Eweida contributed to the writing of the manuscript.
- All authors provided critical feedback, helped shape the research, analysis, and approved the final version of the manuscript.

Funding

This research was funded by the National Research Centre [Project no. 12060170].

Ethical approval

The study was approved by the ethical committee of the National Research Centre, Egypt (Registration number 19-162).

Acknowledgments

The authors would like to thank all participants in this work.

Conflicts of Interest

The authors declare no conflict of interest.

References:

Allain CC, Poon LS, Chan CS, Richmond W and Fu PC. 1974. Enzymatic determination of total serum cholesterol. *Clin Chem.*, **20**: 470-475.

Almeida MI and Calin GA. 2016. The miR-143/miR-145 cluster and the tumor microenvironment: unexpected roles. *Genome Med.*, **8(1)**: 29.

Al-Rawaf HA. 2019. Circulating microRNAs and adipokines as markers of metabolic syndrome in adolescents with obesity. *Clinical nutrition.*, **38(5)**: 2231-2238.

Bartel DP. 2004. MicroRNAs: genomics, biogenesis, mechanism, and function. *Cell.*, **116(2)**: 281-297.

Bergmeyer HU and Hørder M. 1980. International federation of clinical chemistry. Scientific committee. Expert panel on enzymes. IFCC document stage 2, draft 1; 1979-11-19 with a view to an IFCC recommendation. IFCC methods for the measurement of catalytic concentration of enzymes. Part 3. IFCC method for alanine aminotransferase. *J Clin Chem Clin Biochem.*, **18**: 521-534.

Chen H, Wang S, Chen L, Chen Y, Wu M, Zhang Y, Yu K, Huang Z, Qin L and Mo D. 2014. MicroRNA-344 inhibits 3T3-L1 cell differentiation via targeting GSK3 beta of Wnt/beta-catenin signaling pathway. *FebsLett.*, **588(3)**: 429-435.

Cho YK, Son Y, Kim SN, Song HD, Kim M, Park JH, Jung YS, Ahn SY, Saha A, Granneman JG and Lee YH. 2019. MicroRNA-10a-5p regulates macrophage polarization and promotes therapeutic adipose tissue remodeling. *Mol Metab.*, **29**:86-98.

Cortez MA, Bueso-Ramos C, Ferdin J, Lopez-Berestein G, Sood AK and Calin GA. 2011. MicroRNAs in body fluids-the mix of hormones and biomarkers. *Nat Rev Clin Oncol.*, **8(8)**: 467-477.

Cui X, You L, Zhu L, Wang X, Zhou Y, Li Y, Wen J, Xia Y, Wang X, Ji C and Guo X. 2018. Change in circulating microRNA profile of obese children indicates future risk of adult diabetes. *Metab Clin Exp.*, **78**: 95-105.

D'Agati VD, Chagnac A, de Vries AP, Levi M, Porrini E, Herman-Edelstein M and Praga M. 2016. Obesity-related glomerulopathy: clinical and pathologic characteristics and pathogenesis. *Nat Rev Nephrol.*, **12(8)**: 453-471.

Finley PR, Schifman RB, Williams RJ and Lichti DA. 1978. Cholesterol in high-density lipoprotein: use of Mg2+/dextran sulfate in its enzymic measurement. *Clin Chem.*, **24**: 931-933.

Fredrickson DS, Levy RI and Lees RS. 1967. Fat transport in lipoproteins–an integrated approach to mechanisms and disorders. *N Engl J Med.*, **276**:273-281.

Friedewald WT, Levy RI and Fredrickson DS. 1972. Estimation of the concentration of low density lipoprotein cholesterol in plasma, without use of the preparative ultracentrifuge. *Clin Chem.*, **18**: 499-502.

GBD 2015 Obesity Collaborators. 2017. Health effects of overweight and obesity in 195 countries over 25 years. *N Engl J Med.*, **377(1)**: 13-27.

GBD 2015 Risk Factors Collaborators. 2016. Global, regional, and national comparative risk assessment of 79 behavioural, environmental and occupational, and metabolic risks or clusters of risks, 1990–2015: a systematic analysis for the Global Burden of Disease Study 2015. *Lancet.*, **388(10053)**: 1659-1724.

Ghaben AL and Scherer PE. 2019. Adipogenesis and metabolic health. *Nat Rev Mol Cell Biol.*, **20(4)**: 242-258.

Gouda W, Ahmed AE, Mageed L, Hassan AK, Afify M, Hamimy WI, Ragab HM, Maksoud NAE, Allayeh AK and Abdelmaksoud MDE. 2023. Significant role of some miRNAs as biomarkers for the degree of obesity. *J Genet Eng Biotechnol.*, **21(1)**:109.

Guay C and Regazzi R. 2013. Circulating microRNAs as novel biomarkers for diabetes mellitus. *Nat Rev Endocrinol.*, **9(9)**: 513-521.

Guo J, Zhu Z, Zhang D, Chen B, Zou B, Gao S and Zhu X. 2020. Analysis of the differential expression profile of miRNAs in myocardial tissues of rats with burn injury. *Biosci Biotechnol Biochem.*, **84(12)**: 2521-2528.

Heinz F and Beushausen TW. 1981. A new enzymatic method for the determination of glucose. *J Clin Chem Clin Biochem.*, **19**: 977-978.

Heneghan HM, Miller N, McAnena OJ, O'Brien T and Kerin MJ. 2011. Differential miRNA expression in omental adipose tissue and in the circulation of obese patients identifies novel metabolic biomarkers. *J Clin Endocrinol Metabol.*, **96(5)**: E846-E850.

Hu G, Qiao Q, Tuomilehto J, Balkau B, Borch-Johnsen K and Pyorala K. 2004. Prevalence of the metabolic syndrome and its relation to all-cause and cardiovascular mortality in nondiabetic European men and women. *Arch Intern Med.*, **164(10)**: 1066-1076.

Huang Y, Yan Y, Xv W, Qian G, Li C, Zou H and Li Y. 2018. A new insight into the roles of MiRNAs in metabolic syndrome. *Biomed Res Int.*, **2018**:7372636.

Iacomino G, Russo P, Stillitano I, Lauria F, Marena P, Ahrens W, De Luca P and Siani A. 2016. Circulating microRNAs are deregulated in overweight/obese children: preliminary results of the I. Family study. *Genes Nutr.*, **11**: 7.

Ji C and Guo X. 2019. The clinical potential of circulating microRNAs in obesity. *Nat Rev Endocrinol.*, **15(12)**: 731-743.

Kadamkode V and Banerjee G. 2014. Micro RNA: An Epigenetic Regulator of Type 2 Diabetes. *Microrna.*, **3(2)**:86-97.

Kaplan A. 1984. Urea. The C.V. Mosby Co. St Louis. Toronto. Princeton. *Clin Chem.*, **1984**: 1257-1260 and 437 and 418.

Keaver L, Webber L, Dee A, Shiely F, Marsh T, Balanda K and Perry IJ. 2013. Application of the UK foresight obesity model in Ireland: the health and economic consequences of projected obesity trends in Ireland. *PloS One.*, **8(11)**: e79827.

La Sala L, Crestani M, Garavelli S, de Candia P and Pontiroli A. 2021. Does microRNA Perturbation Control the Mechanisms Linking Obesity and Diabetes? Implications for Cardiovascular Risk. *Int J Mol Sci.,* **22**: 143.

Leimena C and Qiu H. 2018. Non-Coding RNA in the Pathogenesis, Progression and Treatment of Hypertension. *Int J Mol Sci.,* **19(4)**: 927.

Leung MY, Pollack LM, Colditz GA and Chang SH. 2015. Life years lost and lifetime health care expenditures associated with diabetes in the U.S. National Health Interview Survey 1997-2000. *Diabetes Care.,* **38(3)**: 460-468.

Lim SS, Vos T, Flaxman AD, Danaei G, Shibuya K, Adair-Rohani H, Amann M, Anderson HR, Andrews KG, Aryee M, Atkinson C, Bacchus LJ, Bahalim AN, Balakrishnan K, Balmes J, Barker-Collo S and et al. 2012. A comparative risk assessment of burden of disease and injury attributable to 67 risk factors and risk factor clusters in 21 regions, 1990–2010: a systematic analysis for the Global Burden of Disease Study 2010. *Lancet.,* **380(9859)**: 2224-2260.

Lin B, Feng DG, Wang F, Wang JX, Xu CG, Zhao H and Cheng ZY. 2016. MiR-365 participates in coronary atherosclerosis through regulating IL-6. *Eur Rev Med Pharmacol Sci.,* **20(24)**: 5186-5192.

Lischka J, Andrea Schanzer A, Hojreh A, Ba-Ssalamah, de Gier AC, Valent I, Item CB, Greber-Platzer S and Zeyda M. 2021. Circulating microRNAs 34a, 122, and 192 are linked to obesity associated inflammation and metabolic disease in pediatric patients. *Int J Obes.,* **45**:1763-1772.

Livak K and Schmittgen T. 2001. Analysis of relative gene expression data using real-time quantitative PCR and the 2 (–delta delta C (T)) methods. *Methods.,* **25**: 402-408.

Mirhafez SR, Ebrahimi M, Saberi Karimian M, Avan A, Tayefi M, Heidari-Bakavoli A, Parizadeh MR, Moohebati M, Azarpazhooh MR, Esmaily H, Nematy M, Safarian M, Ferns GA and Ghayour-Mobarhan M. 2016. Serum high-sensitivity C-reactive protein as a biomarker in patients with metabolic syndrome: evidence-based study with 7284 subjects. *Eur J Clin Nutr.,* **70(11)**: 1298-1304.

Murray RL. 1984. Creatinine In: Kaplan LA, Pesce AJ. (Eds.). The C.V. Mosby Co. St Louis. Toronto. Princeton. *Clin Chem.,* **1984**: 1261-1266 and 418.

Nakamura M and Sadoshima J. 2018. Mechanisms of physiological and pathological cardiac hypertrophy. *Nat Rev Cardiol.,* **15(7)**: 387-407.

Ng M, Fleming T and Gakidou E. 2014. Global, regional, and national prevalence of overweight and obesity in children and adults during 1980-2013: a systematic analysis for the Global Burden of Disease Study 2013. *Lancet.,* **384(9945)**: 766-781.

Ortega FJ, Mercader JM, Catalán V, Moreno-Navarrete JM, Pueyo N, Sabater M, Gómez-Ambrosi J, Anglada R, Fernández-Formoso JA, Ricart W, Frühbeck G and Fernández-Real JM. 2013. Targeting the circulating microRNA signature of obesity. *Clin Chem.,* **59(5)**: 781-792.

Ortega FJ, Mercader JM, Moreno-Navarrete JM, Rovira O, Guerra E, Esteve E, Xifra G, Martínez C, Ricart W, Rieusset J, Rome S, Karczewska-Kupczewska M, Straczkowski M and Fernández-Real JM. 2014. Profiling of circulating MicroRNAs reveals common MicroRNAs linked to type 2 diabetes that change with insulin sensitization. *Diabetes Care.,* **37(5)**: 1375–1383.

Ortiz-Dosal A, Rodil-García P and Salazar-Olivo LA. 2019. Circulating microRNAs in human obesity: a systematic review. *Biomarkers.,* **24(6)**: 499-509.

Pescador N, Pérez-Barba M, Ibarra JM, Corbatón A, Martínez-Larrad MT and Serrano-Ríos M. 2013. Serum circulating microRNA profiling for identification of potential type 2 diabetes and obesity biomarkers. *PloS One.,* **8(10)**: e77251.

Plaisance V, Waeber G, Regazzi R and Abderrahmani A. 2014. Role of microRNAs in islet beta-cell compensation and failure during diabetes. *J Diabetes Res.,* **2014**: 618652.

Prats-Puig A, Ortega FJ, Mercader JM, Moreno-Navarrete JM, Moreno M, Bonet N, Ricart W, López-Bermejo A and Fernández-Real JM. 2013. Changes in circulating microRNAs are associated with childhood obesity. *J Clin Endocrinol Metabol.,* **98(10)**: E1655-E1660.

Price NL and Fernández-Hernando C. 2016. miRNA regulation of white and brown adipose tissue differentiation and function. *Biochim Biophys Acta.,* **1861(12 Pt B)**: 2104-2110.

Qin L, Chen Y, Niu Y, Chen W, Wang Q, Xiao S, Li A, Xie Y, Li J, Zhao X, He Z and Mo D. 2010. A deep investigation into the adipogenesis mechanism: Profile of microRNAs regulating adipogenesis by modulating the canonical Wnt/beta-catenin signaling pathway. *BMC Genomics.,* **11**: 320.

Seravalle G and Grassi G. 2017. Obesity and hypertension. *Pharmacol Res.,* **122**: 1-7.

Shi Y, Xi D, Zhang X, Huang Z, Tang N, Liu Y, Wang L, Tang Y, Zhong H and He F. 2020. Screening and validation of differentially expressed microRNAs and target genes in hypertensive mice induced by cytomegalovirus infection. *Biosci Rep.,* **40(12)**: BSR20202387.

Suksangrat T, Phannasil P and Jitrapakdee S. 2019. miRNA regulation of glucose and lipid metabolism in relation to diabetes and nonalcoholic fatty liver disease. *Adv Exp Med Biol.,* **1134**: 129-148.

Sun L, Xie H, Mori MA, Alexander R, Yuan B, Hattangadi SM, Liu Q, Kahn CR and Lodish HF. 2011. Mir193b-365 is essential for brown fat differentiation. *Nat Cell Biol.,* **13**: 958-965.

Surma S, Czober T, Lepich T, Sierka O and Bajor G. 2020. Selected biomarkers of atherosclerosis: clinical aspects. *Acta Angiol.,* **26(1)**: 28-39.

Vonhögen IGC, Mohseni Z, Winkens B, Xiao K, Thum T, Calore M, da Costa Martins PA, de Windt LJ, Spaanderman MEA and Ghossein-Doha C. 2020. Circulating miR-216a as a biomarker of metabolic alterations and obesity in women. *Noncoding RNA Res.,* **5(3)**:144-152.

Wang L, Shang C, Pan H, Yang H, Zhu H and Gong F. 2021. MicroRNA Expression Profiles in the Subcutaneous Adipose Tissues of Morbidly Obese Chinese Women. *Obes Facts.,* **14(1)**: 1-15.

Wu H, Wang Y, Wang X, Li R and Yin D. 2017. MicroRNA-365 accelerates cardiac hypertrophy by inhibiting autophagy via the modulation of Skp2 expression. *Biochem Biophys Res Commun.,* **484(2)**: 304-310.

Wu HB, Yang CS, Wang YC, Xie YT, Wang XC, Liu HL and Du RP. 2021. The Expression of miR-365 in Serum of Hypertension Patients with Left Ventricular Hypertrophy Was Up-Regulated, Which Was Positively Correlated with Left Ventricular Mass Index. *Pharmgenomics Pers Med.,* **14**: 905-913.

Zhao P, Li X, Li Y, Zhu J, Sun Y and Hong J. 2021. Mechanism of miR-365 in regulating BDNF-TrkB signal axis of HFD/STZ induced diabetic nephropathy fibrosis and renal function. *Int Urol Nephrol.,* **53(10)**: 2177-2187.

Zhu Y, Wen X and Zhao P. 2018. MicroRNA-365 inhibits cell growth and promotes apoptosis in melanoma by targeting BCL2 and cyclin D1 (CCND1). *Med Sci Monit.,* **24**: 3679-3692.

JJBS

Volume 17, Number 4,December 2024
ISSN 1995-6673
Pages 601 – 611
https://doi.org/10.54319/jjbs/170403

Jordan Journal of Biological Sciences

Genetic Differentiation Among Wheat Genotypes Using SDS-PAGE and Molecular Markers

Samira A. Osman*, Samy A.A. Heiba, Hamdy M.H. Abd Elrahman, Rania T. Ali

Genetics and Cytology Department, Biotechnology Research Institute, National Research Centre, Giza, Egypt.

Received: January 21, 2024; Revised: April 9, 2024; Accepted: May 1, 2024

Abstract

Wheat is the most strategic cereal crop worldwide. Studies on the genetic similarities among wheat genotypes are very helpful in the selection of high-quality parents with desirable traits. This study was performed for the discrimination among thirteen wheat genotypes using water-soluble protein, nine Random amplified polymorphic DNA (RAPD) and five Inter simple sequence repeat (ISSR) primers. The maximum genetic similarity percentage was documented between Shandweel1 and Sids12 (96.8%), while the minimum genetic similarity was found between Misr 1 and Sakha 93 (67.7%) based on water-soluble protein profile. On the other hand, the highest percentage of similarty was reported between Sakha 93 and line 18 (95%), while the lowest similarity percentage was found between Gemmeiza 10 and Sids 12 (1.9%), depending on RAPD-PCR. Besides, the highest similarity percentage was recorded between Sakha 93 and Sakha 94 (98.5%), and the least relationship was found between Gemmeiza 9 and sids 12 (66%) based on ISSR-PCR results. RAPD-PCR gave the highest polymorphism (62.35%), followed by ISSR-PCR (54.05%). Finally, SDS-PAGE scored the least polymorphism (35.48%). Despite that, protein analysis provided us with insufficient results, yet it provided us with useful information on the relationships among closely related genotypes and detected the unique band of 13 kDa in the genotype Sids12. Therefore, RAPD and ISSR assays are considered powerful markers for the differentiation among studied wheat genotypes compared with SDS-PAGE.

Keywords: Wheat, Genetic diversity, Biochemical marker, RAPD and ISSR.

1. Introduction:

Triticum aestivum L. (hexaploid wheat, AABBDD, (2n= 6X= 42)) is the most strategic cereal crop worldwide. Wheat grains are rich in proteins (albumins, globulins, prolamins, and glutelins) and carbohydrates, which are used for assessing bread quality (Cooke and Law, 1998; Izadi–Darbandi *et al*., 2010). Developed countries are goals to cultivate wheat crop to afford their population's consumption and trade the excess to developing countries for hard currency. Production of high-quality species is in great need to keep the lead in markets. Studies on the genetic similarities amongst genotypes are very helpful in the selection of high quality parents with desirable traits to breed on a large scale under various agro-climatic conditions and stresses (Qadir *et al*., 2017).

Genetic diversity means the existence of the anchored inherited variation among different varieties within the same species (Salgotra and Chauhan, 2023). Numerous factors influence genetic diversity of plants such as evolutionary factors, mutation, migration, and genetic drift may cause constant changes in allelic frequency. Hence, some morphological, cytological, biochemical, and molecular markers are used for assessing genetic diversity.

Protein banding patterns using the SDS-PAGE technique could be used to analyze the variability of proteins for detecting the phylogenetic relationships and genetic diversity of adapted plant cultivars, improving the productivity of plant breeding programs, and evaluating the genetic diversity among different plant genotypes (Jha and Ohri, 1996; Iqbal *et al*., 2005).

Several molecular markers based on DNA investigation such as RAPD, ISSR, and SSR were utilized to discriminate among different plant genotypes (Gowayed and Abd El-Moneim, 2021; Shaban *et al*., 2022; Abouseada *et al*., 2023). Molecular markers are classified into numerous groups depending on the mode of gene action: co-dominant markers such as SSRs or dominant markers such as RAPD and ISSRs (Souframanien and Gopalakrishna, 2004).

Randomly amplified polymorphic DNA (RAPD) has been widely utilized for determining the genetic difference in *Triticum* because this method is fast, easy to achieve, and inexpensive (Shukre *et al*., 2015). In addition, inter-simple sequence repeats ISSR markers have been performed for resolving intra- and inter-genomic relationships for discrimination of different plant specimens (Khurana-Kaul *et al*., 2012; Velasco-Ramirez *et al*., 2014). ISSR markers are considered reproducible

* Corresponding author. e-mail: s_nrc82@yahoo.com.

** **List of abbreviations**: SDS-PAGE: Sodium dodecyl sulfate polyacrylamide gel electrophoresis; UPGMA:Unweighted Pair-group Arithmetic ; M: Monomorphic bands; P: Polymorphic bands; kDa: kiloDalton; DNA; deoxyribonucleic acid; PCR: Polymerase chain reaction; RAPD: Random Amplified Polymorphic; DNA ; ISSRs:Inter Simple Sequence Repeats

fingerprinting for assessing genetic variability among wheat genotypes (Najaphy *et al*., 2012; Osman and Ramadan, 2020).

The present study is carried out to detect the genetic relationships among thirteen Egyptian bread wheat genotypes using biochemical marker (SDS-PAGE) and two different molecular markers (RAPD and ISSR).

2. Materials and Methods

2.1. Plant Materials

Thirteen hexaploid wheat genotypes (*Triticum aestivum* L.) 2n = 6X = 42, were kindly obtained from the Agricultural Research Center, Ministry of Agriculture, Giza, Egypt as listed in Table (1).

Table 1. The Pedigree and year of release for studied thirteen hexaploid wheat genotypes.

Ser. No.	genotypes	genotype	Pedigree	Source	year
1	Sakha94	Cultivar	Opata/ Rayon//Kauz CMBW90Y31800-TOPM-3Y-010M-010Y-1OM-015Y-0Y-0AP-OS	Egypt	2004
2	Sakha93	Cultivar	Sakha 92TR810328 S 88711-S-2S-1S-0S	Egypt	1999
3	Gemmeiza10	Cultivar	Maya74"S"/On//11603/147-/Bb/4/Chat"S"/5/ctow	Egypt	2004
4	Misr2	Cultivar	SKAUZ/BAV92 CMSS96M03611S-1M-010SY-010M-010SY-8M-0Y-OS	Egypt	2011
5	Sids1	Cultivar	HD 2172/Pavon"S"//1158.57/Maya 74"S"	Egypt	1996
6	Sids12	Cultivar	BUC//7C/ALD/5/MAYA74/ON//1160.1473//BB/GLL/4/CHAT"S"/6/MAYA /VUL//CMMH74A.6304/*SX SD70964-SD-1SD-1SD-0SD	Egypt	2007
7	Giza168	Cultivar	MIL/BUC//Seri CM930468-M-0Y-0M-2Y-0B	Egypt	1999
8	Misr1	Cultivar	OASIS/SKAUZ//4*BCN/3/2*PASTOR CMSS00Y01881T-050M-030Y-030M-030WGY-33M-0Y-0S	Egypt	2010
9	Shandweel1	Cultivar	Site/MO/4/Nac/Th.Ac//3*Pvn/3/Mirlo/Buc CMSS93B00567S-72Y-010M-010Y-010M-3Y-0M-0THY-0SH	Egypt	2011
10	Line12 (Hatcher)	Line	Yuma'PI372129//TAM 200/3/4*Yuma/4/KS91H184/Vista	Colorado, USA	--
11	Line18 (Kofa)	Line	Selection from composite cross *T. dicoccon* alpha-85 5-1	Colorado, USA	--
12	Line20 (Lovrin 34)	Line	Ranin aja 12/Nadodores 63//Lovrin12	Romania	--
13	Gemmeiza9	Cultivar	Ald"S"/Huac"S"//CMH74A.630/5X CGM4583-GM-1GM-0GM.	Egypt	1999

2.2. Protein banding patterns via SDS-PAGE technique:

Sodium dodecyl sulfate-polyacrylamide gel electrophoresis (SDS-PAGE) was performed according to the method of Laemmli (1970) as modified by Studier (1973). After that, the electrophoresis gel was stained with Coomassie Brilliant Blue dye, and then destained to visualize the protein bands. The images were transferred to the analyzer program (Total Lab program) to detect the molecular weight of each band among the examined genotypes. Data was imported into the SPSS program to determine the similarity matrix and dendrogram (UPGMA, using Jaccard's coefficient), which reflect the relationships among the studied genotypes.

2.3. DNA extraction

Young leaves of randomly selected samples of each genotype (0.1 gm) were used for genomic DNA extraction using (bio-basic kits). The extracted plant genomic DNA was quantified via a NanoDrop 1000 spectrophotometer (Thermo Scientific). 50ng/µl was then used as a DNA template for PCR reaction.

2.3.1. RAPD-PCR amplification

Nine RAPD primers were utilized for RAPD amplification (Table 2). The amplification was performed in 25µl reaction mixture, which contained 2 µl of genomic DNA (50 ng/ µl), 3µl primer (10 *p*mol), 10X *Taq* DNA polymerase reaction buffer (2.5µl), *Taq* DNA polymerase (1.5 units) and dNTPs (200 mm). Thermocycler (PTC-100 PCR version 9.0-USA) was adjusted for PCR amplification using the following program: 94°C for 5 min (Initial denaturation, one cycle), followed by 35 cycles of 94°C for 30 s,42°C for 90 sec., 72°C for 90 Sec, and final extension at 72°C for 2 min.

Table 2. Code and sequences of nine RAPD primers.

Primer code	Sequence (5`→3`)
OPA-02	CAGGCCCTTC
OPA-04	AATCGGGCTG
OPA-07	GAAACGGGTG
OPB-07	GGTGACGCAG
OPB-10	CTGCTGGGAC
OPO-10	TCAGAGCGCC
OPO-13	GTCAGAGTCC
OPO-14	AGCATGGCTC
OPO-19	CAATCGCCGT

2.3.2. ISSR-PCR amplification

PCR reactions were carried out by using ISSR primers (Table 3) according to Zietkiewciz *et al*. (1994). The reaction mixture was standardized to 20 µl (2.5 mM PCR buffer 1X, $MgCl_2$, 1 mM dNTPs, Primer 10 *p*mol, 1 unit *Taq* polymerase, genomic DNA (50 ng/ µl). The following PCR program was used in a DNA Thermocycler (PTC-100 PCR version 9.0-USA). Initial denaturation at 94°C for 5 min (one cycle), followed by 38 cycles of 94°C for 30 sec, 56 °C for 1 min annealing, 72°C for 2 min, and a final extension at 72 °C for 10 min (one cycle) then hold at 4°C.

Table 3. Code and sequences of five ISSR primers.

Primer code	Sequence (5`→3`)
A12	$(GA)_6CC$
UBC-811	$(GA)_8$ AC
UBC-817	$(CA)_8A$
UBC-814	$(CT)_8A$
UBC-815	$(CT)_8G$

2.3.3. Gel electrophoresis

100 bp DNA ladder (Ferments Life Sciences) and PCR products of RAPD and ISSR were separated on 1% and 1.5% (w/v) agarose gels (staining with ethidium bromide), respectively in 1X TAE buffer (Sambrook *et al.,* 1989). A gel documentation system (Biometra - Bio Documentations) was used for visualizing PCR products by UV-transilluminator and photographed and detecting the polymorphism among the studied bread wheat genotypes.

2.3.4. Data analysis

The amplified bands of RAPD and ISSR were scored as (1) for presence and (0) for absence for each of the thirteen wheat samples according to the gel analyzer program to detect positive and negative markers. The similarity coefficients were generated by the SPSS program version 10 (Nie *et al.,* 1975) to construct a dendrogram by the unweighted pair group method with arithmetical average (UPGMA).

3. Results

3.1. Identification of wheat genotypes by SDS-PAGE:

Obvious differences in protein banding patterns via the SDS-PAGE technique appeared in the protein profiles of thirteen wheat genotypes, as shown in Figure (1) and Table (4). The electrophoresis was estimated based on the molecular weights (MWs) of each band, which were represented with a unit of kilo Daltons (kDa). The total number of bands was 31 bands, of which twenty were monomorphic and eleven were polymorphic (35.48% polymorphism), including one -ve unique band of MW 13 kDa, which disappeared in Sids12 cultivar. The highest number of bands (31 bands) was exhibited in Sids12 cultivar, while Sakha93 exhibited the least number of bands (26 bands).

After the analysis of the obtained image of protein profiles via Jaccard coefficient similarity index, the genetic similarity index and dendrogram tree of the studied thirteen wheat genotypes were achieved, as shown in Table (5) and Figure (2). The similarity values showed substantial differences among the studied wheat genotypes. For instance, the similarity of soluble protein profiles ranged from 67.7% to 98.6%, with an average of 83.85%. The highest similarity was recorded between Shandweel1 and Sids12 (96.8%) while the least genetic similarity was recorded between Misr1 and Sakha93 (67.7%).

Dendrogram represents the genetic relationships among the thirteen wheat genotypes using UPGMA cluster analysis generated from protein marker, which ended to 4 subgroups and five solitary genotypes. The four subgroups are: (line 12& Gemmeiza 10 with a similarity coefficient 93.1%), (Giza 168& Sids 1 with similarity coefficient 96.6%), (line 20& Misr 2 with a similarity coefficient 93.1%) and (Shandaweel1& Sids 12 with a similarity coefficient 96.8%).

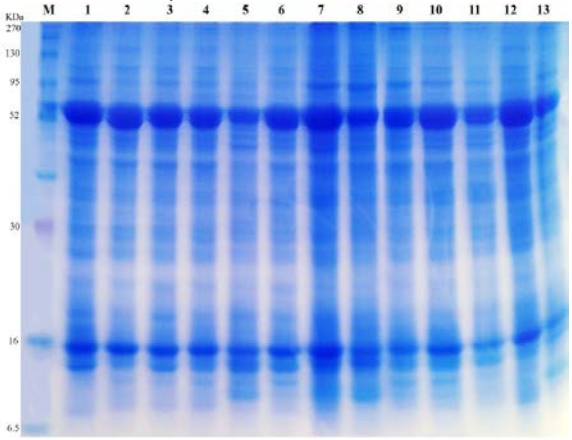

Figure 1. Water soluble proteins banding patterns for thirteen wheat genotypes.

Lane M: Protein marker (270-6.5KDa).

Lane 1: Sakha94. Lane 2: Sakha93. Lane 3: Gemmeiza10. Lane 4: Misr2. Lane 5: Sids1. Lane 6: Sids12. Lane 7: -Giza168. Lane 8: Misr1. Lane 9: Shandweel1. Lane 10: Line12 (Hatcher). Lane 11: Line18 (Kofa). Lane 12: Line20 (Lovrin 34). Lane 13: Gemmeiza9.

Table 4. Banding patterns of water soluble proteins for thirteen wheat genotypes.

Genotype		1	2	3	4	5	6	7	8	9	10	11	12	13
No	MW													
1	253	+	+	+	+	+	+	+	+	+	+	+	+	+
2	209	+	+	+	+	-	+	-	-	+	+	-	+	-
3	135	+	+	+	+	+	+	+	+	+	+	+	+	+
4	125	-	-	-	+	+	+	+	+	+	-	-	+	+
5	115	+	+	+	+	+	+	+	+	+	+	+	+	+
6	108	+	+	+	+	+	+	+	+	+	+	+	+	+
7	95	+	+	+	+	+	+	+	+	+	+	+	+	+
8	82	+	-	-	+	+	+	+	+	+	+	+	+	+
9	56	+++	+++	+++	+++	+++	+++	+++	+++	+++	+++	+++	+++	+++
10	46	+	+	+	+	+	+	+	+	+	+	+	+	+
11	43	+	+	+	+	+	+	+	+	+	+	+	+	+
12	41	+	+	+	+	+	+	+	+	+	+	+	+	+
13	40	-	+	+	-	-	+	-	+	-	+	-	-	-
14	38	++	++	++	++	++	++	++	++	++	++	++	++	++
15	36	+	+	+	+	+	+	+	+	+	+	+	+	+
16	35	+	+	+	+	+	+	+	+	+	+	+	+	+
17	34	+	+	+	+	+	+	+	+	+	+	+	+	+
18	31	+	+	+	+	+	+	+	+	+	+	+	+	+
19	29	+	+	+	+	+	+	+	+	+	+	+	+	+
20	28	+	+	+	+	+	+	+	+	+	+	+	+	+
21	25	+	+	+	+	+	+	+	+	+	+	+	+	+
22	21	+	+	+	+	+	+	+	+	+	+	+	+	+
23	20	+	-	+	+	+	+	+	+	+	+	-	+	+
24	18	+	+	+	+	+	+	+	+	+	+	+	+	+
25	17	+	-	+	+	+	+	+	+	+	+	-	-	+
26	15	++	++	++	++	++	++	++	++	++	++	++	++	++
27	14	-	-	-	-	+	+	+	+	+	-	-	-	-
28	13	+	+	+	+	+	+	+	-	+	+	+	+	+
29	12	-	+	+	+	+	+	+	-	+	+	+	+	-
30	10	-	-	-	-	+	+	+	+	+	+	+	+	+
31	9	+	+	+	+	-	+	+	-	+	+	+	+	+
Total bands		26	25	27	28	28	31	29	27	30	29	26	28	27

Lane 1-Sakha94. Lane 2-Sakha93. Lane 3- Gemmeiza 10. Lane 4-Misr2. Lane 5-Sids1. Lane 6-Sids12. Lane 7-Giza168. Lane 8-Misr1. Lane 9-Shandweel1. Lane 10-Line12 (Hatcher). Lane 11-Line18 (Kofa). Lane 12-Line20 (Lovrin 34). Lane 13- Gemmeiza 9.

(-) absent band. (+, ++ and +++) gradual increase in the band intensity.

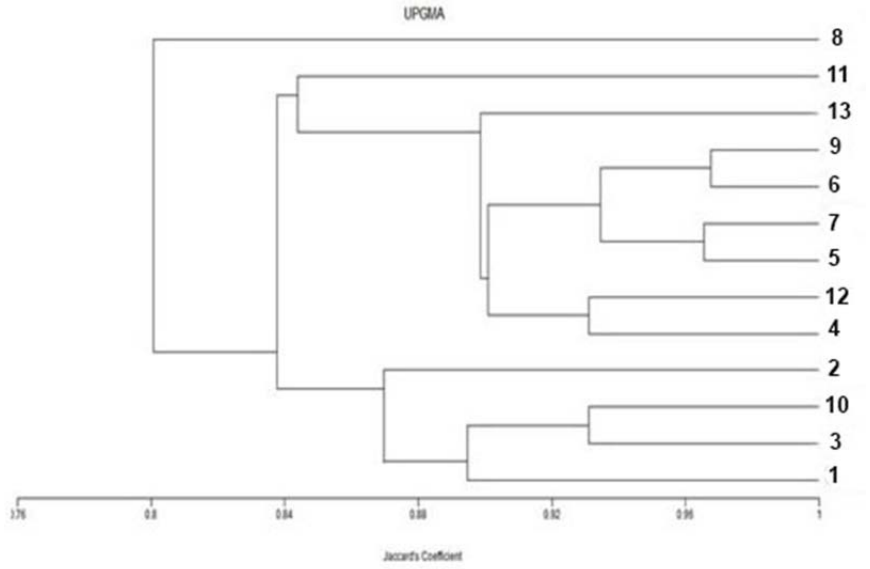

Figure 2. phylogenetic tree using water soluble proteins of thirteen wheat genotypes.

1-Sakha94. 2-Sakha93. 3-Gemmeiza10. 4-Misr2. 5-Sids1. 6-Sids12. 7-Giza168.
8-Misr1. 9-Shandweel1. 10-Line12 (Hatcher). 11-Line18 (Kofa). 12-Line20 (Lovrin 34). 13- Gemmeiza9.

Table 5. proximity matrix of relationship among thirteen wheat genotypes using water soluble proteins.

Case	Sakha 94	Sakha 93	Gemesa 10	Misr2	Sids 1	Sids12	Giza168	Misr1	Shand-weel1	Line12 (Hatcher)	Line18 (Kofa)	Line20 (Lovrin 34)	Gemesa 9
Sakha94	1.000												
Sakha93	0.821	1.000											
Gemmeiza10	0.893	0.926	1.000										
Misr2	0.929	0.828	0.897	1.000									
Sids1	0.800	0.710	0.774	0.867	1.000								
Sids12	0.839	0.806	0.871	0.903	0.903	1.000							
Giza168	0.833	0.742	0.806	0.900	0.966	0.935	1.000						
Misr1	0.767	0.677	0.742	0.774	0.897	0.871	0.867	1.000					
Shandweel1	0.867	0.774	0.839	0.933	0.933	0.968	0.967	0.839	1.000				
Line12 (Hatcher)	0.897	0.862	0.931	0.900	0.839	0.935	0.871	0.806	0.903	1.000			
Line18 (Kofa)	0.821	0.852	0.793	0.828	0.828	0.806	0.862	0.733	0.833	0.862	1.000		
Line20 (Lovrin 34)	0.862	0.828	0.833	0.931	0.867	0.903	0.900	0.774	0.933	0.900	0.893	1.000	
Gemmeiza9	0.893	0.733	0.800	0.897	0.897	0.871	0.931	0.862	0.900	0.867	0.857	0.897	1.000

3.2. Identification of wheat genotypes by RAPD analysis:

Nine of RAPD primers were used to assess relationships among thirteen of Egyptian wheat genotypes. The analysis of results obtained from RAPD revealed differences in number of bands, as shown in Figure (3). The total number of amplified fragments with the nine used primers was 85 bands with 32 monomorphic bands and 53 polymorphic bands to produce 62.35% of polymorphism among the thirteen wheat genotypes (Table 6). The detected band numbers ranged from five bands with OPO-14 primer to 17 bands with OPA-04 primer. The highest percentage of polymorphism was 80% with OPO-14 primer, while the lowest percentage of polymorphism was 5% with OPO-10 primer.

The similarity matrix revealed the highest relationship between Sakha 93 and line 18 with a similarity of 95%. On the other hand, the least relationship was found between Gemmeiza 10 and Sids 12 with a similarity of 1.9% with an average of 48.45% (Table 7). The phylogenetic tree was composed of two clusters; the first one included Gemmeiza10 only, while the second cluster involved all other studied genotypes. The second cluster was divided into two sub-clusters; the first sub-cluster contained Sakha 94 and Sids 1, while the second sub-cluster included the others (ten studied genotypes). The second sub-cluster was divided into two clades; the first clade composed of Giza 168, Shandawel 1, and Line 12 while the second clade involved the remaining seven genotypes. The second clade was divided into two sub-clades; the first sub-clade contained only Sids 12, while the second sub-clade was divided into two groups; the first group included only Misr 1. The second group was divided into two sub-groups; the first sub-group included only Misr 2, while the second sub-group consisted of two sections; the first section included Gemmeiza 9, while the second section included line 18 and Sakha 93 (Figure 4).

Dendrogram represents the genetic relationships among the thirteen wheat genotypes using UPGMA cluster analysis with RAPD primers, which ended to three subgroups (Sakha 93& Line 18) with similarity coefficient 95%, (Shandaweel 1& Line 12) with a similarity coefficient 76.5% and (Sakha 94& Sids 1) with similarity coefficient 66.7%.

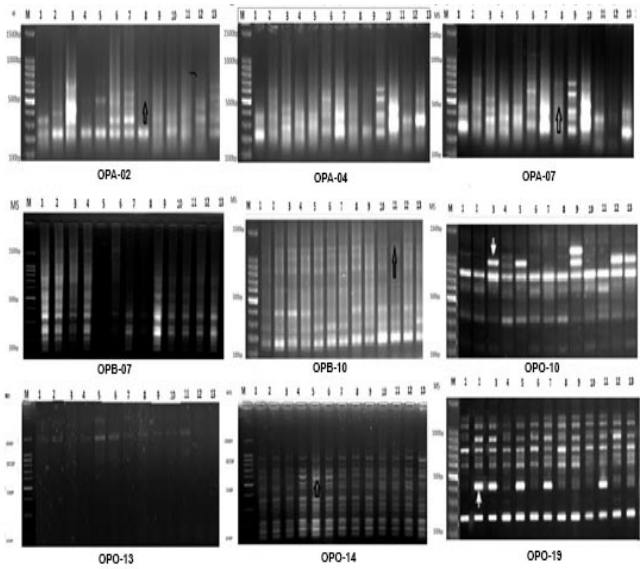

Figure 3.RAPD-PCR banding patterns using RAPD primers for thirteen wheat genotypes.

Lane M: DNA Ladder (100 – 1500 bp).

Lane 1: Sakha94. Lane 2: Sakha93. Lane 3: Gemmeiza10. Lane 4: Misr2. Lane 5: Sids1. Lane 6: Sids12. Lane 7: -Giza168. Lane 8: Misr1. Lane 9: Shandweel1. Lane 10: Line12 (Hatcher). Lane 11: Line18 (Kofa). Lane 12: Line20 (Lovrin 34). Lane 13: Gemmeiza9.

Table 6. Monomorphic and polymorphic bands and %polymorphism for thirteen wheat genotypes using nine RAPD primers.

Code no.	Primer sequences	Monomorphic bands	Polymorphic bands	Total bands	% polymorphism
OPA-02	CAGGCCCTTC	5	7	12	58.3
OPA-04	AATCGGGCTG	6	11	17	64.7
OPA-07	GAAACGGGTG	2	5	7	71.4
OPB-07	GGTGACGCAG	4	5	9	55.6
OPB-10	CTGCTGGGAC	5	6	11	54.5
OPO-10	TCAGAGCGCC	3	3	6	50
OPO-13	GTCAGAGTCC	2	6	8	75
OPO-14	AGCATGGCTC	1	4	5	80
OPO-19	CAATCGCCGT	4	6	10	60
Total		32	53	85	62.35%

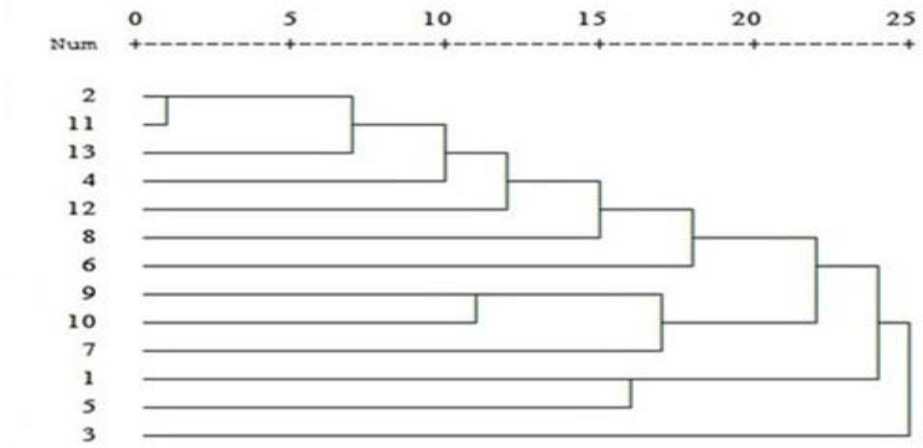

Figure 4. Phylogenetic tree using RAPD-PCR for thirteen wheat genotypes.

1-Sakha94. 2-Sakha93. 3-Gemmeiza10. 4-Misr2. 5-Sids1. 6-Sids12. 7-Giza168. 8-Misr1. 9-Shandweel1. 10-Line12 (Hatcher). 11-Line18 (Kofa). 12-Line20 (Lovrin 34). 13- Gemmeiza9.

Table 7.Proximity matrix of relationship among thirteen wheat genotypes using nine RAPD primers.

Case	Matrix File Input												
	Sakha 94	Sakha 93	Gemmeiza 10	Misr2	Sids1	Sids12	Giza 168	Misr1	Shandweel 1	Line12 (Hatcher)	Line18 (Kofa)	Line20 (Lovrin 34)	Gemmeiza 9
Sakha94	1.000												
Sakha93	0.260	1.000											
Gemmeiza 10	0.260	0.137	1.000										
Misr2	0.468	0.778	0.511	1.000									
Sids1	0.667	0.381	0.392	0.291	1.000								
Sids12	0.033	0.667	0.019	0.260	0.294	1.000							
Giza168	0.532	0.260	0.260	0.319	0.197	.023	1.000						
Misr1	0.468	0.490	0.354	0.552	0.291	0.260	0.617	1.000					
Shandweel 1	0.532	0.552	0.100	0.468	0.197	0.162	0.683	0.468	1.000				
Line12 (Hatcher)	0.468	0.634	0.511	0.552	0.445	0.100	0.468	0.552	0.765	1.000			
Line18 (Kofa)	0.430	0.950	0.319	0.789	0.406	0.532	0.430	0.650	0.430	0.650	1.000		
Line20 (Lovrin 34)	0.713	0.589	0.468	0.650	0.552	0.230	0.571	0.511	0.430	0.511	0.738	1.000	
Gemmeiza 9	0.552	0.713	0.137	0.634	0.230	0.511	0.552	0.778	0.552	0.490	0.863	0.726	1.000

3.3. Identification of wheat genotypes by ISSR analysis:

The discrimination between thirteen wheat genotypes was carried out using five ISSR primers. The PCR products revealed differences in a number of resulting bands, as shown in Figure (5). The total number of bands produced by amplification of all studied primers was 37 bands with 17 monomorphic bands and 20 polymorphic bands to score 54.05% of polymorphism. The highest polymorphism was 62.5% using UBC-817 primer. However, the lowest polymorphism was 37.5% using UBC-815 primer. The number of amplification products generated by primers ranged from 5 (UBC-814) to 9 (A12 primer) bands (Table 8).

UPGMA cluster analysis generated from ISSR marker was translated to generate the dendrogram and similarity index (Figure 6 and Table 9).

The similarity matrix revealed the highest identity between Sakha 93 and Sakha 94 with a similarity of 98.5%. On the other hand, the lowest relationship was found between Gemmeiza 9 and Sids 12 with a similarity of 66% as listed in Table (9). The phylogenetic tree composed of two clusters; the first cluster included only Sakha 94, while the second cluster involved all other studied genotypes. The second cluster was classified to two sub-clusters; the first sub-cluster was divided into two clades, the first clade consisted of Sakha 93 and Line 18, while the second clade involved Gemmeiza 9 and Masr 2. The second sub-cluster was divided into two clades; the first clade composed of two sub-clades; the first sub-clade contained only Misr 1, while the second sub-clade included Sids 1 and Line 20. The second clade was divided into two sub-clades; the first sub-clade included Shandawel 1 only, while the second sub-clade was divided into two groups. The first group included Giza 168 and Sids12, while the second group consisted of Gemmeiza 10 and Line 2 (Figure 6).

Dendrogram represents the genetic relationships among the thirteen wheat genotypes using UPGMA cluster analysis generated from ISSR marker ended to five subgroups and three solitary genotypes. The five subgroups are: (Line 12& Gemmeiza 10 with similarity coefficient 69.4%), (Giza 168 & Sids 12 with similarity coefficient 93.1%), (Line 20& Sids 1 with similarity coefficient75.4), (Line 18& Sakha93 with similarity coefficient 80%) and (Masr 2& Gemmeiza 9 with similarity coefficient 86.5%). While the solitary split genotypes were Sakha 94, Masr 1 and Shandaweel1.

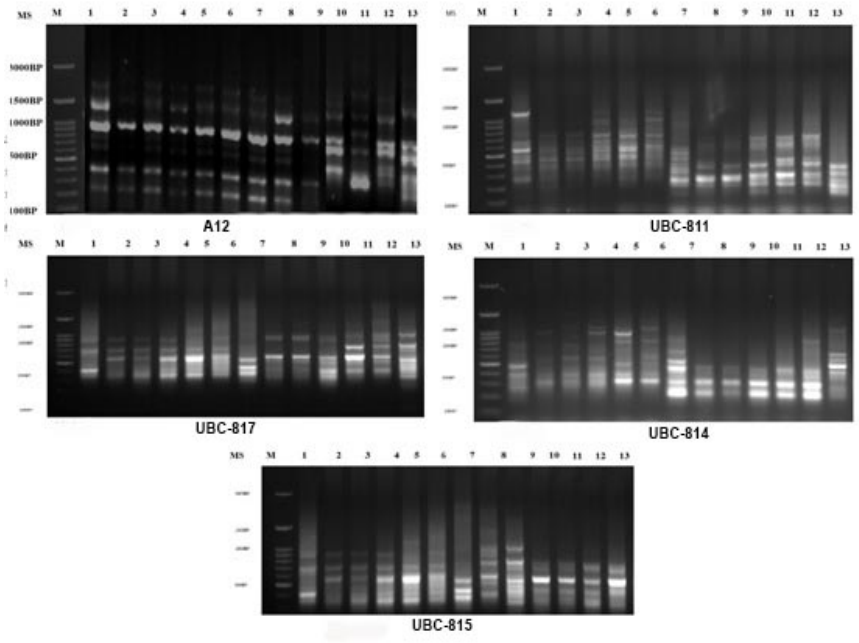

Figure 5. ISSR-PCR banding patterns using RAPD primers for thirteen wheat genotypes.

Lane M: DNA Ladder (100 – 3000 bp).

Lane 1: Sakha94. Lane 2: Sakha93. Lane 3: Gemmeiza10. Lane 4: Misr2. Lane 5: Sids1.

Lane 6: Sids12. Lane 7: -Giza168. Lane 8: Misr1. Lane 9: Shandweel1. Lane 10: Line12 (Hatcher).

Lane 11: Line18 (Kofa). Lane 12: Line20 (Lovrin 34). Lane 13: Gemmeiza9.

Table 8. Monomorphic and polymorphic bands and %polymorphism for thirteen wheat genotypes under study using five ISSR primers.

Primer code	Sequence (5`→3`)	Monomorphic bands	Polymorphic bands	Total bands	% polymorphism
A12	(GA)6CC	4	5	9	55.56
UBC-811	(GA)8 AC	3	4	7	57 14
UBC-817	(CA)8A	3	5	8	62.5
UBC-814	(CT)8A	2	3	5	60
UBC-815	(CT)8G	5	3	8	37.5
Total		17	20	37	54.05%

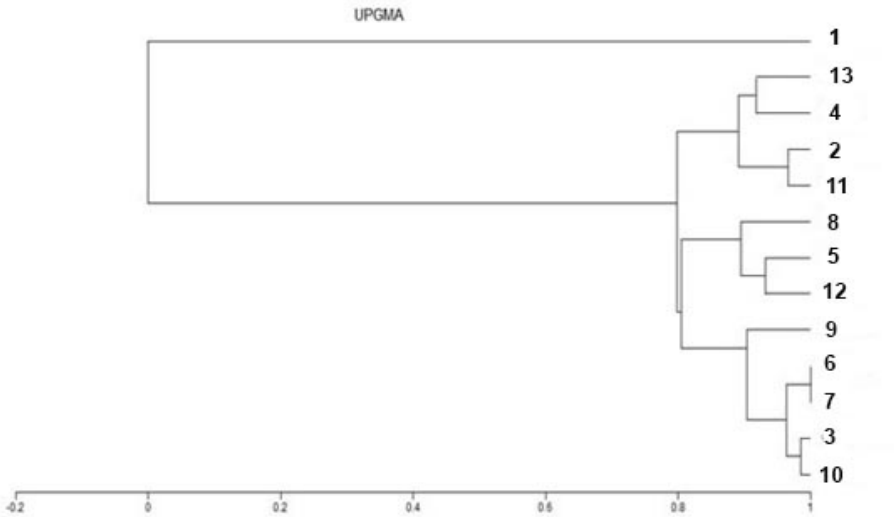

Figure 6. Phylogenetic tree using ISSR-PCR for thirteen wheat genotypes.

1-Sakha94. 2-Sakha93. 3-Gemmeiza10. 4-Misr2. 5-Sids1. 6-Sids12. 7-Giza168.
8-Misr1. 9-Shandweel1. 10-Line12 (Hatcher). 11-Line18 (Kofa). 12-Line20 (Lovrin 34). 13- Gemmeiza9.

Table 9. Proximity matrix of relationship among thirteen wheat genotypes using five ISSR primers

Case	Sakha94	Sakha93	Gemmeiza 10	Misr2	Sids1	Sids12	Giza168	Misr1	Shandweel1	Line12 (Hatcher)	Line 18 (Kofa)	Line20 (Lovrin 34)	Gemmeiza 9
Sakha94	1.000												
Sakha93	0.985	1.000											
Gemmeiza10	0.955	0.971	1.000										
Misr2	0.955	0.971	1.000	1.000									
Sids1	0.875	0.892	0.923	0.923	1.000								
Sids12	0.825	0.844	0.844	0.844	0.918	1.000							
Giza168	0.787	0.806	0.806	0.806	0.847	0.931	1.000						
Misr1	0.721	0.742	0.742	0.742	0.780	0.862	0.929	1.000					
Shandweel1	0.806	0.794	0.794	0.794	0.767	0.780	0.842	0.912	1.000				
Line12 (Hatcher)	0.806	0.794	0.794	0.794	0.733	0.746	0.807	0.877	0.966	1.000			
Line18 (Kofa)	0.813	0.800	0.831	0.831	0.774	0.721	0.780	0.847	0.900	0.933	1.000		
Line20 (Lovrin 34)	0.825	0.844	0.844	0.844	0.754	0.700	0.724	0.793	0.847	0.881	0.918	1.000	
Gemmeiza9	0.780	0.677	0.870	0.865	0.722	0.660	0.730	0.768	0.789	0.765	0.786	0.890	1.000

4. Discussion

Genetic diversity has a critical role in the assessment of the genetic relationships among different plant genotypes by using biochemical markers (Protein electrophoresis) and different molecular markers (Mishra *et al*., 2014).

Protein banding patterns using the SDS-PAGE technique could be considered a reliable tool for the identification and characterization of the similarity among different plant species. This technique was used to analyze the variability of seedling water soluble protein profiles for detecting the phylogenetic relationships and genetic diversity of adapted plant cultivars and improving the productivity of plant breeding programs (Iqbal *et al*., 2005). According to Zahoor *et al. (*2023), genotypes in one cluster should be identical in their protein profile, show less intra-specific genetic variation, and exchange genes smoothly between them, guaranteeing the success of hybrid breeding.

Data obtained from protein profiling as biochemical markers put Line 12 and Gemmeiza 10 in one subgroup, which were highly similar with the exception of three bands missing (82, 20, and 17 kDa) from Gemmeiza 10, two genotypes Giza 168 and Sids 1 were put in one subgroup with high similarity in protein profile with the exception of missing two bands from Giza 168 (207 and 40 kDa), and line 20 and Misr 2 in one subgroup, which have the identical protein fingerprint.

Our obtained data revealed that both protein marker and ISSR marker assessed the genetic similarity coefficient between the two genotypes line 12 and Gemmeiza 10 to reach 93.1 and 79.4%, respectively, and gather them in the same subgroup. The higher induced similarity after protein marker despite the higher genetic diversity on the ISSR molecular marker level may have arisen from paralogue genes (produced to serve the plant evolution) translated into the identical proteins (Koonin, 2005). These paralogue genes expand the genome diversity on the molecular marker side but at the same time summarize the distance among relatives on the protein marker side.

The difference between protein and ISSR was not in the similarity coefficient only but to put different genotypes in different grouping matter. For example, protein electrophoresis gathers Sids 12 and Shandaweel1 in one subgroup with the similarity coefficient 96.8%. At the same time, ISSR marker put Sids 12 and Giza 168 with the similarity coefficient 93.1%.

RAPD-PCR was more precise and informative than SDS-PAGE concerning relationships between *Zea mays* (mays) and *Zea mays* (Mexicana) and between *Sorghum valgare* and *Sorghum bicolor* (Osman *et al*., 2013).

The data recorded herein after the biochemical markers depending on total soluble protein from the thirteen of wheat seedlings agrees with those observed by El-Akkad (1998); El-Akkad and El-Abd El-Kariem (2002), in which they detected genetic variability between and within wheat species and cultivars depending on seed storage protein profiles.

Both of the two molecular RAPD and ISSR markers succeeded to put the two wheat genotypes Sakha 93 and line 18 in same subgroup with a similarity coefficient of 95 and 80% respectively. The difference in resolution of RAPD and ISSR marker systems refers to that the two marker techniques targeted different sequences of the genome.

Comparing the obtained results based on the polymorphism of RAPD and ISSR as molecular markers gave a wide range of the genetic diversity (62.35 and 54.04%, respectively). Therefore, they were considered powerful markers for discrimination among different studied wheat genotypes, compared with biochemical markers (SDS-PAGE) which had the lowest polymorphism (35.48%). This may be explained by that RAPD and ISSR are neutral to environmental influence and indicate variations at the full genome level. Besides, biochemical markers can be affected by extraction methodology, plant

stage, plant tissue, and environmental conditions (Mondini *et al*., 2009).

From the same point of view, our obtained results about the advantage of using molecular markers in assessing the genetic diversity agree with Abdel-Lateif and Hewedy (2018) who recorded that SCoT and ISSR markers were effective in detecting the genetic diversity among different Egyptian wheat and helping breeders to evaluate genetic diversity. Sofalian *et al.* (2008) documented that ISSR markers gave a high value of polymorphism for discrimination of wheat landraces. Also, Pasqualone *et al.* (2000) reported that ISSR markers had productivity, so they used this marker to distinguish all the examined durum wheat cultivars.

Despite that, protein profiling SDS-PAGE of seedling's protein analysis provided us with insufficient results. It provided us with useful information on the relationships among closely related genotypes and detected the unique band at M.W 13 kDa in the genotype Sids12.

In agreement with Abd El-Hady (2010), our results obtained the highest polymorphism using RAPD assays because it targeted the non-coding DNA regions which are very stable, less responsive to external factors, and high tolerance to mutation.

There is a contradiction between our obtained results which revealed the RAPD highest similarity of 95% between (Sakha 93 and line 18) and the least similarity matrix of 1.9% between (Gemmeiza 10 and Sids 12) and the data obtained by Mansour *et al*. (2020) who found the highest similarity matrix between (Sakha 93 and Saheel 1) with a similarity of 86%; while the least similarity matrix was found between (Gemmeiza 9 and Shandaweel 1) with a similarity of 1.9%. This contradiction may be due to the difference in RAPD primers used in their PAPD amplification compared with our used RAPD primers.

5. Conclusions

Thirteen Egyptian wheat genotypes were discriminated using SDS-PAGE, RAPD and ISSR techniques. The discrimination reveals the genetic diversity and, at the same time, points to the relationships between genotypes. RAPD has the highest polymorphism (62.35%), followed by ISSR, which has a polymorphism of 54.05%, and seedling proteins, which have a polymorphism of 35.48%. This means that RAPD and ISSR are more powerful markers than protein marker in the discrimination and identification of different studied wheat genotypes. So, combining the biochemical markers with the molecular markers enriches the study with more informative data. The obtained data can be reliable as a roadmap for the wheat breeders to present more closely related genotypes for estimating new wheat hybrids in great harmony with their surroundings.

Acknowledgement

The authors would like to thank the National Research Centre (Genetics and Cytology Department) Egypt, for providing all the facilities to conduct all experiments in its laboratories. We are thankful to all the researchers whom we cited in this manuscript for their important and beneficial research.

Authors' contributions

Authors S.A.O. and S.A.H. performed RAPD, ISSR, and protein electrophoresis (SDS-PAGE) experiments and analyzed the data. Authors S.A.O. and R.T.A. wrote the manuscript and managed the literature. Author S.A.O. organized the paper. All authors read and approved the final manuscript.

Funding

This research was funded by National Research Centre, Egypt. Project no 11030107.

References:

Abdel-Lateif K and Hewedy O. 2018**.** Genetic diversity among Egyptian wheat cultivars using SCoT and ISSR markers. SABRAO J. Breed. Genet. , **1(50):** 36-45.

Abd El-Hady AA, Haiba AA, El-Hamid RA and Rizkalla A. **2010.** Phylogenetic diversity and relationships of some tomato varieties by electrophoretic protein and RAPD analysis. J. Am. Sci., **6(11):** 434-441.

Abouseada HH, Mohamed AH, Teleb SS, Badr A, Tantawy ME, Ibrahim SD, Ellmouni FY and Ibrahim M. 2023. Genetic diversity analysis in wheat cultivars using SCoT and ISSR markers, chloroplast DNA barcoding and grain SEM. BMC Plant Biol., **23:**193.

Cooke RJ and Law JR. 1998. Seed storage protein diversity in wheat varieties. Plant Var. and Seeds, **11:** 159-167.

El-Akkad SS. 1998. Protein and randomly amplified polymorphic DNA (RAPD) of wheat plant. J. Uni. Ar. Biol., **6(B):** 467-475.

El-Akkad SS and El-Abd El-Kariem SS. 2002. Protein patterns of wheat grains with phylogenetic inferences. Egy. J. Biol., **4:** 31-36.

Gowayed SMH and Abd El-Moneim D. 2021. Detection of genetic divergence among some wheat (*Triticum aestivum* L.) genotypes using molecular and biochemical indicators under salinity stress. PLoS ONE, **16(3):** e0248890.

Iqbal SH, Ghafoor AB and Ayub NA. 2005. Relationship between SDS-PAGE markers and *Ascochyta blight* in chickpea. Pak. J. Bot., **37(1):** 87-96.

Izadi-Darbandi A, Yazdi-Samadi B, Shanejat-Boushehri AA and Mohammadi M. 2010. Allelic variations in Glu-1 and Glu-3 loci of historical and modern Iranian bread wheat (*Triticum aestivum* L.) cultivars. Ind. Acad. Sci., *J. Genet.*, **89(2):** 193-199.

Jha SS and Ohri D. 1996. Phylogenetic relationships of *Cajanus cajan* (L) Millsp. (Pigeonpea) and its wild relatives based on seed protein profiles. Genet. Res. Crop Evol., **43:** 275-281.

Khurana-Kaul V, Kachhwaha S and Kothari SL. 2012. Characterization of genetic diversity in *Jatropha curcas* L. germplasm using RAPD and ISSR markers. Ind. J. Biotech., **11(1):**54–61.

Koonin EV. 2005. Orthologs, paralogs, and evolutionary genomics. Annu. Rev. Genet., **39:** 309–338.

Laemmli UK. 1970. Cleavage of structural proteins during the assembly of the head of bacteriophage T4. Nat., **227**: 680-685.

Mansour HA, Mohamed SE and Lightfoot DA. 2020. Molecular studies for drought tolerance in some Egyptian wheat genotypes under different irrigation systems. Open Agric., **5:** 280–290.

Mishra KK, Fougat RS, Ballani A, Thakur V, Jha Y and Bora M. 2014. Potential and application of molecular markers techniques for plant genome analysis. IJPAB., **2:** 169-189.

Mondini L, Noorani A and Pagnotta MA. 2009. Assessing plant genetic diversity by molecular tools. Divers., **1:** 19-35.

Najaphy A, Parchin RA and Farshadfar E. 2012. Comparison of phenotypic and molecular characterizations of some important wheat cultivars and advanced breeding lines. Aust. J. Crop Sci., **6(2):** 326-332.

Nie NH, Hadlia C, Jenkins JG, Steinbrenner K and Bent DH. 1975. SPSS, statistical package for the social sciences. 2nd ed. New York: **McGraw-Hill**.

Osman G, Munshi A, Altf F and Mutawie H. 2013. Genetic variation and relationships of *Zea mays* and *Sorghum* species using RAPD-PCR and SDS-PAGE of seed proteins. AJB., **12(27):** 4269-4276.

Osman SA and Ramadan WA. 2020. Characterization of Egyptian durum Wheat Genotypes using Biochemical and Molecular Markers. JJBS., **13(4):** 419-429.

Pasqualone A, Lotti C, Bruno A, Vita P, Fonzo N and Blanco A. 2000**.** Use of ISSR markers for cultivar identification in durum wheat. Options Méditerranéennes. Série A, Séminaires Méditerranéens, **40:** 157-161.

Qadir A, Ali N, Jan SA, Rabbani MA, Khurshid H, Nouman A and Ullah F. 2017. Characterization of agromorphological variation in exotic Fenugreek (*Trigonella foenum-graecum* L.) germplasm. JBES., **10(3):** 71-79.

Salgotra RK and Chauhan BS. 2023. Genetic Diversity, Conservation, and Utilization of Plant Genetic Resources. *Genes*, **14(1):** 174.

Sambrook J, Fritsch KF and Maniatis T. 1989. Molecular cloning, second edition (cold spring Harbor, New York).

Shaban AS, Arab SA, Basuoni MM, Abozahra MS, Abdelkawy AM and Mohamed MM. 2022. SCoT, ISSR, and SDS-PAGE Investigation of Genetic Diversity in Several Egyptian Wheat Genotypes under Normal and Drought Conditions. Int. J. Agron., **7024028:** 1-14.

Shukre VM, Chavan NS and Patil YK. 2015. Assessment of Genetic Diversity among Wheat Varieties in Aurangabad Using RAPD Analysis. IJCMAS., **4(8):** 671-694.

Sofalian O, Chaparzadeh N, Javanmard A and Hejazi MS. 2008. Study the genetic diversity of wheat landraces from northwest of Iran based on ISSR molecular markers. IJAB., **10(4):** 466-468.

Souframanien J and Gopalakrishna T. 2004. A comparative analysis of genetic diversity in blackgram genotypes using RAPD and ISSR markers. Theor. Appl. Genet., **109(8):** 1687-1693.

Studier FW. 1973**.** Analysis of bacteriophage T1 early RNAs and proteins of slabgels. J. Mol. Biol., **79(2):** 237-248.

Velasco-Ramirez AP, Torres-Moran MI, Molina-Moret S, Sanchez-Gonzalez JJ and Santacruz-Ruvalcaba F. 2014. Efficiency of RAPD, ISSR, AFLP and ISTR markers for the detection of polymorphisms and genetic relationships in camote de cerro (*Dioscorea* spp.). Electron. J. Biotechnol., **17(2):**65–71.

Zahoor M, Nisar M, Ur Rahman A and Ul Bari W. 2023. Determination of genetic diversity in *Acacia modesta* germplasm using SDS-PAGE. Braz. J. Biol., **84:** e265065.

Zietkiewciz E, Rafalski A and Labuda D. 1994. Genome finger printing by simple Sequence Repeat (SSR)-Anchord Polymerase Chain Reaction Amplification. Genom., **20:**176-183.

JJBS

Volume 17, Number 4,December 2024
ISSN 1995-6673
Pages 613 – 621
https://doi.org/10.54319/jjbs/170404

Jordan Journal of Biological Sciences

Culture Trials and Biochemical analysis of Arabian yellowfin seabream *Acanthopagrus arabicus* Iwatsuki, 2013 to Evaluate Feed Efficacy

Komal Shabbir[1]. Nuzhat Afsar[1,*] , Ghulam Abbas[2], Abdul Malik[2], Rafia Azmat[3] and Shahzad Najam[4].

[1] *Institute of Marine Science, University of Karachi;* [2] *Center of Excellence in Marine Biology, University of Karachi;* [3] *Department of Chemistry, University of Karachi;* [4] *Integrated Biosciences, Karachi-74900*

Received: October 17, 2023; Revised: March 19, 2024; Accepted: May 3, 2024

Abstract

Commonly known Arabian yellow fin sea bream (*Acanthopaqrus arabicus*) were selected for trials. Specimens were procured from the Sonari channel (24°53'13.81"N 66°41'44.57"E.), shifted to laboratory, and placed into 162 liter capacity glass aquaria, where they were subsequently acclimated for 60 days. Fish were fed in ration of 3% live body weight of feed. Two treatments were placed (T1 & T2). Individuals placed under T1 treated with soybean meal (SM) and individuals under T2 treated with fish meal (FM). Physicochemical parameters were recorded. pH, salinity (ppt), and temperature (27°C) were measured on daily basis, while ammonia, dissolved oxygen (DO), and nitrite nitrogen were evaluated on weekly basis. Length (cm) and weight (g) of under treatment individuals recorded thrice in a month. The mean final weight for treatments (T1 and T2) endured 8.11±0.12 and 8.12±0.13 g, respectively, while the mean achieved length was 10.24±0.11 cm and 10.31±0.12 cm. Results showed the minimal weight increase in T2 alongside the slight difference in specific growth rate. Meanwhile, based on weight increase, feed conversion ratio, and specific growth rate there was a minute difference in growth between the two meals (SM & FM), whereas biochemical analysis revealed that SM impacted the individuals as greater levels of crude fat (51.23±0.947), crude protein (62 ±2.8284) found. Hence, soybean meal (SM), which is affordable, proved that it could be a possible diet that can replace traditional fish meal (FM) for cultivation of *A. arabicus* in aquaculture facilities to achieve marketable size.

Keywords*:* Aquaculture; soybean meal; fish feed; omnivorous

1. Introduction

Fish meal is widely regarded as the premier healthy diet for people worldwide, being the most notable source of various proteins, vitamins, low-saturated fats, and omega-3 fatty acids. Seafood is renowned for its ability to reduce the risk of cardiovascular disease due to the presence of n-3 polyunsaturated fatty acids (Dabrowski *et al.*, 2005; Erkan and Ozden 2007). *Acanthopaprus arabicus* is one of the commercially important species in the group of Pisces. So, due to the commercial significance of *Acanthopaprus arabicus* numerous studies have been made to elucidate different aspect of growth and nutrition of yellowfin seabream species globally. For instance, Saffari *et al* (2021) observed the effects of nano-Selenium add-on in plant protein-rich diet on reproductive performance. Results have shown the higher relative fecundity in females fed at the rate of 4 mg Kg^{-1} N-Se diet ($p < .05$). In the same way, Izadpanah *et al.* (2022) and Mohtashemipour *et al.* (2024) concluded and highlighted the preference of augmenting plant protein based diet with nano-selenium (n.Se)/Kg to enhance the survival and larval length of *A. arabicus* on larval stage. AlKatrani (2023) examined the salinity effect on energy and metabolic enzymes in juveniles and adults of yellow fin sea bream. Study undertaken revealed the reflective enzyme activity in adults. So, there are many studies that have achieved successful results on herbal maturation diets in fish (Al Khawli, 2019).

Molecular and biological makeup of fish meat can facilitate effective food amplification (Njinkoue *et al*., 2016). Nearly 50% of the fish products consumed worldwide in 2016 came from aquaculture, clinched 30.1 million tons of aquatic plants and 80.0 million tons of edible fish. As per past reckoning regarding the production of fish and shellfish for human consumption, 54.1 million tons came from fish, 17.1 million tons from mollusks, 7.9 million tons from crustaceans, and 938,500 tons from other aquatic creatures (FAO, 2018). At 15.3 million tons, China is by far the largest produced globally. Other Asian nations like Indonesia, India, Japan, and Viet Nam are next. With production totals of 2.03 and 0.91 million tons, respectively, Norway and Spain are at the top of the list in Europe (Pateiro *et al.*, 2020).

* Corresponding author. e-mail: nafsar@uok.edu.pk.

Along with nutritional sources of protein and critical amino acids, marine fish larvae can boost the potency of their ability to multiply. In general, larvae transform during the advanced phases, and a variety of significant elements can influence the quality of young and prevent improvement (Naess *et al.*, 1995; Njinkoue *et al.*, 2016). Generally, fish size, species, season, and zone are different quotients between food fish and byproducts (Rustad *et al*., 2011). High quantities of fat-soluble vitamins (A and D), necessary macro and micro minerals, i.e. iodine, magnesium, phosphorus, and selenium, as well as high-quality proteins and balanced essential amino acids are all present in seafood or fish species (Gil and Gil, 2015).

Sea bream is an important fish for the entire world due to its ability to grow in both brackish pond and marine environments (Sadek *et al.*, 2004). Iwatsuki (2013) reported that the yellowfin seabream, *Acanthopagrus latus*, which has long been considered a single species in the Indian-Western Pacific, actually comprises five different species, including *Acanthopagrus arabicus* arises in the Middle East towards the western coast of India (excluding the Red Sea).

Ahmad *et al* (2018) assessed growth performance of juvenile *Acanthopagrus arabicus* reared in floating net cages, and juveniles were fed twice daily at the rate of 3%, 5%, 7% and 9% with accordance to their body with a diet containing 42% protein. Results have shown 100% survival rate in all groups up to seven weeks and significant results were found in group three fed with 7% protein to their body weight. Later Ahmad *et al.* (2019 and 2020) investigated the impact of dietary protein level in the practical diet of yellowfin seabream, juveniles to check out optimum growth performance, survival and carcass composition besides feeding frequency influence on growth performance in cage culture was also scrutinized respectively. Previously, Yesser *et al.* (2016) worked on impact of feeding levels on growth performance and food conversion of Acanthopagrus arabicus cultivated in concrete tanks at Basrah province. Recently, Sarvi *et al.* (2023) found out the effect of delayed first feeding on growth and survival of yellowfin seabream (*Acanthopagrus arabicus*) larvae.

There are many studies that have achieved successful results on herbal maturation diets in fish (Dhas *et al*, 2017). Overall, the aquaculture business in Pakistan is developing although at a very modest rate. Despite having a 1001 km long coastline, Pakistan unfortunately ignores mariculture. However, the nation's aquaculture industry has greatly increased GDP (Mohsin *et al.*, 2019). In this context previous study was also carried out to evaluate growth performance, body composition and survival rate of juvenile snakehead (*Channa marulius*) by Kalhoro *et al.*, (2017).

The objectives of the study are to evaluate the growth performance, physiological responses, and biochemical composition of commonly known Arabian yellow fin sea bream (*Acanthopagrus arabicus*) under controlled conditions. Specifically, it seeks to compare the effects of soybean meal (SM) and fish meal (FM) on the growth and health of *A. arabicus*, with the objective of assessing the suitability of soybean meal as a potential alternative to fish meal in the diet of *A. arabicus* for aquaculture purposes. The investigation will include monitoring physicochemical parameters of the water environment, such as pH, salinity, temperature, ammonia levels, dissolved oxygen, and nitrite nitrogen concentrations, to understand their influence on the growth and health of *A. arabicus* under experimental conditions. Key parameters to be investigated include growth performance indicators like weight gain, length gain, and specific growth rate, as well as biochemical composition analysis focusing on crude fat, crude protein, total lipid content, vitamin A and total carbohydrates in the fish specimens. By addressing these objectives, the study aims to contribute valuable insights into optimizing diet composition for the cultivation of *A. arabicus* in aquaculture facilities, potentially enhancing the efficiency and sustainability of sea bream production.

2. Materials and Methods

Acanthopagrus latus which was later re-identified as *Acanthopagrus arabicus* (Iwatsuki, 2013), the experimental fish was identified on the basis of taxonomic features and positioned in glass aquariums according to experimental plan to carry out growth trials based on various feed efficacies. The collection of juveniles of *Acanthopagrus arabicus* was done from the Sonari channel (24°53'13.81"N 66°41'44.57"E) which is located between Sindh and Balochistan provinces near Hub river in October 2019 by using cast net (Figure 1). The experimental fish was identified on the basis of taxonomic features and positioned in glass aquariums according to experimental plan to carry out growth trials based on various feed efficacies. Taxonomic categories of this species are: Phylum Chordata, Class Actinopterygii, Order Perciformes, Family Sparidae (Rafinesque, 1818), Genus Acanthopagrus (Peters, 1855), and the specific identification is *Acanthopagrus arabicus*, Iwatsuki, 2013 (Figure 2). This systematic classification provides a detailed understanding of the organism's biological lineage, facilitating scientific categorization and study within the broader context of marine life (Figure 2). Careful transfer of thriving juveniles from the site to laboratory allowed further experimental research. Taxonomic identification of species was done with the help of Iwatsuki, Y., 2013, FAO (2015), FAO (2018), Froese, and Pauly (Eds.) (2019) and Fish base site. After stocking, all samples were acclimatized for about two weeks within the laboratory conditions, and juveniles were fed on appropriate feed in accordance to research design. Juveniles of fish used in this experiment were fed with two different treatments (T1, T2) and meals: treatment one (T1) received soybean meal (SM), and treatment two (T2) received fish meal FM. Before placing each fish sample into the tanks, its length and weight (g) were measured using a measuring tape or scale and a digital balance, respectively. The samples of fish were then placed in different fish aquariums. Treatments lasted up to eight weeks; there were two replicates used for each treatment. Physicochemical parameters were observed through available devices, i.e. pH (pH meter (EzDO 6011, Taiwan), temperature (digital thermometer), salinity (refractometer), dissolved oxygen (portable test kit (Merck KGaA, 64271, Germany), ammonia test kits (Merck KGaA, 64271, Germany) and nitrite nitrogen test kit (Merck KGaA, 64271, Germany) were used to lookup the water quality for the improved development of juveniles.

Analysis of both treatments was done with the help of statistical analysis (statistical Minitab software (17.0 version) in which one-way analysis of variance (ANOVA) was carried out. The length weight data is presented by means of total mean and standard deviation. Biochemical analysis was performed for following juveniles after culturing of specific juveniles for the provided feeds. Growth indices such as weight gain, mean daily weight gain, percent weight gain, Feed Conversion Ratio, Condition factor (CF), Specific growth rate (SGR) and survival rate (SR) were calculated from the data collected in present research by the help of literature of earlier authors. The nutritional composition of our formulated diets is as listed below and shown in Figure 3.

Figure 1. Collection site: Sonari channel 24°53'13.81"N 66°41'44.57"E (Google Maps 2023).

Figure 2. The overall appearance of *Acanthopagrus arabicus* Iwatsuki, 2013.

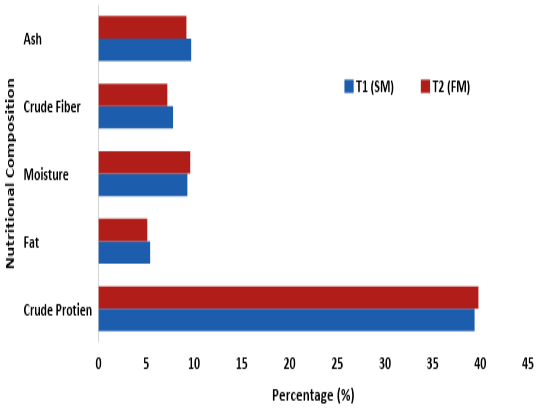

Figure 3. Biochemical analysis of experimental diet.

3. Preparation of samples

Complete proximate analysis of juveniles for two different treatments provided were done such as total lipids, crude protein, vitamin A, organic and inorganic content with the help of classical methods. The samples of *Acanthopagrus arabicus* were prepared for biochemical analysis. First of all, samples from both treatments tanks were sacrificed collected and then they were dissected and then dried at 80- 105 ^{O}C for 24-26 hours. After crushing the samples, placed them in glass vials for further biochemical analysis. The extraction of crude fat was done by following the method as described by Triebold and Aurand (1963) by the help of soxhlet extraction method. The determination of crude protein from the dried sample was done by the micro-kjeldahl distillation method (Hawk *el al*., 1954). The total inorganic content was determined by using the standard method of AOAC (2000). The organic content was determined by the help of official methods of analysis, The Association of Official Analytical Chemists **(**AOAC) standard method (2000). Calcium content was determined by the method of titration with the help of AGQ laboratory. Vitamin A was determined by the SPE (Solid Phase Extraction) method by the Reverse phase HPLC with the help of AGQ laboratory. It was determined by the classical method of phenol sulphuric method in the lab of Institute of Marine Science, University of Karachi.

4. Results

4.1. Growth Indices and Physicochemical parameters

The summary of growth parameters of sea bream (*Acanthopagrus arabicus*) for the duration of experimental trial and water quality parameters were enlisted in Table 1 which are the basic requirements for maintaining the aquaculture set up and maintaining the growth of fish species. In T1, average weight and length were measured 8.11±0.12 gm and 6.65±0.05 cm respectively, and in T2 average weight and length were 8.12±0.13 gm and 6.71±0.04 cm respectively. However, there is no noteworthy difference in the initial length and whole body weight of specimen treatments. Nevertheless, in the end, fish growth was assessed and calculated as difference of mean initial weight and length in both treatments. The average attained final weight ranged in between 22.78±0.4 gm (T1) to 23.15±0.3gm (T2), whereas mean length was

10.24±0.11 cm to 10.31±0.12cm among all treatments respectively. The slightly higher or negligible weight gain was experiential in T2 rather than T1. There is no noteworthy differentiation in specific growth rate, but for T2 it is slightly higher than the T1. The feed conversion ratio of juveniles for soybean meal was slightly greater than as compared to the fish meal but it is non-significant. 100 % Survival rate was observed. (Table 1). Length (cm) and weight (g) relationship showed that fish persisted healthy and in good physical shape during the entire investigational period as values of slopes in all treatments were significant (Figure 4 A-B).

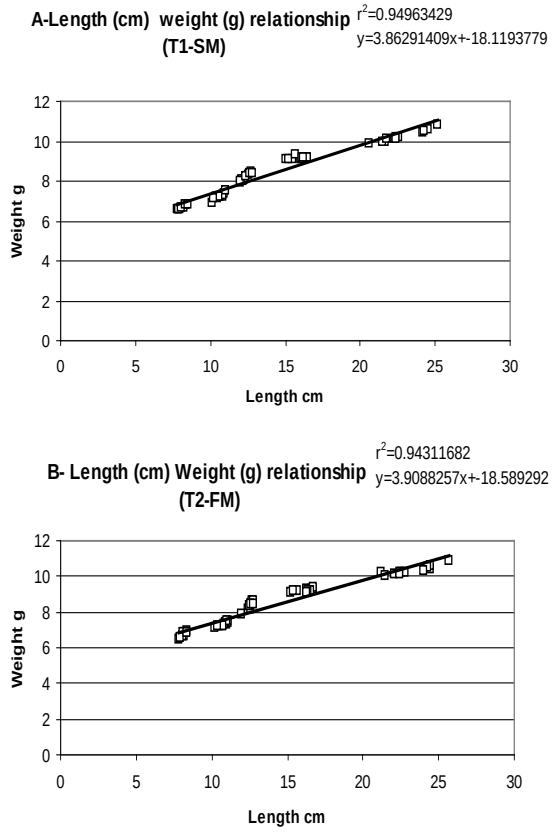

Figure 4.(A-B) Correlation between weight (g) and length (cm) (pooled data) of experimental fish treated with different diet/ treatment. [Treatment 1 (T1) & 2 (T2): FM-fish meal; SM-soybean meal

During the experimental protocol, average temperature was 27.747±1.197^{o}C in T1 and in T2 average temperature was 27.468 ± 1.277 ^{o}C, average salinity was about 30.263 ± 0.452‰ in T1 and 30.105±0.459‰ in T2 , pH of water ranged between 7.4 to 7.5 with average of 7.4784 ± 0.2274 throughout the experimental period in T1 and 7.4926 ± 0.1980 in T2, average levels of dissolved oxygen were measured 7.335±0.021 during the experimental period in T1 and in T2 it was observed with the average of 7.35 ± 0.021, Nitrite nitrogen concentration was observed in T1 and T2 with average of 0.019±0.0007 mg/l and 0.015±0.0007 mg/l correspondingly, The ammonia concentration estimated between 0.01 to 0.05 with average of 0.0465±0.0064 and 0.01±0.0007 mg/l in T1 and T2.

Table 1 (a) Growth indices of sea bream (*Acanthopagrus arabicus*) for both treatments over 60 days (FM-fish meal; SM-soybean meal) and **(b)**Summary of physicochemical parameters for both treatments over 60 days (FM-fish meal; SM-soybean meal).

Parameters	Treatment 01 (SM)	Treatment 02 (FM)
For Growth indices		
Initial Length (cm)	6.65±0.05	6.71±0.04
Final length (cm)	10.24±0.11^{b}	10.31±0.12^{a}
Initial weight (g)	8.11±0.12	8.12±0.13
Final weight (g)	22.78±0.4^{b}	23.15±0.3^{a}
Weight gain	14.67±0.2^{b}	15.03±0.5^{a}
Specific growth rate	1.72±0.03^{b}	1.75±0.02^{a}
Feed conversion ratio	1.69±0.01^{a}	1.67±0.02^{b}
Condition factor	2.12±0.03^{a}	2.11±0.04^{b}
Survival rate	100±0.0	100±0.0
WG% IW	14.6±1.67^{b}	15.03±1.7^{a}
Physicochemical parameters		
Water Temperature (^{0}C)	27.747±1.197	27.468±1.277
Salinity(‰)	30.263 ± 0.452	30.105±0.459
pH	7.4784 ± 0.2274	7.4926±0.1980
Dissolved Oxygen (mg/l)	7.335±0.021	7.35±0.021
Nitrite Nitrogen (mg/l)	0.019±0.0007	0.015±0.0007
Ammonia (mg/l)	0.0465±0.0064	0.01±0.0007

ANOVA (P<0.05) Duncan new multiple test range (Mean±SE). Different superscripts showed significant differences among groups.

4.2. Biochemical Analysis

In the current research, we have performed certain biochemical tests to evaluate the rate of growth, activity and development of the cultured species. Following are the tests which were performed after the experimental period for comparing the quality of meat according to their feed utilization and the results were being analyzed by different experimental protocol which are listed below and summary of all outcomes are presented in Table 2.The concentration of total lipid was found higher in T2 (which was fed with fish meal) than that of T1.The results showed the average values in percentage of total lipid content is 0.8±0.1414 gm in T1 and 1.45±0.4949 gm in 22 (Figure 5), the concentration of crude fat in T1 was 51.23±0.947 % and in T2 was 28.53±0.671 % which is shown in Figure 6, the resultant values of crude protein were 62±2.8284 % for T1 in which juveniles were fed with soybean meal and 33.5±2.121 % in T2 (Figure 7), The ash content was found about 0.936 ±1.50 % in first treatment and it was found 0.676±1.06 % in the other treatment (Figure 8), The moisture content was found about 0.426±0.133 % in first treatment and in the other treatment it was found 0.518±0.064 % (Figure 9), In T1 the calculated value of calcium content was 19.94±0.091 % whereas in T2 it was found approximately 20.25±0.35 % (Figure 10), The calculated values of vitamin A was 9±1.414 % and 10±1.414 % in T1 and T2 respectively(Figure 11), total carbohydrates content was 12.75±0.4949 % and 15±0.707 % in T1 and T2 respectively (Figure 12).

Table 2. Summary of proximate analysis of the fish meat according to the different diets which were fed in the whole experimental period.

Proximate Analysis	Treatment 1	Treatment 2
Total lipid content (%)	0.8 ± 0.1414	1.45±0.4949
Crude Fat (%)	51.23±0.947	28.53±0.671
Crude protein (%)	62 ±2.8284	33.5±2.121
Ash content (%)	0.936±1.50	0.676±1.06
Moisture Content (%)	0.426±0.133	0.5185±0.064
Calcium content (%)	19.94±0.091	20.25±0.35
Vitamin A (%)	9±1.414	10±1.414
Total carbohydrates (%)	12.75±0.4949	15±0.707

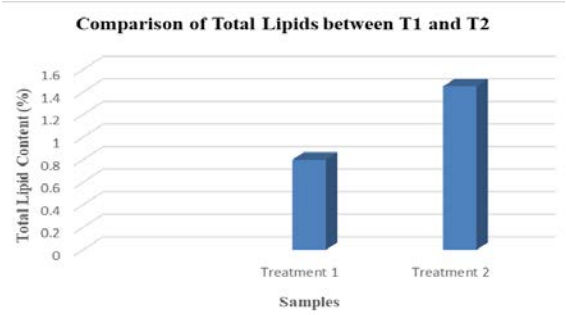

Figure 5. Comparison of total lipids in fish body between two different diets

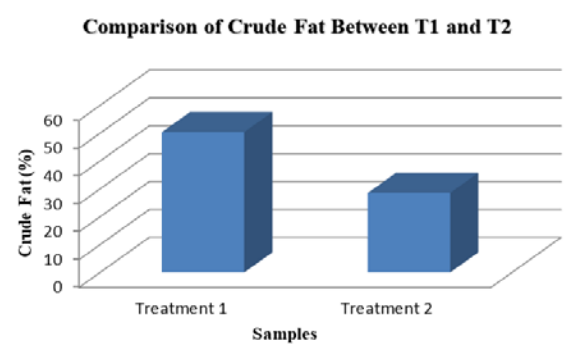

Figure 6. Comparison of crude fat in fish body between two different diets

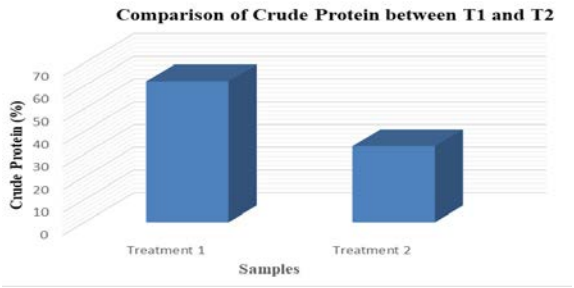

Figure 7. Comparison of crude protein in fish body between two different diets

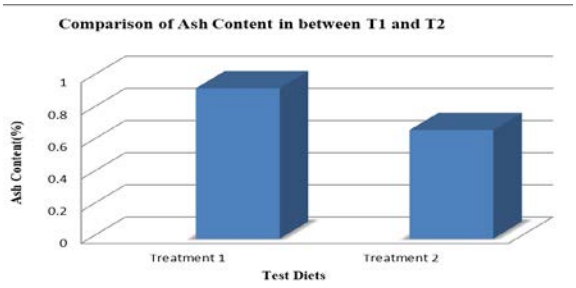

Figure 8. Comparison of ash content in fish body between two different diets

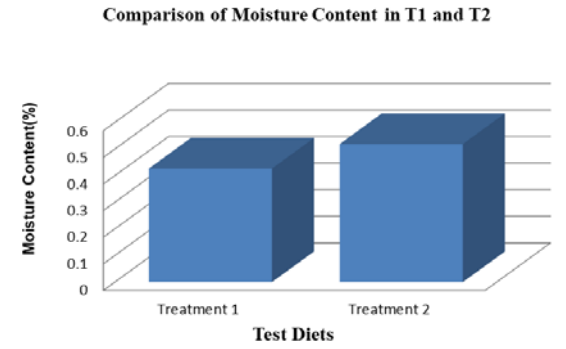

Figure 9. Comparison of Moisture content in the body of fish between two different diets

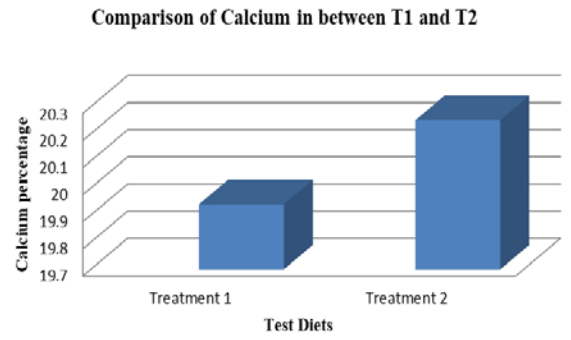

Figure 10. Comparison of calcium content in the body of fish between two different diets

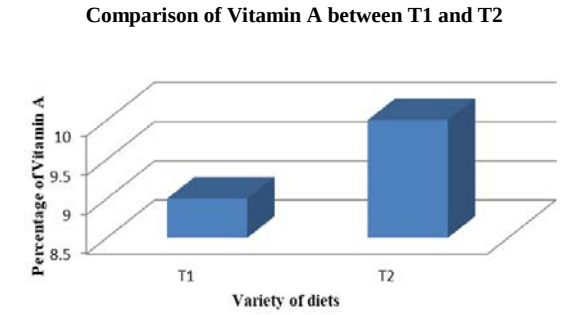

Figure 11. Comparison of Vitamin A content in the body of fish between two different diets

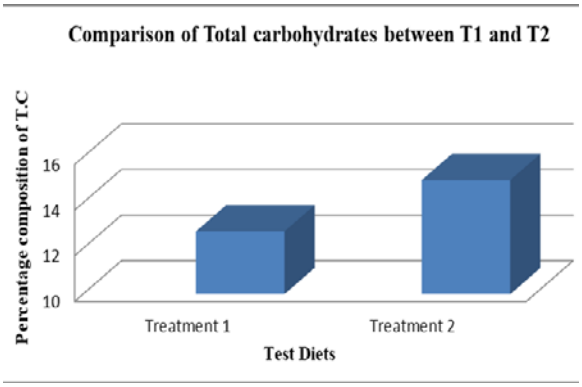

Figure 12. Comparison of Total carbohydrates content in the body of fish between two different diets

5. Discussion

In this current research, juveniles of yellow fin sea bream *Acanthopagrus arabicus* were utilized and they fed on two different compositional diets for eight weeks with different nutritional qualities under controlled conditions with weekly assessment of water quality parameters along with length and weight relationship. According to the results, the weight gain of the juveniles nourished using fish meal diet was a little higher than the juveniles fed with soybean meal but there was no significant difference so it is suggested that fish meal can be substituted by the cheaper soybean meal because it can be the appropriate diet for juveniles of *Acanthopagrus arabicus* that can give us an idea about better growth similarly like the fish meal. According to the Gallagher (1994), it was observed that the swapping of the soybean meal with the fish meal has been performed in the hybrid striped sea bass fish with different protein concentrations for 12 weeks trial and found that the gained weight of fish as compared to the initial weight in both the treatments was not significantly different and this trial was performed on variety of juveniles having different body weight and size then concluded that there were no noteworthy difference has been found for changing the diet so it was suggested that fish meal can be replaced by vegetable meal (Gallagher,1994). In 2019, Huaqun *et al.* conducted an eight-week trial focusing on the replacement of fish meal with soybean meal in the juveniles of the obscure puffer (*Takifugu obscurus*). During this trial, they meticulously observed various growth parameters. As a result, they came to the same conclusions: there was no significant difference in weight gain, and the juvenile fish showed a specific growth rate (Huaqun *et al.*, 2019). Kissil *et al.* (2000) claims that they carried out a 56-day experiment in which they investigated biochemical parameters by substituting soybean and rapeseed meal for fish meal. Following the trial, the concentration of protein and ash showed no discernible variances; however, the lipid and energy levels varied. In summary, they found that young sea bream can successfully get protein from both soybean and rapeseed (Kissil *et al.*, 2000). De Francesco *et al.* claim that they conducted an experimental trial on the eating behavior of gilthead sea bream in 2007 and switched the FM diet intended for a diet high in plant protein. It was determined that whereas feed efficacy and protein efficacy ratio were better in the sea bream PP diet, the intake of feed was higher in the sea bream FM diet. In contrast to PP, meals containing Fish Meal (FM) exhibited higher levels of moisture content but lower amounts of PUFA (polyunsaturated fatty acids) and MUFA (monounsaturated fatty acids) (De Francesco *et al.*, 2007).

Ajani *et al.* (2016) conducted a trial in which fish meal was relieved with four altered types of soybean meal: partial soybean meal, no soybean meal, only soybean meal, and soybean with methionine; the results revealed the average gain in weight, that was 22.77 grams and length was 16.90 grams which is notably raised in partial soybean meal (PSM) and a smallest amount found in no soybean meal (NSM) that was 17.54 grams and 14.63 cm (Ajani *et al.*, 2016). According to the previous studies, the outcomes showed that the specific growth rate and feed conversion ratios were slightly higher in diet 2 than the diet 1, while the conversion of feed was slightly greater in diet 1.

In 12-weeks trial on gilthead sea bream, fish oil and fish meal were substituted by different plant proteins, and the findings revealed that there was no statistically significant difference in weight gain between the two diets when 40 or 60 percent of the fish meal was interchanged by the plant proteins, but there was a slight loss of weight when 65 percent of the FM and 65 percent of the FO were substituted (Dias *et al.*, 2009). According to Wang *et al.* (2006), they studied *Nibea miichthioides* growth after replacing fish meal with soybeans, and they came to the conclusion that as the concentration of fish meal in the diet decreased, so did weight decreases, and it was noted that replacing 20% of the fish meal with soybeans had no discernible special effects, while replacing 100% of the fish meal had weight loss (Wang *et al.*, 2006). The results of the 12 week experimental study showed no discernible differences in weight increases; nevertheless, the rate of specific growth was higher in the control diet, which contains animal meal, than in the other diets, which used soybean meal as a substitute at rates of 12 and 36 percent. The FCR was also lower than with the other interventions (Karalazos *et al.*, 2007). After 125-day trial substituting soybean meal for fish meal in the diets of rainbow trout (*Oncorhynchus mykiss*), it was found that there were no significant differences in weight, specific growth rate, or feed conversion ratio. As a result, it was recommended that soybean meal can be substituted for 80 percent fish meal in rainbow trout adults (Voorhees, 2019). According to the results of the contemporary study, it was found that we can either completely replace fish meal (FM) with soybean meal (SM) because there is no noteworthy change in the growth and survivability of fish juveniles thus the meal having the vegetable origin would be the good replacement for the aqua culturist.

Moreover, fish species' growth indices would be adequate, and their survival rates would be 100%. In our research trial, we have adjusted the physicochemical parameters at optimum level as mentioned in our results to avoid any discrepancy. Jian and Cheng (2003) worked on the salinity and temperature tolerance of *A. latus* in which they concluded that the highest tolerated salinity could be 50‰ when they gradually increased the salinity levels (Jian and Cheng, 2003). Iqbal *et al.* (2012), worked on *Oreochromis niloticus* to reveal the impact of salt concentration on the progression of fish and the outcomes revealed the mean WG (weight gain) and mean LG (length gain) greater at higher levels of salinity and in contrast

reduced growth was observed in control group. Moreover, feed conversion ratio (FCR) was also found increasing with the raised levels of salinity thus better growth was observed in increasing salinity levels (Iqbal *et al*., 2012). Endurance and growth in juveniles of fish were not being affected at various salinity levels until temperature would be greater than 27 ^{0}C, but it can produce prominent effects when the temperature would be beneath 25 ^{0}C (Watanabe *et al*., 1989). The species of sea bream are susceptible to oxidative stress, and it was determined that the fatal concentration of dissolved oxygen was approximately 0.1 milligrams per litre; for this reason, *Sparidentex hasta* is classified as an oxy-conformer (Zainal, 2016). In the current thesis, DO was adjusted at 7 to 8 mg/l, which is thought to be a satisfactory range for the species of sea bream to grow more successfully. Rahim *et al.* (2017) studied the growth factors of juveniles of black fin sea bream in brackish water ponds where fish were fed a variety of artificial diets and the physicochemical properties of the ponds modified such as salinity ranged between 15 and 20 parts per thousand, range of temperature stayed between 25 °C to 28 °C, pH ranged from 7.6 to 7.8, both ponds remained slightly alkaline; nitrite, nitrogen and ammonia concentrations was less than 0.001 mg/l. DO ranged from 5.6 to 7.5 mg/l. In their 2015 study, Rahim *et al.* conducted a controlled cultivated experiment, maintaining optimal values for water quality parameters. Specifically, dissolved oxygen (DO) was held at 6.5±0.4 mg/l, pH around 7.3±0.2, temperature at 26±0.3°C, ammonia and nitrites registering less than 0.01 mg/l, and salinity maintained between 15 and 16 parts per thousand (Rahim *et al*. 2015). Tseng and Hsu (1984) conducted an experiment in which they cultured marine copepods and *Acanthopagrus latus*, as well as these copepods used as a diet for the juveniles of *A. latus* that housed in aquaria with optimum aeration in sea water, with specific gravity of 1.015, temperature ranging from 25 to 28 ^{0}C, and salinity of 24 ppt (Tseng and Hsu, 1984). The study of proximate composition for the total body meat of juvenile fish was carried out in the current research experiment, and the findings for diets 1 and 2, which contain soybean meal and fish meal respectively, were discovered. Yang *et al.* (2015) conducted an experimental trial in which they observed the effects of substituting fish meal with soybeans on the growth of juveniles of *Litopenaeus vannamei*. Their main finding was that the amount of crude protein in the juveniles' bodies was higher in the diets containing 4.28% ESBM than the diets containing 25.26% ESBM, while the concentration of crude lipid of the juveniles' bodies was higher in the diets containing 11% ESBM (Yang *et al*., 2015). Thus the dietary interventions very minimally changed the contents of fatty acids (Karalazos *et al.,* 2007). Rahim *et al.* (2017) contributed a preliminary study on growth factors using juvenile black fin sea bream as the target species in brackish water ponds. Fish were fed a variety of artificial diets, and the proximate composition of the treated groups was analogous to the control groups in terms of moisture and ash concentration. However, the lipid and protein concentration of the treated clusters was greater than that of the control groups, and it was determined that feeding diets with a combined 42 percent protein content and 20 percent lipid content is optimum for cultivating black fin sea bream. Also, it was determined that there was no discernible difference between the treated and control groups' body compositions (Rahim *et al.,* 2017). The Gilthead sea bream (*Sparus aurata*) was used in an experiment to define the effects of mannan oligosaccharides on two different intakes made of fish meal and soybeans, which have different nutrient compositions. The findings showed that neither diet significantly changed the nutrient composition of the body nor the final WG, PER, SGR, or FCR (Dimitroglou *et al*., 2010). Rahim *et al.* (2016) conducted an experiment on young *A. berda* fish in which artificial diets with varying protein composition were fed to the fish. The results showed increased weight gain and growth intensity at 40% and 50% protein ratios, and the biochemical analysis of the whole fish showed that the moisture content was higher in the fish fed diets of 40% to 50% than the 20 to 40% protein diet, while the lipid content at 40% to 50% was observed (Rahim *et al*., 2016). Rahim *et al.* (2015) studied different lipid concentrations and observed changes in growth indices in *A. berda*. They fed 42 percent protein diet with various lipid concentrations as 15%, 20%, 25%, and 30%. It was found that the 20 percent lipid-containing diet revealed the highest WG, SGR, and lowest FCR, and that the product quality of meat, particularly ash content, protein, and lipid profile, was unaffected by any lipid variations in diet (Rahim *et al.,* 2015).

Alasalvar *et al.* (2002) studied the *Dicentrarchus labrax* commonly named as sea bass and determined that there were substantial changes between wild and cultivated sea bass based on the amount of fatty acids and minerals in the flesh of fish (Alasalvar *et al*., 2002). Similar work has been done by another researcher who assessed the differences between the wild and farmed gilthead sea bream. In this study, the analytical units were flesh attributes, and the main factors were morphological traits, fat content, and fatty acid profile. Higher lipid content and lower GSI levels were detected in cultured fish than in wild fish, respectively. Moreover, morphological traits were varied between fish from the wild and those raised in captivity (Grigorakis et al., 2002). Similar research was done by Orban *et al.* (2003) using two other species of fish, *Sparus aurata* and *Dicentrarchus labrax*, to assess the variations in lipid content between farmed and wild fish. They discovered that each of the cultured species had higher levels of lipid content than the wild species (Orban *et al.,* 2003). The juveniles of *Acanthopagrus arabicus* were the target species in Ahmad *et al.* (2018) study; the work has been done on the relationship between feeding frequency proportions and defensive capabilities, body nutritional composition, and growth rate. The results showed that growth rates were best at 7 percent body weight/day, with the smallest growth rates being 5 percent, 9 percent, and 1 percent weight gain after treatments. Protein and ash levels did not alter much; however, fat content did increase with increasing feeding frequency (Ahmad *et al.* (2018). Peres and Oliva-Teles (1999) studied the effects of feed modifications in terms of the developmental growth of juvenile European sea bass. They fed the juveniles feed containing 48 percent protein with higher lipid intensity levels of 12, 18, and 30 percent. In contrast to other diets with larger amounts of lipid, it was found that low lipid diets had higher quantities of protein, and their lipid and calorie contents were also reduced. The results showed that raising the nutritive lipid percentage

from 12 to 24% does not impact growth developmental rates, feed competence, or protein. Liver lipid concentration was greater in diets with the highest levels of lipids, but it had no impact on the lipid content of the muscles. Yet, a diet with 30 percent lipids can reduce protein and calorie content while having no negative effects on development (Peres and Oliva-Teles, 1999). Fish oil is one of the best sources of efficiency, intensity, and strength, followed by soybean oil, according to Rahim *et al.* (2017), who conducted a preliminary research trial on the juveniles of *A. berda* and fed them on four different feeds with oil: fish oil, soybean oil, palm oil, and olive oil (Rahim *et al*., 2017).

6. Conclusion

The current research was intended to carry out some fundamental investigations on the effectiveness of feed on *Acanthopagrus arabicus* in light of market requirements and the importance of produced fish's nutritional quality. The work that was scheduled was intended to provide knowledge and information on the evaluation of macromolecules using a variety of biochemical analyses and chemical tests to correlate with the obvious characteristics necessary for a particular fish species' culture to advance robustly. Therefore, in the light of our results it is concluded that fish meal can be substituted by the soybean meal because it can be the appropriate diet for juveniles of *Acanthopagrus arabicus.* Research undertaken gives an idea for cheap ad cost-effective soybean meal that can replace effortlessly other high cost fish meal to achieve good market oriented results.

Acknowledgments

The authors of the paper would like to express sincere thanks to Mr. Iqbal for graciously granting us access to the multitude of cutting-edge facilities available at the AGQ lab. Our project has greatly benefited from the unwavering assistance provided by the Dean’s grant, whose support has been instrumental in our research endeavors ((DFS-KURP No. 139/2021-22).

References

Ahmad, N., Pirzada, J. A. S., Khan, K. M., Ali, A., Khokhar, F. N., and Amir, S. A. 2020. Feeding frequency influences the growth performance of yellowfin seabream (Acanthopagrus arabicus) in cage culture. *Iran. J. Fish. Sci.*, **19**, 1073-1082.

Ahmad, N., Siddiqui, P. J. A., Akbar, N. U., Rashid, M., and Masroor, R. 2018. The growth performance of juvenile yellow fin seabream (*Acanthopagrus arabicus*) fed at different feeding rates while reared in floating net cages. *J. Anim. Plant Sci.*, **28**:1014-1020.

Ahmad, N., Siddiqui, P. J. A., Ali, A., Khan, K. M., Masroor, R., ul Akbar, N., and Attaullah, M. 2019. Dietary protein level in the practical diet of yellowfin seabream, acanthopagrus arabicus, juveniles for optimum growth performance, survival and carcass composition. *Pak. J. Zool.*, **51**, 1003.

Ajani, E. K,. Orisasona, O., Omitoyin, B.O. and Osho, E. F. 2016. Total Replacement of Fishmeal by Soybean Meal with or Without Methionine Fortification in the Diets of Nile Tilapia, *Oreochromis niloticus. J. Fish, Aquat. Sci.,* **11**: 238-243.

Al Khawli, F., Pateiro, M., Domínguez, R., Lorenzo, J.M., Gullón, P., Kousoulaki, K., Ferrer, E. Berrada, H. and Barba, F.J. 2019. Innovative green technologies of intensification for valorization of seafood and their by-products. *Mar. Drugs,* **17**: 689.

Alasalvar, C., Taylor, K. D. A., Zubcov, E., Shahidi, F., and Alexis, M. 2002. Differentiation of cultured and wild sea bass (*Dicentrarchus labrax*): total lipid content, fatty acid and trace mineral composition. *Food Chem.*, **79**: 145-150.

AlKatrani, L. M. A. A. 2023. Direct transfer to different salinities and its effect on energy and metabolic enzymes in juveniles and adults of yellowfin sea bream *Acanthopagrus arabicus. J. Fish Biol.*, **102**: 1510-1516

AOAC. 2000. Official Methods of Analysis. 17th Edition, The Association of Official Analytical Chemists, Gaithersburg, MD, USA. Methods 925.10, 65.17, 974.24, 992.16.

Dabrowski, K., Terjesen, B. F., Zhang, Y., Phang, J. M. and Lee, K. J. 2005. A concept of dietary dipeptides: a step to resolve the problem of amino acid availability in the early life of vertebrates. *J. Exp. Biol.*, **208**: 2885-2894.

De-Francesco., Parisi, M., Perez-Sanchez, G., Gomez-Requeni, J., Medale, P., Kaushik, S. J. and Poli, B. M. 2007. Effect of high level fish meal replacement by plant proteins in gilthead sea bream (*Sparus aurata*) on growth and body/fillet quality traits. *Aquac. Nutr.*, 13: 361-372.

Dias, J., Conceição, L. E., Ribeiro, A. R., Borges, P., Valente, L. M. and Dinis, M. T. 2009. Practical diet with low fish-derived protein is able to sustain growth performance in gilthead seabream (*Sparus aurata*) during the grow-out phase. *Aquaculture*, **293**: 255-262.

Dimitroglou, A., Merrifield, D. L., Spring, P., Sweetman, J., Moate, R. and Davies, S. J. 2010. Effects of mannan oligosaccharide (MOS) supplementation on growth performance, feed utilisation, intestinal histology and gut microbiota of gilthead sea bream (*Sparus aurata*). *Aquaculture*, **300**: 182-188.

Erkan, N. and Özden, Ö. 2007. Proximate composition and mineral contents in aqua cultured sea bass (*Dicentrarchus labrax*), sea bream (*Sparus aurata*) analyzed by ICP-MS. *Food Chem.*, **102**:721-725.

FAO. 2018. *The State of World Fisheries and Aquaculture 2018*. Meeting the sustainable development goals. *Rome. Italy*, **223**: 1-227.

Gallagher, M. L. 1994. The use of soybean meal as a replacement for fish meal in diets for hybrid striped bass (*Morone saxatilis M. chrysops*). *Aquaculture*, **126**:119-127.

Gil, A.; Gil, F. 2015. Fish, a Mediterranean source of n-3 PUFA: Benefits do not justify limiting consumption. *Br. J. Nutr.*, **113**: 58–67.

Grigorakis, K., Alexis, M. N., Taylor, K. A. and Hole, M. 2002. Comparison of wild and cultured gilthead sea bream (*Sparus aurata*); composition, appearance and seasonal variations. *Int. J. Food Sci & Tech.*, **37**: 477-484.

Hawk. H. W.. Tvler. W. J.. and Casida. L. E. 1954. Some factors affecting age at puberty in Holstein-Friesian heifers. *J. Dairy Sci.*, 37, 252-258. https://doi.org/10.1111/jfb.15393

Huaqun Ye, Minglei Xu , Qingying Liu, Zhenzhu Sun, Cuiyun Zou, Leling Chen, Ningning Su. and Chaoxia Ye. 2019. Effects of replacing fish meal with soybean meal on growth performance, feed utilization and physiological status of juvenile obscure puffer, *Takifugu obscures. Comp. Biochem. Physiol. C: Pharmacol. Toxicol. Endocrinol.*, **216**:75-81.

Iqbal, K. J., Qureshi, N. A., Ashraf, M., Rehman, M. H. U., Khan, N., Javid, A. and Majeed, H. 2012. Effect of different salinity levels on growth and survival of Nile tilapia (*Oreochromis niloticus*). *J. Anim. Plant Sci.*, **22**: 919-922.

Iwatsuki, Y., 2013. Review of the *Acanthopagrus latus* complex (Perciformes: Sparidae) with descriptions of three new species from the Indo-West Pacific Ocean. *J. Fish Biol.*, **83**: 64-95.

Izadpanah, E., Saffari, S., Keyvanshokooh, S., Torfi Mozanzadeh, M., Mousavi, S. M. and Pasha-Zanoosi, H. 2022. Nano-selenium supplementation in plant protein-based diets changed thyroid hormones status and hepatic enzymes activity in Acanthopagrus arabicus female broodfish and their offspring, *Aquac. Rep*., **24**: 1-6.

Jian, C.Y. and Cheng, S. Y. 2003. Temperature and salinity tolerances of yellowfin sea bream (*Acanthopagrus latus*) at different salinity and temperature levels. *Aquac. Res.*. **34**:175 - 185.

Kalhoro, H., Malik, A., Abbas, G., Kalhoro, I. B., Shah, S. A., and Kalhoro, H. (2017). Evaluation of the Growth Performance, Body Composition and Survival Rate of Juvenile Snakehead (Channa marulius) Fed on Different Feeds. *Pak. J. Zool.*, *49*.

Karalazos, V., Treasurer, J., Cutts, C. J., Alderson, R., Galloway, T. F., Albrektsen, S. and Bell, J. G. 2007. Effects of fish meal replacement with full-fat soy meal on growth and tissue fatty acid composition in Atlantic cod (*Gadus morhua*). *J. Agric Food Chem.*, **55**: 5788-5795.

Kissil, G. W., Lupatsch, I., Higgs, D. A. and Hardy, R. W. 2000. Dietary substitution of soy and rapeseed protein concentrates for fish meal, and their effects on growth and nutrient utilization in gilthead seabream *Sparus aurata*, L. *Aquacult Res.*, **31**: 595-601.

Mohsin, M., Mu, Y. T., Hengbin, Y., Memon, A. M., Noman, M., and Mehak, A. (2019). Implications of historic development and economic performance of molluscan fisheries in China 1950-2017. *Indian J. Mar. Sci.*, *48*.

Mohtashemipour, M., Mohammadian, T., Torfi Mozanzadeh, M., Mesbah, M. and Nejad, A. J. 2024. Dietary Selenium Nanoparticles Improved Growth and Health Indices in Asian Seabass (*Lates calcarifer*) Juveniles Reared in High Saline Water", *Aquac Nutrn*, 2024:1-13. https://doi.org/10.1155/2024/7480824

Næss, T., Germain-Henry, M. and Naas, K. E. 1995. First feeding of Atlantic halibut (*Hippoglossus hippoglossus*) using different combinations of Artemia and wild zooplankton. *Aquaculture*, **130**: 235-250.

Njinkoue, J. M., Gouado, I., Tchoumbougnang, F., Ngueguim, J. Y., Ndinteh, D. T., Fomogne-Fodjo, C. Y., and Schweigert, F. J. 2016. Proximate composition, mineral content and fatty acid profile of two marine fishes from Cameroonian coast: Pseudotolithus typus (Bleeker, 1863) and Pseudotolithus elongatus (Bowdich, 1825). *Nutr. Food Sci J.*, 4, 27-31.

Orban, E., Nevigato, T., Lena, G. D., Casini, I. and Marzetti, A. 2003. Differentiation in the lipid quality of wild and farmed seabass (*Dicentrarchus labrax*) and Gilthead Sea bream (*Sparus aurata*). *J. Food Sci*, **68**: 128-132.

Pateiro, M., Munekata, P. E., Domínguez, R., Wang, M., Barba, F. J., Bermúdez, R., and Lorenzo, J. M. 2020. Nutritional profiling and the value of processing by-products from gilthead sea bream (*Sparus aurata*). *Mar. Drugs*, 18, 101.

Peres, H., and Oliva-Teles, A. 1999. Effect of dietary lipid level on growth performance and feed utilization by European sea bass juveniles (*Dicentrarchus labrax*). *Aquaculture*, **179**:325-334.

Rahim, A., Abbas, G., Naeem, M., Ferrando, S., Gallus, L., Hafeez-ur-Rehman, M. and Mateen, A. 2017. Effect of Different Dietary Oils on Growth, Feed Conversion and Body Composition of Juvenile Black Fin Sea Bream, Acanthopagrus berda (Forsskal, 1775). *Pak. J. Zool.*, **49**: 655-661.

Rahim, A., Abbas, G., Waryani, B., Ghaffar, A., Monwar, M., Hafeez-ur-Rehman, M., and Dastagir, G. 2015. Influence of Varying Dietary Lipid Levels on Growth, Feed Conversion and Chemical Composition of Meat and Liver of the Juvenile Blackfin Sea Bream, Acanthopagrus berda (Forsskal 1775). *Pak J. Zool.*, **47**: 1467-1473

Rahim, A.., Abbas, G., Ferrando, S., Gallus, L., Ghaffar, A., Mateen, A., Hafeez-ur-Rehman, M. and Waryani, B. 2016. Effects of Varying Dietary Protein Level on Growth, Nutrient Utilization and Body Composition of Juvenile Blackfin Sea Bream, Acanthopagrus berda (Forsskal, 1775). *Pak J. Zool*., **48**: 1089-1097.

Rustad, T., Storro, I. and Slizyte, R. 2011. Possibilities for the utilisation of marine by-products. *Int. J. Food Sci. Technol.,* **46**: 2001–2014.

Sadek, S., Osman, M. F. and Mansour, M.A. 2004. Growth, survival and feed conversion rates of sea bream (*Sparus aurata*) cultured in earthen brackish water ponds fed different feed types. *Aquac. Intl*., **12**: 409–421.

Saffari, S., Keyvanshokooh, S., Torfi Mozanzadeh, M., and Shahriari, A. 2021. Effects of nano Selenium supplementation in plant protein rich diet on reproductive performance. *Aquac. Nutr*., 27: 1959-1971.https://doi.org/10.1111/anu.13332

Sarvi, B., Kolkovski, S., Rafiee, G. R., Pourmozaffar, S., Nazemroaya, S., and Alibeygi, T. 2023. The effect of delayed first feeding on growth and survival of yellowfin seabream (Acanthopagrus arabicus) larvae. *Aquac. Rep*., ***32***: 101695.

Triebold, H.O. and Aurand, L.W. (1963). **Food Composition and Analysis, Van Nostrand (Eds.),** New York , pp. 23-24

Tseng, W. Y. and Hsu, C. K. 1984. Studies on the culture of the marine copepod Tigriopus japonicus Mori and its value as a food for juveniles of the yellow-fin sea bream Acanthopagrus latus (Houttuyn). *Crustaceana. Supplement.*: 381-389.

Voorhees, J. M., Barnes, M. E., Chipps, S. R., and Brown, M. L. 2019. Bioprocessed soybean meal replacement of fish meal in rainbow trout (*Oncorhynchus mykiss*) diets. *Cogent Food Agric*., **5**: 1579482.

Wang, Y., Kong, L. J., Li, C. and Bureau, D. P. 2006. Effect of replacing fish meal with soybean meal on growth, feed utilization and carcass composition of cuneate drum (*Nibea miichthioides*). *Aquaculture*, **261**: 1307-1313.

Watanabe, W. O., French, K. E., Ernst, D. H., Olla, B. L. and Wicklund, R. I. 1989. Salinity during early development influences growth and survival of Florida red tilapia in brackish and seawater. *J. World Aquac. Soc.*, **20**: 134-142.

Yang, Q., Tan, B., Dong, X., Chi, S. and Liu, H. 2015. Effect of replacing fish meal with extruded soybean meal on growth, feed utilization and apparent nutrient digestibility of juvenile white shrimp (*Litopenaeus vannamei*). *J. Ocean Univ. China*, **14**: 865-872.

Yesser, A. K. T., Al-Faiz, N. A., and Hussein, S. A., 2016. Impact of feeding levels on growth performance and food conversion of Acanthopagrus arabicus cultivated in concrete tanks at Basrah province. *Iraqi J. Aquacult.*, **13**: 109-124.

Zainal, K. 2016. Aspects on respiratory physiology of cultured Sea bream, *Sparidentex hasta* (Valenciennes 1830), Kingdom of Bahrain. *J. Assoc. Arab Univ. Basic Appl. Sci*., **20**: 1-7.

JJBS

Volume 17, Number 4,December 2024
ISSN 1995-6673
Pages 623 – 628
https://doi.org/10.54319/jjbs/170405

Jordan Journal of Biological Sciences

Assessing the Productivity and Effectiveness of Various Sorghum (Sorghum bicolor L. Moench) Genotypes in Semi-arid Environments

Fakher J. Aukour[1,*]; Nabeel Bani Hani[2] and Omar Mahmoud Al zoubi[3]

[1] Dept. Land Management and Environment. Prince Al-Hassan Bin Talal Faculty of Natural Resources and Environment. The Hashemite University, Jordan. ; [2]Nabeel Bani Hani. Director of Laboratory. Irrigation and Soil Researcher. National Agricultural Research Center (NARC), Jordan; [3]Omar Mahmoud Al zoubi. Biology Department, Faculty of Science Yanbu, Taibah University, Yanbu El-Bahr 46423, Saudi Arabia;

Received: March 15, 2024; Revised: April 28, 2024; Accepted: May 13, 2024

Abstract

Jordan as a Mediterranean country is facing climatic change which results in increasing temperatures and a reduction in precipitation. So, there is a need to find sorghum genotypes that can resist such variations in environmental conditions. Field experiments were conducted under semi-arid conditions at the Dir-Alla agriculture research station in Jordan Valley to evaluate eight sorghum genotypes (ICSV_745, CSV_93046_9, CSV_15, JJ_1041, ICSV_112, S_35, ICSR_93034, EZRA' 7) for their stability, above-ground biomass, seed yield, and number of cuts under drought-prone environment. Results showed genotypic differences in WUE, above-ground biomass, seed yield, and HI. WUE increased with an improved HI leading to higher above-ground biomass. Linear relationships were observed between aboveground biomass, HI, and WUE. The results showed differences between the first cut compared to the following cuts. We recommend using VSV-15 with the highest value for both above-ground biomass and seed yield, followed by S_35. The S-35 showed optimistic potential to be used as fresh green forage when the whole plant is used at maturity, or can simply utilize the highest fresh weight achieved from its first cut.

Keywords: semi-arid, Jordan Valley, sorghum, climate change, above-ground biomass, Sorghum bicolor L.

1. Introduction

One of the perilous defies that face the world is the necessity to fulfill the food requests of the intensely rising population (Al-Ghzawi et al., 2018). The world population is estimated to rise by 34% by 2050, with an extra 2.3 billion people, based on the FAO forecasts (FAO, 2009). To confirm worldwide growth, cereal production must be increased by 43% on a global scale**.** This growth will be enhanced by changing climate and new defies facing agriculture (Barbeau et al., 2015; Al-Ghzawi et al., 2019). The most significant obstacle to agricultural productivity in arid and semi-arid regions is water, which is usually caused by low and/or uneven rainfall distributions (Jahanzad et al., 2013, Keshavarz et al., 2014). Crop growth depends on climate as plant physiological processes react directly to changes in temperature and moisture availability (McKenzie and Andrews, 2010). These factors have numerous impacts on established plant behaviors, including defects in photosynthesis, reductions in leaf area, and the sugar content of cereals including sorghum (Sorghum bicolor L.) (Plaut, et al., 2004).

Several studies have been conducted to improve crop production including sorghum to fulfill the higher demand to face the expected increase in world population. Since the future scenarios of climate change predict decreasing precipitation and increasing temperature, Jordanian scientists demonstrated that sustainable cereal yield growth is crucial, and new breeding strategies are needed to develop high-yielding, stress-resistant genotypes. Developing new genotypes with improved drought adaptation and increased yield per unit area is also essential for crop improvement under rainfed conditions in Jordan (Al-Abdallat et al., 2017).

In Jordan, the climate varies considerably across different regions. For instance, the western areas experience a Mediterranean climate, marked by hot, dry summers and mild, wet winters (Al-Bakri et al., 2011). Rainfall in this region exhibits notable variability both within and between years. The climate in the highlands of Jordan and its surrounding areas is characterized by mild summers and cold winters (Al-Bakri et al., 2011). Rainfall starts in October up to March. The annual rainfall ranges from 30 to 100 mm in the steppe desert, while it exceeds 600 mm in the highlands, with significant variability between and within the regions. Rainfall decreases while moving from west to east and from north to south. Since almost 91.4% of Jordan's land is desert and has no economic significance except from occasional, short-term grazing during specific seasons of the year, the country is categorized as a low rainfall zone (Al-Karablieh and Jabarin, 2010). According to the Third National Communication on Climate Change produced by Jordan in 2014 (MoEnv, 2014), it is predicted that Jordan is anticipating a warm climate with possible temperature increases of 2.1 ºC to 4 ºC by the end of the

* Corresponding author. e-mail: fakagr67@hu.edu.jo.

century. It also expects a dry climate with potential cumulative precipitation decreases of up to 21%, particularly in the western region of the country, and more frequent and severe droughts.

Sorghum is the fifth-most significant cereal crop regarding global sowing and distribution (Kimber, 2000, Gognsha and Hiruy, 2020). Rainfed crops adapted to dry climates in arid and semiarid environments (Saddam, S. et al., 2014) and are utilized for both seed and biomass purposes as food, fodder, forage, and biofuel (Assefa et al., 2020; Bollam, 2021; Ostmeyer et al., 2022). Sorghum forage production is influenced by various factors such as high-yielding cultivars, effective weed control strategy, seed vigor, sowing date, and depth, fertilizer, and irrigation. Because it can withstand unusual abiotic challenges like heat and drought (Pennisi, 2009; Chiluwal et al., 2018), use available resources efficiently (Van Oosterom et al., 2001, Qi et al., 2016), and adapt genetically to a variety of ecological conditions with limited water and soil fertility (Ahmad, W., et al., 2016), it is a great alternative feed source. It also shows promise for future growth. (Bibi and others, 2012).

In Jordan, Sorghum is not well known and is distributed as animal feed and mostly grown by limited resource farmers with low inputs and limited resources. Sorghum is planted in very small quantities in Jordan as a winter crop (FAO, 2022). Therefore, the objective of the current study was to evaluate the productivity of sorghum grown under full irrigation using mixed water (fresh and treated wastewater) effluent based on potential evapotranspiration calculated from meteorological data.

2. Materials and Methods

2.1. Study area and site description

This study was conducted at Deir-Alla Regional Agriculture Research Center, Located in Jordan Valley at 35°37′N longitude, 32° 13′ E latitude, and 224 m below sea level. Deir-Alla has a semi-arid climate with warm winters (minimum temperature is 15 ºC) scorching summers and an average of 280 mm of yearly rainfall. The mean yearly temperature is 30 ºC. In summer, the typical relative humidity is 30% compared to 70% in winter. The area experiences erratic rainfall patterns and is particularly vulnerable to drought. A potential evapotranspiration measures 2175.065 mm. The soil is extremely calcareous and non-saline.

2.2. 2.2 The experimental design and field experiment

2.2.1. water and irrigation schedules

The King Talal Dam (KTD) at the Zarqa River provided the study area's water resources through pressurized convey pipes. The water's moderate salinity ranges from 1.4 dS m-1 in the winter to roughly 3.0 dS m-1 in the summer, which could have a negative impact on salt accumulation in the soil profile and the degradation of land productivity.

Based on potential evapotranspiration calculated using the Penman-Monteith equation from meteorological data, the drip irrigation method used various kinds with mixed water effluent from King Talal Dam as full irrigation. It was used with 0.4 meters between lateral emitters and inline emitters (4 l h^{-1}). Disc filters was employed to reduce clogging of the water outflow to achieve and maintain irrigation efficiency. A drip irrigation system with four-liter-per-hour inline emitters spaced 40 centimeters apart and 40 centimeters apart between lateral lines based on the water demand of the crop (every 10 days).

To make sure that the water content in the soil was within the permitted range (75% of field capacity), soil water content was measured for each location at three distinct soil depths: 0–20, 20–40, and 40–60 cm. Soil water measurements were obtained in the time domain "Trime -FM3 TDR" (Imko GmbH, Ettlingen, Germany) using a reflectometer. Experimental plots were managed following the standard practices of the National Agriculture Research Center (NARC) including the application of fertilizers and pathogen and weed control.

2.2.2. cultivation and experimental design

At the end of June 2019, eight different Sorghum genotypes (ICSV_745, CSV_93046_9, CSV_15, JJ_1041, ICSV_112, S_35, ICSR_93034, EZRA' 7) were planted at Dair Alla agricultural station. The eight genotypes were grown in a randomized complete block design with twelve replications. Four replicates were kept for harvest, while the other eight replicates were used for growth analysis throughout the growing season. The plot area was 3 m^2 with 8 rows (0.40 m apart and 3.2 m long). The eight cultivars were randomly distributed in each plot, and two rows were cultivated with EZRA' 7 as borders to avoid edge effect.

To evaluate the crop productivity throughout the season, four replicates were kept to measure green above-ground biomass at harvest (before pod formation) with no cuttings throughout the season. The other four replicates were used to measure seed production at maturity (4 replicates) with no cuttings throughout the season, while the rest of the replicates (4 replicates) were cut three times throughout the season to measure the green above-ground biomass at three different growth stages to examine progressive vegetative growth (i.e. fresh forages from different cuts were subjected to air drying).

The first cut was harvested 65 days after planting; the second cut was taken 35 days after the first cut; and the third cut was taken at harvest time (physiological maturity), leaving at least 10 to 18 cm of stubble for fast recovery purposes following each cut.

The following traits were measured: Number of Branches Plant Height (cm); Stem Diameter (cm); Brush Length (cm); above-ground Biomass Fresh Weight (ton/ha); above-ground Biomass Dry Weight (ton/cut); Total Mature Fresh above-ground biomass (ton/ha); Total Mature Dry above-ground biomass (ton /ha); Seed Yield (ton /ha). Data for forage above-ground biomass & seed yields were calculated based on plants cut at ground level (net plot area) after physiological maturity (total above-ground biomass) or needed growth stage (cut). The height of the plant (cm) measured at 50% of its linear meter blooming from the bottom to the top. The green forage above-ground biomass per plot were determined using a spring balance and converted into fresh above-ground biomass weight per hectare, the dried plants were weighed again using a precision balance after being left in the sun for 10 days to determine the dry weight (DW). The weight

loss percentage was calculated by dividing DW / FW by 100 for each sample.

2.3. Water Use Efficiency and HI

Three WUEs were calculated as water use efficiency at maturity fresh weight, at maturity dry weight, and seed harvesting, measuring fresh weight / each cut and dry weight/cut. The water use efficiency (WUE) was calculated by dividing the produced above-ground biomass weight (fresh above-ground biomass, dry above-ground biomass, and seed weight) per amount of water applied (m^3). Harvest Index (HI): the weight of grain produced expressed as a proportion of the total weight of the plant.

2.4. Statistical Analyses

A Turkey-Kramer test within JMP statistical software version 11.0.0 (SAS Institute Inc., 2011) was used to evaluate the differences in means for all crop parameters among different Sorghum genotypes. The test is a genuine test with a 95% confidence level.

3. Results and Discussion.

Significant differences (P≥0.05) were observed among the eight tested genotypes in terms of plant height, stem diameter, and brush length (Table 1). Plant heights range from 97.0 cm in EZRA' 7 to 226 cm in ICSV_93046_9. Similarly, the stem diameter ranged from 1.4 cm in JJ_1041 to 2.20 cm in EZRA' 7. The brush length was 21.00 cm in S_35, followed by 20.88 cm in ICSR_93034, and the least was seen in EZRA' 7 with 8.96 cm.

Table 1. Comparison of mean physical parameters of different genotypes of sorghum*

Genotypes	Number of Branches	Plant height	Stem Diameter	Brush Length
		cm		
ICSV_745	4.8a	118.8g	2.02b	19.25e
ICSV_93046_9	3.3e	226.0a	1.91e	18.96f
CSV_15	4.3b	176.8d	1.78f	18.67g
JJ_1041	3.8d	200.3b	1.40h	20.42c
ICSV_112	4.0c	142.0f	1.68g	20.21d
S_35	2.8f	187.3c	1.99c	21.00a
ICSR_93034	3.8d	150.8e	1.97d	20.88b
EZRA' 7	4.8a	97.0h	2.20a	8.96h

*Means followed by the same letter are not statistically significant at P<0.05

S-35 genotype showed optimistic potential to be used as fresh green forage (147.6 ton/ha) when the whole plant is used at maturity, while EZRA' 7 was the lowest (32.9 ton/ha; Table 2). S-35 ranked first among the genotypes and yielded 147.6 ton/ha of above-ground biomass (Table 2). The same trend was observed in the three cuttings with a total of 138.2 ton/ha (Table 4). S-35 produced 41.3 ton/ha still has the highest dry weight (Table 2), followed by ICSR93034 (40.2 ton/ha), while the least dry weight was produced by EZRA' 7 (8.3 ton/ha). Table 2 illustrates that S-35 loses 72% of its original fresh weight, which represents a moderate value of percentage water loss compared to the rest of the genotypes. The highest percentage of water loss was seen at ICSR93034 with 90.3%, followed by CSV-15 with 88%, while EZRA' 7 lost just (43.4 %) as the least weight loss. WUE followed the same trend as fresh above-ground biomass weight, in that S-35 showed the highest value with 9.84 kg/m^3, as well as in the case of dry above-ground biomass weight with 2.75 kg/m3. EZRA' 7 has the lowest WUE value (2.19 & 0.55 kg/m3) at fresh and dry above-ground biomass respectively

Table 2. aboveground biomass (ton/ha) and WUE (kg/m^3) *

Genotypes	Aboveground biomass ton/ha (Yield)		%weight loss after drying	Aboveground biomass WUE (kg/m3)	
	Fresh	Dry		Fresh	Dry
ICSV_745	110.1d	28.0e	71.35937c	7.34d	1.87e
ICSV_93046_9	126.4c	32.0c	77.48677b	8.43c	2.14c
CSV_15	136.2b	28.6d	88.00977a	9.08b	1.91d
JJ_1041	65.3g	16.5g	62.16353d	4.35g	1.10g
ICSV_112	97.4e	24.6f	57.48891e	6.50e	1.64f
S_35	147.6a	41.3a	72.53442c	9.84a	2.75a
ICSR_93034	85.9f	40.2b	90.28372a	5.72f	2.68b
EZRA' 7	32.9h	8.3h	43.36373f	2.19h	0.55h

*Means followed by the same letter are not statistically significant at P<0.05.

3.1. Seed Production and WUE

The seed yield (Table 3) showed CSV_15 with 12.72 ton/ha as the highest value, followed by JJ_1041 with 11.36 ton/ha. In contrast, the ICSR_93034 and ICSV_745 genotypes show the least seed yield of 0.06 ton/ha. The same trend is shown in terms of seed WUE, in that the CSV_15 genotype exhibits the highest WUE value with 0.85 kg/m^3 followed by JJ_1041 with 0.76 kg/m^3, while the lowest value is seen at ICSR_93034 with a 0.004

kg/m^3. The highest HI value was seen for JJ_1041 genotypes with 0.687, and the lowest HI value was seen at the S-35 genotype.

Table 3. Seed productivity of different genotypes of sorghum at maturity*

Genotypes	Seed wt. ton/ha (Yield)	Seed WUE (kg/m^3)	HI
ICSV_745	0.06g	0.004g	0.002g
ICSV_93046_9	2.05d	0.137d	0.064e
CSV_15	12.72a	0.848a	0.444b
JJ_1041	11.36b	0.757b	0.687a
ICSV_112	5.22c	0.348c	0.212c
S_35	1.59e	0.106e	0.039f
ICSR_93034	0.06g	0.004g	0.001h
EZRA' 7	1.30f	0.087f	0.156d

*Means followed by the same letter are not statistically significant at P<0.05.

3.2. Productivity of sorghum genotypes at various cuts.

Table 4 shows the extent of statistical significance in the first cut (P≥0.05). The S-35 genotype showed the highest above-ground biomass obtained in the first cut with a 92.2 ton/ha, as well as WUE with a 13.2 ton/m^3, followed by the ICSR-93034 genotype with an 86 ton/ha above-ground biomass and a 12.3 kg/m^3 WUE. The lowest value was shown in EZRA'7 with 48.3 ton/ha of aboveground biomass and 6.9 kg/m^3 for WUE.

Table 4. Productivity of different genotypes of sorghum at different cuts*

Genotypes	Cut1		Cut2		Cut3		Total Yield		Average WUE	
	Yield	WUE	Yield	WUE	Yield	WUE	Fresh	Dry	Fresh	Dry
	ton/ha	kg/m3	ton/ha	kg/m3	ton/ha	kg/m3	ton/ha		kg/m3	
ICSV_745	70.8f	10.1f	64.5b	12.9b	5.7g	0.99g	141.0c	42.3c	8.00b	2.38c
ICSV_93046_9	85.2c	12.2c	48.6d	9.7d	7.9d	1.37d	141.6b	45.9b	7.75c	2.58b
CSV_15	77.6e	11.1e	33.3h	6.7h	3.9h	0.67h	114.8h	34.4g	6.14h	1.94h
JJ_1041	65.0g	9.3g	56.3c	11.3c	7.2e	1.24e	128.5f	38.5f	7.26g	2.17f
ICSV_112	84.6d	12.1d	44.0f	8.8f	11.4c	1.99c	140.0d	42.0d	7.62d	2.37d
S_35	92.2a	13.2a	40.2e	8.0g	5.8f	1.00f	138.2e	41.5e	7.41e	2.31e
ICSR_93034	86.0b	12.3b	68.3a	13.7a	13.7b	2.38b	168.1a	50.4a	9.45a	2.84a
EZRA' 7	48.3h	6.9h	47.2g	9.4e	32.0a	5.56a	127.5g	38.4g	7.30f	2.16g

*Means followed by the same letter are not statistically significant at P<0.05.

The results of the second cut demonstrate variations in above-ground biomass cuts and WUE. ICSR-93034 genotype demonstrates the highest above-ground biomass with 68.3 ton/ha as well as with a WUE of 13.7. kg/m^3, followed by ICSU-745 with 64.5 ton/ha and a WUE value of 12.9 kg/m^3. On the other hand, the values that were the lowest in WUE (Table 4) were seen at CSV_15 with 33.3 ton/ha and a WUE of 6.7 kg/m^3.

On the other hand, in the third cut, the EZRA' 7 genotypes showed the highest above-ground biomass with 32.0 ton/ha as well as with a WUE of 5.56. kg/m3. Followed by ICSR_93034 with 13.7 ton/ha and a WUE of 2.38 kg/m3. The lowest above-ground biomass in the second cut was seen for ICSV_745 with 5.7 ton/ha and a WUE of 0.99 kg/m3. The total above-ground biomass obtained as a sum of all the three cuts illustrated in Table 4 showed that ICSR_93034 has the highest above-ground biomass with 168.1 ton/ha and a WUE average value of 7.3 kg/m3, whereas CSV_15 had the lowest above-ground biomass, measuring 114.8 tons/ha and having a WUE of 34.4 kg/m3..

4. Discussion

Currently, Jordan's mean annual temperatures have increased dramatically, and this increase has been accompanied by less and unequal precipitation distribution (Ormann, 2018). This effect was seen in changes in vegetative cover deterioration and reduction in dominated genotype production (Aukour et al., 2013). Consequently, using well-adapted germplasm is a useful strategy to mitigate climate change related to heat stress and drought (Fita et. al., 2015; Al-Ghzawi et al., 2017). Predictions indicate that water demand will rise significantly owing to population growth, climate change, and the development of agricultural practices. Therefore, plant breeders are focused on creating water-use-efficient cultivars to avoid heat stress and drought in order to preserve sustainable agricultural production.

Sorghum is a vital crop in drier areas assisting more than 500 million people (Yahaya et al., 2021). It is a reasonably drought-tolerant crop adapted to cultivate and yield in marginal locations where it is difficult to other leading crops such as maize and wheat to survive. However, the yield of sorghum in the semi-arid regions is still below the world average of 2.5 ton/ha, primarily due to repeated droughts and heat stress. Therefore, the objectives of this study were to assess the impact of drought stress on eight sorghum genotypes to identify their ability to withstand semiarid conditions in the Jordan Valley. Results showed differences among tested genotypes. At maturity, statistical analysis for the whole cultivated (without cut) plants showed significant

differences among genotypes regarding above-ground biomass, percentage of weight loss after drying, and WUE for above-ground biomass. In other words, sorghum genotypes varied in their adaptation to arid environments and thus their aboveground biomass at drought-prone conditions. This was consistent with Zegada-Lizarazu et al. (2012) and Bani Hani et al. (2022), who demonstrated that Under drought stress, WUE is the main concern rather than the production itself, keeping in mind that WUE is the amount of above-ground biomass produced per unit of water used. Indeed, the current study revealed that WUE is the determinant of yield under stress and even as a component of crop drought resistance, since genotypes with the highest WUE produce the highest above-ground biomass and seed yield. In the current study, JJ_1041 genotypes showed the highest HI followed by CSV_15 as the most tolerant genotypes to the semiarid environment, while the least tolerant genotype (ICSR_93034), had the lowest HI values. This indicates that this genotype is non-tolerant to drought and cannot grow properly. These results suggested that HI can be a useful indicator by breeders for sorghum tolerance to semi-arid environments.

The current study showed a converse relationship was observed between the above-ground biomass production and the number of cuts. It is noticeable that in all genotypes above-ground biomass yield is reduced by repeated cuts, whereas the third cut yield is always the lowest in all genotypes. On the other hand, all other genotypes show that the WUEs were high in the second cut compared to the third cut. The results showed a slight difference in the case of the first cut compared with the second cut. For example, in the first cut, S-35 sorghum genotypes do not conserve the same orientation as other genotypes, the production value drops to the closest lower value. The genotype S-35 showed the highest WUE at the first cut which might be related to high production records when compared to other genotypes. Variations in WUE are shown in the second cut results, with ICSR-93034 showing the highest value and ICSU-745 following. In the second cut, the above-ground biomass obtained in all genotypes was less than that in the first one. ICSR_93034 genotype showed the highest above-ground biomass as well as WUE, while S-35 became the fifth genotype in harvested above-ground biomass. The same trend was seen in the third cut in which EZRA' 7 showed the highest above-ground biomass as well as the highest WUE. Additionally, the sum of the above-ground biomass from the three cuts revealed that ICSR_93034 had the highest above-ground biomass and WUE, while S-35 had the freshest above-ground biomass from the entire plant and CSV_15 had the lowest above-ground biomass and WUE. From all the above, the results show that the S-35 genotype has a high level of above-ground biomass production. This genotype has the potential to be drought-resistant and can be used as a substitute for animal feeds in Jordan, provided that continuous feeds are obtained through multiple rapid cultivations, first cut, or the entire plant. In terms of propagation characteristics, Sorghum JJ_1041 yielded 11.36 tons/ha, which was less compared to the highest seed output of 12.72 tons/ha produced by CSV_15. However, the S_35 genotype had a significantly low seed yield of just 1.59 tons/ha, indicating its inability to reproduce well under dry and drought-prone conditions

5. Conclusions

Results presented in this study showed that as the number of cuts increased during the sorghum lifespan, above-ground biomass decreased. A significant difference is presented among genotypes. Also, the high HI genotype had high WUE, hence producing more above-ground biomass and seed yield. To cultivate sorghum for dual purposes (fresh above-ground biomass and seed production), it is recommended to use VSV-15 with the highest value for both above-ground biomass and seed production.

Ethical Responsibilities of Authors

The manuscript is not under consideration or submitted to other journals for simultaneous consideration. The submitted work is original and has not been published elsewhere in any form or language (partially or in full).

Acknowledgment

This work has been accomplished under the supervision and support of the National Center for Agriculture Research and Extension, Jordan.

References

Fita, A. Rodr´ıguez-Burruezo, M. Boscaiu, J. Prohens, and O. Vicente, (2015). “Breeding and domesticating crops adapted to drought and salinity: a new paradigm for increasing food production,” Front. Plant Sci., vol. 6, p. 978, 2015

Abebe Assefa, Aemiro Bezabih, Getawey Girmay, Tesfaye Alema yehu & Alemu Lakew | Manuel Tejada Moral (Reviewing editor) . (2020). Evaluation of sorghum (*Sorghum bicolor (L.) Moench*) genotype performance in the lowlands area of wag lasta, north eastern Ethiopia, Cogent food agric, **6**:1, DOI: 10.1080/23311932.2020.1778603.

Ahmad, W., Noor, M. A., Afzal, I., Bakhtavar, M. A., Nawaz, M. M., Sun, X., Zhou, B., Ma, W., & Zhao, M. (2016). Improvement of Sorghum Crop through Exogenous Application of Natural Growth-Promoting Substances under a Changing Climate. Sustainability, **8(12),** 1330. https://doi.org/10.3390/su8121330.

M. Al-Abdallat, A. Karadsheh, N. I. Hadadd, M. W. Akash, S. Ceccarelli, M. Baum, M. Hasan, A. Jighly and J. M. Abu Elenein. 2016. Assessment of genetic diversity and yield performance in Jordanian barley (Hordeum vulgare L.) landraces grown under Rainfed conditions. BMC Plant Biol. (2017) **17**:191 DOI 10.1186/s12870-017-1140-1.

Al-Bakri JT, Suleiman A, Abdulla F, Ayad J (2011) Potential impacts of climate change on the rainfed agriculture of a semi-arid basin in Jordan. Phys Chem Earth **36(5–6):**125–134

Al-Ghzawi, A. L. A., Al-Ajlouni, Z. I., Sane, K. O. A., Bsoul, E. Y., Musallam, I., Khalaf, Y. B. & Al-Saqqar, H. (2019). Yield stability and adaptation of four spring barley (*Hordeum vulgare* L.) cultivars under rainfed conditions. ROC, **20(1),** 10-18.

Al-Ghzawi, A. L. A., Khalaf, Y. B., Al-Ajlouni, Z. I., AL-Quraan, N. A., Musallam, I., & Hani, N. B. (2018). The effect of supplemental irrigation on canopy temperature depression, chlorophyll content, and water use efficiency in three wheat (*Triticum aestivum* L. and *T. durum* Desf.) genotypes grown in dry regions of Jordan. Agriculture, **8(5),** 67.

AL-karablieh, E. and Amer S. Jabarin (2010). Different rangeland management systems to reduce livestock feeding costs in arid and semi-arid areas in Jordan. Q. J. Int. Agric." 49 (2010), No. **2**: 91-109.

Ararso Gognsha and Berhanu Hiruy. (2020). Genotypes Composition and Status of Stored Sorghum Pests in Traditional Farmer's Storages of Kena District of Koso Zone, Southern Ethiopia. J. Exp. Agric. Int. **42(1):** 12-22, 2020; Article no. JEAI.53994

Aukour, F. J., Al-Hammouri, A. and Al-Ghzawi, A. L. A. (2013): Recovery of plant species, richness, and composition in abandoned grassland in arid region. Acta Bot. Hung. 55(3–4).

B.A. McKenzie and M. Andrews (2010). Modelling climate change effects on cool season grain legume crop production: LENMOD, a case study. In: Yadav S.S., McNeil D.L., Redden R. (eds.), **Climate change and management of cool season grain legume crops.** Springer, Heidelberg/New York.

Bani Hani, N.; Aukour, F.J.; Al-Qinna, M.I. (2022). Investigating the Pearl Millet (Pennisetum glaucum) as a Climate-Smart Drought-Tolerant Crop under Jordanian Arid Environments. *Sustainability* 2022, 14, 12249. https://doi.org/10.3390/ su141912249

Barbeau, C.; Oelbermann, M.; Karagatzides, J.; Tsuji, L. (2015). Sustainable agriculture and climate change: Producing potatoes (*Solanum tuberosum* L.) and bush beans (*Phaseolus vulgaris* L.) for improved food security and resilience in a canadian subarctic First Nations community. *Sustainability* 2015, *7*, 5664–5681.

Bibi, A., H. A. Sadaqat, M. H. N. Tahir and H. M. Akram (2012). Screening of sorghum (*Sorghum bicolor* Var moench) for drought tolerance at seedling stage in polyethylene glycol. J. Anim. Plant Sci. **22(3):** 671-678.

Bollam, S., Romana, K. K., Rayaprolu, L., Vemula, A., Das, R. R., Rathore, A., et al. (2021). Nitrogen use efficiency in Sorghum: exploring native variability for traits under variable N Regimes. Front. Plant Sci. **12**:643192. doi: 10.3389/fpls.2021. 643192

Chiluwal, A., Bheemanahalli, R., Perumal, R., Asebedo, A. R., Bashir, E., Lamsal, A., et al. (2018). Integrated aerial and destructive phenotyping differentiates chilling stress tolerance during early seedling growth in sorghum. *Field Crops Res.* **227**, 1–10. doi: 10.1016/j.fcr.2018.07.011

DeLucia, E. H., and Heckathorn, S. A. (1989). The effect of soil drought on water-use efficiency in a contrasting Great Basin Desert and Sierran montane genotypes. PLANT CELL ENVIRON, **12(9),** 935-940. https://doi.org/10.1111/j.1365-3040.1989.tb01973.x.

FAO, 2009. Acipenser sturio. Fisheries and Aquaculture Information and Statistics Service. URL: http://www.fao.org/fishery/genotypes/2876/en.

FAO, 2022. Global Information and Early Warning System. Reference Date: 29-August-2022. https://www.fao.org/giews/countrybrief/country.jsp?code=JOR&lang=ar.

Ormann, P. Reeves, S. umm et al., "Changes in barley (Hordeum vulgare L. subsp. vulgare) genetic diversity and structure in Jordan over a period of 31 years," **Plant Genetic Resources: Characterization and Utilization,** vol. 16, no. 2, pp. 112–126, 2018

Jahanzad E, Jorat, M. Moghadam, H. Sadeghpour A., Chaich, M.R. and Dashtaki. M. (2013). Response of a new and commonly [illegible] var to limited irrigation and planting density. Agric. Water Manag**.** **117**: 62-69.

Keshavarz Afshar, R., Chaichi, M.R. Asareh, M.H. Hashemi, M. and Liaghat. A. (2014). Interactive effect of deficit irrigation and soil organic amendments on seed yield and flavonolignan production of milk thistle (*Silybum marianum* L. Gaertn.). Ind Crops Prod **58**: 166-172.

Kimber, C. T. (2000). "**Origins of domesticated sorghum and its early diffusion to India and China," in Sorghum: Origin, History, Technology, and Production,** eds C. W. Smith and R. A. Frederiksen (New York, NY: John Wiley & Sons), 3–98. doi: 10.1163/9789004497412_004.

Kumari, S. 1988. The effects of soil moisture stress on the development and yield of millet. Agron. J., 57: 480- 487.

Meena, G. L., Latika Sharma, Kailash Chand Bairwa, Phool Chand Meena, Hemant Sharma. (2022). Growth and variability in sorghum production in Bhilwara district vis-à-vis Rajasthan. Ama-Agricultural Mechanization in Asia Africa and Latin America. Vol.53, Issue 06, 2022.

MoEnv. Ministry of Environment in Jordan (2014). Jordan's Third National Communication on Climate Change Submitted to The United Nations Framework Convention on Climate Change (UNFCCC). The Hashemite Kingdom of Jordan, Ministry of Environment, 2014.

Muhammad Ahmad Yahaya, Hussein Shimelis. 2021. Drought stress in sorghum: Mitigation strategies, breeding methods and technologies—A review. J. Agron. Crop Sci... https://doi.org/10.1111/jac.12573

Ostmeyer TJ, Bahuguna RN, Kirkham MB, Bean S and Jagadish SVK (2022). Enhancing Sorghum Yield Through Efficient Use of Nitrogen – Challenges and Opportunities. Front. Plant Sci. **13**:845443. doi: 10.3389/fpls.2022.845443.

Plaut, Z.; Butow, B.; Blumenthal, C.; Wrigley, C. (2004). Transport of dry matter into developing wheat kernels and its contribution to grain yield under post-anthesis water deficit and elevated temperature. Field Crops Res. 2004, *86*, 185–198.

Pennisi, E. (2009). How sorghum withstands heat and drought. *Science* **323**:573. doi: 10.1126/science.323.5914.573.

Qi, G., Li, N., Sun, X. S., Wang, D., Ciampitti, I., and Prasad, V. (2016). "Overview of *Sorghum* industrial utilization," in ***Sorghum: A State of the Art and Future Perspectives***, eds I. Ciampitti and V. Prasad (Madison WI: American Society of Agronomy and Crop Science Society of America, Inc.), 463–476. doi: 10.2134/ agronmonogr58.c21.

Saddam, S. Bibi, A. Sadaqat, H. A. and Usman, B. F. (2014). Comparison of 10 sorghum (*Sorghum bicolor*) genotypes under various water stress regimes. JAPS. 24(6): 2014, Page: 1811-1820

SAS Institute. 2011. SAS for Windows. Version: 9.3. SAS Institute, Cary, NC.

Tessema Tesfaye Atum and Getachew Gudero Mengesha. (2022). Growth and yield performance of sorghum (*Sorghum bicolor* L.) crop under anthracnose stress in dryland crop-livestock farming system. Experimental Results (2022), 3, e14, 1–15. doi:10.1017/exp.2022.12.

Van Oosterom, E. J., Chapman, S. C., Borrell, A. K., Broad, I. J., and Hammer, G. L.(2010b). Functional dynamics of the nitrogen balance of sorghum. II. Grain filling period. Field Crops Res. **115**, 29–38.

JJBS

Volume 17, Number 4,December 2024
ISSN 1995-6673
Pages 629 – 636
https://doi.org/10.54319/jjbs/170406

Jordan Journal of Biological Sciences

Growth, Water Relation and Physiological Responses of Eggplant (*Solanum melongena* L.) under Different Olive Mill Waste Water Levels

Shorouq Jaradat[1], Emad Y. Bsoul[1,*], Salman Al-Kofahi[2] and Rami Alkhatib[3]

[1]*Department of Biology and Biotechnology, Faculty of sciences, The Hashemite University, Zarqa, Jordan;* [2]*Department of Lands Management & Environment, The Hashemite University, Zarqa, Jordan;* [3]*Department of Biotechnology and Genetic Engineering, Jordan University of Science and Technology, Irbid, Jordan*

Received: January 25, 2024; Revised: May 6, 2024; Accepted: May 14, 2024

Abstract

Eggplant (*Solanum melongena* L.) is an important traditional crop, cultivated worldwide. Olive mill wastewater (OMW) is an important olive oil extraction byproduct due to its high concentration of different valuable compounds. Three eggplant cultivars were evaluated under different concentrations of olive mill wastewater. Seedlings were treated with four OMW levels (control, 25% OMW, 50% OMW and 100% OMW). Eggplant cultivars expressed different physiological responses when irrigated with OMW at different levels. Many physiological parameters such as growth, stomatal conductance, transpiration, relative water content, relative growth rate, stem diameter and chlorophyll content were examined. It has been found that many of these responses were adversely affected when plants were irrigated with OMW. Unexpectedly, the water status of eggplants was not affected by the different levels of OMW as plants maintained transpiration rate similar to the control values. Our findings clearly suggest that the physiological responses of eggplant to OMW vary among cultivars. However, the ability of plants to absorb water were not affected by OMW. We recommend that the sensitivity of the eggplant cultivars to OMW be taken into consideration before irrigating eggplants with OMW.

Keywords: *Solanum melongena*; Olive mill wastewater; Phenolic compounds; transpiration, diffusive resistant, Plant relative growth rate; Net assimilation rate.

1. Introduction

Demand for food is much more than ever before. The food production chain including agriculture and industry leads to accumulation of wastes that need to be assimilated or safely disposed with minimum environmental impacts. Olive mill wastewater (OMW) is an example of olive oil extraction byproduct that can be of beneficial for some uses due to the high concentration of different compounds. Olive (*Olea europea* L.) trees are drought tolerant ones commonly grown in Mediterranean region as viable trees that do not require much effort (Brito *et al.*, 2019, Torres-Ruiz *et al.*, 2013). Olive oil marketing is an expanding worldwide industry especially in the olive-growing regions due to the high demand for its fruits and oil and the associated economical value (Khdair and Abu-Rumman, 2020, Brito *et al.*, 2019). The production of olive oil in Mediterranean countries represents 95-98% of the entire worldwide total production (Arvaniti *et al.*, 2012).

Processing of olive fruits to extract olive oil generates two types of waste which are a large quantity of solid waste called pomace (Khdair and Abu-Rumman, 2020) or olive cake and OMW that is generating a main ecological problem (Khdair and Abu-Rumman, 2020, Arvaniti *et al.*, 2012). Olive pressing industry produces 1,000 metric tons of this OMW per harvesting season (annually) in Mediterranean countries in a short period of time (October to late January) (Khdair and Abu-Rumman, 2020, Paraskeva and Diamadopoulos, 2006). The amount of OMW differs according to the extraction method, with a range of 50 and 80 m^3 ha^{-1} using pressure or centrifuge extraction techniques (Belaqziz *et al.*, 2008 , Hanifi and El Hadrami, 2009).

OMW is a dark brown color acidic waste, highly saline, and rich in organic matter and minerals (Arvaniti *et al.*, 2012, Comegna *et al.*, 2022, Rusan and Malkawi, 2016, Lopes *et al.*, 2009). The organic matter composition differs in its phenolics, sugars, polysaccharides, proteins, lignins and fatty acids content according to type of olive, treatment procedure, the level of fruit maturity, time of harvest, and processing method (Arvaniti *et al.*, 2012, De Marco *et al.*, 2007).

The ecological problem of OMW arises from the high concentration of phenolic, tannins and flavonoids compounds that negatively impacts plant growth and microorganisms if approaching toxicity levels (Comegna *et al.*, 2022, Arvaniti *et al.*, 2012, Isidori *et al.*, 2005). In addition, OMW is characterized with unpleasant odor after anaerobic digestion (Arvaniti *et al.*, 2012) and represents a threat to pollute surface and groundwater sources, with an adverse impact on the environment aesthetic value (Khatib *et al.*, 2009 , Arvaniti *et al.*, 2012). Therefore,

* Corresponding author. e-mail: ebsoul@hu.edu.jo.

some European countries prohibit discharging of this wastewater in nature (Hanifi and El Hadrami, 2009).

The uncontrolled disposal of OMW on soil leads to reduction in soil water retention ability and infiltration rate, increases soil hydrophobicity, adversely affects soil acidity, salinity, nitrogen immobilization, and nutrient leakage (Khdair and Abu-Rumman, 2020, Sierra *et al.*, 2007) . Different methods have been proposed for OMW treatment based on evaporation ponds, thermal concentration, and different physicochemical and biological treatments (Martinez *et al.*, 1994). Unfortunately, most of these methods are costly, and still the end by-products need to be disposed and uploaded to an environment system (Khdair and Abu-Rumman ,2020, Arvaniti *et al.*, 2012, Paredes *et al.*, 1999) . However, some researchers reported advantages and benefits associated with OMW where incorporating OMW with soil changes soil physicochemical and microbiological properties, reduces evapotranspiration in arid and semi-arid zones and improves soil water balance, amends soil structure, decreases soil erosion, increases infiltration rate and water holding capacity with no negative impacts on soil properties (Kurtz *et al.*, 2021, Khdair and Abu-Rumman, 2020, Rusan and Malkawi, 2016 , Rusan *et al.*, 2015, Rigane *et al.*, 2015, Ayoub *et al.*, 2014, Wahsha *et al.*, 2014, Barbera *et al.*, 2013). Furthermore, OMW can replenish soil with macronutrients (nitrogen, phosphorus and potassium) along with organic matter that is beneficial to soils (Comegna *et al.*, 2022 , Khdair and Abu-Rumman, 2020, Rusan and Malkawi, 2016 , Rusan *et al.*, 2015) . Therefore, there is a potential for OMW to be exploited in agricultural as source for nutrient, soil conditioner, and a water conservation technique.

Eggplant (*Solanum melongena* L.) is a vegetable crop belonging to *solanaceae* family. Eggplant is a traditional crop mainly in Asia, Southern Europe and the Mediterranean countries. It is the fifth most economically important solanaceous crop after potato, tomato, pepper, and tobacco (Taher *et al.*, 2017). In 2008, about 1.96 million ha were devoted to cultivating eggplant worldwide (FAO, 2010). The large annual quantities of OMW production accompanied with both its climatic hazards and its nutritive values to plants nominated this product for more investigation. The aim of this work was to investigate the growth rate, water relations, and physiological responses of three eggplant cultivars under different concentrations of the olive mill waste water applications.

2. Materials and Methods

2.1. Study location

This study was conducted in a greenhouse at the Hashemite University, Zarqa, 32°05' N Latitude and 36°06 E Longitudes. Greenhouse day temperatures were in the range of 20-35°C, and mean midday photosynthetic photon flux density (PPFD) was 365 µmol.s^{-1}.m^2 measured by a quantum sensor (LI_250A; LICOR.)

2.2. Plant Material and Experimental Design

Seeds of three eggplants (*S. melogena* L.) cultivars (Blacky, Hi-Tech, Denmark; Pearly F1, Hi-Tech, Denmark; and Classic, Harris moran, China) were used for this experiment. Seeds were germinated in trays containing peatmoss (KEKKILA, European Union). After 30 days of seeding date, seedlings were transplanted into 5 L pots containing autoclaved mixture of fumigated media composed of peatmoss: perlite: soil (1:1:1v/v). Cloth screens were placed in the bottom of the pots to prevent soil loss and allow drainage of extra irrigation water. Transplanted seedlings were kept well irrigated in the greenhouse for a month. Plants were fertilized using Nutri-Leaf 60, USA (20N-20P- 20K) at a rate of 5g/L of irrigation water once a week after transplantation.

The plants were gradually irrigated with OMW solution until the disignated treatment levels were reached in order to acclimatize the plants and avoid shock. Four levels of irrigation water mixed with OMW were used (control, 25% OMW, 50% OMW and 100% OMW). Uniform plants from each cultivar were assigned randomly to one of four irrigation treatments and allowed to grow for 65 days. The experimental design was completely randomized block design with five replications. Each block contained 12 plants (3 cultivars x 4 irrigation solution). An extra 24 plants (8 per cultivar) were used to determine the initial plant growth characteristics before initiating salinity treatment application.

2.3. Initial Seedling Traits

Initial plant growth characteristics were collected for each cultivar using the extra plants maintained for this purpose. The harvested plants were separated into leaves, stems and roots. The collected baseline data included leaf area, leaf dry weight, stem dry weight and root dry weights. Leaf area (cm^2) was measured using a portable leaf area meter (LI-3000A; LICOR; Lincoln, Nebr. USA). Roots were washed by tab water to remove soil mixture. Oven dry weights of leaves, stems, and roots were determined after drying at 65 ^oC to a constant weight (data not shown).

2.4. Treatments preparation

2.4.1. Determination of total phenol content in the OMW

Total phenol content (TPC) was determined according to Slinkard and Singleton, (1977) with Folin–Ciocalteu reagent using Gallic acid as a standard. Briefly, 1 ml of approximately diluted samples and a standard solution of Gallic acid were added to a 25 ml volumetric flask containing 9 ml of distilled water. Distilled water was used as blank reagent; one ml of folic–Ciocalteu phenol reagent was added to the mixture and were shaken for 5 min. Then, 10 ml of 7% Na_2CO_3 solution were mixed and then allowed to stand for 2 h. Next, the absorbance was measured at 760 nm using spectrophotometer. The samples TPC was averaged to 0.753 mg.l^{-1} , and that was considered as stock OMW solution (100%). The remaining treatments were prepared from the stock solution and diluted to (50% and 25%) and that was equivalent to 0.377 and 0.188 mg.l^{-1} , respectively.

2.4.2. OMW solution characteristics

Electrical conductivity (EC) using EC meter (Milwaukee SPEM500), TPC and pH were determined for the OMW irrigation solutions (Table 1).

Table 1: Electrical conductivity, pH and TPC of OMW irrigation solutions.

Parameters	OMW irrigation solution		
	100%	50%	25%
pH	5.5	5.8	5.8
Electrical Conductivity (EC) (dS. m^{-1})	1.870	1.325	1.092
TPC ($mg.l^{-1}$)	0.753	0.377	0.188

On the same day when the initial data were recorded, the five blocks were irrigated with OMW treatment (25%, to prevent shock, except for the control that was watered with tap water only. The OMW concentration was then gradually increased for two weeks until each desired OMW treatment level was achieved (control, 25% OMW, 50% OMW and 100% OMW). Once all the experimental plants had started receiving their designated treatments levels, all treatments were irrigated manually every two days to the field capacity for the total duration of 65 days.

2.5. Physiological Traits

Chlorophyll Concentration Index (CCI) was determined biweekly by averaging two midday readings of each plant. The SPAD was measured on the two youngest fully-expanded mature healthy leaves (LI-250A OPTICSCIENCES CCM-200). Transpiration and stomatal conductance (g_s) were measured biweekly using a steady state porometer (LI-1600; LICOR; Lincoln, Nebr.). The height of each plant was measured biweekly from soil surface to the top of the plant.

2.6. Final Harvest

All plants were harvested after 65 days of initiating the experiment. Harvested plants were washed, air dried on filter paper, separated into leaves, stems and roots. Leaf area (cm^2) was determined using a portable leaf area meter (LI-3000A; L-ICOR; Lincoln, Nebr. USA). Stem diameters were measured using an electronic 0-150 mm digital caliper (Swiss). The oven dry weights of plant leaves, stems and roots were determined after the dry weight was stabilized at 65 ^oC. Leaf discs from two youngest fully expanded mature leaves of all plants were used to determine Relative Water Content (RWC).

RWC was calculated using the equation (FW-DW/TW-DW) (100), where FW is the fresh weight, DW represents fresh weight sample oven dried at 68 °C and TW represents the turgid (saturated) weight of sample, which was immersed overnight in distilled water (Bsoul *et al.,* 2006). Relative growth rates were calculated using the equation of Gutschick and Kay, (1995): RGR = (ln W2 -ln W1)/ (T2 - T1), where W2 was the final dry weight at day 65 (T2), and W1 was the initial DW determined from initial data harvest on day 1 (T1). Net assimilation rates (NAR) were calculated as: NAR = M2 - M1/T2 - T1 X log L2 - log L1/L2 - L1, where M2 was the final dry weight at day 65 (T2), and M1 was the initial DW determined from the initial weight recorded on day one of the experiment (T1). Leaf area ratio (cm^2.g-1) was calculated as SLA= leaf area/leaf dry weight where SLA represents Specific Leaf Area. Specific stem length (cm.g-1) was calculated as SSL= stem height/ stem dry weight.

2.7. Statistical Analysis

Statistical analysis was performed using SAS 9.1 software for Windows (2003). Significant differences between values of all parameters were determined at $P \leq 0.05$ using Proc GLM, PDIFF option, ANOVA and Duncan's Multiple Range Tests were used.

3. Results

There was no significant interaction observed between cultivars and teatments. Stem dry weight had no significant differences among cultivars or treatments. Pearly cultivar had the lowest leaf dry weight, shoot dry weight, plant dry weight, plant height and stem diameter (Table 2). In addition, Pearly had the lowest relative growth rate, but the three cultivars had similar NAR (Table 3). Olive mill wastewater has reduced most of the growth parameters of the eggplants when compared to the control (Table 2). Classic cultivar had the thickest stem diameter (5.02 mm). However, the stem diameter had no significant differences among OMW treatments (Table 2). Noticeably, irrigation with high olive mill wastewater concentration (100%) had no effect on the plant height (Table 2) and NAR (Table 3). Olive mill wastewater treatments hand no significant effect on the RWC of eggplants cultivars (Table 3). The CCI values were highest for classic cultivar and were negatively affected by all the OMW concentrations as compared to the control (Table 3).

Table 2. Plant biomass dry weights, shoot to root ratio, plant height, and stem diameter of three eggplant cultivars (Blacky, Pearly, and Classic) subjected to four OMW treatments (control, 25%, 50%, and 100%) for 65 days.

Cultivar	Stem DW (g)	Leaf DW (g)	Shoot DW (g)	Root DW (g)	Plant DW (g)	Shoot/ Root (g)	Plant height (cm)	Stem diameter (mm)
Blacky	0.84^{zA}	0.84^{AB}	1.77^{AB}	0.74^{A}	2.32^{AB}	3.97^{A}	16.55^{AB}	4.43^{AB}
Pearly	0.65^{A}	0.52^{B}	1.18^{B}	0.43^{A}	1.61^{B}	4.76^{A}	14.13^{B}	4.21^{B}
Classic	0.87^{A}	1.02^{A}	1.90^{A}	0.84^{A}	2.72^{A}	3.23^{A}	18.85^{A}	5.02^{A}
Treatment								
Control	0.96^{A}	1.52^{A}	2.51^{A}	1.16^{A}	3.53^{A}	3.21^{AB}	17.67^{AB}	4.78^{A}
25%	0.73^{A}	0.80^{B}	1.54^{B}	0.57^{B}	2.09^{B}	5.65^{A}	14.35^{B}	4.56^{A}
50%	0.68^{A}	0.57^{BC}	1.25^{B}	0.51^{B}	1.77^{B}	4.34^{AB}	16.05^{AB}	4.37^{A}
100%	0.77^{A}	0.29^{C}	1.16^{B}	0.45^{B}	1.48^{B}	2.74^{B}	17.97^{A}	4.51^{A}
P-value								
Cultivar	0.296	0.032	0.033	0.111	0.039	0.036	0.005	0.0423
Treatment	0.371	0.0001	0.0003	0.0065	0.0004	0.0003	0.0937	0.7277

^{z}Means (n = 5) within columns followed by the same letter were not statistically different. Means were assessed at $P \leq 0.05$ using Proc GLM, PDIFF option.

Table 3. Plant net assimilation rate (NAR), relative growth rate (RGR), leaf relative water content (RWC), and chlorophyll content index (CCI), of three eggplant cultivars (Blacky, Pearly, and Classic) subjected to four olive mill wastewater treatments (control, 25%, 50%, and 100%) for 65 days.

Cultivar	NAR ($mg \cdot cm^{-2} \cdot d^{-1}$)	RGR ($g \cdot g^{-1} \cdot d^{-1}$)	RWC %	CCI
Blacky	0.090^{A}	0.016 ^{AB}	0.36^{A}	8.12^{B}
Pearly	0.067^{A}	0.014 ^{B}	0.40^{A}	8.96^{AB}
Classic	0.099^{A}	0.019 ^{A}	0.39^{A}	13.30^{A}
Treatment				
Control	0.115^{A}	0.021^{A}	0.37^{A}	15.65^{A}
25%	0.069^{AB}	0.016^{B}	0.40^{A}	9.11^{B}
50%	0.066^{B}	0.015^{B}	0.35^{A}	8.08^{B}
100%	0.105^{AB}	0.013^{B}	0.42^{A}	7.67^{B}
P-value				
Cultivar	0.0539	0.0227	0.5218	0.0179
Treatment	0.0092	0.0042	0.3289	0.002

^{z}Means (n = 5) within columns followed by the same letter were not statistically different. Means were assessed at $P \leq 0.05$ using Proc GLM, PDIFF option.

The three cultivars had similar LA, LAR, and LWR values with no significant differences among them (Table 4). On the other hand, Pearly had recorded the highest SLA. However, LA, SLA, LAR and LWR were significantly impacted by OMW treatments. It is obvious that high OMW concentration (100%) had significantly reduced the eggplants LA, SLA, LAR and LWR (Table 4).

Table 4. Leaf area (LA), specific leaf area (SLA), leaf area ratio (LAR), and leaf weight ratio (LWR) of three eggplant cultivars (Blacky, Pearly, and Classic) subjected to four olive mill wastewater treatments (control, 25%, 50%, and 100%) for 65 days.

Cultivar	LA (cm^2)	SLA ($cm^2.mg^{-1}$)	LAR ($cm^2.mg^{-1}$)	LWR ($g.g^{-1}$)
Blacky	180.09^{A}	225.49^{B}	68.62^{A}	0.31^{A}
Pearly	148.58^{A}	271.77^{A}	96.70^{A}	0.33^{A}
Classic	191.20^{A}	194.23^{B}	77.48^{A}	0.38^{A}
Treatment				
Control	298.00^{A}	225.31^{B}	87.71^{A}	0.40^{A}
25%	193.07^{B}	264.01^{A}	109.34^{A}	0.41^{A}
50%	145.11^{B}	249.38^{A}	89.58^{A}	0.36^{A}
100%	56.96^{C}	183.29^{B}	37.10^{B}	0.19^{B}
P-value				
Cultivar	0.4992	0.0062	0.1965	0.2826
Treatment	0.0001	0.0268	0.0016	0.0002

^{z}Means (n = 5) within columns followed by the same letter were not statistically different. Means were assessed at $P \leq 0.05$ using Proc GLM, PDIFF option.

The biweekly data showed that eggplant CCI continued to decrease throughout the experiment progress under all OMW concentration as compared to the control (Fig 1A). On the other hand, Classic cultivar had the highest chlorophyll content (Fig 1B).

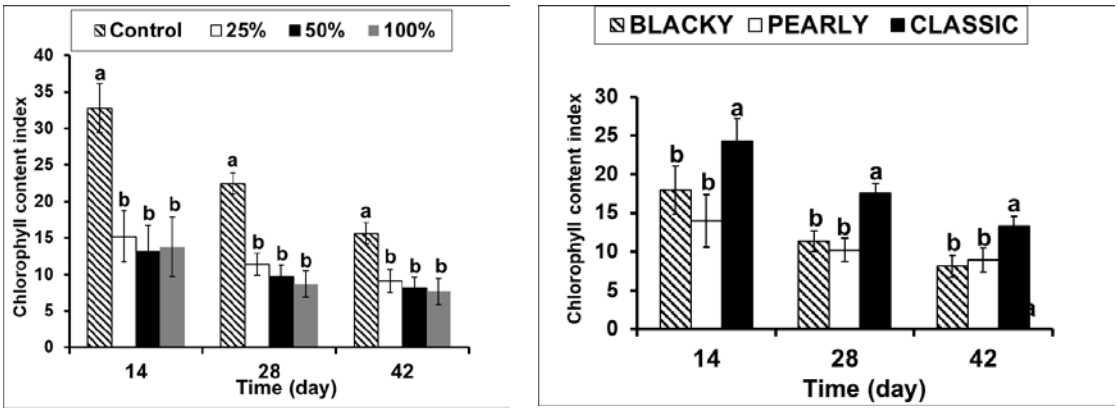

A B

Figure 1: Chlorophyll content index: Biweekly CCI values of three eggplant cultivars (Blacky, Pearly, and Classic) subjected to four olive mill wastewater treatments (control, 25%, 50%, and 100%). Data are means ± SE of 5 replicates. Means among the neighbored columns marked with the same letter were not significantly different at the $P \leq 0.05$ using Proc GLM, PDIFF option.

Eggplant transpiration rate was not affected by the increased OMW concentration in the experiment. However, transpiration rate was increased throughout the experiment (Fig 2A). After 42 days, the Classic cultivar started to show less transpiration rate than Blacky and Pearly cultivars (Fig 2B).

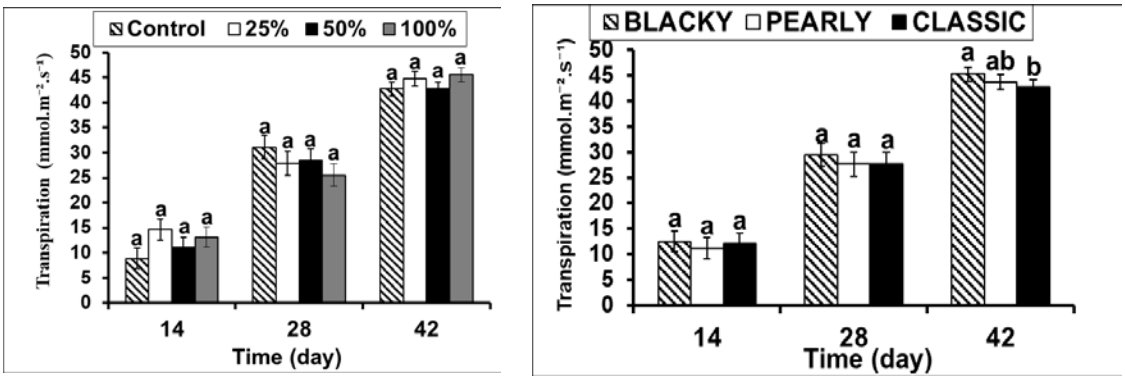

A B

Figure 2: Transpiration: Biweekly transpiration values of three eggplant cultivars (Blacky, Pearly, and Classic) subjected to four olive mill wastewater treatments (control, 25%, 50%, and 100%) Data are means ± SE of 5 replicates. Means among the neighbored columns marked with the same letter were not significantly different at the $P \leq 0.05$ using Proc GLM, PDIFF option.

The three eggplants had similar stomatal diffusive resistance under the different OMW concentration, but they all had high stomatal diffusive resistance values after 28 days (4 weeks) (Fig 3B).

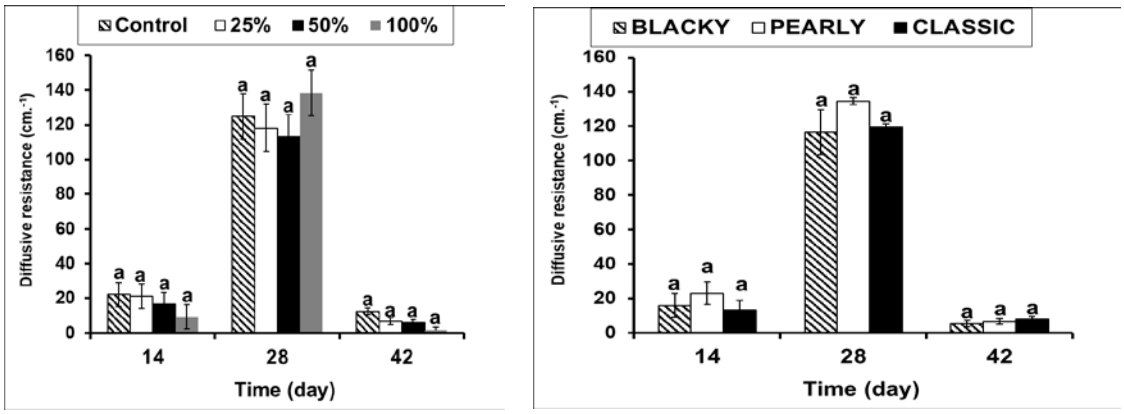

A B

Figure 3: Diffusive resistance: Biweekly Diffusive resistance values of three eggplant cultivars (Blacky, Pearly, and Classic) subjected to four olive mill wastewater treatments (control, 25%, 50%, and 100%). Data are means ± SE of 5 replicates. Means among the neighbored columns marked with the same letter were not significantly different at the $P \leq 0.05$ using Proc GLM, PDIFF option.

4. Discussion

Our data obviously reported that olive mill wastewater negatively impacted the growth of the eggplants, specially at high concentration. However, some cultivars such as Pearly might be affected more than the other cultivars. Rusan *et al.,* (2016) reported that plant growth was reduced when irrigated with untreated OMW. Our data is consistent with Asfi *et al.* (2012) who reported that plant biomass was more affected than plant height under OMW treatments. In addition, negative effect of OMW treatment on dry biomass production was reported in many other plants (Mekki *et al.,* 2006; Ouzounidou *et al.,* 2008; Ouzounidou *et al.,* 2010).

However, OMW had no effect on the eggplant water status at all concetration levels as the RWC was not affected and maintained values similar to the control at all OMW treatments concentrations. Moreover, the three cultivars had similar RWC. Our data might suggest that the OMW treatments had no effect on the absorbtion and the hydrulic conductance of water, specially when we refere to the shoot/root ratio (Table 2) which showed that the plants maintained good root system even when irrigated with 100% OMW. In addition, the plants transpiration rate and the stomatal diffusive resistance maintaind similar readings with the control throughout the experiment (Fig. 2 and Fig. 3). Chartzoulakis *et al.* (2010) reported that the application of raw OMW had no effect on plants stomatal conductance and showed similar values to control plants.

Our data might suggest that the impaired growth of the eggplants in our expirement was not a consequence of water deficit. Bsoul *et al.*(2022) mentioned that water availability is a factor that usually reduces NAR and growth. Based on the results of CCI data (Table 3), we believe that the RGR and NAR are directly impacted by chlorophyll content. Fitter and Hay (2002) reported that RGR represents the extent to which a plant invests its photosynthesis in current growth and improves its ability for upcoming photosynthesis. High OMW concentration (100%) had significantly reduced the eggplants LA, SLA, LAR and LWR (Table 4). Ben-Rouina *et al.* (1999) also reported that the increased levels of OMW irrigation were phytotoxic, and plants might die. The variation of cultivars growth indices (LA, SLA, LAR and LWR) could be attributed to the variable sensitivity among these cultivars as reported in previous research (Montemurro *et al.,* 2011). Specifically, these growth indices are associated with the leaf photosynthetic mesophyll cells (Benincasa *et al.,* 2003).

In conclusion, many physiological parameters were adversely affected when the plants were irrigated with OMW. On the other hand, the water status of the eggplants was not affected by the different levels of OMW as the plants maintained transpiration rate similar to the control values. In addition, our findings clearly suggest that the physiological responses of eggplant to OMW vary among cultivars, and the reason behind that was not the effect of OMW on the ability of the plants to absorb water. We recommend that before irrigating eggplants with OMW it is important that the sensitivity of the cultivar to OMW be taken into consideration. Moreover, the unobservable advanges of irrigating *S. melongena* with OMW for some physiological parameters do not necessarily make a recommendation for not investigating OMW as a source for bioactive molecules that support plant growth and development. In addition, OMW is rich in nutreints such as nitrogen, phosphorus, potasium, carbon, sodium (Santos *et al.,* 2019), anthocyanins, flavinoids, and many other useful compounds (Sciubba *et al.,* 2020). Therefore, we suggest that further experiments with some manipulations can deliver potential applicable findings. For example, diluting the OMW below 25% is expected to maintain the nutritional value of OMW without arresting plant growth and development. Furthermore, investigaing the physiological responses of different crops to different OMW might be needed primarily befor heading to investigate cultivars responses. For example, Santos *et al.,* (2019) investigated different crop growth and development in realtion to olive wastewater solution applications.

5. Author Contributions

Conceptualization, Emad Y. Bsoul
Methodology, Shorouq Jaradat and Emad Y. Bsoul
Validation, Emad Y. Bsoul and Shorouq Jaradat
Formal analysis, Emad Y. Bsoul and Salman Al-Kofhai
Investigation, Emad Y. Bsoul and Shorouq Jaradat
Resources, Emad Y. Bsoul and Salman Al-Kofahi
Data curation, Emad Y. Bsoul, Shorouq Jaradat, and Salman Al-Kofahi
Writing— Emad Y. Bsoul, Shorouq Jaradat. and Salman Al-Kofahi, and Rami Alkhatib
Review and editing, Emad Y. Bsoul, Shorouq Jaradat. and Salman Al-Kofahi, Rami Alkhatib
Visualization, Emad Y. Bsoul
Supervision, Emad Y. Bsoul
Project administration, Emad Y. Bsoul
All authors have read and agreed to the published version of the manuscript.

6. Funding

This research received no external funding.

7. Data Availability Statement

Data supporting reported results are available with the corresponding author.

Acknowledgments

We recognize the Hashemite University for allowing us to use their facilities and equipment. In addition, we are thankful for the greenhouse technicians Yahya Al-Sayfi and Ayoub for their help during the experiment.

Conflict of Interests

The authors declare that there is no conflict of interests.

References

Author 1 A B, Author 2 C D and Author 3 E. Year. Title of the article. *Abbreviated Journal Name*, **Volume**: page range.

Arvaniti E C, Zagklis D P,Papadakis V G and Paraskeva C A. 2012. High-Added Value Materials Production from OMW: A

Technical and Economical Optimization. *Int. J. Chem. Eng.*, **6**: 7219-7226.

Asfi M, Ouzounidou G, Panajiotidis S, Herios I and Moustakas M. 2012. Toxicity effects of olive-mill wastewater on growth, photosynthesis and pollen morphology of spinach plants. *Ecotoxicol. Environ. Saf*., **80**: 69-75.

Ayoub S, Al-Absi K, Al-Shdiefat S, Al-Majali D and Hijazean D. 2014. Effect of olive mill wastewater land-spreading on soil properties, olive tree performance and oil quality. *Sci. Hortic.*, **175**: 160–166.

Barbera A C, Maucieri C, Cavallaro V, Ioppolo A and Spagna G. 2013. Effects of spreading olive mill wastewater on soil properties and crops, a review. *Agric Water Manag.*,**119**: 43-53.

Belaqziz M, Lakhal EK, Mbouobda HD and El Hadrami I. 2008. Land Spreading of Olive Mill Wastewater: Effect on Maize (Zea *mays*) Crop. *Journal of Agronomy*, **7 (4)**: 297-305.

Benincasa M. 2003. **Análise de Crescimento de Plantas (Noções Básicas),** third ed. FUNEP: Jaboticabal, Brazil.

Ben-Rouina B, Taamallah H and Ammar E. 1999. Vegetation water used as a fertilizer on young olive plants. *Acta Hort*., **474**: 353–355.

Brito C, Dinis L, Moutinho-Pereira J and Correia C M. 2019. Drought Stress Effects and Olive Tree Acclimation under a Changing Climate. *Plants*, **8 (7)**: 232-252.

Bsoul E St, Hilaire R and VanLeeuwen D. 2006. Bigtooth maples exposed to asynchronous cyclic irrigation show provenance differences in drought adaptation mechanisms. *J. Amer. Soc. Hort. Sci.*, **131**: 459-468.

Bsoul E Y, Othman SA, Al-Ghzawi AA and Massadeh M I. 2023. Effect of silver nanoparticles on growth and physiological responses of spinach (*Spinacia oleracea* L.) under Salt Stress. *Jordan J. Biol. Sci.,* **16**: 1-6.

Chartzoulakis K, Psarras G, Moutsopoulou M and Stefanoudaki E. 2010. Application of olive mill wastewater to a Cretan olive orchard: Effects on soil properties, plant performance and the environment. *Agric Ecosyst Environ AGR.*, **138**: 3–4.

Comegna A, Dragonetti G, Kodesova R and Coppola A. 2022. Impact of olive mill wastewater (OMW) on the soil hydraulic and solute transport properties. *Int J Environ Sci Technol*., **19**: 7079-7092.

De Marco E, Savarese M, Paduano A and Sacchi R. 2007. Characterization and fractionation of phenolic compounds extracted from olive oil mill wastewaters. *Food Chem.*, **104**: 858-867.

FAO. 2010. http://faostat.fao.org/site/567/default.aspx#ancor.

Fitter A and Hay R. 2002. Environmental Physiology of Plants. *Academic Press*, San Diego.

Gutschick VP and Kay LE. 1995. Nutrient-limited growth rates: quantitative benefits of stress responses and some aspects of regulation. *J. Exp. Bot*., **46**: 995-1009.

Hanifi S and El Hadrami I. 2009. Olive Mill Wastewaters: Diversity of the Fatal Product in Olive Oil Industry and its Valorisation as Agronomical Amendment of Poor Soils: A Review. *J. Agron*., **8 (1)**: 1-13.

Isidori M, Lavorgna M, Nardelli A and Parrella A. 2005. Model study of the effect of 15 phenolic olive mill wastewater constituents on seed germination and Vibrio fischeri metabolism. *J. Agric. Food Chem.*, **53**: 8414-8417.

Khatib A, Aqra F, Yaghi N, Subuh Y, Hayeek B, Musa M, Basheer S and Sabbah I. 2009. Reducing the Environmental Impact of Olive Mill Wastewater. *Am. J. Environ. Sci.*, **5 (1)**: 1-6.

Khdair A and Abu-Rumman G. 2020. Sustainable Environmental Management and Valorization Options for Olive Mill Byproducts in the Middle East and North Africa (MENA) Region. *Processes*, **8 (6):** 671-693.

Kurtz MP, Dag A, Zipori I, Laor Y, Buchmann CH, Saadi I, Medina Sh, Raviv M, Zchori-Fein E, Schaumann G E and Diehl D. 2021. Toward Balancing the Pros and Cons of Spreading Olive Mill Wastewater in Irrigated Olive Orchards. *Processes* **9 (5)**: 780-798.

Lopes M, Araujo C, Aguedo M, Gomes N, Goncalves C, Teixeira J A and Belo I. 2009. The use of olive mill wastewater by wild type *Yarrowia lipolytica* strains: medium supplementation and surfactant presence effect. *Chem. Technol. Biotechnol*., **84**: 533-537.

Martinez NL, Garrido H SE and El alpechin. 1994. Un problema medioambiental en vias de solucion (I). *Quibal*, **41**: 755-765.

Mekki A, Dhouib A and Sayadi, S. 2006. Changes in microbial and soil properties following amendment with treated and untreated olive mill wastewater. *Microbiol. Res.*, **161**: 93–101.

Montemurro F, Diacono M, Vitti C and Ferri, D. 2011. Potential use of olive mill wastewater as amendment: Crops yield and soil properties assessment. *Commun. Soil Sci. Plant Anal*., **42 (21)**: 2594-2603.

Ouzounidou G, Asfi M, Sortirakis N, Papadopoulou P and Gaitis F. 2008. Olive mill wastewater triggered changes in physiology and nutritional quality of tomato (Lycopersicon esculentum Mill.) depending on growth substrate. *J. Hazard. Mater.*, **158**: 523–530.

Ouzounidou G, Zervakis GI and Gaitis F. 2010. Raw and microbiologically detoxified olive mill waste and their impact on plant growth. *Terr Aquatic Environ Toxicol* 4 (special Issue 1), 21–38.

Paraskeva P and Diamadopoulos E. 2006. Technologies for olive mill wastewater (OMW) treatment: A review. *J. Chem. Technol. Biotechnol*., **81**: 1475–1485.

Paredes C, Cegarra J, Roig A, Sfinchez- Monedero M A and Bernal M P. 1999. Characterization of olive mill wastewater (alpechin) and its sludge for agricultural purposes. *Bioresour. Technol*., **67**: 111-115.

Rigane H, Chtourou M, Ben Mahmoud I, Khaled Medhioub Kh and Ammar E. 2015. Polyphenolic compounds progress during olive mill wastewater sludge and poultry manure co-composting, and humic substances building (Southeastern Tunisia). *Waste Manag Res.*, **33 (1)**: 73-80.

Rusan MJ and Malkawi HI. 2016. Dilution of olive mill wastewater (OMW) eliminates its phytotoxicity and enhances plant growth and soil fertility. *Desalin. Water Treat.*, **57**: 27945-27953.

Rusan M, Albalasmeh A, Zuraiqi S and Bashabsheh M. 2015. Evaluation of phytotoxicity effect of olive mill wastewater treated by different technologies on seed germination of barley (Hordeum vulgare L.). *Environ. Sci. Pollut*., **22**: 9127–9135.

De los Santos, B, Brenes M, Garcia P, Aguado A, Medina E.and Romero C. 2019. Effect of table olive wastewaters on growth and yield of cucumber, pepper, tomato and strawberry. *Sci. Hortic.*, **256**: 108644.

Sciubba F, Chronopoulou L, Pizzichini D, Lionetti V and Fontana C. 2020. Olive mill wastes: A source of bioactive molecules for plant growth and protection against pathogens. *Biology*., **9**: 1-20.

Sierra J, Marti E, Garau AM and Cruanas R. 2007. Effects of the agronomic use of olive oil mill wastewater: Field experiment. *Sci. Total Environ.*, **378**: 90–94.

Slinkard K and Singleton V L. 1977. Total phenol analyses: Automation and Comparison with Manual Methods. *AJEV* ., **28 (1)**: 49-55.

Taher D, Solberg SØ, Prohens J and Chou Y. 2017. World Vegetable Center Eggplant Collection: Origin, Composition, Seed Dissemination and Utilization in Breeding. Front. *Plant Sci*., **8**: 1484-1496.

Torres-Ruiz J M, Diaz-Espejo A, Morales-Sillero A, Martín-Palomo M J, Mayr S, Beikircher B and Fernández J E. 2013. Shoot hydraulic characteristics, plant water status and stomatal response in olive trees under different soil water conditions. *Plant Soil*, **373**: 77–87.

Wahsha M, Bini C and Nadimi-Goki M. 2014. The impact of olive mill wastewater on the physicochemical and biological properties of soils in northwest Jordan. *EQA*, **15**: 25-31.

JJBS

Volume 17, Number 4,December 2024
ISSN 1995-6673
Pages 637 – 643
https://doi.org/10.54319/jjbs/170407

Jordan Journal of Biological Sciences

An *in vitro* Study into Antioxidant, Antibacterial, and Toxicity Impacts of *Artocarpus altilis* Leaf Extract

Nguyen Minh Tue[1], Nguyen Trung Quan[2], Hoang Thanh Chi[3], Bui Thi Kim Ly[3,*]

[1] *Faculty of Chemical Engineering, Ho Chi Minh City University of Technology – HCMUT, Viet Nam National University Ho Chi Minh City, 740030, Ho Chi Minh City, Vietnam;* [2] *Faculty of Biology - Biotechnology, University of Sciences, Viet Nam National University Ho Chi Minh City, 72711, Ho Chi Minh City, Vietnam;* [3] *Department of Medicine and Pharmacy, Thu Dau Mot University, Thu Dau Mot City 820000, Binh Duong Province, Vietnam*

Received: November 4, 2023; Revised: May 19, 2024; Accepted: May 25, 2024

Abstract

Artocarpus altilis (Parkinson) Fosberg, which was first discovered in 1769, mainly grows in subtropical and tropical areas. This plant is famous for having multiple applications in Asia, where people use fruits for food, leaves for drinks, and trunks for wood. *A. altilis* is also famous for treating human diseases such as diarrhea, dysentery, and other intestinal diseases. Various phytochemicals are determined in this plant and predicted to create biological activities. The bio-effects of the leaf extract were evaluated in order to supply scientific evidence contributing to this plant into the orthodox medical application. A free radical scavenging assay, a reducing power assay, a broth-diluted assay, and a brine shrimp lethality assay were performed to evaluate the extract's antioxidant, antibacterial, and toxicity capacities. The extract was clarified to be able to scavenge the free radical DPPH (EC50 = 48.65 ± 1.86 µg/mL) and active ABTS (EC = 29.27 ± 4.38 µg/mL) as well as reduce the Fe^{3+} into Fe^{2+} in solution. Moreover, the anti-positive gram bacteria were detected as an activity of the extract, also causing death to the brine shrimp with an LC50 of 87.68 ± 4.67 µg/mL. Hence, the bio-activities of the *A. altilis* extract were initially demonstrated to inhibit Gram-positive microorganisms and balance the activity of redox.

Keywords: *Artocarpus altilis*, antibacterial, shrimp lethality, antioxidants.

1. Introduction

Moraceae is a family with 60 genera consisting of over 1400 species, mainly growing in the tropical and subtropical areas of Asia, in which the genus *Artocarpus* is widely used in folk remedies (Sikarwar et al., 2014; Jagtap and Bapat, 2010). Plenty *Artocarpus* members have been proven to have the potential to treat inflammation, skin diseases, blood pressure, diabetes, etc. (Jagtap and Bapat, 2010; Tiraravesit et al., 2015; Adewole and Ojewole, 2007; Juliastuti et al., 2017). *Artocarpus altilis* (Parkinson) Fosberg is one of the standout members of the genus due to its phytochemical diversity, which includes over 50 species mainly distributed in the subtropical and tropical areas, including South Asia, Southeast Asia, Northern Australia, and Central America (Sikarwar et al., 2014; Aliefman, 2010). Sydney Parkinson discovered this plant in 1769 when he was on James Cook's first voyage (Ferrer-Gallego and Boisset, 2018). In 1773, this plant was named *Sitodium altile* and trustee at the Natural History Museum, London (Ferrer-Gallego and Boisset, 2018; Ragone et al., 1997). *Artocarpus altilis* (Parkinson) Fosberg has been officially used since 1941 (F. R. Fosberg and Swinggle, 1941). In folk therapy, each part of the plant serves as a different remedy. For example, the resin was used for the treatment of sprain, sciatica pain, diarrhea, dysentery, and other stomach diseases. Meanwhile, the bark was used for headaches, and the root was used as a purgative drug (Ragone et al., 1997). Additionally, *A. altilis* leaves are the most widely used folk remedies for inflammatory diseases (Fakhrudin et al., 2015). However, using leaves of this plant for medicine is only at the "word of mouth" level and has not been official yet despite the recorded therapeutic effects, especially the antibacterial ability. Bacterial infections are the most common threat to human health, especially those with solid toxicity or drug resistance (Mancuso et al., 2021). The problem of bacterial drug resistance has become complicated, causing many health and economic consequences despite many WHO and national policies (Zaman et al., 2017). According to WHO, although Ciprofloxacin is one of the most common antibiotics used, its restriction is predicted to rise to 93% in *Escherichia coli* and 80% in *Klebsiella pneumoniae*. In 2019, Methicillin-Resistant *Staphylococcus aureus* infection in the bloodstream was reported in 25 countries while the number recorded on *E. coli* was 49 countries. Thus, research for new bacterial therapeutics has become important, and many proposals were suggested, such as phage therapy, and modulating the microbiome in a situation where antibiotics gradually lose their effectiveness (Hauser et al., 2016). Several plant extracts are also considered a source of materials of interest in the process of finding novel treatments for bacteria (Deka and

* Corresponding author. e-mail: lybtk@tdmu.edu.vn.

Jha, 2018; Adaramola et al., 2018). Most secondary compounds exhibit antibacterial and antioxidant activity (Tungmunnithum et al., 2018). The diversity of medical compounds in *A. altilis* was recorded to be related to human healthcare (Sikarwar et al., 2014). *A. altilis* was reported for its antibacterial capacity on different strains of bacteria and fungi (Qamar et al., 2014; Pradhan et al., 2013; Riasari et al., 2017a). In addition, essential compounds with promising biological activities can be found in this plant, including antioxidant activity (Tungmunnithum et al., 2018). A comprehensive investigation of the inherent bio-activities of *A. altilis* leaf extract can contribute authentic scientific evidence to guide the safe and legitimate use of this plant in medicine. To achieve this aim, a synthetic investigation of the biological activities of *A.altilis* leaf extract was investigated to illustrate the antioxidant, antibacterial, and poisonous features.

2. Materials and methods

2.1. Herbal material and extract preparation

Artocarpus altilis (Parkinson) Fosberg leaves (Voucher No. BD-2018-1050) were collected from downtown Thu Dau Mot, Binh Duong, Vietnam. The intact leaves were rinsed with distilled water. The leaves were further dried in an oven at a stable 40^{o}C until the weight was unchanged. The herbal powder was formed by grinding it into flour. The plant extract was macerated for a week with absolute methanol. The 200 mg/mL stock solution was obtained by sterile filtering, removing solvents from samples by evaporation, and dissolving them into dimethyl sulfoxide (DMSO, Merck, Germany). The *A. altislis* leaf extract (abbreviated as AE) was stored at -20°C until use.

2.2. Antioxidant capacity evaluation

2.2.1. DPPH assay

The antioxidant ability of the AE was recorded through the capacity of free radical scavenging measurements (Ly et al., 2019; Ponnusamy and Pramadas, 2011). The *A. altilis* extract ranging from 0 to 200 µg/mL was mixed with α, α-diphenyl-β-picrylhydrazyl (DPPH, Sigma-Aldrich, USA) 0.3 mM at a proportion of 1:1 (v/v) then incubated at room temperature for 30 min in the dark. The reacted solution was recorded for absorbance at 517 nm. The reactions of vitamin C and solvent to DPPH were positive and negative controls. The percentage of DPPH radical scavenging was measured as the proportion of the discoloured DPPH and the initial DPPH.

2.2.2. ABTS assay

2,2'-azino-bis-3-ethylbenzothiazoline-6-sulfonic acid (ABTS, Sigma-Aldrich, USA) 7 mM solution was reacted with 2,45 mM $K_2S_2O_8$ solution at a ratio of 1:1 at room temperature in a dark room for 14 h to form active ABTS cation radical (Ly et al., 2019). The active ABTS solution was standardized with methanol to get a reagent with an absorbance at 734 nm of 7.00 ± 0.02. The *A. altilis* extract (0 to 200 µg/mL) was mixed with the standardized ABTS at a ratio of 1:1 (v/v), and then the mixture was left in the dark at room temperature for 7 minutes. The reacted solution was recorded for absorbance at 734 nm. The solvent and vitamin C reactions to ABTS were negative and positive controls, respectively. The percentage of ABTS radical scavenging was calculated as the proportion of the original ABTS and the initial ABTS. The non-linear regression was analyzed to calculate the extract's half-maximal effective concentration (EC50).

2.2.3. Potassium ferricyanide reducing antioxidant power (PFRAP) assay

The reduction capacity indirectly demonstrates the antioxidant ability of the AE. The PFRAP assay was used to indicate the reducing power of *A. altilis* extract by using the modified method (Ly et al., 2019). A volume of 1 mL of extract was added to 2.5 mL of PBS (phosphate buffered saline, TBR Technology CO., Vietnam) at pH 6.6 and mixed with 2.5 mL of potassium ferricyanide 1% (Sigma-Aldrich, USA). The mixture was vortexed and heated at 50°C for 20 minutes before adding a volume of 2.5 mL of 10% trichloroacetic acid (Sigma-Aldrich, USA). After a 10-minute incubation, 2.5 mL of the supernatant layer was collected and mixed in 2.5 mL of water supplemented with 0.5 ml of 0.1% $FeCl_3$ (Sigma-Aldrich, USA). The blue-green colour of the solution was computed by the absorbance at 700 nm. The extract at 0 to 1600 µg/mL concentration was tested; Vitamin C was a positive control.

2.3. Pathogenic bacterial lethality

The agar diffusion assay was carried out on selected pathogenic bacteria to determine the antibacterial effect of AE, including *Escherichia coli* (ATCC 25922 and ATCC 8739), *Proteus mirabilis* (ATCC 25933), and *Salmonella enterica* (ATCC 14028), *Staphylococcus aureus* (ATCC 25923 and ATCC 6538), *Rhodococcus equi* (ATCC 6939), *Listeria monocytogenes* (ATCC 13932). The microorganisms used in this study were derived from the American Type Culture Collection (ATCC, USA). The biomass was activated in TSA (Tryptic Soy Agar, HiMedia, India) at 37^{o}C overnight for analysis. Bacterial concentrations at 10^8 CFU/mL were regressed using the McFarland 0.5 method (Leber, 2016). Biomass was diluted with saline to obtain a density of 10^5 CFU/mL for the experiments. 100 µL of 10^5 CFU/mL spread on Muller-Hinton Agar plates, and then 6 mm wells were created using a punch stopper perforator for 50 µL AE extract loading. After a 20-hour incubation at 37^{o}C, the inhibition zones reflected the difference of the observed diameter and 6mm of the well.

The AE-sensitive strains were further detected for MIC (minimum inhibitory concentration) and MBC (minimum bactericidal concentration) (Ly et al., 2019). To demonstrate the MIC of the extract, the biomass of bacteria at 10^5 CFU/mL in Mueller-Hinton broth (MHB; HiMedia, India) was exposed to the AE at different concentrations, and the results were recorded by resazurin 0.02 % (Merck, Germany) supplementation. The MIC values were the most diluted AE concentration in which the biomass solution was still in blue. The treated biomass was further spread onto Mueller-Hinton Agar to clarify the MBC, which was considered as the lack of colonies' expression.

2.4. Toxicity of the extract investigation

The brine shrimp lethality assay indicated the toxicity of the extract, and the assay followed the reported description with a slight modification (Banti and

Hadjikakou, 2021). An amount of 1 mg of dried cysts (*Artemia nauplii*) was incubated in a hatcher with aeration under continuous light for egg hatching. The shrimps were cultured in separate test cups containing 2 mL of buffer saline; thirty individuals were used for a test. The larvae were exposed to the extract at a concentration of 0 to 1000 µg/mL with aeration under continuous light and without feeding for 24 hours. The solvent was a control. The larvae without movement during the 10 seconds of observation were considered dead. The survival rate was determined as a proportion of the number of alive in the test and control groups. The non-linear regression analysis was built up to indicate the median lethal dose (LD_{50}) of the extract on *A. nauplii*.

2.5. Data analysis

All of the experiments were performed at least three times. The GraphPad Prism software v.9.0.0 was used for data analysis, which was expressed as mean ± standard deviation. The differences were computed for the statistical significance at a p-value less than 0.05.

3. Results

The AE was extracted independently with 200 initial herbal powders. The extraction yield was recorded as 11.74 ± 0.04 %. The phytochemical content of AE extract was reported previously in the presence of polyphenols, especially tannins and flavonoids, cardiac glycoside, reducing sugar, and organic acid compounds (Chi, 2022a). The total polyphenol content was determined to be 13.57 ± 1.88 mg/100g dry weight, with the standard being Gallic acid. Meanwhile, the total flavonoid content was 29.64 ± 7.93 mg/100g dry weight, with the standard being Quercetin (Chi, 2022a)

3.1. The antioxidant ability of the AE

The antioxidant capacity of the extract is illustrated through its ability to scavenge free radicals and reduce redox reactions. The results showed that the AE and vitamin C scavenging effects, both at the concentration of 200 µg/mL, were not statistically different, with about 90% capturing DPPH radical (Figure 1A). The oxidizing radical scavenging capacity of the AE was recorded to be less active than that of the positive control, vitamin C. The activity of vitamin C reached saturation at a dose of 50 µg/mL and maintained this state at higher concentrations. The free radical scavenging efficiency of the AE observed on the ABTS gave similar results to the DPPH. However, the antioxidant activity of the extract tested on ABTS radical tended to be more effective than that on DPPH. For example, at a 100 µg/mL concentration, the ABTS cation scavenging capacity peaked while more than 75% of the DPPH radical was trapped (Figure 1B). In this assay, the effect of the extract reached the peak of 100% asymptotically from the concentration of 100 µg/mL to the higher concentration, and the saturation state was set up at higher coordinates than the positive control. The percentages of DPPH and active ABTS radicals were recorded to decline in an AE dose-dependent manner. The EC50 of the AE was calculated as 48.65 ± 1.86 µg/mL for DPPH and 29.27 ± 4.38 µg/mL for ABTS.

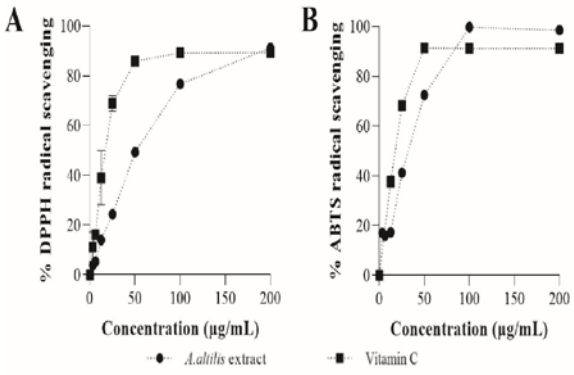

Figure 1. The antioxidant capacity of the *Artocarpus altilis* extract expressed through the free radical scavenging

The PFRAP assay was performed to assess the reducing power of AE, indirectly illustrating the antioxidant capacity (Cheng and Li, 2004). By reducing the Fe^{3+} solution into a Fe^{2+} solution with a maximum absorbing wavelength of 700nm, a curve for the extract's reduction potential was constructed to reflect the electron donor capacity (Ponnusamy and Pramadas, 2011). As illustrated in Figure 2, the reducing power of the extract was clearly shown through the gradual inflating of the amount of Fe^{2+} with the increasing AE concentration. However, the reducing power of the AE was observed to be much less effective than that of positive control.

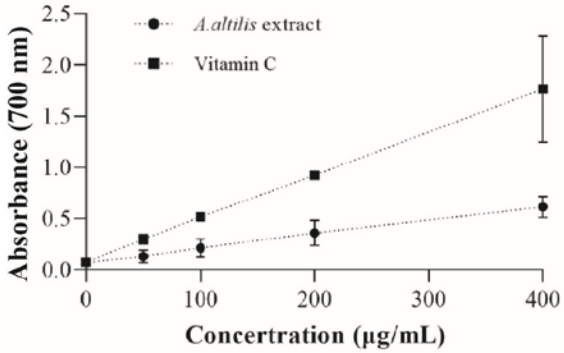

Figure. 2. The antioxidant capacity of the Artocarpus altilis extract expressed through reducing power

3.2. AE inhibited gram-positive microorganisms.

The different diameters of inhibitory zones on tested bacteria are shown in Table 1. The effect was only observed on gram-positive bacteria, with an approximate range of inhibition diameter (mm) of 5–8 for *S. aureus* ATCC 25923, 5.7–9 for *S. aureus* ATCC 6538, 8–10.5 for *R. equi* ATCC 6939; and 5.5–7.6 for *L. monocytogenes* ATCC 13932. One-way ANOVA analysis and the post-hoc Tukey's range analysis were performed and indicated that the AE showed the most potent effect on *R. equi* ATCC 6939, P-value = 0.0003.

In Figure 3, the increasing zone diameter of inhibition with increasing concentration alluded to the dose-dependent manner of the effect. This study used disk diffusion assay as a primary screening method for bacterial susceptibility, followed by the broth dilution method as a secondary screening assay. The affected bacterial strains were further analyzed for MIC and MBC values. The MIC and MBC values are detailed in Table 2. The MIC of the AE ranged from 0.1 mg/mL to 0.39 mg/mL, while the MBC was from 0.2 mg/mL to 0.78 mg/mL.

Table 1: Antimicrobial ability of the *Artocarpus altilis* extract expressed as inhibition zones

Organism	Extract concentration (mg/ml) – Inhibition zone (mm)			
	0	12.5	50	200
S.aureus ATCC 25923	-	5.01 ± 0.16	5.76 ± 0.04	7.96 ±0.49
S.aureus ATCC 6538	-	5.70 ± 0.37	6.70 ± 0.19	8.95 ± 0.13
R.equi ATCC 6939	-	8.04 ± 0.10	9.04 ± 0.04	10.46 ± 0.20
L.monocytogenes ATCC 13932	-	5.59 ± 0.25	6.79 ± 0.12	7.56 ± 0.21
E.coli ATCC 8739	-	-	-	-
E.coli ATCC 25922	-	-	-	-
P.mirabilis ATCC 25933	-	-	-	-
S.enterica ATCC 14028	-	-	-	-

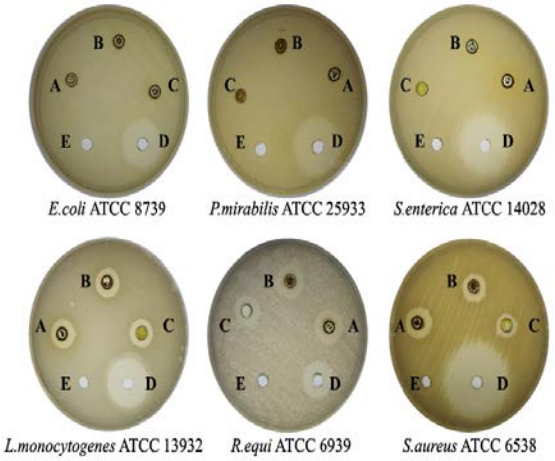

Figure. 3. The zone diameter of inhibition on various pathogenic bacteria of the Artocarpus altilis extract

Table 2. The MIC and MBC of the *Artocarpus altilis* extract and ampicillin

Organism	The AE extract (mg/mL)		Ampicillin (µg/ml)	
	MIC	MBC	MIC	MBC
S.aureus ATCC 6538	0.39	0.78	3.13	3.13
S.aureus ATCC 25923	0.39	0.39	6.25	12.50
R.equi ATCC 6939	0.10	0.20	3.13	6.25
L.monocytogenes ATCC 13932	0.10	0.20	3.13	6.25

3.3. The toxicity of AE on brine shrimp

The extract toxicity was investigated by adding the extract in different concentrations to the biomass of *A. nauplii* and then determining the percentage of mortality (Figure 4). The results showed that dead larvae increased dose-dependent and peaked at 400 µg/mL extract concentration. The EA exhibited a decisive lethality with an LD_{50} value on *A. altilis* of 87.68 ± 4.67 µg/mL.

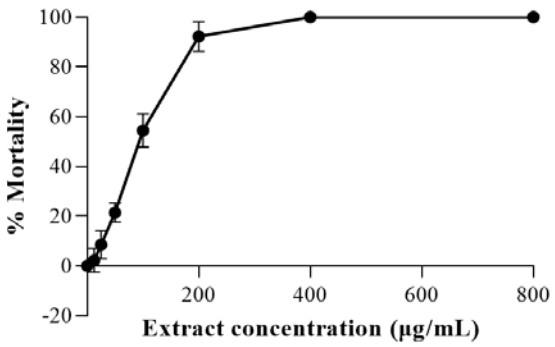

Figure. 4. The lethality effect of the Artocarpus altilis extract on brine shrimp A. nauplii after 24 hours of exposure

4. Discussion

The phytochemical content of AE was previously published at the total phenolic and flavonoid content level at 13.57 ± 1.88 mg GAE/100 g.d.w. (mg/100 g gallic acid equivalent in dried weight) and 29.64 ± 7.93 mg QE/100 g.d.w. (mg/100 g quercetin equivalent in dried weight), respectively (Chi, 2022b). The highest flavonoid content was reported to belong to the seed extract of *A. altilis* (400.86 ± 40.33 mg/100g catechin equivalent), followed by the leaf extract (334.13 ± 11.38 mg/100g catechin equivalent) (Yoanes Maria Vianney et al., 2020). Many scientific reports illustrate that antioxidant capacity mainly comes from the phenolic derived from plants, especially fruits and vegetables, instead of ascorbic acid, as popular belief holds (Wang et al., 1996). The antioxidant properties of the phenolics are formed by electron H-atom transfer, which is present in the structure (Tungmunnithum et al., 2018). The radical-induced neutralization of hydroxyls helps balance the redox in the cell (Lobo et al., 2010). The concept of free radicals, proposed by Denham Harman, was first mentioned in the *Journal of Gerontology* in 1956, suggesting that endogenous free radicals were derived from cellular activity or specifically as by-products of enzyme redox reactions (Harman, 1956). Thus far, many studies have shown the negative impact of free radicals on cellular components, namely DNA, proteins, and lipids, leading to the development of chronic human diseases, namely degenerative neurological diseases, heart-related diseases, and cancer (Sharifi-Rad et al., 2020). Maintaining redox balance helps cells avoid unwanted damage caused by free radicals, which are caused by reducing elements known as antioxidant agents (Lobo et al., 2010). The antioxidant capacity was indirectly depicted through the *in vitro* reduction of free radicals such as DPPH or ABTS of the AE. The antioxidant effect of the AE in this study was more effective than the previous research, showing the EC50 values of *A. altilis* leaf extract in DPPH assays were 140.54 µg/ml and 66.60 µg/ml (with 10% tamarind leaf co-combination) (Devi et al., 2019). In addition, the antioxidants of the other parts of *A. altilis* were also investigated, such as the fruit pulp extract, with an EC50 of 55 ± 5.89 µg/mL (Jalal et al., 2015). The AE showed an approximate antioxidant effect for the relative species, including jackfruit (*Artocarpus heterophyllus*) (Devanandan et al., 2016). The experiments with vitamin C specified the EC50 at 16.26 ± 1.54 µg/ml and 16.28 ±

1.39 µg/ml for DPPH and ABTS, which followed a similar curve to the previous report (Ly et al., 2019). The asymptote in free radical scavenging action between AE and Vitamin C shows the potential to exploit AE as a source of antioxidant materials. The donation of free electrons is also recorded through the reducing property of the extract; the higher the electron donation is, the greater is the observed reducing property (Zhong and Shahidi, 2015). The results reflect the high reducing power of AE when the extract concentration is high and vice versa. However, AE's reducing power was recorded as unrelated to radical scavenging, where there was an enormous difference between the reduction of AE and vitamin C.

In another aspect, the ability of AE to inhibit bacterial growth was observed by inhibition rings where the AE extract diffused. No inhibitory zones were observed in the Gram-negative bacterial experiments, indicating that the AE effect on these tested Gram-negative was negligible. The presence of the outer membrane and the distinction of gram-negative from gram-positive bacteria hinder the hydrophilic agents' access and permeation (Breijyeh et al., 2020). Therefore, the drug resistance in gram-negative bacteria is more conspicuous than in gram-positive (Breijyeh et al., 2020). The bias in the impact on the Gram-positive and the Gram-negative was reflected in previous reports (Shadid, 2018; Alhumaid et al., 2021).

The response to ampicillin of the tested bacteria was also investigated, and the MIC and MBC values were recorded. The anti-bacterial activity of an extract is determined by the growth-retarding and lethality of the extract against bacteria (Wallace, 2004). By comparing the MIC index of ampicillin with previous studies, it was shown that the microorganisms had average growth during the experiment (Ly et al., 2019). The antibacterial potential of A. altilis was previously reported by using agar diffusion experiments on fungi ***c***andida albicans; gram-positive bacteria streptococcus mutans**,** propionibacterium acnes, staphylococcus epidermidis, *and* staphylococcus aureus; and gram-negative bacteria *p*seudomonas aeruginosa**,** escherichia coli (Riasari et al., 2017b). The biological statuses of the leaves of A. altilis, such as green leaves, yellow leaves, and fallen leaves, also influenced antimicrobial activity; fermented green leaves were more effective than the others (Riasari et al., 2017b). In fact, according to folk remedies, the fallen leaves of *A. altilis* are usually steeped in hot water to drink, cooling the liver.

In contrast, the green leaves are exploited to cure inflammatory diseases. The ability to decrease the growth of Gram-positive bacteria at low doses suggests the possibility of exploiting AE in treating bacterial diseases. Furthermore, the safety of *A. altilis* leaf extract has been reported previously, promising a potential material for extensive antimicrobial research. The investigation of the bio-effects of AE extract was tested simply by experimenting with a brine shrimp viability assay (Sarah et al., 2017). Because the shrimp can live for up to 48 hours without being fed, the experimental time of 24 hours was appropriate and ensured the vitality of the larvae (Carballo et al., 2002). The LC50 of this assay worked as a preliminary evaluation of the bioactive components as well as the general toxicity indicator of an extract (Wakawa, 2017). The LD_{50} value of less than 250 µg/mL for crude extract and less than 40 µg/mL for pure compound was considered significantly active (Rieser et al., 1996). Moreover, the safety of the A. altilis aqueous and 80% of the leaf and stem methanol extracts were also investigated on the Wistar rat model, which did not show any negative influences on the experimental host (Sairam and Urooj, 2014). The effect on brine shrimp reinforces the strong biological potential of AE extract, which is recognized as a worthy object for further in-depth studies for academic purposes and application.

5. Conclusion

The investigation into the biological activities of AE extract depicted the potent free radical scavenging capability compared to vitamin C but has a weak reducing power in a dose-dependent manner. Besides, a potent activity against Gram-positive bacteria was also recorded, notably against *R. equi* and *L. monocytogenes* with MIC values of about 100 µg/mL. The extract did not affect Gram-negative evaluated strains. Moreover, the ability to kill 50% of brine shrimp at concentrations below 100 µg/mL also confirmed the bio-effects of AE extract. Therefore, it is necessary to consider the leaves of A. altilis as a potential source of research that can be well exploited for medical applications.

Conflict of interest

The authors declare no conflict of interest.

Acknowledgements

No application

References

Sikarwar M, Hui B, Subramaniam K, Valeisamy B, Yean L, and Balaji K. 2014. A Review on Artocarpus altilis (Parkinson) Fosberg (breadfruit). *J. Appl. Pharm. Sci.,* **4**: 91-97. https://doi.org/10.7324/JAPS.2014.40818.

Jagtap UB and Bapat VA. 2010. Artocarpus: a review of its traditional uses, phytochemistry and pharmacology. *J Ethnopharmacol.*, **129(2)**: 142-66. https://doi.org/10.1016/j.jep.2010.03.031.

Tiraravesit N, Yakaew S, Rukchay R, Luangbudnark W, Viennet C, Humbert P, and Viyoch J. 2015. Artocarpus altilis heartwood extract protects skin against UVB in vitro and in vivo. *J Ethnopharmacol.*, **175**: 153-62. https://doi.org/10.1016/j.jep.2015.09.023.

Adewole SO and Ojewole JO. 2007. Hyperglycaemic effect of Artocarpus communis Forst (Moraceae) root bark aqueous extract in Wistar rats. *Cardiovasc. J. Afr.,* **18(4)**: 221-227.

Juliastuti H, Novianti A, Fatawi B, and Yuslianti E. 2017. Ethanol-based Breadfruit Leaf (Artocarpus altilis) Extract as Hepatoprotective in Carbon Tetrachloride-induced Liver Injury. *J. Pharm. Toxicol.,* **12**: 136-141. https://doi.org/10.3923/jpt.2017.136.141.

Aliefman H. 2010. Diversity of secondary metabolites from Genus Artocarpus (Moraceae). *Nusantara bioscie.,* **2(3)**: 146-156. https://doi.org/10.13057/nusbiosci/n020307.

Banti CN, Hadjikakou SK. 2021. Evaluation of Toxicity with Brine Shrimp Assay. *Bio Protoc,* **11(2)**:e3895. https://doi.org/10.21769/BioProtoc.3895.

Ferrer-Gallego PP and Boisset F. 2018. The naming and typification of the breadfruit, Artocarpus altilis , and breadnut, A. camansi (Moraceae). *Willdenowia.,* **48**: 125-135. https://doi.org/10.3372/wi.48.48109

Ragone D, Heller J, and Engels J. 1997. Breadfruit, Artocarpus altilis (Parkinson) Fosberg. [In:] **Promoting the conservation and use of neglected and underutilized crops**. (J Heller; JMM Engles; K Hammer [editor]). Rome, Italy. IPK and IPGRI.

FR Fosberg and Swinggle WT. 1941. Botany - Name un Amaranthus, Artocarpus, and Inocarpus. *J. Wash. Acad. Sci.,* **3(3)**: 93 - 96.

Fakhrudin N, Hastuti S, Andriani A, Widyarini S, and Nurrochmad A. 2015. Study on the antiinflammatory activity of Artocarpus altilis leaves extract in mice. *Int. J. Pharmacogn. Phytochem*., **7**: 1080-1085.

Mancuso, G, A Midiri, E Gerace, and C Biondo (2021). Bacterial Antibiotic Resistance: The Most Critical Pathogens. *Pathogens.* **10(10)**: 1310.

Zaman SB, Hussain MA, Nye R, Mehta V, Mamun KT, and Hossain N. 2017. A Review on Antibiotic Resistance: Alarm Bells are Ringing., *Cureus.* **9(6)**: e1403-e1403. https://doi.org/10.7759/cureus.1403.

Hauser A R, Mecsas J, and Moir DT. 2016. Beyond Antibiotics: New Therapeutic Approaches for Bacterial Infections. *Clin. Infect. Dis.,* **63(1)**: 89-95. https://doi.org/10.1093/cid/ciw200.

Deka D and Jha D. 2018. Antimicrobial activity of endophytic fungi from leaves and barks of Litsea cubeba Pers., a traditionally important medicinal plant of North East India. *Jordan J. Biol. Sci.,* **11**: 73-79.

Adaramola F, Benjamin G, Oluchi O, and Fapohunda S. 2018. Antimicrobial and antioxidant activities of crude methanol extract and fractions of Andrographis paniculata leaf (Family: Acanthaceae) (Burm. f.) wall. Ex Nees. *Jordan J. Biol. Sci.,* **11**: 23-30.

Tungmunnithum D, Thongboonyou A, Pholboon A, and Yangsabai A. 2018. Flavonoids and Other Phenolic Compounds from Medicinal Plants for Pharmaceutical and Medical Aspects: An Overview. *Medicines (Basel).,* **5(3)**: 93. https://doi.org/10.3390/medicines5030093.

Qamar M, Budiasih S, Kaleemullah M, and Elhassan G. 2014. Evaluation of Antioxidant and Antimicrobial Activity of Artocarpus altilis Against Human Pathogens. *UK. J. Pharm. Biosci.,* **2**: 10-14.

Pradhan C, Mohanty M, and Rout A (2013). Assessment of the antibacterial potential of breadfruit leaf extracts against pathogenic bacteria. *Int. J. Pharm.*, **3(2)**: 374-379.

Riasari H, Ulfah M, Prayugo D, and Komariah N. 2016. Antibacterial and antifungal activities of various bread fruit leaves (Breadfruit (Artocarpus altilis (Parkinson) Fosberg). *Int. J. Pharm. Sci. Res.,* **11**: 1066-1073. https://doi.org/10.13040/IJPSR.0975-8232.8(3).1066-73.

Ly B, Quan N, Ly MD, Nguyen H, Lam M, and Chi HT. 2019. Evaluation of Antimicrobial, Antioxidant and Cytotoxic Activities of Dialium cochinchinensis Seed Extract. *Indian. J. Pharm. Sci.,* **81(5)**:975-980. https://doi.org/10.36468/pharmaceutical-sciences.594.

Ponnusamy J and Pramadas L. 2011. Reducing power of the solvent extracts of Eichhornia crassipes (Mart.) Solms. *Int. J. Pharm. Pharm. Sci.* **3**: 126-128.

Leber AL. 2016. Preparation of Routine Media and Reagents Used in Antimicrobial Susceptibility Testing. [In:] **Clinical Microbiology Procedures Handbook**. (Amy LL [editor]). Wiley Online Library.

Chi HT. 2022. Screening and measuring the total amount of phenols and flavonoids in Artocarpus altilis leaf extract. *Int. J. Pharm. Res.,* **14(3)**: 169-172. https://doi.org/10.31838/ijpr/2022.14.03.023.

Cheng Z and Li Y. 2004. Reducing power: the measure of antioxidant activities of reductant compounds? *Redox. Rep.* **9(4)**: 213-217.

Yoanes MV, Sulistyo Emantoko DP, and Purwanto MGM. 2020. Antioxidant and toxicity activity of aqueous extracts from various parts of breadfruit and breadnut. *Int. J. Fruit. Sci.,* **20(3)**: S1639-S1651. https://doi.org/10.1080/15538362.2020.1828222.

Wang, H, Cao G, and Prior RL. 1996. Total Antioxidant Capacity of Fruits. *J. Agric. Food Chem.,* **44(3)**: 701-705.

Lobo V, Patil A, Phatak A, and Chandra N. 2010. Free radicals, antioxidants and functional foods: Impact on human health. *Pharmacogn. Rev.*, **4(8)**: 118-126. https://doi.org/10.4103/0973-7847.70902.

Harman D. 1956. Aging: a theory based on free radical and radiation chemistry. *J. Gerontol.,* **11(3)**: 298-300.

Sharifi-Rad M, Anil Kumar NV, Zucca P, Varoni EM, Dini L, Panzarini E, Rajkovic J, Tsouh FPV, Azzini E, Peluso I, Prakash MA, Nigam M, Rayess YE, Beyrouthy ME, Polito L, Iriti M, Martins N, Martorell M, Docea AO, Setzer WN, Calina D, Cho WC, and Sharifi-Rad J. 2020. Lifestyle, Oxidative Stress, and Antioxidants: Back and Forth in the Pathophysiology of Chronic Diseases. *Front. Physiol.,* **11**: 694. https://doi.org/10.3389/fphys.2020.00694.

Devi M, Wibowotomo B, Soekopitojo S, and Merawati D. 2019. Study of Antioxidant Activity in Sinom Drinks From Breadfruit (Artocarpus Altilis) Leaves. *J. Adv. Soc. Sci. humanit.,* **242**: 7-12. https://doi.org/10.2991/icovet-18.2019.3.

Jalal TK, Ahmed IA, Mikail M, Momand L, Draman S, Isa ML, Abdull RMS, Omar MN, Ibrahim M, and Abdul WR. 2015. Evaluation of antioxidant, total phenol and flavonoid content and antimicrobial activities of Artocarpus altilis (breadfruit) of underutilized tropical fruit extracts. *Appl. Biochem. Biotechnol.* **175(7)**: 3231-3243. https://doi.org/10.1007/s12010-015-1499-0.

Devanandan P, Chowdary P, Thanmayi G, Poojitha G, and Muthukumar VA. 2016. Antioxidant and Analgesic Activity of Leaf Extracts of Artocarpus heterophyllus. *Res. J. Pharm. Technol.,* **9**: 257.

Zhong, Y and F Shahidi. 2015. Chapter 12 - Methods for the assessment of antioxidant activity in foods Handbook of Antioxidants for Food Preservation. Woodhead Publishing. 287-333. https://doi.org/10.5958/0974-360X.2016.00047.0.

Breijyeh Z, Jubeh B, and Karaman R. 2020. Resistance of Gram-Negative Bacteria to Current Antibacterial Agents and Approaches to Resolve It. *Molecules (Basel, Switzerland).,* **25(6)**: 1340. https://doi.org/10.3390/molecules25061340.

Shadid K. 2018. Phytochemical screening: Antioxidant and Antibacterial Activities of Verbena supina L. Aqueous, Hexane and Methanol Extracts., *Jordan J. Biol. Sci.,* **11 (5)**: 495-498.

Alhumaid S, Mutair AA, Alawi ZA, Alzahrani AJ, Tobaiqy M, Alresasi AM, Bu-Shehab I, Al-Hadary I, Alhmeed N, Alismail M, Aldera AH, AlHbabi F, Al-Shammari H, Rabaan AA, and Al-Omari A. 2021. Antimicrobial susceptibility of gram-positive and gram-negative bacteria: a 5-year retrospective analysis at a multi-hospital healthcare system in Saudi Arabia. *Ann. Clin. Microbiol. Antimicrob.,* **20(1)**: 43. https://doi.org/10.1186/s12941-021-00450-x.

Wallace RJ. 2004. Antimicrobial properties of plant secondary metabolites. *Proc. Nutr. Soc.,* **63(4)**: 621-9.

Sarah Q, Anny F, and Misbahuddin M. 2017. Brine shrimp lethality assay. *Bangladesh J. Pharmacol.,* **12**: 5. https://doi.org/10.3329/bjp.v12i2.32796.

Carballo JL, Hernández-Inda ZL, Pérez P, and García-Grávalos MD. 2002. A comparison between two brine shrimp assays to detect in vitrocytotoxicity in marine natural products. *BMC Biotechnology.* **2(1)**: 17.

Wakawa H. 2017. brine shrimp lethality bioassay of abrus precatorius (linn) leaves and root extract. *J. Pharm. Pharm. Sci.,* **9**: 179-181. https://doi.org/10.22159/ijpps.2017v9i1.15057.

Rieser MJ, Gu ZM, Fang XP, Zeng L, Wood KV, and McLaughlin JL. 1996. Five novel mono-tetrahydrofuran ring acetogenins from the seeds of Annona muricata. *J. Nat. Prod.* **59(2)**: 100-8.

Sairam, S and Urooj A. 2014. Safety Evaluation of Artocarpus altilis as Pharmaceutical Agent in Wistar Rats. *J. Toxicol.,* **2014**: 980404. https://doi.org/10.1155/2014/980404.

JJBS

Volume 17, Number 4,December 2024
ISSN 1995-6673
Pages 645 – 655
https://doi.org/10.54319/jjbs/170408

Jordan Journal of Biological Sciences

The Role of Chitosan in Improving the Cold Stress Tolerance in Strawberry varieties

Sherin A. Mahfouze*, Heba A. Mahfouze, Radwa Y. Helmi, Fathallah B. Fathallah, Kamal A. Aboud, and Mahmoud E. Ottai

Genetics and Cytology Department, Biotechnology Research Institute, National Research Centre, Dokki, Giza, 12622, Egypt.

Received: March 22, 2024; Revised: June 3, 2024; Accepted: June 13, 2024

Abstract

Cold stress is considered one of the main factors that influence strawberry production in an open field. This study aimed to estimate the effects of three different concentrations of chitosan (COS) solution used by foliar spraying on the vegetative growth and yield parameters of three strawberry varieties. Moreover, the impact of foliar spraying of COS solutions on the induction of biochemical changes linked to cold stress was assessed. In this study, three different concentrations of COS solution (250, 500, and 1000 ppm) were applied to three strawberry varieties that genetically different by foliar spraying, compared with the untreated control (0 ppm COS). The results showed that the COS solution led to significant and non-significant increases in the vegetative and fruit growth parameters, depending on the concentration of COS and strawberry variety. On the other hand, it was shown that foliar application of strawberry varieties with COS solution under chilling stress causes changes in gene expression in strawberry varieties, either up-regulated or down-regulated. Furthermore, novel proteins related to cold tolerance, including pathogen-related proteins (PRPs), were identified in three strawberry varieties. For instance, new polypeptides of MWs (53 and 44 kDa) and (53; 44; and 8 kDa) were scored in Fortuna variety that was sprayed with 250 and 500 ppm COS respectively, compared with the corresponding control. In addition, one subunit of 29 kDa was detected in Florid and Festival varieties treated with 500 and 1000 ppm COS solutions. Consequently, these proteins could be used as biomarkers related to cold tolerance. Therefore, foliar spraying of COS can be used in strawberry breeding programs to protect them from cold stress.

Keywords: Abiotic stress, *Fragaria* x *ananassa* Duch, fruit yield, gene expression, vegetative growth.

1. Introduction

Strawberry (*Fragaria* × *ananassa* Duch.) belongs to the *Rosaceae* family; it is an herbaceous plant. The strawberry plant is considered to be an economically significant crop yield in Egypt and worldwide (Tan *et al*., 2003). It is considered to be one of the richest resources of bioactive chemical substances, e.g. vitamins, anthocyanins, flavonoids, carotenoids, and phenolics, all of which have marked antioxidant properties. In addition, phenolic substances like flavonoids, carotenoids, and anthocyanins found in strawberry plants have important anticancer activities (Zhang *et al.*, 2008; Hossain *et al.*, 2016; Rahman *et al.*, 2018). Recently, the production of strawberries in Egypt has been impacted by climate change. Temperature is considered a crucial environmental factor affecting strawberry plant growth under short-day conditions. In temperate regions, strawberry plant freezing injury is a main factor in decreasing the quantity and quality of crop yield (Roussos *et al*., 2020; Li *et al*., 2021; Han *et al*., 2023).

One of several natural substances that have demonstrated effectiveness against diseases in strawberries and different crops is chitosan (COS), a biopolymer chemically produced from crustaceans and soluble in organic acids (Malerba and Cerana, 2018). COS is considered ecologically sound for agricultural applications due to its easy environmental degradation and non-toxicity to people. Plant defense was elicited by COS and its derivatives, so it was applied as a natural compound to manage diseases before and after harvest (El Ghaouth *et al.*, 1991). Numerous studies have found that strawberry fruit treated with chitosan improves storage stability and increased anthocyanin content (Malerba and Cerana, 2018; El Ghaouth *et al.*, 1991). COS was commonly used as a coating agent for various fruits, to protect against post-harvest losses due to microbial diseases (Sakif *et al.*, 2016). The use of chitosan as a foliar spray has been reported previously by many investigators to increase vegetative growth, yield, and biochemical contents in plants (El-Miniawy *et al.*, 2013; Mukta *et al.*, 2017). Transcriptomic analysis revealed that COS stimulates the expression of genes in a variety of physiological processes, involving photosynthesis, the plant immune system, systemic acquired resistance, and hormone metabolism. Additionally, it affected the expression of the heat-shock protein (HSP) and the re-programming of protein metabolism with an increase in storage proteins (Landi *et al.*, 2017). However, there is little information available regarding the use of chitosan in plant growth, crop productivity, and quality. Therefore, the current

* Corresponding author. e-mail: sherinmahfouze@yahoo.com.

investigation aims to estimate the effects of three different doses of COS solution by foliar spraying on the vegetative growth and fruit yield parameters of three strawberry varieties. Besides, the impact of foliar spraying of COS on the induction of biochemical changes with reference to cold stress.

2. Materials and Methods

2.1. Plant materials

The current study was conducted out in the South of Tahrir, Beheira Governorate, during the 2022/23 season (latitude: 30° 31' 48.3312", and longitude 30° 31' 48.3312" and altitude N 30° 31.8055'). Planting strawberry runners of three varieties (Fortuna, Festival, and Florida) were done in four lines, 30 cm apart, on terraces 120 cm wide, and the distance between plants was 30 cm. The experimental unit contained 40 plants. Thirty-day-old strawberry plug plants were transplanted in the field during the winter season. The chitosan treatment was applied in cold conditions, with temperatures ranging from 18-22/5-13°C daylight/night from mid-December, 2022 until the end of January 2023 and 50–60% humidity. All agricultural practices, including irrigation, fertilization, and pesticides, were performed as recommended by the Ministry of Agriculture, Egypt.

2.2. Chemical analysis of soil (pre-experiment)

Chemical analysis was done at Land Resources Evaluation and Mapping, National Research Centre, Dokki, Giza, Egypt. The results showed that the soil was suitable for growing strawberry plants (Table 1).

Table 1. Determination of soil chemical properties of strawberry.

Parameters	Experimental soil
pH	7.79*
EC dSm^{-1}	0.67**
EC ppm	428.8
Soluble cations and anions	meq/L
Ca^{++}	2.0
Mg^{++}	1.2
K^{+}	0.3
Na^{+}	2.8
$CO_3^{=}$	-
HCO_3^{-}	1.1
Cl^{-}	3.7
$SO_4^{=}$	1.5
Macro- and micro-elements	ppm
N	175.6
P	8.04
K	202.8
Fe	18.5
Mn	13.2
Zn	2.2
Cu	2.5

EC is electrical conductivity. * Determined in 1:2.5 soil suspension, ** measured in 1:5 soil extraction.

2.3. Chilling treatments

Practical-grade chitosan (COS) biopolymer (poly-ß-1,4-D-glucosamine) available in powder form was purchased from Bioworld company, Egypt. It was commercially prepared by the alkaline deacetylation of chitin obtained from shrimp shells (*Pandalus borealis*). The degree of de-acetylation was ≥ 75-85%, and viscosity was 200-800 cP. Three different concentrations, 250, 500, and 1000 ppm of COS solution were prepared by measuring the required amount of product, and diluting with distilled water and pH adjusted to 6.5 by adding drops of 0.1 M NaOH, or 0.1 M HCL (Benhamou *et al*., 1998). Freshly prepared COS solutions were sprayed on strawberry plants in each experimental unit before the flowering stage by spraying up to run off level for five successive times with an interval of 10 days between each. Control plants were sprayed with an equal volume of sterile water amended with an equal volume of 0.1 N HCl and NaOH to adjust pH at 6.5 (without chitosan).

2.4. Data collection

To determine the impact of spraying with COS on the plant's growth of three strawberry varieties, observations were recorded on randomly selected ten guarded plants for the number of leaves per plant, plant height (cm), root length (cm), leaf area (cm^2), shoot fresh and dry shoot weights (g), and root fresh and dry weights (g). Fruit yield characteristics were also estimated by repeated collection at intervals 1^{st}, 2^{nd}, and 3^{rd} harvests according to the flowering growth cycles of strawberry plants during the growing season according to the prevailing temperatures for number of fruits/plant, and weight of fruits/plant (g/plant).

2.5. Sodium dodecyl sulfate–polyacrylamide gel electrophoresis (*SDS-PAGE)*

2.5.1. Extraction of total protein

Protein was extracted and purified from ground samples using sodium dodecyl sulfate (SDS) extraction followed by trichloroacetic acid (TCA)-acetone precipitation, according to (Zheng *et al.*, 2007).

2.6. Electrophoresis on PAGE

SDS-PAGE was performed according to Laemmli, (1970) as modified by Studier, (1973) by using 12.5% SDS gel for total protein profiling. After that, the electrophoresis gel was stained with Coomassie Brilliant Blue dye G-250 and then was destained to visualize the protein bands.

2.7. Statistical analysis

The field experiment was laid out in a randomized complete block design (RCBD) with three replicates. Observations were recorded on randomly selected 10 guarded plants from each plot. The obtained data was statistically analysed using a two-way ANOVA (Snedecor and Cochran, 1980) to compare the treatments and varieties for all traits. Tukey's test was applied to compare significant differences between treatment means at $p<0.05$. The analysis was performed using 'GraphPad- prism' software (version 9.3.1, www.graphpad.com).

2.8. Cluster analysis

A matrix for SDS-PAGE was generated by scoring reproducible bands as 1 for their presence and as 0 for their absence across treated and untreated strawberry varieties. Genetic similarity coefficients were computed according to (Nei and Li, 1979). A dendrogram based on

Jaccard similarity coefficients was constructed by using the unweighted pair group method of arithmetic averages (UPGMA) (Sneath and Sokal, 1973), employing sequential, agglomerative hierarchic, and non-overlapping clustering (SAHN). All the computations were carried out using the PAST software (Ryan *et al.*, 1995). Correlation coefficients were calculated using similarity coefficients obtained from SDS-PAGE analysis.

3. Results

3.1. Effect of COS on vegetative growth parameters of strawberry varieties

The ANOVA analysis showed positive effects on vegetative growth parameters **(**number of leaves per plant**,** plant height, root length, shoot fresh and dry weight, and root fresh and dry weight) between treatments for each strawberry variety separately and the corresponding control (Figs. 1, 2, 3, and 4). It was observed that strawberry var. Festival treated with 500 ppm COS led to an increase in the number of leaves/plant, shoot fresh and dry weight, and root fresh and dry weight compared with the control. However, the plants sprayed with 1000 ppm COS solution caused a non-statistically significant increase in the plant height and leaf area (Figures 1, 2, 3, and 4). For the Fortuna variety, the application of 250 ppm COS led to an increase in root length, while the dose of 500 ppm COS induced positive changes in the number of leaves/plant and root fresh and dry weights. Moreover, the plants treated with 1000 ppm COS led to a significant increase in leaf area at $p<0.05$, compared with the untreated control. However, the dose of 1000 ppm COS caused a non-significant variation in the plant height (Figures 1, 2, 3, and 4). Finally, it was observed that the foliar spraying of 500 ppm COS solution on strawberry plants var. Florida caused an increase in the plant height, the root length, the number of leaves, and shoot fresh and dry weight, while the dose of 1000 ppm COS solution had positive effects on root fresh and dry weight (Figures 1, 2, 3, and 4). On the other hand, there were significant differences among three strawberry varieties sprayed with COS and the controls. For example, significant variations were recorded between strawberry var. Fortuna (500 ppm COS) and Florida (500 ppm COS). Also, Florida (500 ppm COS) and Fortuna (1000 ppm COS). Two strawberry varieties, Fortuna and Florida treated with 500 ppm COS had highly significant differences in the number of leaves, compared with Fortuna (250 ppm COS) and Festival (500 ppm COS), respectively (Figure 3). It is clear that 1000 ppm COS of var. Florida caused a substantial impact in the number of leaves, compared with var. Festival (250 and 1000 ppm COS) at $p<0.05$. In contrast, strawberry var. Florida (250 and 500 ppm COS) resulted in a significant increase in the number of leaves compared with Festival (1000 ppm COS). The latter significantly increased the number of leaves, compared with the Fortuna variety (1000 ppm COS) (Figure 3).

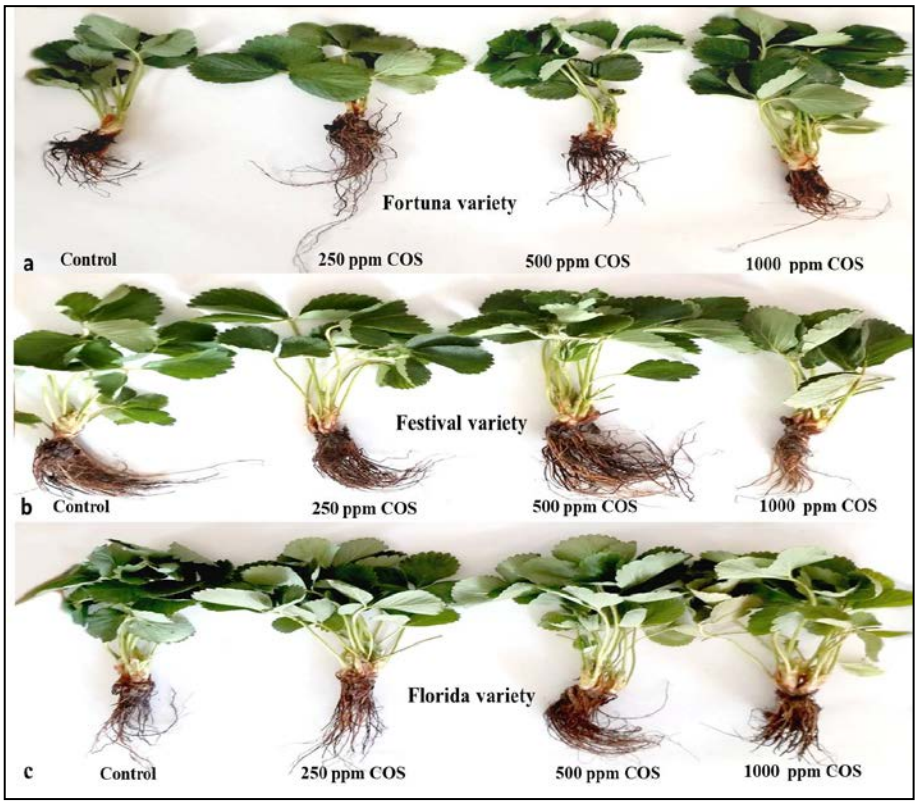

Figure 1. Showing variability in vegetative growth parameters of three different strawberry (**a**: Fortuna, **b**: Festival, and **c**: Florida) varieties, treated with three different concentrations of COS solution under cold-stress conditions, compared with untreated control. After 60 days of treatment with COS. Error bars represent cm.

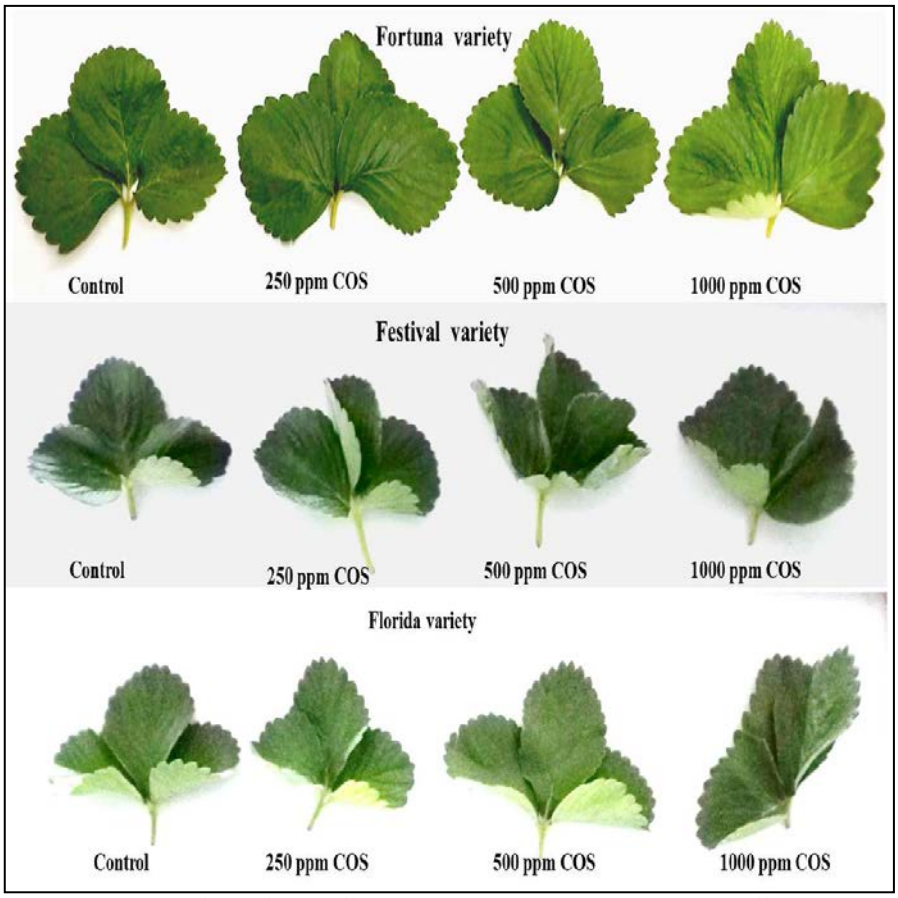

Figure 2. Showing variability in leaf area of three different strawberry varieties, treated with three different concentrations of COS solution under cold-stress conditions, compared with un-treated control. After 60 days of treatment with COS. Error bars represent cm.

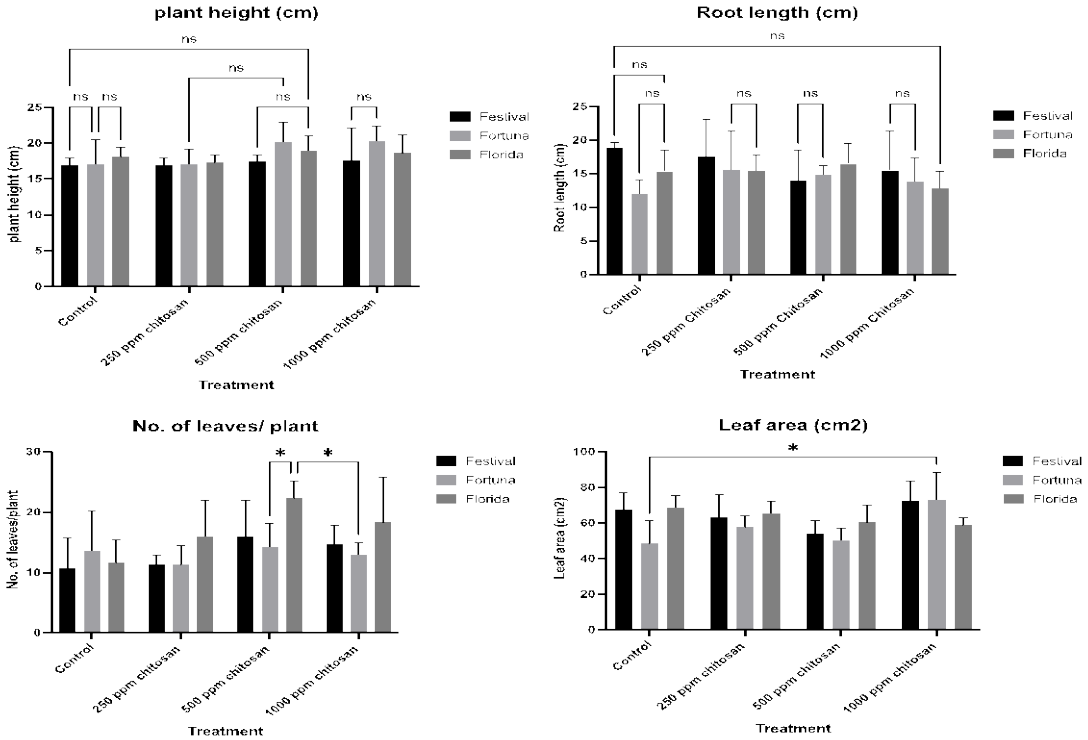

Figure 3. Bar plots show morphological characterization (plant height, root length, No. of leaves/plant, and leaf area) of three different strawberry varieties, treated with three different concentrations of COS solution under cold-stress conditions, compared with un-treated control. The asterisk means significant differences among treatments and genotypes according to range, $p<0.05$, and ns: non-significant.

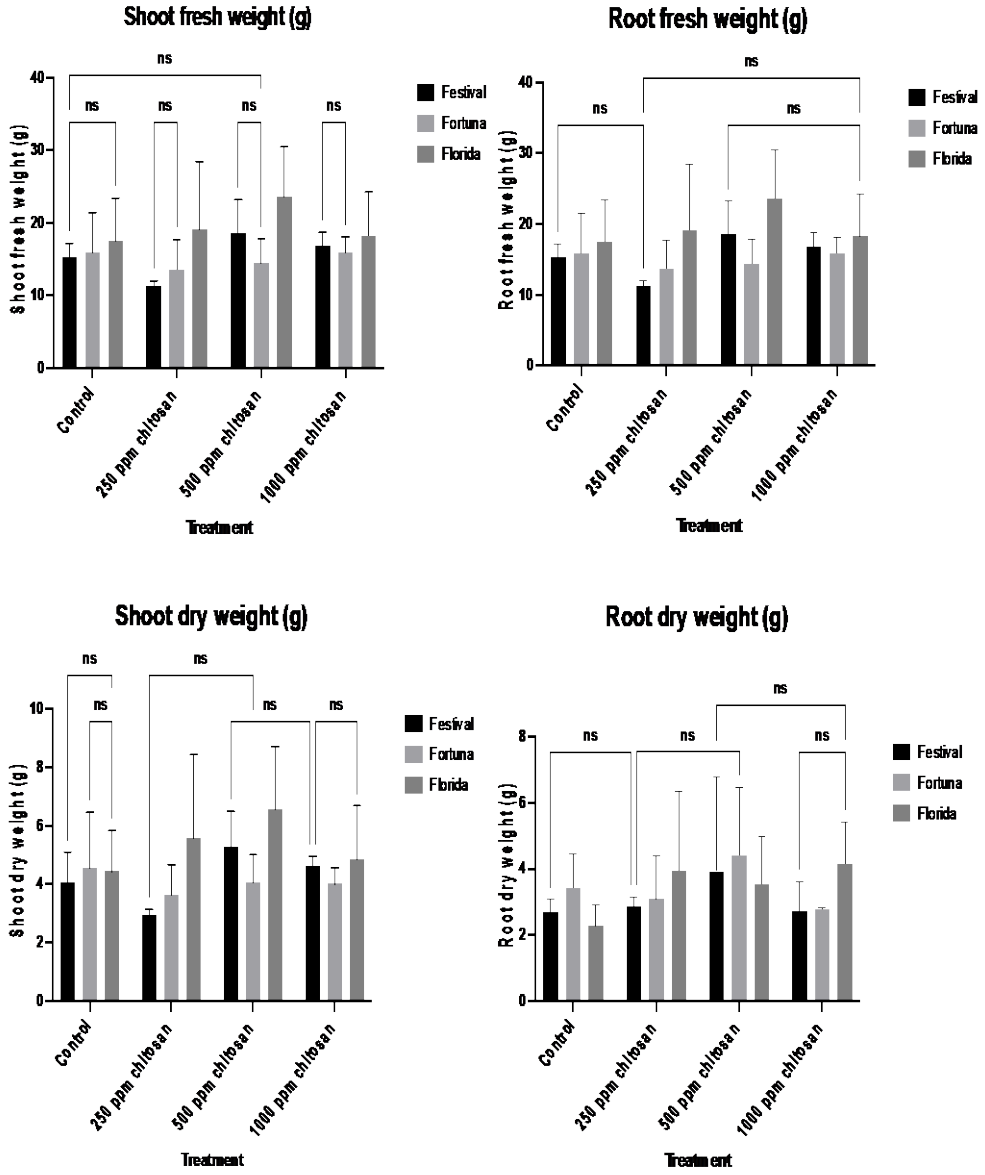

Figure 4. Bar plots show morphological characterization (shoot and root fresh weight and shoot and root dry weight) of three different strawberry varieties, treated with three different concentrations of COS solution under cold-stress conditions, compared with un-treated control. ns: non-significant.

3.2. Effect of COS on reproductive growth parameters of strawberry varieties

3.2.1. Number of fruits in the 1st, 2nd, and 3rd harvests

The strawberry var. Festival treated with 500 ppm COS solution had a highly significant increase in the number of fruits in the 1st harvest, compared with the control. Furthermore, the foliar spraying of 500 ppm COS caused positive effects on the number of fruits in the 2nd and 3rd harvests. For the Fortuna variety, it was shown that a dose of 250 ppm COS solution improved the number of fruits in three harvest times. However, the foliar application of 500 ppm COS of strawberry var. Florida grown in the field caused a significant increase in 1st harvest yield under cold stress conditions, compared with the control at $p<0.05$ (Figure 5). Also, plants treated with 500 and 1000 ppm COS improved the number of fruits in (the 1st and 2nd) and the 3rd harvests, respectively, compared with un-treated plants. On the other side, there were significant variations in the number of fruits in three harvests, between treatments and control of three different strawberry varieties. In the 1st harvest, control var. Florida positively and significantly influenced the number of fruits, compared with the control vars. Fortuna and Festival. Besides, the strawberry plants of Florida treated with different concentrations of COS solution (500 and 1000 ppm) induced significant effects compared with the control vars. Fortuna and Festival. Also, Festival (500 and 1000 ppm COS) led to significant changes in fruit yield, compared with Florida and Fortuna controls, respectively (Figure 5). For the 2nd harvest, results of the study showed that var. Festival sprayed with 500 ppm COS caused a highly significant increase in the fruit numbers, compared with the control plants. Besides, var. Fortuna (500 ppm COS) showed statistically significant differences in fruits number, compared with the control. It was observed that

var. Fortuna (250 and 500 ppm COS) led to highly significant changes in the number of fruits, compared with Festival var. treated with 250 ppm COS. There were substantial variations between 500 ppm COS of the Florida variety and control var. Fortuna as well as Fortuna (250 and 500 ppm COS) and Festival (1000 ppm COS) (Figure 5). In the 3rd harvest, it was clear that both Fortuna and Florida controls recorded highly significant differences in the number of strawberry fruits, compared with Festival control. On the contrary, there were no significant variations between each strawberry variety separately and controls (Figure 5).

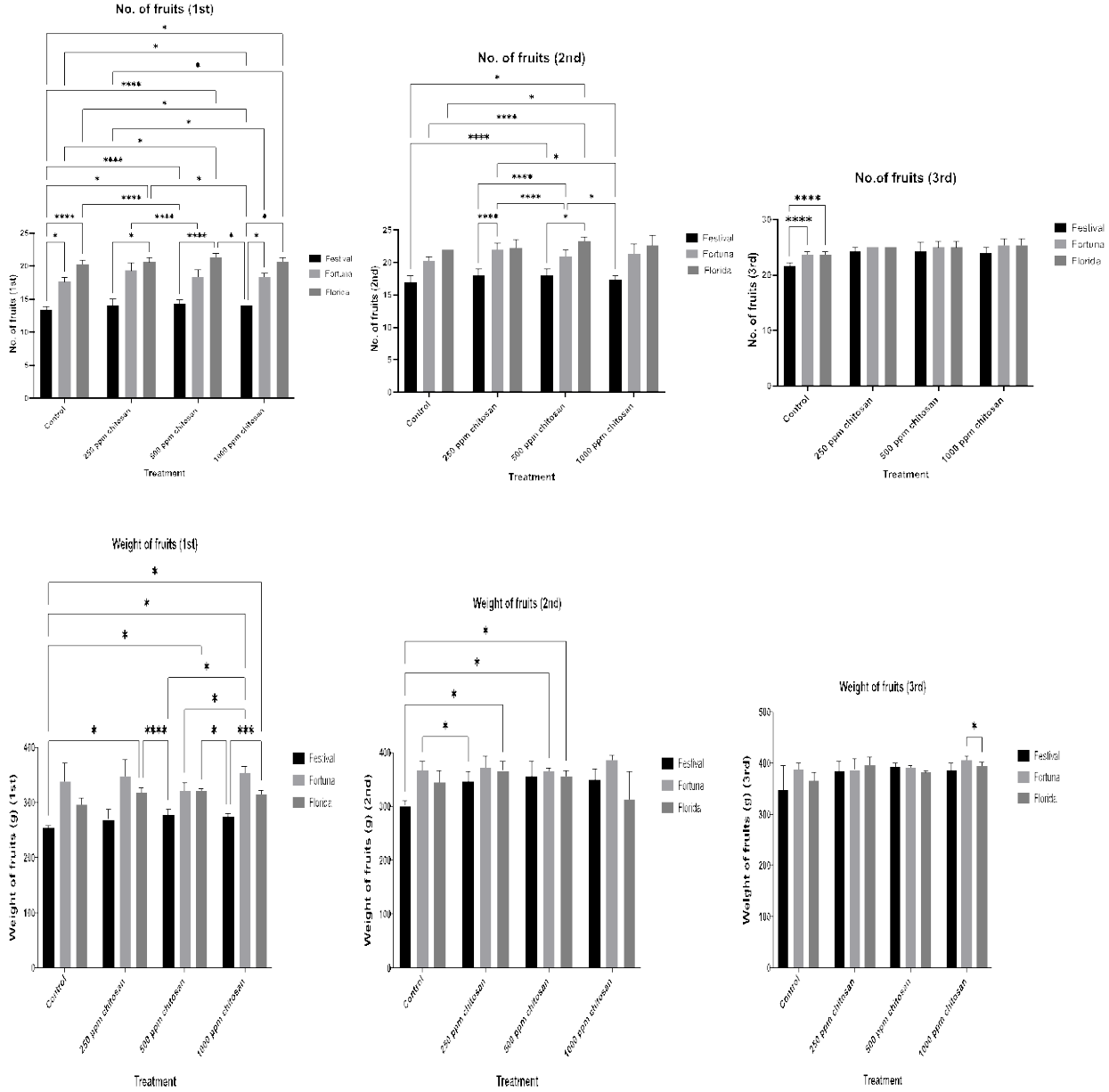

Figure 5. Charts show fruit yield (number and weight of fruits in 1st, 2nd, and 3rd harvests) of three different strawberry varieties, treated with three different concentrations of COS solution under cold-stress conditions, compared with untreated control. The asterisk means significant differences among treatments and genotypes according to range, $p<0.05$.

3.2.2. Weight of fruits in 1st, 2nd, and 3rd harvests

Regarding the results of the weight of fruits of three strawberry varieties in three harvests, it was found that foliar application of 500 ppm COS led to an increase in the fresh biomass in var. Festival through three harvests, compared with the untreated control. Moreover, the foliar spraying of 1000 ppm COS of strawberry var. Fortuna cultivated in the field induced a significant ($p<0.05$) increase in the weight of fruits under cold stress conditions in the 1st harvest and a non-significant increase in the 2nd, and 3rd harvests, compared with un-treated plants. Furthermore, strawberry var. Florida sprayed with 250 and 500 ppm COS solutions had positive effects on fruit yield in (the 2nd and 3rd) and the 1st harvests, respectively (Figure 5). On the other hand, it was clear that strawberry var. Florida treated with three different concentrations of COS solution (250, 500, and 1000 ppm) caused a significant increase in weight of fruits, compared with the control Festival (Figure 5). Moreover, Fortuna var. sprayed with 1000 ppm COS recorded a remarkable increment in fruit yield in the 1st harvest, compared with Festival

(control and 500 ppm COS). It was shown that 250 and 1000 ppm COS solution significantly increased fruits weigh in strawberry var. Florida, compared with 500 and 1000 ppm COS of var. Festival, respectively at $p<0.05$. Moreover, strawberry var. Florida treated with 500 ppm COS solution had a positive effect on the weight of the fruit, compared with 1000 ppm Festival variety. For 2nd harvest, it was found that vars. Florida (250 and 500 ppm COS) and Fortuna (500 ppm COS) stimulate a significant increase in yield, compared with the control Festival (Figure 5). According to the 3rd harvest, it was observed that 1000 ppm COS of var. Fortuna scored a statistically significant increase in fruit weight compared with 1000 ppm COS of Florida (Figure 5).

3.3. Gene expression of strawberry plants treated with COS by SDS-PAGE

SDS-PAGE revealed the differences in protein banding patterns of three varieties of strawberry (Florida, Festival, and Fortuna), treated with the three different concentrations of COS (250, 500, 1000 ppm, and un-treated control) (Figure 6). The electrophoregrams were estimated depending on the number of subunits and molecular weights of polypeptides (MWs) (kDa). A total of 26 polypeptides were recorded, ranging from 8 to 120 kDa; 18 bands out of 26 were monomorphic (69.23%). However, eight were polymorphic (30.77% polymorphism). The application of foliar spraying with COS under cold stress led to inducing changes in gene expression in strawberry varieties that were either up-regulated or down-regulated. The highest content of proteins was found in Fortuna variety treated with 500 ppm COS (25 subunits). In contrast, the lowest content of proteins was recoded in Florida variety sprayed with 250 ppm COS (19 polypeptides) (Figure 6). On the other hand, new proteins were induced in three strawberry varieties treated with COS under cold stress. For example, the Fortuna variety sprayed with 250 and 500 ppm COS recorded novel polypeptides of MWs (53 and 44 kDa) and (53; 44; and 8 kDa), respectively, compared with the corresponding control. Interestingly, Florid and Festival varieties sprayed with 500 and 1000 ppm COS induced only one band of 29 kDa (Figure 6).

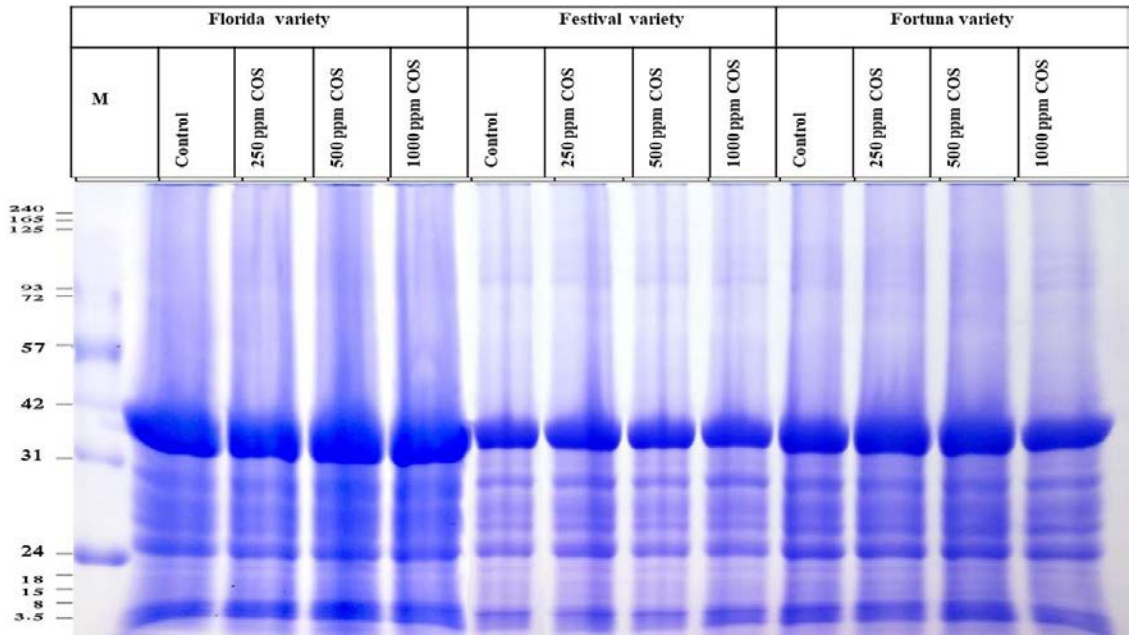

Figure 6. SDS-PAGE banding patterns of three strawberry varieties (Florida, Festival, and Fortuna) sprayed with three different concentrations of chitosan (COS) compared with the control. Lane M: Protein ladder.

3.4. Cluster analysis

The genetic similarity values among three strawberry varieties (Florida, Festival, and Fortuna) COS-treated ranged from 0.73 to 0.96 (Figure 7). The highest genetic similarity was 0.96, found between (Fortuna; 250 ppm) and (Fortuna; 500 ppm), while the lowest genetic similarity was 0.73, recorded between (Fortuna; 500 ppm) and (Festival; 1000 ppm) (Figure 7). A dendrogram showed two different clusters. The first cluster (I): composed of two groups. The first group (a) has COS-treated and untreated plants of Florida variety. However, the second group (b) included treated and untreated plants of Festival variety. Finally, the second cluster (II): contained the Fortuna variety treated with three different concentrations of COS and control, which conferred a higher genetic distance between the two clusters Fortuna and (Florida and Festival) (Figure 8).

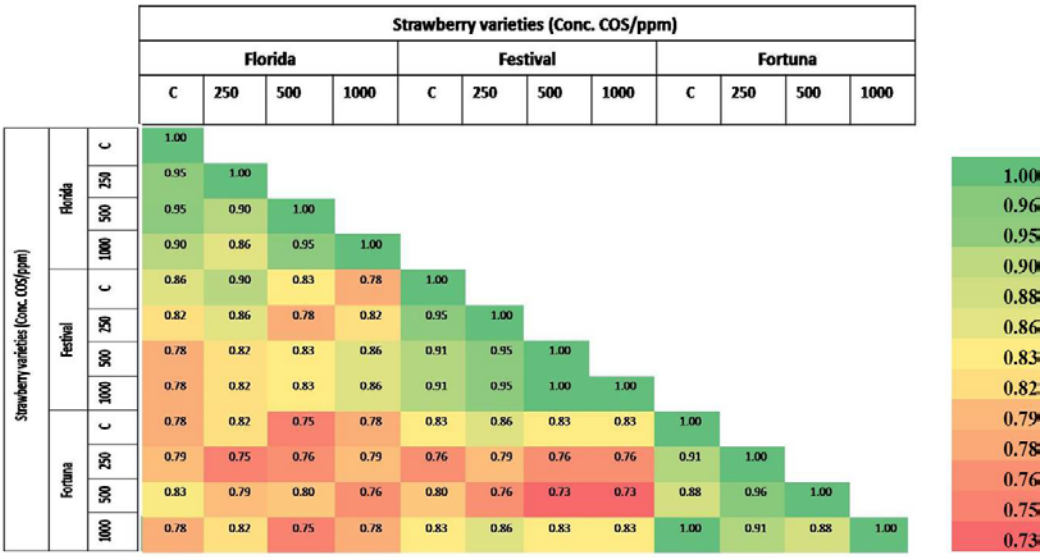

Figure 7. Heatmap was determined using the Jaccard index of three strawberry varieties (Florida, Festival, and Fortuna) sprayed with three different concentrations of chitosan (COS), compared with the control (C).

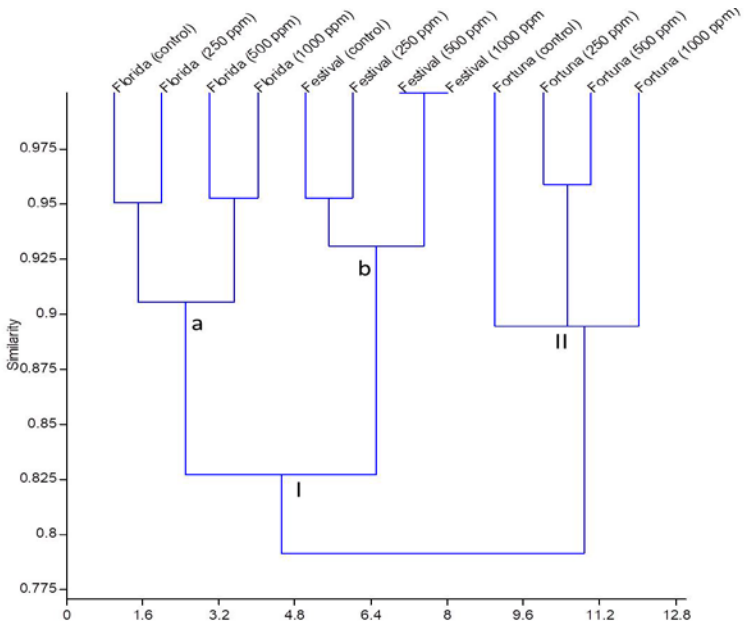

Figure 8. Dendrogram of three strawberry varieties (Florida, Festival, and Fortuna) sprayed with three different concentrations of chitosan (COS), compared with the control.

4. Discussion

Chilling is considered a very serious threat as a result of its harmful effects on the growth of different crops in the field. Also, climate change can impact quantity and quality of the vegetable and fruit yields in Egypt and worldwide, consequently affecting the accessibility of food in the future (Eissa *et al.*, 2013; Hasanuzzaman *et al.*, 2020). One of these climatic changes' manifestations is cold stress, which has a severe impact on the productivity of various crops, such as strawberry plants (Roussos *et al.*, 2020; Li *et al.*, 2021; Han *et al.*, 2023). A low temperature can affect biochemical and physiological operations in plants, causing different symptoms such as necrosis, chlorosis, and wilting (Ruelland and Zachowski, 2010). In this study, the ANOVA analysis showed positive effects in vegetative growth parameters (number of leaves/plant, leaf area, plant height, root length, shoot fresh and dry weight, root fresh, and dry weight) and reproductive growth (number of fruits and weight of fresh biomass) between COS treatments for each strawberry variety separately and the healthy control and among the tested strawberry varieties. Our findings showed that foliar application of COS solution to strawberry plants in an open field improved the plant growth, which depends on the concentration and variety. Similar results were observed by Pongprayoon *et al.*, (2022) who found that COS-treated plants induce beneficial responses in plants against abiotic

stresses. Thus, COS influence depends on concentration, plant species, structure, and the growth stage of the plant.

In the current investigation, the lowest vegetative and fruit growth parameters were recorded in the COS-untreated control. However, foliar spraying of 500 ppm COS solution on strawberry var. Festival led to improvements in vegetative and reproductive growth, while a dose of 1000 ppm had positive changes in plant height and leaf area. Moreover, a remarkable increment in both vegetative growth and yield of strawberry var. Fortuna depends on COS dose. For example, a dose of 250 ppm COS positively influenced root length, and the number of fruits in three harvests, whilst a dose of 500 ppm COS solution increased the number of leaves/plant and root fresh and dry weight, and the number of fruits in the 3rd harvest. Nevertheless, 1000 ppm COS induced remarkable changes in plant height, leaf area, and weight of fruits in the 1st, 2nd, and 3rd harvests. However, strawberry var. Florida treated with a dose of 500 ppm COS caused an increase in plant height, root length, no. of leaves, shoot fresh and dry weight, no. of fruits in the 1st, and 2nd harvests, weight of fruit in the 1st harvest, and root fresh, dry weight and the number of fruits in the 3rd harvest. These results agree with Pichyangkura and Chadchawan, (2015) and Rahman *et al*., (2018) who found that foliar spraying with different doses of COS enhanced the growth of strawberry plants compared with untreated control. However, a dose of 500 ppm recorded the highest growth parameters and improved resistance to diseases by mechanisms involving induced systemic resistance. The positive effect of COS on vegetative growth may be attributed to an increase in the uptake of water and nutrient elements by altering the osmotic pressure of the cell and decreasing the aggregation of harmful free radicals through increasing antioxidants, e.g. glutamine synthetase, nitrate reductase, and protease. It encourages the production of large quantities of phenolics, flavonoids, carotenoids, and anthocyanins. Besides, COS enhanced the transportation of nitrogen to leaves. Consequently, COS increased photosynthesis, which enhanced the growth and development of plants. In addition, COS has several characterization including being less expensive, safe for human health, and environment-friendly, abundantly available, and biodegradable (Guan *et al.*, 2009; Mondal *et al.*, 2012). Wang *et al.*, (2021) indicated that COS nanoparticles increase the efficiency of *Musa* sp. plants in the tolerance of chilling by decreasing the accumulation of reactive oxygen species (ROS) and the induction of non-enzymatic antioxidants, such as phenolic compounds, and increasing antioxidant enzyme activities. Besides, it causes the accumulation of osmoprotectants, such as amino acids, soluble carbohydrates, and proline. Therefore, it aids in enhancing the plants' tolerance to cold stress.

In this context, it was shown that foliar application of strawberry plants with COS solution under chilling stress stimulates changes in gene expression in strawberry varieties, either up-regulated or down-regulated. Furthermore, novel proteins belonging to pathogen-related proteins (PRPs) were induced in three strawberry varieties treated with COS under abiotic stress. For example, new polypeptides of MWs (53 and 44 kDa) and (53; 44; and 8 kDa) were scored in the Fortuna variety sprayed with 250 and 500 ppm COS, respectively compared with the corresponding control. Also, one subunit of 29 kDa was detected in Florid and Festival varieties treated with 500 and 1000 ppm COS solutions. These results agree with Lukoševičiūtė, (2014) who observed a significant increase in the content of 18 kDa protein in the shoots of two strawberry varieties during the freezing stress. Vítámvás and Prášil, (2008) found that one of the characteristics of acclimatization to cold stress is an increase in the concentration of soluble proteins and carbohydrates, which significantly reduces the damage that freezing causes to plant tissues. Besides, low temperatures cause an increase in total soluble proteins involving lipocalins and dehydrins that accumulate in plasma membranes when plants are exposed to freezing. Ouellet and Charron, (2013) indicated that these proteins play an important role in protecting cell structures from chilling damage and decreasing oxidative stress development. Kuwabara and Imai, (2009) found that some PRPs were induced under cold stress conditions, such as ß-1,3-glucanases, which were shown to be low temperature-induced and were cryoprotective activity similar to other extracellular PRPs (Hincha *et al.*, 1997). The evidence on the role of PRPs in cold tolerance in strawberry plants is little. Gharechahi *et al.*, (2014) mentioned that PRPs other than the PR-1 class are linked to the chilling stress of plants, and it was supposed that they could be included as components of the stress-regulated signal transduction pathway. Pihakaski-Maunsbach *et al.*, (2001) suggested that low temperatures interact with other environmental cues in plants. Interestingly, numerous studies have found a strong correlation between chilly signals and defensive reactions. There were a variety of PRPs, including -1,3-glucanases, endochitinases, and thaumatin-like proteins, that built up in winter rye during cold stress. These proteins play the main role in freezing tolerance (Griffith and Yaish, 2004). How cold stress stimulates their accumulation is still understood. The synthesis of PRPs under cold stress conditions ensures an appropriate strategy of defense against infection with pathogens that multiply during cold seasons. All this information shows the existence of a variety of signaling interactions between pathogens and cold responses. Van Loon *et al.*, (2006) mentioned that senescence, injury, or cold stress all cause the induction of several defense-related proteins, some of which have antifreeze functions. Numerous defense-related proteins are found in floral tissues on a constitutive basis, and a sizable number of PR-like proteins in pollen, fruits, and vegetables. Besides, these proteins play major roles in plant life, whether in defense or not.

Therefore, the exogenous application of COS led to the induction of novel polypeptides in all tested strawberry varieties. These new proteins were up-regulated compared with the corresponding control.

5. Conclusions

Chilling injury is considered one of the most important environmental stresses that affect the growth and productivity of strawberry crops in the world. In this study, it was observed that foliar spraying of three strawberry varieties with different concentrations of COS solution (250, 500, and 1000 ppm) in an open field, resulted in a significant increase in leaf area, and number of leaves of var. Fortuna. Furthermore, there was a substantial increment in the number of fruits in vars. Festival, Fortuna,

and Florida, compared with the un-treated control. On the other hand, COS had positive effects in vegetative growth parameters for the tested strawberry varieties **(**number of leaves/plant**,** leaf area, plant height, root length, shoot fresh and dry weight, root fresh, and dry weight) and reproductive growth (weight of fresh biomass) between COS treatments for each strawberry variety separately and the corresponding control. Therefore, the foliar application of COS solution decreases the negative effects of cold stress and improves the strawberry plants' tolerance to chilling by increasing the content of total soluble proteins.

Competing interests

The authors declare that they have no competing interests.

Funding

This work was supported by project ref. 13050511 funded by National Research Centre, Dokki, Giza, Egypt.

References

Benhamou N, Kloepper JW and Tuzun S. 1998. Induction of resistance against Fusarium wilt of tomato by combination of chitosan with an endophytic bacterial strain: ultrastructure and cytochemistry of the host response. *Planta*, **204** (**2**): 153±68.

Eissa MA, Nafady M, Ragheb H and Attia K. 2013. Effect of soil moisture and forms of phosphorus fertilizers on corn production under sandy calcareous soil. *World Appl. Sci. J*., **26**: 540–547.

El Ghaouth A, Arul J, Ponnampalam R and Boulet M. 1991. Chitosan coating effect on storability and quality of fresh strawberries. *J. Food Sci.*, **56**(**6**): 1618±20.

El-Miniawy SM, Ragab ME, Youssef SM and Metwally AA. 2013. Response of strawberry plants to foliar spraying of chitosan. *Res. J. Agric. & Biol. Sci.*, **9**(**6**): 366±72.

Gharechahi J, Alizadeh H, Naghavi R and Sharifi G. 2014. A proteomic analysis to identify cold acclimation associated proteins in wild wheat (*Triticum urartu* L.). *Mol. Biol. Rep.*, **41**: 3897–3905.

Griffith M and Yaish MWF. 2004. Antifreeze proteins in overwintering plants: A tale of two activities. *Trends Plant Sci*., **9**: 399–405.

Guan YJ, Hu J, Wang XJ and Shao CX. 2009. Seed priming with chitosan improves maize germination and seedling growth in relation to physiological changes under low temperature stress. *J. of Zhejiang Univ. Sci. B*, **10**(**6**): 427-433.

Han J, Li X, Li W, Yang Q, Li Z, Cheng Z, Lv L, Zhang L and Han D. 2023. Isolation and preliminary functional analysis of *FvICE1*, involved in cold and drought tolerance in *Fragaria vesca* through overexpression and CRISPR/Cas9 technologies. *Plant Physiol. and Biochem*., **196**: 270-280.

Hasanuzzaman M, Bhuyan M, Zulfiqar F, Raza A, Mohsin S, Mahmud J, Fujita M and Fotopoulos V. 2020. Reactive oxygen species and antioxidant defense in plants under abiotic stress: Revisiting the crucial role of a universal defense regulator. *Antioxidants*, **9**: 681.

Hincha DK, Meins F Jr and Schmitt JM. 1997. [beta]-1,3-Glucanase is cryoprotective in vitro and is accumulated in leaves during cold acclimation. *Plant Physiol*., **114**: 1077-1083.

Hossain A, Begum P, Zannat MS, Rahman MH, Ahsan M and Islam SN. 2016. Nutrient composition of strawberry genotypes cultivated in a horticulture farm. *Food Chem.*, **199**: 648±52.

Kuwabara C and Imai R. 2009. Molecular basis of disease resistance acquired through cold acclimation in overwintering plants. *J. Plant Biol*., **52**: 19-26.

Laemmli UK. 1970. Cleavage of structural protein during the assembly of the head of bacteriophage T. *Nature*, **227**: 680-689.

Landi L, De Miccolis Angelini RM, Pollastro S., Feliziani E, Faretra F and Romanazzi G. 2017. Global transcriptome analysis and identification of differentially expressed genes in strawberry after preharvest application of benzothiadiazole and chitosan. *Front. Plant Sci*., **8**: 235.

Li Y, Hu J, Xiao J, Guo G and Jeong BR. 2021. Foliar thidiazuron promotes the growth of axillary buds in Strawberry. *Agronomy*, **11**(**3**):1–11.

Lukoševičiūtė V. 2014. Characterization of cold acclimation and cold hardiness of strawberry *in vitro* and *in vivo*. PhD Thesis. Aleksandras Stulginskis University.

Malerba M and Cerana R. 2018. Recent advances of chitosan applications in plants. *Polymers*, **10**(**2**): 118.

Mondal MMA, Malek MA, Puteh AB, Ismail MR, Ashrafuzzaman M and Naher L. 2012. Effect of foliar application of chitosan on growth and yield in okra. *Aust. J. Crop Sci.*, **6**: 918-921.

Mukta JA, Rahman M, Sabir AA, Gupta DR and Surovy MZ *et al.* 2017. Chitosan and plant probiotics application enhance growth and yield of strawberry. *Biocatal Agric Biotechnol*, **11**: 9±18.

Nei M and Li WH. 1979. Mathematical model for studying genetic variation in terms of restriction endonucleases. *Proceedings of the National Academy of Sciences of the United States of America* (PNAS), **76**(**10**): 5269-5273.

Ouellet F and Charron JB. 2013. Cold acclimation and freezing tolerance in plants. In: eLS. Chichester: Wiley.

Pichyangkura R and Chadchawan S. 2015. Biostimulant activity of chitosan in horticulture. *Sci. Hortic*., **196**: 49±65.

Pihakaski-Maunsbach K, Moffatt B, Testillano P, Risueño M, Yeh S, Griffith M and Maunsbach AB. 2001. Genes encoding chitinase-antifreeze proteins are regulated by cold and expressed by all cell types in winter rye shoots. *Physiol. Plant*., **112**: 359–371.

Pongprayoon W, Siringam T, Panya A and Roytrakul S. 2022. Application of chitosan in plant defense responses to biotic and abiotic stresses. *Appl. Sci. Eng. Prog*., **15**(**1**): 1-10. https://doi.org/10.14416/j.asep.2020.12.007.

Rahman M, Mukta JA, Sabir AA, Gupta DR, Mohi-Ud-Din M and Hasanuzzaman M *et al*. 2018. Chitosan biopolymer promotes yield and stimulates accumulation of antioxidants in strawberry fruit. *PLoS ONE*, **13**(**9**): e0203769. https://doi.org/10.1371/journal.pone.0203769.

Roussos PA, Denaxa NK, Ntanos E, Tsafouros A, Mavrikou S and Kintzios S. 2020. Organoleptic nutritional and anti-carcinogenic characteristics of the fruit and rooting performance of cuttings of black mulberry (*Morus nigra* L.) genotypes. *J. Berry Res.*, **10**: 77–93.

Ruelland E and Zachowski A. 2010. How plants sense temperature. *Environ. Exp. Bot*., **69**: 225–232.

Ryan PD, Harper DAT and Whalley JS. 1995. PALSTAT, Statistics for paleontologists. Chapman & Hall (now Kluwer Academic Publishers).

Sakif TI, Dobriansky A, Russell K and Islam T. 2016. Does Chitosan Extend the Shelf Life of Fruits? *Adv. Biosci. Biotechnol.*, **7**(**08**): 337.

Sneath PHA and Sokal RR. 1973. Numerical taxonomy. In: Freeman WH, Co. San Francisco, (Eds.): **The Principles and Practices of Classification**: 588 p.

Snedecor GW and Cochran WG.1980. **Statistical Methods**.7th ed., Iowa Stat. Univ., Press, Ames, Iowa, USA.

Studier FW. 1973. Analysis of bacteriophage T, early RNAs and proteins of slab gel. *J. Mol. Biol.*, **79**: 237-248.

Tan C, Dai H and Lei J. 2003. World strawberry production and trade status and development trend. *World Agric*., **5**: 10–12, 40.

van Loon LC, Rep M and Pieterse CMJ. 2006. Significance of inducible defense-related proteins in infected plants. *Annu. Rev. Phytopathol*., **44**:135–62.

Vítámvás P and Prášil IT. 2008. WCS120 protein family and frost tolerance during cold acclimation, deacclimation and reacclimation of winter wheat. *Plant Physiol. Biochem*., **46**: 970–6.

Wang A, Li J, AL-Huqail AA, AL-Harbi MS, Ali EF, Wang J, Ding Z, Rekaby SA, Ghoneim AM and Eissa MA. 2021. Mechanisms of chitosan nanoparticles in the regulation of cold stress resistance in banana plants. *Nanomaterials*, **11**: 2670. https://doi.org/10.3390/ nano11102670

Zhang Y, Seeram NP, Lee R, Feng L and Heber D. 2008. Isolation and identification of strawberry phenolics with antioxidant and human cancer cell antiproliferative properties. J. *Agric. Food Chem*., **56**(**3**): 670±5.

Zheng Q, Song J, Doncaster K, Rowland E and Byers DM. 2007. Qualitative and quantitative evaluation of protein extraction protocols for apple and strawberry fruit suitable for two-dimensional electrophoresis and mass spectrometry analysis. *J. Agric. Food Chem*., **55**: 1663−1673. doi: 10.1021/jf062850p.

JJBS

Volume 17, Number 4,December 2024
ISSN 1995-6673
Pages 657 – 665
https://doi.org/10.54319/jjbs/170409

Jordan Journal of Biological Sciences

Functional Group of Spiders on Durian Plantations in Tarakan Island: The Influence of Ant Predator *Oecophylla smaragdina* on Spiders

Abdul Rahim[1,*], Kyohsuke Ohkawara[2], Oshlifin Ruchmana Saud[3]

[1]*Department of Agrotechology, Faculty Of Agriculture, Borneo University. Jl. Amal Lama No. 01 Tarakan, North Kalimantan, Indonesia. Tel./Fax. +82-50882116, [*]email: rahim@borneo.ac.id; [2]Laboratory of Ecology, Division of Biological Sciences, Graduate School of Natural Science andTechnology, Kanazawa University, Kanazawa 920-1192, Japan; [3]Faculty of Forestry, Universitas Mulawarman. Jl. Penajam, Kampus Gn. Kelua, Samarinda 75123, East Kalimantan, Indonesia.Tel./fax.: +62-541-735379.*

Received: January 12, 2024; Revised: May 22, 2024; Accepted: July 3, 2024

Abstract.

This study aimed to examine the guild composition of spiders in durian plantations, specifically focusing on the influence of *O. smaragdina*. For data collection, branch sampling was employed to gather *O. smaragdina* and spiders from Durian (*Durio zibethinus*) trees in the plantations, and the density of both predators was determined by counting the number of individuals. The results showed that a total of 3,049 individual belonging to 74 species of spiders were collected from 44 durian trees, and the community exhibited eight distinct functional groups, namely Stalkers, Orb Weavers, Foliage Runners, Ambushers, Tangled Weavers, Ground Runners, and unknowns. Stalkers also emerged as the dominant group within the durian trees, and the average number of *O. smaragdina* workers in trees did not show a negative correlation with Foliage Runners. However, there was a negative effect of the nest presence and the number of workers on the spider community, particularly impacting the Foliage Runners and Ambusher groups. This study also suggested that *O. smaragdina* acted as a competitor and predator for certain guilds of spiders in durian plantations, but the influence on the functional groups within mixed cropping systems was found to be relatively weak.

Keywords: Durian, *Oecophylla*, Plantations, Predator, Spider

1. Introduction

Grouping spiders into guilds or functional groups based on similar behaviour in accessing resources is an important approach to understanding their roles and interactions within plantations (Perkins *et al*. 2017). Furthermore, the structure and distribution patterns in farming systems can be influenced by microclimatic conditions, emphasizing the importance of studying their guild composition and functional groups in different agricultural landscapes (Rosas-Ramos *et al*. 2020). The diversity of species and groups is also influenced by the structure of vegetation (Lia *et al*. 2022). It has been reported that various biological components exert an influence on spider composition within ecosystems. Certain biological components, such as insects microorganisms and birds, have been found to significantly impact their respective habitats(Katayama *et al*. 2015; Zhang *et al*. 2018; Gunnarsson and Wiklander 2015).

In terrestrial ecosystems, both ants and spiders have been identified as generalist predators (Samiayyan, 2014). In the specific context of a plantation area using a mixed cropping system, this approach has been found to provide benefits for promoting predator biodiversity and the availability of prey within the ecosystem (Lia *et al*. 2022). Consequently, these predators play a crucial role in pest control within the plantation. It is also important to acknowledge that the system can also give rise to competition among predators and an increase in pest populations due to the diverse range of available food sources. For instance, ants and spiders, being potential competitors or engaging in intraguild predation, may exhibit such dynamics (Potter *et al*. 2018). The abundance of natural enemies does not always exhibit a strong correlation with pest populations since simple taxa, including spiders and predatory insects, can display varying responses (Paredes *et al*. 2015). In contrast, predators can coexist and have similar effects on plant ecosystems (Rákóczi and Samu 2014; Stefani *et al*. 2015), or may mutually interfere with the functional response of an omnivorous animal (Papanikolaou *et al*. 2020).

There have been reports highlighting the interaction between ants and other predators within plantations. Specifically, ants have been found to exert a disadvantageous effect and interfere with the competition faced by others, such as spiders (Yip 2014). In terrestrial ecosystems, the diversity of spiders (Araneae) indicates whether the correlation is positive or negative. This observation supports the hypothesis that insects act as predators of spiders (Dimitrov and Hormiga 2021). A study conducted in the Bornean tropical forest showed that ants and spiders exhibited significant spatial distribution exclusively in canopy trees (Katayama *et al*. 2015).

[*] Corresponding author. e-mail: rahim@borneo.ac.id.

Another study reports a case in which spiders coexist with predators of ants (Stefani *et al*. 2015). However, studies examining the relationship between ants and spiders remain limited, particularly regarding the impact of the predators on various functional groups.

The utilization of biological agents, specifically ants, has been widely implemented in plantation areas. The strategy of biological control encompasses three key approaches, namely introduction or transfer, augmentation, and conservation of ants (Offenberg 2015). These techniques are implemented through various means, such as relocating ant nests to different locations, employing artificial nests with supplementary food sources, and transferring workers from one colony to another tree using ropes, among other methods (Offenberg 2015; Abdulla *et al.* 2015). The weaver ants *O. smaragdina* are most plentifully and widely distributed in Southeast Asia and northeast Australia (Wetterer 2017). Meanwhile, *Oecophylla* has been recognized as biological control in cashew plants (Offenberg 2015; Olotu *et al.* 2013), mango fruits, and citrus (Offenberg *et al*. 2013). In another case, these predators are known to affect pollinators (Gonzálvez *et al*. 2013), parasitoids (Appiah *et al*. 2014; Tanga *et al.* 2016), and other beneficial insects. This is because weaver ants are general predators which can provide benefits and be harmful to other organisms (Thurman *et al.* 2019).

Durian (*Durio* spp) cultivation and distribution in Kalimantan primarily involve a mixed cropping system that provides resources for *O. smaragdina* (green ants) and spiders (Rahim 2015, unpublished data). However, these areas may also have a higher presence of herbivorous insects. To evaluate the hypothesis regarding the predation dynamics between insects and spiders, as well as the impact of *O. smaragdina* within the spider guild, studying this interaction in the mix cropping system becomes interesting. This study assesses species classifications that share similarities in resource exploitation or guild membership. Additionally, the relationship between *O. smaragdina* and spiders, both acting as predators, is investigated. The results provide insights into the conservation of predators in mixed tree cropping systems and offer guidance on managing local predators in plantations. The conservation of *O. smaragdina* by efforts to move one colony to another tree with a rope is an attempt to ensure the ant colony can access other types of trees. (Offenberg 2015). However, it needs to be combined with additional feed (Abdulla *et al.* 2015) to prevent competition between predators.

2. Materials AND METHODS

2.1. Study area

This study was carried out in the plantation area in Tarakan Island, North Kalimantan (3°18'15"N, 117°37'12"E). The study site was chosen in a mixed tree plantation, where durian trees dominate over other crops. In addition, the site was located near both urban areas and horticulture plantations. *Durio zibethinus*, *Citrus spp*, and *Musa spp* were the dominant species, occupying more than 80%. The average temperature and humidity recorded on the site were 27.7 ℃ and 84%, respectively, as shown in Figure 1.

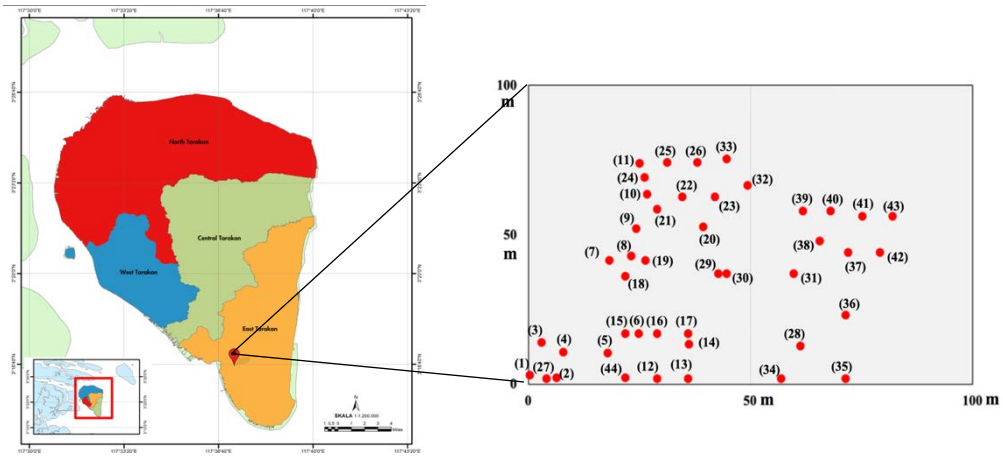

Figure 1. Location of the studied sites in Tarakan Island of North Kalimantan. The point of distribution of sampling in the durian plant cultivation area

2.2. Field collection of O. smaragdina and spiders

The collection of *O. smaragdina* and spiders was conducted on 44 durian trees on Tarakan Island. The age of durian was 5-6 six years old and it was not fruiting periods. In the studied sites, 10 branches measuring between 50 and 80 cm in length, with a diameter ranging from 5 to 10 cm, were selected. The branches were chosen at the bottom, middle and top of the canopy as the place for the beating method. Furthermore, each branch point is given a code so that the next sampling is carried out at the same place. In addition, we measured the number of nests of *O. smaragdina* in each durian tree sample which used direct observation methods.

From March to September 2016, we sampled seven times with an interval of 30 days between each sampling. All the collected samples, including spiders, were preserved in specimen tubes filled with 99% ethanol and sorted in the laboratory. The identification of spiders was conducted in both the field and laboratory. The families, genera, and species (morphospecies) were identified using manual guides and online resources, e.g.

https://www.asianarachnology.com/online-spider-identification-websites/.

The spiders have been classified into different functional groups based on their scientific classification and foraging traits. These functional groups are as follows: (1) Ambushers, Foliage runners, Stalkers, and Orb weavers belonging to the family Thomisidae (Uetz *et al*. 1999), Clubionidae (Uetz *et a*l. 1999), Salticidae and Oxypidae (Uetz *et a*l. 1999), and Araneidae and Tetragnathidae (Lia *et al*. 2022).

2.3. Data analysis

For the examination of species composition and collection frequency in the sites, the average number of spiders collected on each tree branch during sampling was calculated. Based on the Kolmogorov-Smirnov test and the Shapiro-Wilk test, the data were normally distributed. To assess the interactions between ant *O. smaragdhina* and spiders, the R-value (rank Spearman correlation) was computed between the dominant spider species and functional spider groups. Additionally, differences were analyzed using a one-tailed t-test to estimate the effects of *O. smaragdina* on the spider groups. The statistical analysis of the data was conducted using SPSS Ver 23 software.

3. Results and Discussion

3.1. Taxonomic and guild composition of spiders

In this study, a total of 3049 individuals were collected, representing 74 species/morphospecies from 12 families. The results showed that the dominant families on the durian trees were Salticidae (41.1%), Araneidae (22.7%), and Thomisidae (11.7%). Additionally, it was observed that 10 species were frequently collected and exhibited dominance on the durian trees. All samples from the tree were occupied by species belonging to the Araneus genus, as shown in Table 1 and Fig. 1. Among the collected species, 10 stood out as dominant and accounted for over 50% of the spider population on the durian trees. Furthermore, the average number occupying more than 80% of the trees ranged from 2 to 7 individuals per tree, indicating a relatively high density, as shown in Table 1.

Table 1. Species/Morphospecies dominant of spider collected in Durian tree. The functional group were classified into eight groups: Stalkers (S), Orb Weavers (OW), Foliage Runners (FR), Space Web Builders (SWB), Ambusher (A), Tangle Weavers (TW), Ground Runners (G) and Unknown (U).

Family	Species/Morphospecies	Functional Group	Number of Trees Occupied	Total Individuals	Percentage Individuals (%)
Araneidae	*Araneus* sp2	OW	44	314	10.3
Salticidae	*Neon* sp2	S	43	309	10.1
Salticidae	*Neon* sp1	S	43	281	9.2
Thomisidae	Unknown sp1	A	39	181	5.9
Salticidae	Unknown sp2	S	38	124	4.1
Liocranidae	Liocranidae sp1	U	37	107	3.5
Araneidae	*Araneus* sp6	OW	29	91	3.0
Salticidae	*Leptorechestes* sp1	S	35	90	3.0
Araneidae	*Araneus* sp3	OW	27	83	2.7
Salticidae	*Leptorechestes berolinensis*	S	30	80	2.6
Thomisidae	*Xysticus* sp1	A	21	69	2.3
Oxypidae	*Oxyopes* sp3	S	26	66	2.2
Clubionidae	*Clubiona* sp1	FR	32	65	2.1
Araneidae	*Cyrtarachne* sp1	OW	21	64	2.1
Oxypidae	*Oxyopes* sp2	S	27	60	2.0
Salticidae	*Myrmachine formacaria*	S	18	58	1.9
Araneidae	*Araneus* sp4	OW	29	56	1.8
Salticidae	*Neon valentulus*	S	24	56	1.8
Dictynidae	*Dcytina* sp1	SWB	16	51	1.7
Tetragnathidae	*Tetragnatha dearmata*	OW	20	47	1.5
Salticidae	*Chalcoscirtus* sp1	S	23	45	1.5
Clubionidae	*Clubiona* sp4	FR	25	42	1.4
Salticidae	*Chalcoscirtus* sp2	S	24	41	1.3
Salticidae	Salticidae sp1	S	21	41	1.3
Salticidae	*Synageles* sp1	S	17	36	1.2
Pscheridae	*Psechrus* sp1	U	17	34	1.1
Linyphidae	*Floronia* sp1	TW	17	33	1.1

Salticidae	Unknown sp3	S	19	33	1.1
Oxypidae	*Oxypidae* sp1	S	22	32	1.0
Oxypidae	*Oxypidae* sp2	S	19	31	1.0
Clubionidae	*Clubiona* sp7	FR	19	30	1.0
Salticidae	*Neon* sp3	S	15	27	0.9
Oxypidae	*Oxyopes* sp1	S	14	26	0.9
Araneidae	*Araneus* sp5	OW	12	24	0.8
Thomisidae	Unknown sp2	A	14	24	0.8
Thomisidae	*Xysticus* sp3	A	13	23	0.8
Oxypidae	*Oxyopes* sp4	S	13	20	0.7
Linyphidae	*Floronia* sp2	TW	11	18	0.6
Linyphidae	*Drapetisca* sp1	TW	7	17	0.6
Pholcidae	*Pholcus* sp1	SWB	9	17	0.6
Araneidae	*Araneus praesignis*	OW	12	16	0.5
Clubionidae	*Clubiona* sp2	FR	13	15	0.5
Salticidae	*Agorius* sp1	S	7	13	0.4
Salticidae	*Marpissa* sp1	S	9	13	0.4
Clubionidae	*Clubiona* sp5	FR	8	12	0.4
Salticidae	*Plexippus* sp1	S	5	12	0.4
Clubionidae	*Clubiona* sp3	FR	9	10	0.3
Salticidae	*Leptorechestes* sp2	S	8	10	0.3
Salticidae	*Salticus* sp1	S	6	9	0.3
Thomisidae	*Thomisus* sp1	A	5	9	0.3
Lycosidae	*Lycosa* sp1	GR	4	8	0.3
Salticidae	*Euophrys* sp1	S	5	7	0.2
Salticidae	*Myrmachine melanostrata*	S	4	7	0.2
Salticidae	*Myrmarachn*e sp1	S	4	7	0.2
Araneidae	*Araneus* sp1	OW	5	6	0.2
Araneidae	*Araneus* sp7	OW	4	4	0.1
Clubionidae	*Clubiona* sp6	FR	3	4	0.1
Salticidae	Salticidae sp1	S	3	4	0.1
Tetragnathidae	*Tetragnatha* sp1	OW	4	4	0.1
Thomisidae	*Thomisus* sp2	A	2	4	0.1
Thomisidae	*Xysticus* sp2	A	4	4	0.1
Liocranidae	Unknown sp3	U	3	3	0.1
Salticidae	*Neon* sp6	S	3	3	0.1
Thomisidae	*Diaea* sp1	A	3	3	0.1
Thomisidae	Thomisidae sp3	A	3	3	0.1
Araneidae	*Zygiella* sp1	OW	2	2	0.1
Linyphidae	*Micrargus* sp1	TW	1	2	0.1
Salticidae	Unknown sp4	S	2	2	0.1
Salticidae	*Neon* sp8	S	2	2	0.1
Araneidae	*Araniella* sp1	OW	1	1	<0.1
Linyphidae	*Hypselistes* sp1	TW	1	1	<0.1
Salticidae	Unknown sp	S	1	1	<0.1
Salticidae	*Thianitara* sp1	S	1	1	<0.1
Thomisidae	*Misumena* sp1	A	1	1	<0.0

Furthermore, the spiders were classified into eight functional groups: Stalkers, Orb Weavers, Foliage Runners, Space Web Builders, Ambushers, Tangle Weavers, Ground Runners, and Unknown. Among these groups, four dominant categories were identified, namely Stalkers (50.8%), Orb Weavers (23.3%), Ambushers

(10.5%), and Foliage Runners (5.8%), as shown in Fig. 2. These results align with previous data, which show the presence or occurrence of the Stalkers functional group in all sampled trees.

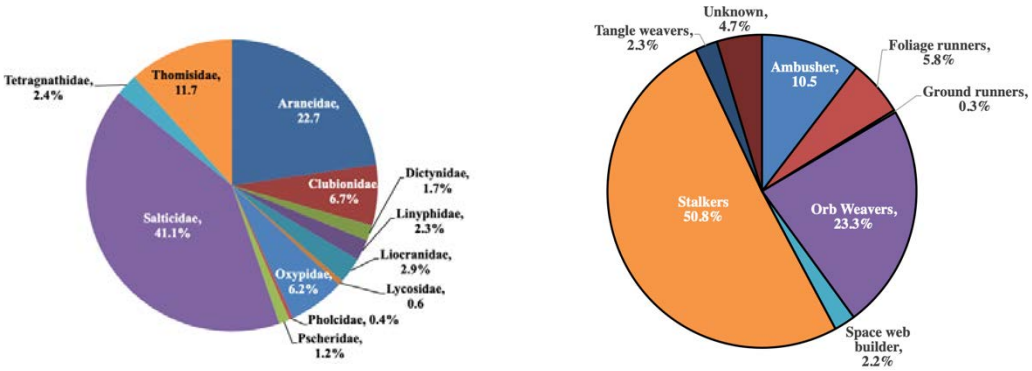

A **B**

Figure 2. Percentage of spider group (A) family (B) guild or functional group in the studied site

3.2. Relationships among O. smaragdina and functional group of spiders

During this study, all relationship analyses consistently indicated a negative correlation between the number of *O. samaragdina* per branch or tree and the average abundance of the functional groups of spiders. The number of worker ants had no significant negative correlation on the functional group of spiders (Ambusher, R^2=0.025; Stalkers, R^2=0.02; Orb weavers, r=0.04, Fig. 3). However, the correlation among *O. smaragdina* was significant on Foliage Runner (R^2=0.07, P=0.012, Fig. 3). The result showed that *O. smaragdina* had no strong relationship on functional groups of spiders.

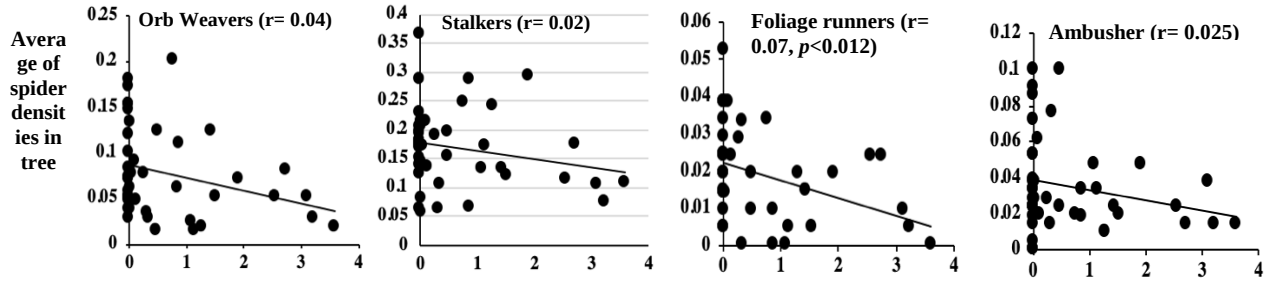

Figure 3. The relationships among the worker densities of *O. smaragdina* and of spider densities by Functional group in durian tree

3.3. Effect of Predator O. smaragdina Presence on Spiders

This study further assessed the impact of *O. smaragdina* presence on durian trees on the spiders guild. The analysis showed a significant difference in the average number of individual spiders observed on durian trees (Ambusher, p = 0.03, Fig. 4a; Foliage Runner p = 0.04, Fig. 4b; Orb Weavers, p = 0.015, Fig. 4d). However, there was no significant result on Foliage Runner (Stalkers, p = 0.06; Fig. 4c). The data showed that the number of spiders in the absence of *O. smaragdina* workers was lower.

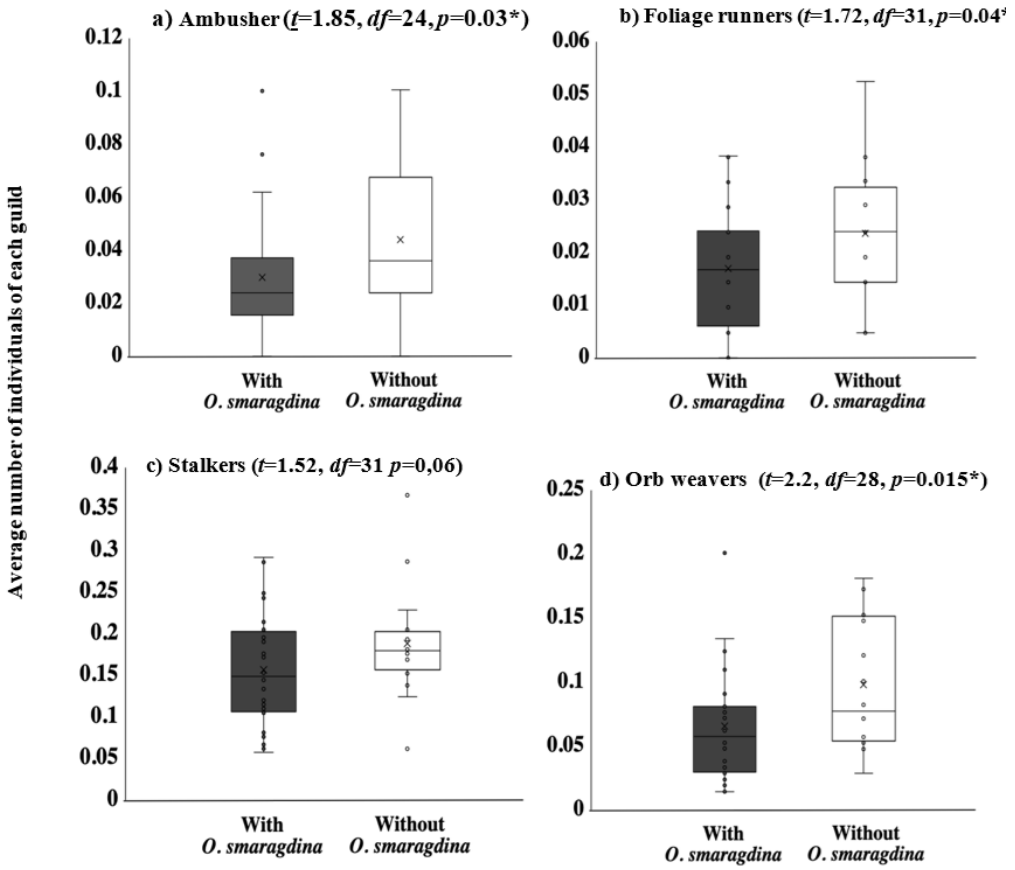

Figure 4. Box plot the differences between the average number of spiders and trees with and without *O. smaragdina* workers densities on durian trees. The average of the collected number (/branch/tree/collection time) was compared by using a t-test. Bar means standard error. Asterisk (*) means a significant difference between trees with and without *O. smaragdina* workers

This study investigated the impact of the presence or absence of *O. smaragdina* nests on the spider guild. The results showed that the average number of nests at the sampling locations ranged from 2 to 3 per tree. A significant difference in the average number of individual spiders was observed on durian trees with *O. smaragdina* nests (Ambusher, p = 0.04, Fig. 5a; Foliage Runner p = 0.002, Fig. 5b). However, there was no significant result on Foliage Runner (Stalkers, p = 0.32; Fig. 5c; Orb Weavers, p = 0.13 Fig. 5d). The presence of *O. smaragdina* nests in trees was associated with a lower number of individual spider.

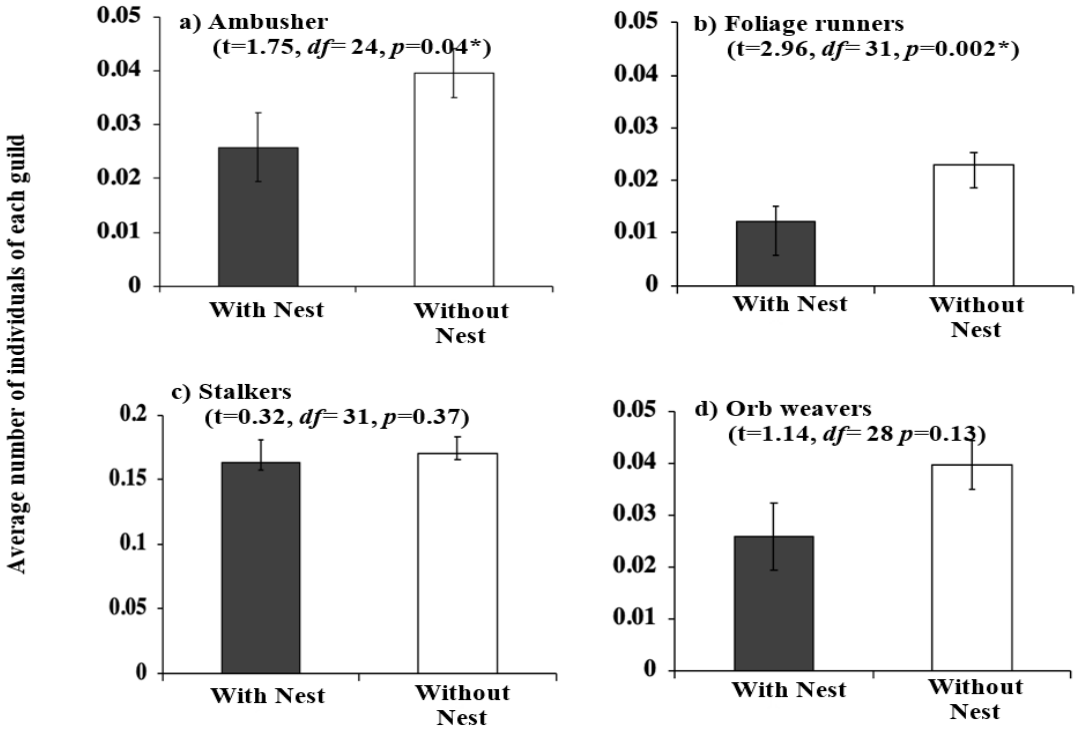

Figure 5. Comparison of average number of four groups of spiders among trees with and without *O. smaragdina* nests in durian trees

4. Discussion

More than seventy morphospecies were recorded within the study region, indicating high species richness in the mixed crop ecosystem. The coexistence of various plant species within this ecosystem provides ample space and food sources for insects, particularly herbivorous insects. Meanwhile, Rahim and Ohkawara (2019) documented the presence of more than 50 species of herbivorous insects thriving in mixed plant ecosystems dominated by horticultural crops. The dominant functional group of herbivores consists of aphids, mealybugs, and leaf beetles. This finding reinforces the notion that the species richness of predators is influenced by the richness of herbivorous insects. Furthermore, a direct proportional relationship is observed between the species richness of herbivorous and other predatory insects.

The species belonging to the families Aranneidae and Salticidae are dominant and can live in the canopy of plants and parts of tree branches. This result has also been described by Lia *et al*. (2020) where the Araneidae family dominates forest vegetation and oil palm plantations, specifically in the canopy. The genera Lycosidae and Oxyopidae dominated the corn plantation area.

The spider community within the Durian tree plantations is confirmed by examining the composition of functional groups or guilds. The Stalkers and Orb Weavers are the dominant groups in the plantations. Previous studies reported that these two groups were associated with canopies in tropical trees. In addition, two species stand out as more dominant than others due to their behavior (Battirola *et al*. 2016). The Stalkers consist of two families, namely Salticidae and Oxypidae, and there are several reasons why Salticidae are currently dominant in this study. Firstly, they exhibit behavior that allows access to all parts of the tree, including branches, leaves, and flowers. Moreover, they are active throughout the middle, bottom, and upper canopy of the tree. Another reason is that the beating sampling method may be influenced by the Salticidae families due to their ability to jump. The Orb Weaver species also emerge as dominant due to their ability to construct intricate webs on the Durian trees. According to Lia *et al*. (2022), spider families are denser and more prevalent in fully-grown vegetation. The Orb Weavers in particular are represented by the families Araneidae and Tetragnathidae, which have shown dominance in certain plantation areas. For example, the Araneidae family has been reported as dominant in Cocoa plantations (Oyewole and Oyelade, 2014) and Coffee agroecosystems (Marin and Perfecto, 2013). These findings indicate that the Durian tree provides a conducive environment for spider coexistence within the plantations.

This study examines the relationship between the number of workers and spiders in functional groups in Durian trees. It confirms that *O. smaragdina* tends to have a negative interaction with spider groups in the ecosystem, particularly with Foliage Runners on leaves (Fig 2). This is attributed to similarities in resource access, specifically leaves. According to Patel and Bhat (2020), weaver ants are eusocial insects that form nests in trees, forage for food, and protect their colony. However, *O. smaragdina* does not exhibit a negative relationship with Stalkers, Orb Weavers, and Ambushers due to their different behaviors in accessing resources. For example, jumping spiders that mimic weaver ants employ various mimicry strategies to coexist with other social insects, including ants (Ceccarelli, 2013). The low population density of *O. smaragdina* per branch per tree also contributes to these findings. Consequently, the presence of the worker insects has a negative relationship with the spiders based on their functional groups.

The activities of *O. smaragdina* are supported by the presence of a nest, and the organization is polydomous.

The colonies of *O. smaragdina* consist of reproductive castes, non-reproductive castes, workers, and soldiers (Offenberg *et al*. 2013). In this study, the presence of workers and nests significantly influenced two groups of spiders. Meanwhile, the average number of Foliage Runners and Ambushers is slightly lower on the durian tree, indicating competition between these predator groups. The presence of *O. smaragdina* does not impact Stalkers and Orb Weavers. Previous studies reported that *O. smaragdina* did not affect spiders and can coexist with other predators (Rákóczi and Samu, 2014; Stefani et al. 2015). They may also exhibit mutual interference (Papanikolaou *et al*. 2020) and avoid predation through mimicry (Ceccarelli, 2013). In addition, the ant predator is more active and distributed in the canopy, potentially accessing a wide range of resources. Then the location uses a mixed cropping system which will influence predator activity through competition from other possible groups of organisms.

In conclusion, the mix cropping system provides a richness of spider species and supports the presence of the predatory ant *O. smaragdina*. Several functional groups of spiders exist in the canopy of durian plantation trees, with the Salticidae group occupying a larger proportion. The relationship between the number of *O. smaragdina* and the spiders in each guild shows a moderate influence, suggesting a potential competition. Consequently, further study is needed to investigate the potential use of biological control agents, particularly focusing on the effects of spiders and *O. smaragdina* on herbivorous insects in mixed plantations.

Acknowledgements

The authors are grateful to the Dean of the Faculty of Agriculture and the Head of Research and Services Center University of Borneo Tarakan for the support provided during the study activities. The authors are also grateful to the field assistants (Muttaqien, Wisnu Ageng, Philipus and others) and the owner of the durian plant location.

References

Abdulla NR, Rwegasira RM, Jensen KMV, Mwatamala MW, Offenberg J. 2016. Control of mango seed weevils (*Sternochetus mangiferae*) using the African Weaver Ant (*Oecophylla longinoda* Latreille) (Hymenoptera: Formicidae). *J. Appl. Entomol*, **140**: 500–506. DOI: 10.1111/jen.12260.

Appiah EF, Ekesia S, Afreh-Nuamah K, Obeng-Ofori D, Mohamed SA. 2014. African weaver ant-produced semiochemicals impact on foraging behavior and parasitism by the Opiine psarasitoid, *Fopius arisanus* on *Bactrocera invadens* (Diptera: Tephritidae). *Biological Control*, **79**: 49-57, DOI: 10.3390/insects7010001.

Battirola LD, Batistella BA, Rosado-Neto GH, Brescovit AD, Marques MI. 2016. Spider assemblage (Arachnida: Araneae) associated with canopies of *Vochysia divergens* (Vochysiaceae) in the northern region of the Brazilian Pantanal. *Zoologia* **33(4)**: 1-9. DOI: 10.1590/S1984-4689zool-20150170.

Ceccarelli FS. 2013. Ant-Mimicking Spiders: Strategies for Living with Social Insects. *Psyche* **2013**: 1-16. DOI: 10.1155/2013/839181

Dimitrov D, Hormiga G. 2021. Spider Diversification Through Space and Time. *Annu. Rev. Entomol*. **66**: 225–41. DOI: 10.1146/annurev-ento-061520-083414.

Gunnarsson B, Wiklander K. 2015. Foraging mode of spiders affects risk of predation by birds. *Biological Journal of the Linnean Society*, **115(1)**: 58–68. DOI: 10.1111/bij.12489.

Gonzálvez FG, Santamaría L, Corlett RT, Rodríguez-Gironés MA. 2013. Flowers attract weaver ants that deter less effective pollinators. Journal of *Ecology* **101(1)**: 78-85. DOI: 10.1111/1365-2745.12006.

Katayama M, Yamada KK, Tanaka HO, Endo T, Hashimoto Y, Yamane S, Itioka T. 2015. Negative Correlation between Ant and Spider Abundances in the Canopy of a Bornean Tropical Rain Forest. *Biotropica*, **47(3)**: 363–368. https://doi.org/10.1111/btp.12208.

Lia M, Rauf A, Hindayana D. 2022. Comparisons of the composition of spider assemblages in three vegetation habitats in Bogor, West Java, Indonesia. *Biodiversitas* **23(1)**: 244–255. DOI: 10.13057/biodiv/d230130.

Marin L, Perfecto I. 2013. Spider Diversity in Coffee Agroecosystems: The Influence of Agricultural Intensification and Aggressive Ants. *Environmental Entomology*, **42(2)**: 204-213. 2013. http://www.bioone.org/doi/full/10.1603/EN11223.

Offenberg J, Cuc NTT, Wiwatwitaya D. 2013. The effectiveness of weaver ant (*Oecophylla smaragdina*) biocontrol in Southeast Asian citrus and mango. *Asian Myrmecology*, **5**: 139–149. DOI: 10.20362/am.005015.

Offenberg J. 2015. Ants as tools in sustainable agriculture. Journal of Applied Ecology, 52: 1197-1205. DOI: 10.1111/1365-2664.12496.

Olotu MI, Du Plessis H, Seguni ZS, Maniania NK. 2013. Efficacy of the African weaver ant *Oecophylla longinoda* (Hymenoptera: Formicidae) in the control of *Helopeltis* spp. (Hemiptera: Psyllidae) and *Pseudotheraptus wayi* (Hemiptera: Coreidae) in cashew crop in Tanzania. *Pest Management Science*, **69(8):** 911-918. DOI: 10.1002/ps.3451.

Oyewole OA, Oyelade OJ. (2014). Diversity and Distribution of Spiders in Southwestern Nigeria. *Natural Resources* **5**: 926-935. http://dx.doi.org/10.4236/nr.2014.515079.

Papanikolaou NE, Dervisoglou S, Fantinou A, Kypraios T, Giakoumaki V, Perdikis D. 2021. Predator size affects the intensity of mutual interference in a predatory mirid. *Ecol. Evol*., **11**: 1342–1351. DOI: 10.1002/ece3.7137.

Paredes D, Cayuela L, Gurr GM, Campos M. 2015. Single best species or natural enemy assemblages? a correlational approach to investigating ecosystem function. *BioControl*, **60**: 37–45. DOI: 10.1007/s10526-014-9620-9.

Patel B, Bhatt N. 2020. Nesting, Protective and Foraging Behavior of *Oecophylla smaragdina* (Weaver Ants) in Anand, Gujarat. *Advances in Zoology and Botany* **8(4)**: 351-357. DOI: 10.13189/azb.2020.0804.

Perkins MJ, Inger R, Bearhop S, Sanders D. 2017. Multichannel feeding by spider functional groups is driven by feeding strategies and resource availability. *Oikos*, **127(1)**: 23–33. DOI:10.1111/oik.04500.

Potter TI, Greenville AC, Dickman CR. 2018 Assessing the potential for intraguild predation among taxonomically disparate micro-carnivores: marsupials and arthropods. *R. Soc. open sci*. **5**: 171872. http://dx.doi.org/10.1098/rsos.171872.

Rosas-Ramos N, Baños-Picón L, Tormos J, Asís JD. 2020. Farming system shapes traits and composition of spider assemblages in Mediterranean cherry orchards. *PeerJ*. DOI 10.7717/peerj.8856.

Rahim A, Ohkawara K. 2019. Species composition of herbivorous insects and ants on trees in the plantations of durian *Durio zibethinus* and citrus fruits *Citrus amblycarpa* in Tarakan Island of Borneo. *Sci. Rep. Kanazawa Univ*, **63**: 45-58.

Rákóczi AM, Samu F. 2014. Coexistence Patterns Between Ants and Spiders in Grassland Habitats. *Sociobiology*, **61(2)**: 171-177. DOI: 10.13102/sociobiology.v61i2.171-177.

Samiayyan K. 2014. Spiders - The Generalist Super Predators in Agro-ecosystems. In: Abrol DP (eds). Integrated Pest Management. Current Concepts and Ecological Perspective. Academic Press, San Diego.

Stefani V, Pires TL, Torezan-Silingardi HM, Del-Claro K. 2015. Beneficial Effects of Ants and Spiders on the Reproductive Value of *Eriotheca gracilipes* (Malvaceae) in a Tropical Savanna. *PLoS ONE* **10(7)**: e0131843. DOI: 10.1371/journal.pone.0131843

Tanga CM, Sunday E, Prem G, Nderitu PW, Samira AM. 2016. Antagonistic interactions between the African Weaver Ant *Oecophylla longinoda* and the parasitoid *Anagyrus pseudococci* potentially limits auppression of the invasive mealybug *Rastrococcus iceryoides*. *Insects*, **7**, DOI:10.3390/insects7010001.

Thurman JH, Northfield TD, Snyder WE. 2019. Weaver Ants Provide Ecosystem Services to Tropical Tree Crops. Front. *Ecol. Evol*. **7**:120: 1-9. DOI: 10.3389/fevo.2019.00120

Uetz GW, Halaj J, Cady AB. 1999. Guild structure of spiders in major crops. *J Arachnol*, **27**: 270-280.

Wetterer JK. 2017. Geographic distribution of the weaver ant *Oecophylla smaragdina*. *Asian Myrmecology*, **9**: e009004. DOI: 10.20362/am.009004

Yip EC. 2014. Ants versus spiders: interference competition between two social predators. *Insectes Sociaux* **61**: 403–406. DOI: 10.1007/s00040-014-0368-0

Zhang L, Yun Y. Hu G, Peng, Y. 2018. Insights into the bacterial symbiont diversity in spiders. *Ecology and Evolution* **8**:4899–4906. DOI: 10.1002/ece3.4051

JJBS

Volume 17, Number 4,December 2024
ISSN 1995-6673
Pages 667 – 680
https://doi.org/10.54319/jjbs/170410

Jordan Journal of Biological Sciences

The Impact of Rhizosphere Bacterial Strains as Biofertilizers: Inhibiting Fungal Growth and Enhancing the Growth and Immunity of Sprouted Barley as an Alternative Livestock Feed

Walaa Hussein[1,*], Walaa A Ramadan[1], Fatma E Mahmoud[1] and Sameh Fahim[2]

[1]*Genetics and Cytology Department, Biotechnology Research Institute, National Research Centre (Affiliation ID: 60014618), Dokki, Egypt;*
[2]*Agricultural Microbiology and Biotechnology, Botany Department, Faculty of Agriculture, Minoufia University, Shibin El-Kom, Egypt.*

Received: May 9, 2024; Revised: June 26, 2024; Accepted: July 4, 2024

Abstract

Egypt faces challenge in supplementing animal feed requirements, which add huge pressure on the budget and foreign currency reserves annually, making it necessary to find alternative solutions. The sprouted barley is considered one of these recent alternatives to animal feed. Sprouted barley faces challenges represented in fungal growth, which have strong competition for oxygen with the embryo and can inhibit seed germination in addition to producing aflatoxins, biofertilizers of plant growth-promoting bacteria (PGPB) are considered a practical and safe solution for these challenges. In this work, five tomato rhizobacterial strains were isolated and identified using the 16SrRNA gene and were found to belong to *Bacillus amyloliquefaciens*, *Peribacillus frigoritolerans*, *Pseudomonas flourescens*, *Bacillus pumilus*, and *Paenibacillus uliginis*, respectively. We reported here that most of these five isolates exhibited multiple PGP properties (PGPP), including the production of ACC deaminase, Indole-acetic acid (IAA), chelating siderophores and phosphate solubilization. *Bacillus amyloliquefaciens* BMG150 isolate exhibited the highest values for all the PGPP except siderophores production (1457 nmol, 37.4 µg/ ml, and 3.7 mg/ml, respectively). We also scanned the presence/ absence of the NRP gene clusters in the five isolates as an important PGPP using bioinformatics tools and NRPs degenerate primers. All five isolates showed NRPs gene clusters presence with the superiority of NRPs number for the strain *Bacillus amyloliquefaciens* BMG150 (surfactin, plipastatin, iturin and bacillibactin siderophore). Accordingly, we used *Bacillus amyloliquefaciens* BMG150, *Pseudomonas flourescens* PMG01 separately and a formula of the other three isolated strains as biofertilizers in sprouted barley cultivation which proved their efficiency in promoting their growth characteristics and reflected on protein pattern.

Keywords: Biofertilizers, Livestock feeding, NRPs, PGPB, Rhizosphere bacteria, Sprouted barley.

1. Introduction

The use of PGPB as biofertilizers is widely applied to improve the safety, quality and production of crops (Hussein *et al*., 2016). The rhizosphere is considered the wealthy source of a variety group of beneficial plant microorganisms. It has the prospective to improve plant growth, health and soil fertility which can be determined through the beneficial interactive relationship between roots and microbes (Parray *et al*., 2016; Kalam *et al*., 2017a). These beneficial interactive relationships possess several characteristics which can be determined and referred to plant growth-promoting bacteria (Dutta and Podile, 2010; Asriatno *et al*., 2023). Almost all important and abundant biofertilizers are Bacilli and Pseudomonas groups which are easily cultivable PGP, colonize rhizosphere intensely (Orozco-Mosqueda *et al*., 2020) and possess PGP properties (Zhou *et al*., 2016; Sansinenea, 2019). Among these PGP properties of Bacilli, their role in increasing minerals availability, chelating iron through siderophores production, fixing nitrogen and producing the phytohormones. Moreover, the ACC deaminase role in ethylene catabolism, detoxification and pathogens virulence factors degradation are considered among this PGP properties (Ahmad *et al*., 2008; Barea *et al*., 2015; Asriatno *et al*., 2023). Besides these latter PGP properties for the Bacilli group, there is the production of a group of highly diverse and effective secondary metabolites called non-ribosomal peptides synthesized by huge modular enzymes called non-ribosomal peptide synthetases (NRPs) (Süssmuth and Mainz, 2017). The high diversity of non-ribosomal peptides is due to their machine's ability to incorporate several non-proteogenic amino acids with different modifications compared to ribosomal machine (Walsh *et al*., 2013). Among these Bacilli NRPS are the lipopeptide families; surfactin, fengycin or plipastatin, iturins and kurstakins known as biosurfactants and have antifungal, antibacterial and antiviral activities. They are used in biocontrol of plant diseases which showed antagonistic activities against various phytopathogens (Ongena and Jacques, 2008). Pseudomonas group also is considered one of the most important producers of a wide spectrum of NRPs natural products. Among Pseudomonas NRPs, the cyclic lipopeptides (CLPs) which are classified into amphisin, syringomycin, viscosin, syringopeptin, or

* Corresponding author. e-mail: : wh.amin@nrc.sci.eg; nourwalaa@hotmail.com.

tolaasin group (Gross and Loper, 2009). In addition, other CLPs have been identified, namely putisolvin, orfamide (Kuiper *et al*., 2004; Gross *et al.*, 2007; Vallet-Gely *et al*., 2010), and entolysin. Also, few linear lipopeptides have been characterized, namely syringafactin and peptin 31 (Berti *et al*., 2007; Fiore *et al*., 2008; Chaida *et al*., 2022).

Egypt faces difficulties in supplementing animal feed requirements; it produces only 20 % of its feed corn and soybean while importing 50 % of feed corn and 90 % of soybean as an annual requirement, which places huge pressure on budget and foreign currency reserves. Cattle feed consists of about 50 % corn feed and 30 % soybeans, while poultry feed requires larger ratios of these ingredients than cattle feed. There are local alternatives that can go into the feed mixes for livestock, such as sprouted grains that have multiple benefits represented in increasing both the quality and quantity of protein and increasing some nutrients (sugars, minerals and vitamins) (Cuddeford, 1989; Gebremedhin, 2015). Sprouted grains fodders are considered a wealthy source for enzymes able to improve animals' productivity, which is rich in chlorophyll and grass juice which improves the animal's performance (Finney, 1983).

Among barely seeds, microbiome communities are fungi which have strong competition for oxygen with the embryo and can inhibit seed germination. (Harper *et al*., 1981) reported that aspergilli and penicillia when colonize the seed under the husk, they can participate the seed for their limited oxygen content. When 100 pg fungus colonized 80 % of the seed under the husk, maximum reduction in germination percentage was recorded.

The SDS-PAGE tool can explain the effect of both environment and the interactions between genotypes genes on protein (Johansson *et al*., 2012; Ling *et al*., 2012) by determining the genetic diversity between various species of crops as barley and wheat (Miháliková *et al*., 2016; Banta *et al*., 2021). SDS-PAGE technique is commonly used in biological analysis for determination of shifting in protein bands (proteins or enzymes) caused under bio-stress, due to the hormonal changes (Ghasempour *et al*., 2001; Ghasempour and Kianian, 2002; Ghasempour and Maleki, 2003) which reflect on protein patterns by increasing bands upon transition from control to environmental stress (Vyomesh and Pitambara, 2018; Ramadan and Soliman, 2020).

This work aims to prove the efficiency of some *Bacillus* and *Pseudomonas* strains producers for NRPs as biofertilizers by inhibiting fungal growth, enhancing sprouted barely growth and immunity to use the sprouted barely as an alternative feeding for animals.

2. Materials and methods

2.1. Soil strains isolation and counting

Nine various soil samples from three different locations in three replicates were collected from tomato field located in the Faculty of Agriculture, Menoufia University, Shibin-Elkom, Egypt. Counting of rhizosphere microbiome communities was performed in two replicates. Microbial colonies different in shape, color and viscosity were selected for cultivation and identification.

2.2. Rhizosphere soil sampling

Three replicates from three zones of tomato field were used for rhizosphere community preparation. 10 ml of sterilized 0.5% NaCl was added to 1 g rhizosphere soil. Serial soil dilutions technique was prepared 10^{-1}, 10^{-2}, 10^{-3}, 10^{-4} and 100 µl of each dilution was plated on LB medium plates and incubated for 24-48 hours at 28 °C.

2.3. Plant samples

The Giza 126 barely seeds variety used in this study was obtained from the field of crops Research Institute, Agricultural Research Center (ARC), Egypt.

2.4. Isolation and identification barely seed associated fungi

Associated fungi were isolated from Giza 126 barely seeds by barely seeds surface sterilization (Hussein *et al*., 2018) and then placed on PDA plates for five days at 25°C. To purify the fungi, they were sub-cultured three times on the same medium PDA. Pathogen identification was firstly performed based on morphology and microscopy observation followed by molecularly identification using the ITS gene after DNA extraction using the Zymo fungal/bacterial DNA miniprep. ITS gene was amplified using the universal primers; ITS_1-Fwd (TCCGTAGGTGAACCTGCGG) /ITS_4- Rev (TCCTCCGCTTATTGATATGC) followed by sequencing. The obtained sequences were aligned using BLASTN (https:// blast.ncbi.nlm.nih.gov/Blast.cgi).

2.5. ACC Deaminase Activity determination

The rhizobacterial isolates from tomato soil were scanned for their ACC deaminase activity on MDFS media (Minimal Dworkin and Foster Salts) supplemented with 3 mM ACC) (Dworkin and Foster, 1958; Penrose and Glick, 2001). After 3 days of incubation at 28 °C, the grown colonies were considered ACC deaminase producers. ACC deaminase quantification was performed using a Carry 100 UV-Vis spectrophotometer by measuring α-ketobutyrate production levels at 540 nm and comparing the results to a standard curve (0.1 to 1.0 mmol) as previously described (Honma and Shimomura, 1978).

2.6. Production of IAA

The isolated strains were incubated on Lauria Bertani medium supplemented with (5 mM Tryptophan) for 7 days at 28 °C under 200 rpm of shaking. The IAA determination was performed by Salkowski reagent colorimetric method (0.5 M Ferric chloride, 70% perchloric acid). The Cell free culture supernatant was mixed with Salkowski reagent in a 4:1 ratio to form indolic compounds, which exhibited a red colour. The absorbance was measured at 530 nm using a Carry 100 UV–Vis spectrophotometer as previously described (Gordon and Weber, 1951). A standard curve of pure indole-3-acetic acid (0-100 mg/ml) was used to determine IAA concentrations.

2.7. Phosphate solubilisation determination

The determination of phosphate solubilization by the rhizobacterial isolates was performed using Pikovaskya's agar medium supplemented with 2% Ca_3PO_4. A 10 µl spot of each bacterial culture was placed on the medium and incubated for 4 days at 28 °C as described by (Nautiyal, 1999). Phosphate solubilization was measured by the development of a clear area formed around the colony.

Additionally, quantitative determination of phosphate solubilization was carried out in NBRIP medium as described by (Nautiyal, 1999). The phosphate concentration in the culture supernatant was calculated as described by (Olsen *et al*., 1982).

2.8. Siderophores production

Siderophores production was assessed by inoculation bacterial colonies on CAS (Chrome Azurol S) plates at 28 °C for 4 days. An orange-yellow halo around the growth indicated siderophores production. For quantification of siderophores production, 100 µl of rhizobacterial isolate culture (10^8 cfu/ml) was inoculated in King B liquid medium for 72 hours at 28 °C. The cultures were then centrifuged at 5000 rpm for 30 minutes. Subsequently, 500 µL of the supernatant was mixed with an equal volume of CAS solution (1:1). After 20 minutes of incubation, the colour change from blue to orange indicated siderophore production, which was measured using a Cary UV-Vis spectrophotometer at 630 nm. The percentage of siderophores produced was estimated using the following equation:

$$\text{Siderophores \%} = RA–SA/RA \times 100$$

Where RA refers to the blank absorbance (CAS reagent) and SA refers to the sample absorbance.

2.9. DNA extraction, primers and 16S rRNA PCR conditions

Bacterial DNAs extraction was carried out using the Wizard genomic DNA extraction kit, Promega. PCR amplification of the 16S rRNA gene was carried out using primers 27F (AGAGTTTGATCMTGGCTCAG) and 1525R (AAGGAGGTGWTCCARCC) (DeLong, 1992). The PCR protocol included an initial denaturation step at 95°C for 10 minutes, followed by 40 cycles of denaturation at 95°C for 30 seconds, annealing at 55°C for 30 seconds, and extension at 72°C for 2 minutes.

Amplified fragments were purified using the Wizard® SV Gel and PCR Cleanup kit from Promega and subsequently sent for sequencing.

2.10. Non-ribosomal peptide synthetase genes detection using bioinformatics tools and degenerate primers

The complete genome sequences of the related species for the five-tomato rhizosphere bacterial isolates were retrieved from GenBank - microbial genomes database-NCBI. These complete genomes were analyzed for the secondary metabolites' genes using AntiSmash (https://antismash.secondarymetabolites.org) (Blin *et al*., 2023).

Two sets of degenerate primers were used; Serie 1 designed for the *Bacillus* group, previously described by (Tapi *et al*., 2010; Abderrahmani *et al*., 2011); and Serie 2, designed for the *Pseudomonas* group, as described by (Rokni-Zadeh *et al*., 2011) Table (1).

Table 1. Degenerate primers list used for detection of genes involved in NRPS.

Primer name	Primer sequence	Expected fragment size (bp)	NRLPs identified	References
Bacillus group				
AP1-F	AGMCAGCKSGCMASATCMCC	959, 929, 893	Plipastatin	(Tapi *et al*., 2010)
TP1-R	GCKATWWTGAARRCCGGCGG			
AS1-F	CGCGGMTACCGVATYGAGC	419, 422, 424, 431	Surfactin	
TS1-R	ATBCCTTTBTWDGAATGTCCGCC			
Af2-F	GAATAYMTCGGMCGTMTKGA	443, 452 455	Fengycins	
Tf1-R	GCTTTWADKGAATSBCCGCC			
Am1-F	CAKCARGTSAAAATYCGMGG	416, 419	Mycosubtilin	
Tm1-R	CCDASATCAAARAADTTATC			
Abl1-F	GATSAWCARGTGAAAATYCG	428, 431, 434	Bacillomycin	(Abderrahmani et al., 2011)
Tbl1-F	ATCGAATSKCCGCCRARATCRAA			
AKs-F	TCHACWGGRAATCCAAAGGG	1125, 1152, 1161, 1167, 1173	Kurstakin	
TKs-R	CCACCDKTCAAAKAARKWATC			
Pseudomonas group				
PGPRB-5045 C1Fwd	YTG ATY STY GAY GGY TGG GG	321, 325	Depend on strain	(Rokni-Zadeh et al., 2011)
PGPRB-5046 C1 Rev	RSA CRT RSA IBG CIG CCA GC			
PGPRB-4681 TE1 Fwd	TCI TTY GGY GGS GTI CTG GC	819, 825		
PGPRB-4682 TE2 Rev	SIC CIG GNG MYT CRC TGT CG			

2.11. Protein pattern determination.

Soluble proteins extraction from samples was carried out following the method described by (Laemmli, 1970) and subsequently analyzed as detailed by (Stegmann, 1979).

Table 2: Bacterial inoculant used in soaking barely seeds treatment before planting

Sample code	Sample description
Inoculant 1	*Paenibacillus uliginis* PMG250, *Peribacillus frigoritolerans* PMG200 and *Bacillus pumilus* BMG300.
Inoculant 2	*Pseudomonas flourescens* PMG01.
Inoculum 3	*Bacillus amyloliquefaciens* BMG150
A	control 1: barely seeds washed with water and sterilized using sodium hypochlorite (after 9 days)
A'	control 1: barely seeds washed with water and sterilized using sodium hypochlorite (after 12 days)
B	control 2: barely seeds washed with water (after 9 days)
B'	control 2: barely seeds washed with water (after 12 days)
C	barely seeds washed with water, sterilized with sodium hypochlorite, and soaked overnight in inoculant 1 (after 9 days)
C'	barely seeds washed with water, sterilized with sodium hypochlorite, and soaked overnight in inoculant 1 (after 12 days)
E	barely seeds washed with water, sterilized with sodium hypochlorite, and soaked overnight in inoculant 2 (after 9 days)
E'	barely seeds washed with water, sterilized with sodium hypochlorite and soaked overnight in inoculant 2 (after 12 days)
G	barely seeds washed with water, sterilized with sodium hypochlorite and soaked overnight in inoculum 3 (after 9 days)
G'	barely seeds washed with water, sterilized with sodium hypochlorite and soaked overnight in inoculum 3 (after 12 days)

3. Results

3.1. Counting, isolation, and identification of rhizobacterial community

The rhizosphere bacterial communities were quantified by colony counting. The highest colony count was observed in zone 2 with 766 colonies, decreasing to 460 and 136 colonies in subsequent dilutions. A total of sixteen rhizobacterial strain were isolated, five of which revealed considerable values of PGP properties. These strains were identified using 16SrRNA gene, and their sequences closely matched *Bacillus amyloliquefaciens*, *Peribacillus frigoritolerans*, *Pseudomonas flourescens*, *Bacillus pumilus*, and *Paenibacillus uliginis*. The phylogenetic tree illustrated the genetic relationships between these isolated rhizosphere strains depending on 16SrRNA gene sequence (Figure 1). Similarity percentage and GenBank accession numbers for these isolated strains are shown in table 3.

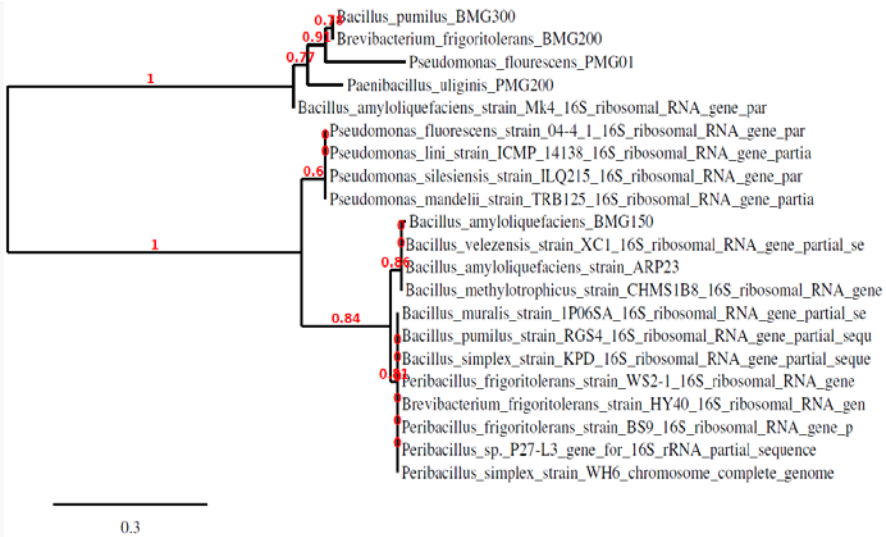

Figure 1. Phylogenetic tree of tomato rhizosphere bacterial isolates depending on 16SrRNA sequenced genes.

Table 3. Tomato rhizosphere bacterial isolates closest relativity.

Strain	Closest relativity	GenBank accession n°	Identity (%)
BMG150	*Bacillus amyloliquefaciens*	OR914616	99.57
PMG01	*Pseudomonas fluorescens*	OR914617	98.25
BMG300	*Bacillus pumilus*	OR914618	98.61
PMG200	*Peribacillus frigoritolerans*	OR914619	98.81
PMG300	*Paenibacillus uliginis*	OR914620	98.50

3.2. Identification of barely seeds associated fungi

Three phytopathogenic fungal strains were isolated from barley seeds and identified based on morphological traits and molecular analysis. Sequence alignment with the NCBI database using BLAST revealed 98.75% identity with *Rhizopus stolonifer*, 98.61% with *Aspergillus niger*, and 100% with *Alternaria alternata*. Thus, the isolated fungi were identified as *Rhizopus stolonifer*, *Aspergillus niger*, and *Alternaria alternata*. Fungal isolates and accession numbers are listed in Table 4.

Table 4. Barely seeds fungal isolates closest relativity.

Strain	Closest relativity	GenBank accession n°	Identity (%)
AMG01	*Alternaria alternata*	PP495831	100
AMG02	*Aspergillus niger*	PP495830	98.61
RMG01	*Rhizopus stolonifers*	PP495829	98.75

3.3. Quantification of ACC deaminase, IAA, phosphate solubilization, and siderophore activities

The activities of ACC deaminases for the five rhizobacterial isolates were quantified by measuring α-ketobutyrate produced from ACC deamination reaction on DF minimal salt broth media at 540 nm. The five bacterial isolates revealed activities of ACC deaminase ranged from 312–1457 nmol α-ketobutyrate/ mg protein. The *Bacillus amyloliquefaciens* BMG150 exhibited the highest activity (1457 nmol), followed by *Pseudomonas flourescens* PMG01 (1078 nmol), *Paenibacillus uliginis* PMG250 (1021 nmol), *Bacillus pumilus* BMG300 (978 nmol) and *Peribacillus frigoritolerans* PMG200 (312 nmol) (Figure 2A).

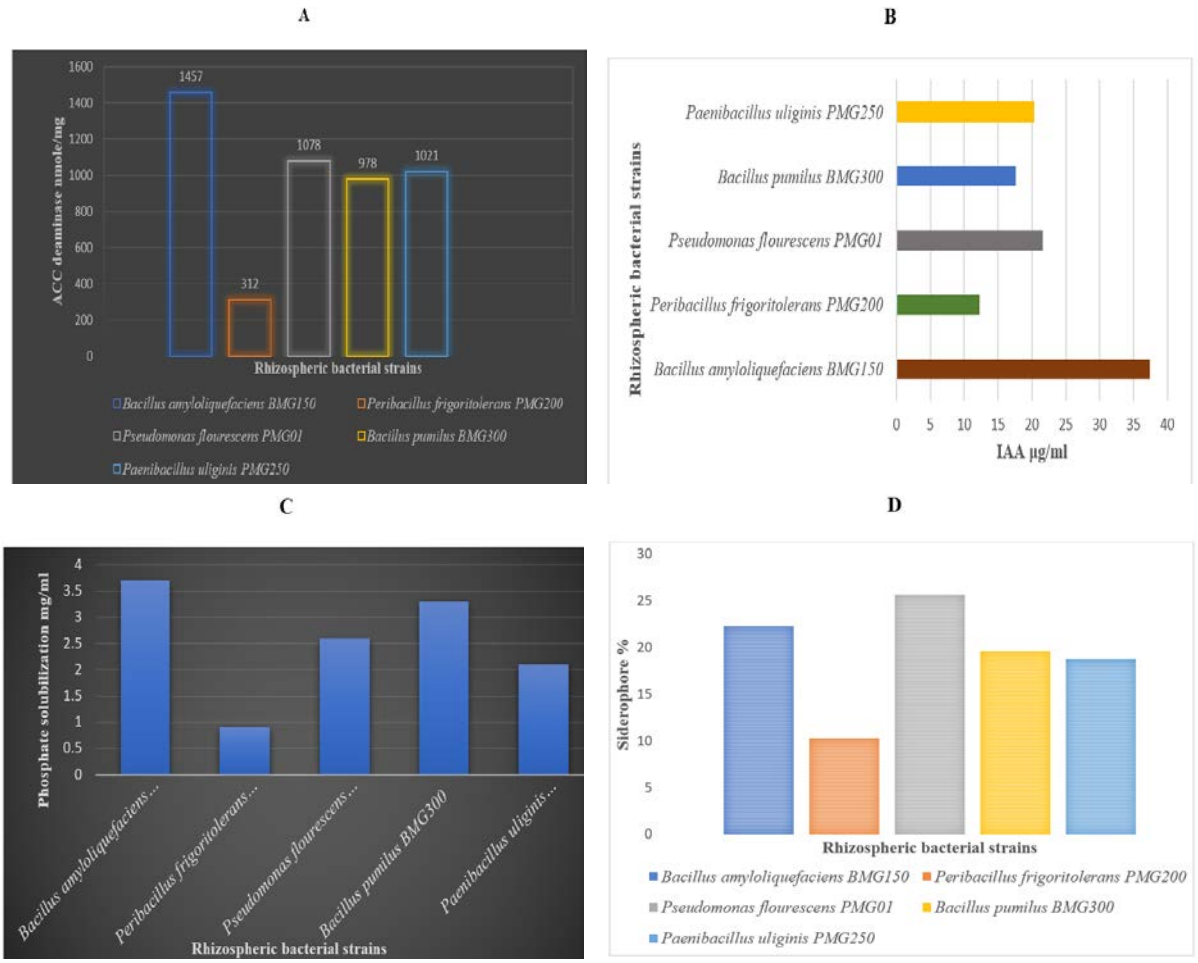

Figure 2. a. Activities of ACC deaminase; b. IAA production, c. phosphate solubilization (mg/ml); d. siderophores % of tomato rhizobacterial five isolates.

The IAA production by the five tomato rhizobacterial isolates was quantified by measuring the formation of indolic compounds at 530 nm. All isolates IAA production ranged between 12.3 µg/ml (*Peribacillus frigoritolerans* PMG200) and 37.4 µg/ml, whereas *Bacillus amyloliquefaciens* BMG110 displayed the highest IAA production followed by isolate *Pseudomonas flourescens*PMG01 (21.6 µg/ml), *Peribacillus frigoritolerans* PMG200 (20.3 µg/ml) and *Bacillus pumilus* BMG300 (17.6 µg/ml) (Figure 2B).

All the five tomato rhizobacterial isolates were solubilized phosphate in solid NBRIP medium by converting the inorganic form of phosphorous (Ca_3PO_4) into the solubilized form by development of yellow colour zone around the colonies on (Pikovaskya agar supplemented with 2% Ca_3PO_4). In liquid medium, *Paenibacillus uliginis* PMG250 displayed the highest solubilized phosphate (2.1 mg/ml) followed by *Peribacillus frigoritolerans* PMG200 (0.9 mg/ml) (Figure 2C). Siderophores production was proved for all the five isolates by development of greenish blue to yellow colour (CAS agar media) on both solid and liquid media. The maximum siderophore % showed for *Pseudomonas flourescens* PMG01 (25.7%) followed by *Bacillus amyloliquefaciens* BMG150 (22.3 %) (Figure 2D).

3.4. Non-ribosomal peptide synthetase genes detection using bioinformatics tools and degenerate primers

The detection of NRPs genes of the selected five tomato rhizobacterial isolates were performed using complete genome sequence accession number of the closest relativity strains available on GenBank: *Bacillus amyloliquefaciens* DSM7, *Peribacillus frigoritolerans*, *Pseudomonas flourescens*, *Bacillus pumilus* SAFR- 032 and *Paenibacillus uliginis* N3975. Using AntiSmash version 7.0, all these complete genome sequences have been analysed, and the most similar known clusters of different secondary metabolites were revealed. Only NRPs clusters from each genome were summarized in Table 4, whereas *Bacillus amyloliquefaciens* DSM 7 showed the largest number of NRPs clusters (5) represented in surfactin, fengycin, iturin, bacillibactin siderophore and bacillaene (polyketide-NRPs hybrid), followed by *Pseudomonas flourescens* which showed three NRPs clusters; viscosin, tolassin and lankacidin (hybrid polyketide-NRPs). *Bacillus pumilus* SAFR- 032 complete genome sequence analysis using AntiSmash detected two NRPs clusters of lichenysin (85% similarity), but when analyzed by PKS/NRPS analysis website, were identified as pumilacidin (surfactin family) and another cluster with 53 % identity to fengycin but with PKS/NRPS website analysis, no PKS/NRPS related domains were detected. *Peribacillus frigoritolerans* complete genome showed two NRPs clusters for koranimine and another cluster with 46 % similarity to fengycin which re-analyzed by PKS/NRPS analysis website and no PKS/NRPS related domains were detected. *Paenibacillus uliginis* N3975 complete genome showed the presence of two NRPs clusters with very low similarity 1% to pyoverdine with no PKS/NRPS related domains detected when analyzed by PKS/NRPS website, and 11% similarity to zwittermicin which was predicted as: (pks-x-Gly-x) by PKS/NRPS analysis website and might indicate the novelty of this NRPs cluster. All known NRPs clusters for the rhizosphere bacterial isolates were summarized in Table 5.

Table 5. AntiSmash Most similar known clusters detected for the five-tomato rhizosphere bacterial isolates.

Strain	Accession n	Region	Type	From	To	Similar known cluster AntiSmash	Similar known cluster PKS-NRPS& Norine	Similarity
Bacillus amyloliquefaciens DSM7	FN597644.1	1	NRP-Lipopeptide	314,040	378,185	Surfactin	Surfactin	82%
		5	Polyketide-NRP	1,766,333	1,867,399	Bacillaene	Bacillaene	100%
		6	NRP	1,948,676	2,058,873	Fengycin	Fengycin	93%
		9	NRP	2,506,988	2,551,970	Iturin	Iturin	100%
		10	NRP siderophore	3,033,649	3,085,384	Bacillibactin	Bacillibactin	100%
Bacillus pumilus SAFR-023	CP000813.4	1	NRP	323,520	403,989	Lichenysin	Pumilacidin	85%
		5	NRP	1,815,669	1,842,788	Fengycin	No NRP	53%
Pseudomonas flourescens	LT907842.1	1	NRP	114,934	144,184	Ambactin	No NRP	25%
		4	NRP	2,512,939	2,574,494	Viscosin		68%
		7	NRP	3,485,149	3,484,280	Pf-5 Pyoverdine	Pyoverdine partial	11%
		8	NRP	3,824,046	3,847,199	Fengycin	No NRP	13%
		9	NRP	3,951,152	3,996,195	Tolassin lipopeptide	Tolassin lipopeptide	70%
		11	NRP	4,325,050	4,377,946	Pf-5 Pyoverdine	Pyoverdine partial	9%
		14	NRP-polyketide	5,702,542	5,724,689	Lancacidin	No NRP	13%
Peribacillus frigoritolerans	CP091882.1	1	NRP	718,980	777,857	Koranimine	Koranimine	87%
		3	NRP	2,496,957	2,521,117	Fengycin	No NRP	46%
*Paenibacillus uliginis*N3975	LT840184.1	1	NRP	804,360	845,517	Pf-5 Pyoverdine	No NRP	1%
		2	NRP-polyketide	1,419,149	1,490,535	Zwittermicin	Unknown NRP-polyketide	11%

Degenerate primers Serie 1 were designed using the conserved nucleic acid sequences after the alignment of the adenylation and thiolation domains of different *Bacillus* strains for the NRPs lipopeptides known clusters; surfactin, fengycin or plipastatin, iturin (mycosubtilin and bacillomycin) and kurstakin (Tapi *et al*., 2010; Abderrahmani *et al*., 2011). Serie 2 of degenerate primers was designed before by the alignment of the amino acids sequence of the condensation domain (C) and the thioestrase domain (TE) of NRPs synthetases from *Pseudomonas* lipopeptides biosynthesis systems to detect the conserved sequences (Rokni-Zadeh *et al*., 2011). *Bacillus* degenerate primers amplified four fragments of the expected sizes for the presence of the NRPs lipopeptides surfactin, fengycin, plipastatin, mycosubtilin in strain *Bacillus amyloliquefaciens* BMG150, which is consistent with the AntiSmash analysis for the genome of the closest relativity strain *Bacillus amyloliquefaciens* DSM 7. Using surfactin primers, the Bacillus degenerate primers amplified a fragment from *Bacillus pumilus* BMG300 of the predicted size, which is also in agreement with the AntiSmash analysis of the genome of the nearest relativity strain, *Bacillus pumilus* SAFR-032.

On the other hand, *Pseudomonas* degenerate primers amplified two fragments of the expected sizes from *Pseudomonas flourescens* PMG01 isolate which often belongs to viscosin and tolassin NRPs clusters detected by AntiSmash analysis of the closest relativity strain *Pseudomonas flourescens*. On the contrary, both strains *Peribacillus frigoritolerans* PMG200 and *Paenibacillus uliginis* PMG250 amplified fragments of different sizes with fengycin primers (580 bp) which revealed 100 % similarity to Koranimine NRPs gene (Figure 3) as detected AntiSmash analysis for the closest relativity strains *Peribacillus frigoritolerans*, and revealed 100 % similarity to amino acid adenylate gene (684 bp) involved into the NRPs-PKS cluster (pks-x-Gly-x) predicted by AntiSmash and PKS/NRPS analysis website of the closest relativity strain *Paenibacillus uliginis* N3975 (Figure 4). All the positive amplification of degenerate primers for the rhizosphere bacterial isolates is listed in Table 6.

Table 6. Detected NRPs clusters for the tomato rhizosphere bacterial isolates using degenerate primers.

Isolated strains	Degenerate primers							
	***Bacillus* primers**							
	plipastatin	**surfactin**	**fengycin**	**mycosubtilin**	**bacillomycin**	**kurstakin**	***Pseudomonas* primers**	
	Ap, Tp	As, Ts	Af, Tf	Am, Tm	Abl, Tbl	Aks, Tks	C1	TE1, TE2
Bacillus amyloliquefaciens BMG150	+	+	+	+	-	-	-	-
Peribacillus frigoritolerans PMG200	-	-	+	-	-	-	-	-
Pseudomonas flourescens PMG01	-	-	-	-	-	-	+	+
Bacillus pumilus BMG300	-	+	-	-	-	-	-	-
Paenibacillus uliginis PMG250	-	-	+	-	-	-	-	-

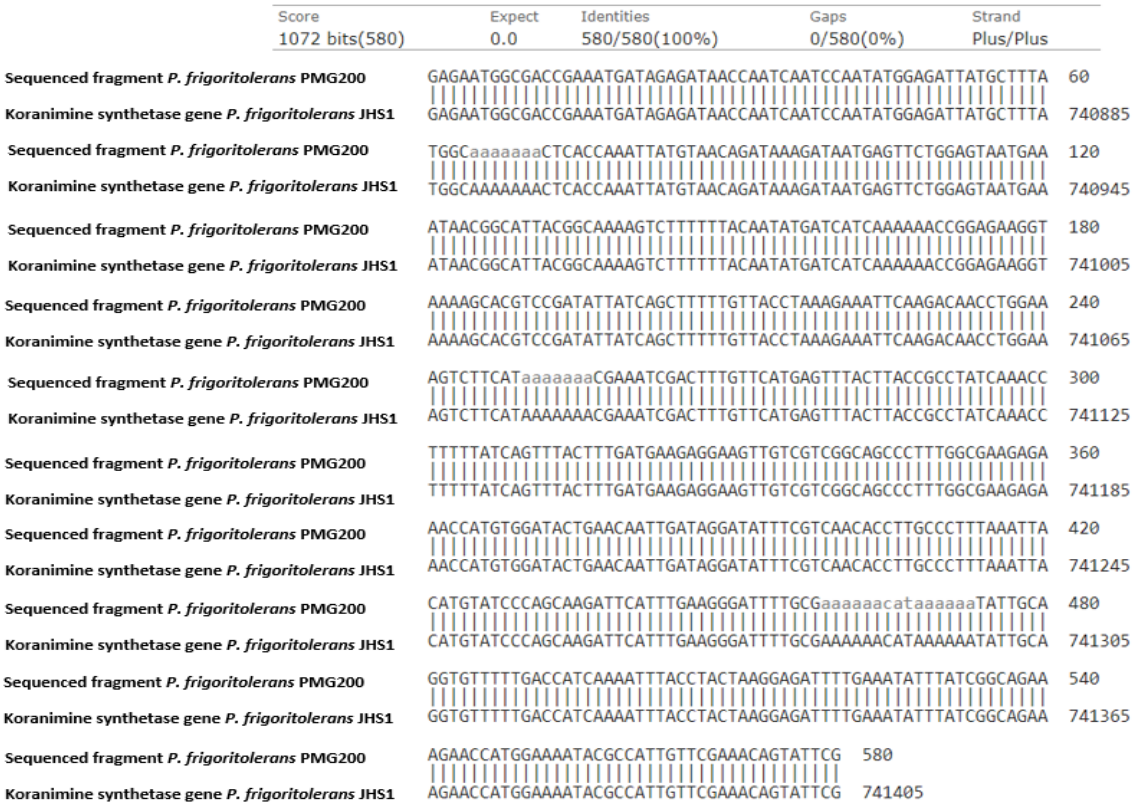

Figure 3. BlastN sequence alignment of fragment amplified using fengycin degenerate primers from strain *Peribacillus frigoritolerans* PMG200.

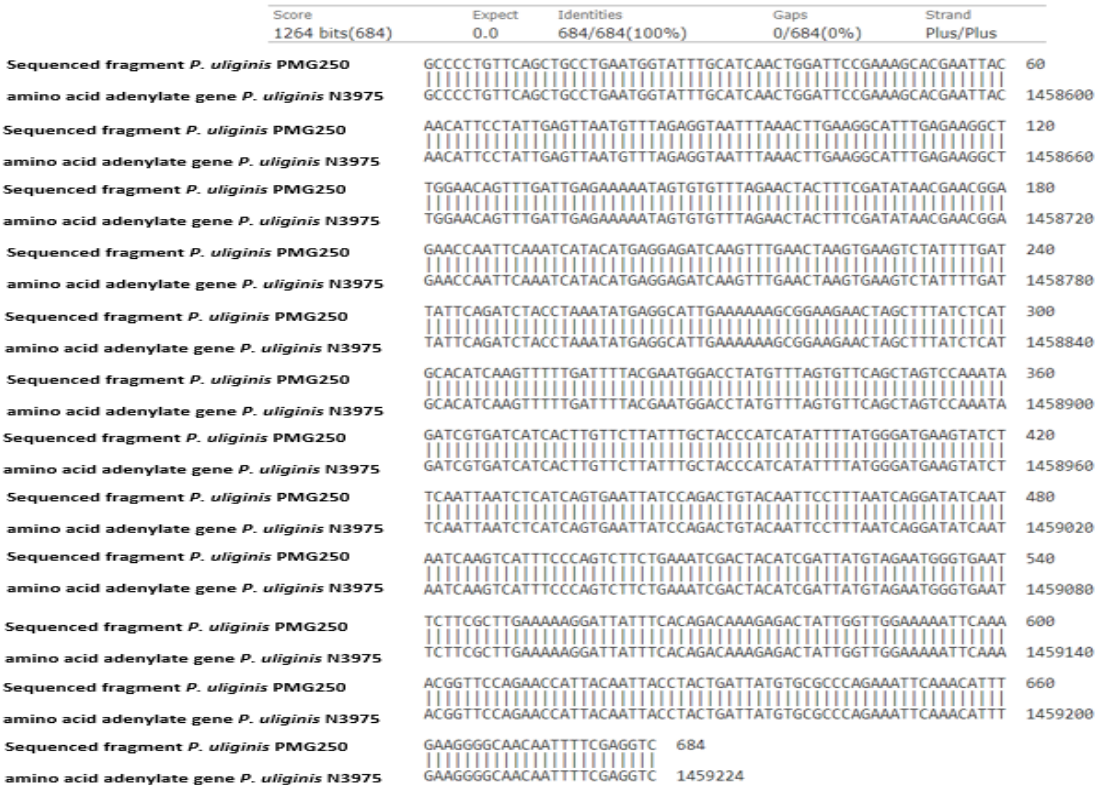

Figure 4. BlastN sequence alignment of fragment amplified using fengycin degenerate primers from strain *Paenibacillus uliginis* PMG250.

3.5. Sprout barely invivo experiment

In this experiment and after 12 days, results were interpreted depending on two main points: (1) production efficiency and (2) seedling length. For the production efficiency, it was remarked that the sample G (soaked in *Bacillus amyloliquefaciens* BMG150) recorded the highest values (7 folds), and seedling length (22.4 cm) followed by the sample E (soaked in *Pseudomonas flourescens* PMG01) (3.8 folds and 16.2 cm), respectively. On the other hand, the lowest production efficiency, and seedling length was observed for the samples B (control 2: washed only with water) (1.3 folds and 11.2 cm), followed by A (control 1: washed and sterilized using Sodium hypochlorite) (1.6 folds and 13.3 cm), C (soaked in *Paenibacillus uliginis* PMG250, *Peribacillus frigoritolerans* PMG200 and *Bacillus pumilus* BMG300,) (3 folds and 15.8 cm), respectively (Figure 5 and Table 7). These results underscore the importance and the efficiency of the use of strain *Bacillus amyloliquefaciens* BMG150 in enhancing sprouted barely seedling germination ratio, strength and length followed by the strain *Pseudomonas flourescens*PMG01.

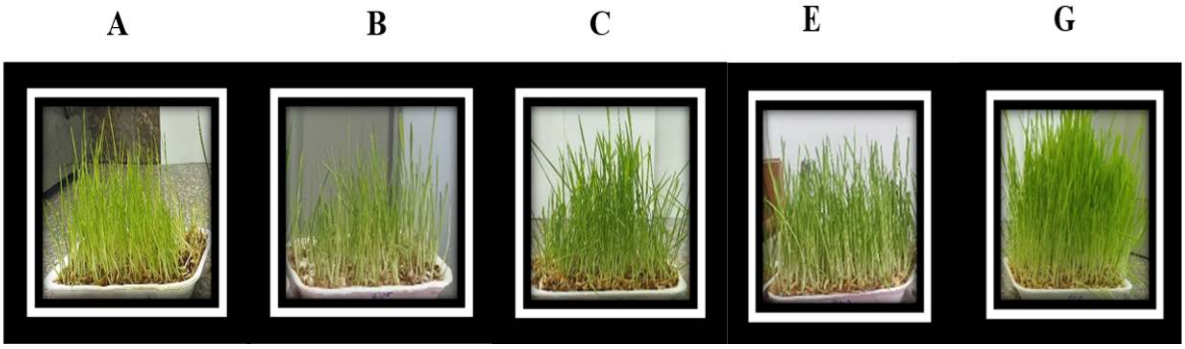

Figure 5. Sprouted barely cultivated for 12 days, (A) control 1: washed and sterilized using Sodium hypochlorite, (B) control 2: washed only with water, (C) barely seeds washed by water, sterilized by Sodium hypochlorite, and soaked in *Paenibacillus uliginis* PMG250, *Peribacillus frigoritolerans* PMG200 and *Bacillus pumilus* BMG300, (E) barely seeds washed by water, sterilized by Sodium hypochlorite and soaked in *Pseudomonas flourescens* PMG01, (G) barely seeds washed by water, sterilized by Sodium hypochlorite and soaked in *Bacillus amyloliquefaciens* BMG150.

Table 7. Sprout barley characteristics after 12 days of plantation using tomato rhizobacterial biofertilizers and fungal inoculants.

Characteristics	A	B	C	E	G
Seed weight	125g	125g	125g	125g	125g
Sprout barely weight	200g	168g	386g	478g	883g
Production efficiency	1.6 folds	1.3 folds	3 folds	3.8 folds	7 folds
Leave length	13.3 cm	11.2 cm	15.8 cm	16.2 cm	22.4 cm

3.6. Soluble protein banding patterns

Protein profile determination by SDS-PAGE for barley samples showed different banding patterns between the treatments. Many alterations in protein patterns were recorded for barley leaves *soaked in different rhizobacterial strains* (*Paenibacillus uliginis* PMG250, *Peribacillus frigoritolerans* PMG200 and *Bacillus pumilus* BMG300, *Pseudomonas flourescens* PMG01 and *Bacillus amyloliquefaciens* BMG150) under two controls. There is a number of bands totalling 21; ten of them were monomorphic bands with 47.6 %, while eleven polymorphic bands appeared with 52.4 %. There is one unique band at MW 15 KDa appeared in samples G (treated with *Bacillus amyloliquefaciens* BMG150 after 9 days). Also, there is one unique band that appeared at MW 40 KDa in samples C (treated with *Paenibacillus uliginis* PMG250, *Peribacillus frigoritolerans PMG200* and *Bacillus pumilus BMG300* after 9 days) *and G* (treated with *Bacillus amyloliquefaciens* BMG150 *after 9 days),* respectively. The highest number of bands was revealed in sample C *(treated* with *Paenibacillus uliginis* PMG250, *Peribacillus frigoritolerans* PMG200 and *Bacillus pumilus* BMG300 after 9 days) and sample G with 20 and 19 bands, respectively. On the other hand, sample B**'** (control 2 at 12 days) were the lowest number of bands (10) as shown in (Table 8 and Figure 6). These results were in harmony with barely invivo experiment**.** The density, strength and length of the weakest seedlings in growth were observed for the sample B (control 2: washed only with water).

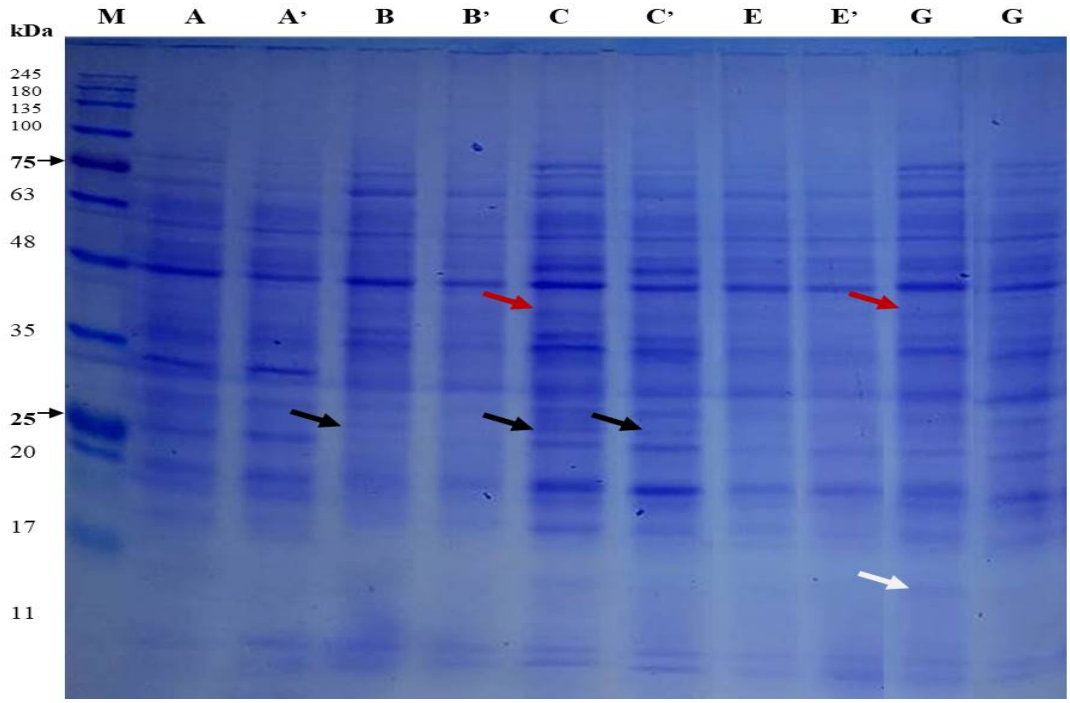

Figure 6. Electrophoretic patterns soluble proteins of the sprouted barely leaves treated with rhizobacterial isolates performed by SDS-PAGE. M: is standard protein.

Table 8. Densitometric analysis water soluble protein patterns for sprouted barley plants treated with rhizobacterial strains. (+) presence of bands; (-) absence of bands.

		Samples										
Band NO.	**size KDa**	**A**	**A'**	**B**	**B'**	**C**	**C'**	**E**	**E'**	**G**	**G'**	
1	**90**	-	-	-	-	+	-	-	-	+	+	**3**
2	**85**	+	-	+	-	+	+	+	-	+	+	**7**
3	**70**	+	+	+	+	+	+	+	+	+	+	**10**
4	**65**	+	+	+	-	+	+	-	-	+	+	**7**
5	**60**	+	+	+	+	+	+	+	+	+	+	**10**
6	**55**	-	-	-	-	+	+	-	-	+	+	**4**
7	**48**	+	+	+	+	+	+	+	+	+	+	**10**
8	**40**	-	-	-	-	+	-	-	-	+	-	**2**
9	**38**	-	-	+	-	+	+	-	-	+	+	**5**
10	**36**	+	+	+	+	+	+	+	+	+	+	**10**
11	**32**	+	+	+	+	+	+	+	+	+	+	**10**
12	**30**	+	+	+	+	+	+	+	+	+	+	**10**
13	**27**	-	-	+	-	+	+	-	-	-	-	**3**
14	**25**	+	+	-	-	+	+	+	+	+	+	**8**
15	**20**	+	+	+	+	+	+	+	+	+	+	**10**
16	**19**	+	+	-	-	+	+	-	-	+	+	**6**
17	**18**	+	+	+	+	+	+	+	+	+	+	**10**
18	**15**	-	-	-	-	-	-	-	-	+	-	**1**
19	**11**	+	+	+	+	+	+	+	+	+	+	**10**
20	**10**	+	+	+	+	+	+	+	+	+	+	**10**
21	**8**	-	+	-	-	+	+	-	+	-	+	**5**
Total bands		**14**	**14**	**14**	**10**	**20**	**18**	**12**	**12**	**19**	**18**	**151**

4. Discussion

Plant-microbe interactions type is often responsible for plant growth and development in the rhizosphere, whereas various studies reported the presence of various Bacillus species in the soil rhizosphere and as PGPR (Kumar *et al*., 2012; Singh *et al*., 2014) according to their promoting plant growth role or suppressed several phytopathogens (Mumtaz *et al*., 2017; Akinrinlola *et al*., 2018).

Here, we highlighted the potential of some tomato rhizosphere beneficial bacteria isolates which are considered the first line defense against pathogens by choosing the more efficient growth promoting characteristics bacteria. In this work, a total of 16 tomato bacterial isolates were evaluated for their PGP characteristics. Only five strains of which revealed considerable values for ACC deaminase, IAA, siderophores and solubilizing phosphate. The five rhizobacterial isolates showed their ACC deaminase production ability in accordance with (Singh *et al*., 2019) who confirmed this ability for rhizobacterial isolated from various crop plants. Furthermore, the ACC deaminase activity quantification ranged from 312–1457 nmol α-ketobutyrate/ mg protein and the isolate *Bacillus amyloliquefaciens* BMG150 exhibited the highest ACC deaminase activity; therefore, ACC deaminase values determination is vital (Singh *et al*., 2019) and the rhizobacteria that can combine both the activity of ACC deaminase and other PGP properties is considered an amended symbiotic associate for the host plants (Tiwari *et al*., 2018; Gowtham *et al*., 2020).

The five isolates are positive producers of IAA which is considered growth regulator of different plant growth stages (Etesami *et al*., 2015). Furthermore, the isolates were assessed for their potential for producing siderophores which enhance iron availability to the plant and reduce iron availability for phyto-pathogens, respectively (Saha *et al*., 2016; Sansinenea, 2019). Phosphate solubilization ability was also tested by the five isolates, which can be interpreted by the production of several components capable of transforming insoluble phosphates into easily absorbed substances by plants (Rodríguez and Fraga, 1999; Chen *et al*., 2006; Patel *et al*., 2008; Brígido and Glick, 2017). Among the selected isolates, the high values were recorded to isolates *Bacillus amyloliquefaciens* BMG150, *Pseudomonas flourescens* PMG01 and *Bacillus pumilus* BMG300. The five efficient rhizosphere bacterial isolates were identified with the 16SrRNA gene sequences, which were similar by 99–100% with genera: Bacillus, Pseudomonas and Peribacillus. The results agree with the finding of (Hariprasad, 2014).

Here, we demonstrated the efficiency of using degenerate primers in detecting NRPs synthetase genes, whereas it empowered us to take insight view about several genes involved in this mechanism side by side with bioinformatics using AntiSmash and PKS-NRPS analysis websites. The use of degenerate primers in detecting NRPs genes became commonly applied. Several studies designed series of these primers, and (Marahiel, 1997) designed a set of primers depending on the motif A2 (KAGGAY) LV P which are highly conserved for peptide synthetases. The second set was designed by (Neilan *et al*., 1999; Viscaino *et al*., 2005) depending on the conserved motif of the adenylation domain (A) aligned from various bacteria and fungi. Recently, the design of NRPs degenerate primers became more specialized depending on bacteria genera; Bacillus, for instance, is considered as one of the first genera for which this kind of NRP degenerate primers was

designed. *Bacillus* non-ribosomal lipopeptide synthetase genes degenerate primers were designed depending on the extraction of the conserved nucleic acids sequence of the (A) and the (T) domains after their alignment from different Bacillus members (Tapi *et al.,* 2010; Chen *et al*., 2006), while Pseudomonas degenerate primers were designed before by the alignment of the amino acids sequence of the condensation domain (C) and the thioestrase domain (TE) of NRPs synthetases from Pseudomonas lipopeptides biosynthesis systems to detect the conserved sequences (Rokni-Zadeh *et al*., 2011). In our study, *Bacillus* degenerate primers (Tapi *et al*., 2010; Chen *et al*., 2006) proved their efficiency in detecting NRLPs clusters of surfactin (As1-F/Ts2-R primers), fengycin (Af2-F/Tf1-R primers), plipastatin (Ap1-R/Tp1-R primers), mycosubtilin (Am1-F/Tm1-R primers) in strain *B. amyloliquefaciens* BMG150, pumilacidin (As1-F/Ts2-R primers) from *B. pumilus* BMG300, koranimine (Af2-F/Tf1-R primers) from *Peribacillus frigoritolerans* PMG200 and unknown NRPs (Af2-F/Tf1-R primers) from *Paenibacillus uliginis* PMG250. The previous results agree with (Tapi *et al*., 2010) who amplified fragments of expected sizes with As1-F/Ts2-R primers from *B.s* 168 and *B. licheniformis* ATCC 14580 (99%) similarity with surfactin and lichenysin (surfactin family), respectively, amplified fragments of expected sizes with plipastatin (Ap1-R/Tp1-R) primers from *Bs* 168 similar (99%) to plipastatin and detected mycosubtilin gene by (Am1-F/Tm1-R) primers in *Bs* ATCC6633. (Tapi *et al*., 2010) also confirmed the amplification of fragments of different sizes with Af2-F/ Tf1-R primers from *Bs* ATCC6633, similarly to bacillaene polyketide synthase of *B. amyloliquefaciens* FZB42 (88%) and of *B.s* 168 (Chen *et al*., 2009; Al-shebly, 2022). The fengycin primer pairs can detect unexpected NRPs genes. These results agree with our finding for the isolates *Peribacillus frigoritolerans* PMG200 and *Paenibacillus uliginis* PMG250 amplified fragments corresponding to another NRPs gene rather than fengycin (Koranimine and unknown NRPs), respectively. On the other hand, *Pseudomonas* degenerate primers amplified two fragments of the expected sizes from *Pseudomonas flourescens* PMG01 isolate similar to viscosin and tolassin, as reported (Rokni-Zadeh *et al*., 2011) who amplified fragments similar to viscosin and tolassin with the expected size from three maize rhizosphere *Pseudomonas florescent* isolates (PGSB3962, PGSB7828, and PGSB8273).

The usage of rhizobacterial strains with PGP characteristics proved their efficiency in promoting barely growth and reduced fungal growth during sprout barely plantation. The production efficiency and leaves length decreased in control 1 and control 2; these results agree with (Paul and Nair, 2008) who confirmed that the presence of *Aspergillus flavus* decreased barley seeds germination and seedlings growth. We suggest that the use of microbial biofertilizers overcome the negative effects of salt by producing osmolytes and salt stress-induced proteins and therefore enhance sprouted barley production efficiency and leave length, which agrees with (Ryu *et al*., 2004). Also, our results agree with (Murphy *et al*., 2003) who described the capability of *Bacillus subtilis* GBO3 in inducing defense-related pathways like, salicylic acid (SA) and jasmonic acid (JA). These results agree with (Aliasgharzad, 2006) who confirmed the enhancement of tomato immunity against tomato mottle virus by the application of *Bacillus amyloliquefaciens* 937b and *Bacillus pumilus* SE-34 as PGPR.

The effect of different bacterial treatments appears in the expression of some genes encoding proteins by switching on or off. Based on our results, we found different bacterial treatments by combination formula of the three strains *Paenibacillus uliginis* PMG250, *Peribacillus frigoritolerans* PMG200 and *Bacillus pumilus* BMG300 and the use of *Bacillus amyloliquefaciens* BMG150 separately revealed the highest number of bands with 20 and 19 bands, respectively. These findings are in accordance with (Murphy *et al*., 2003; Aliasgharzad, 2006) who reported that PGPR strains can induce defense-related pathways like, Salysalic Acid and Jasmonic Acid and enhance tomato immunity. The findings might reflect on protein patterns by the appearance of newly synthesized bands and the absence of others. (Boston *et al*., 1996; El-Saber, 2021) observed that under different stress conditions, molecular chaperones are involved in various cellular functions which agrees with our findings of the low molecular weight proteins accumulation.

5. Conclusion

The use of biofertilizers isolated from soil rhizosphere is considered an alternative to chemical substances and enhances plant growth. The soaking of barely seeds before planting in these rhizosphere isolates suspension enhances the growth of sprouted barely.

References

Abderrahmani A, Tapi A, Nateche F, Chollet M, Leclère V, Wathelet B, Hacene H and Jacques P. 2011. Bioinformatics and molecular approaches to detect NRPS genes involved in the biosynthesis of kurstakin from *Bacillus thuringiensis*. *Appl Microbiol Biotechnol*., **92**: 571–581.

Ahmad F, Ahmad I and Khan MS. 2008. Screening of free-living rhizospheric bacteria for their multiple plant growth promoting activities. *Microbiol Res*., **163**: 173–181.

Aliasgharzad N, Reza M and Neyshabouri Salimi G. 2006. Effects of arbuscular mycorrhizal fungi and *Bradyrhizobium japonicum* on drought stress of soybean. *Biologia*., **19**: 324–328.

Akinrinlola RJ, Yuen, GY, Drijber RA and Adesemoye AO. 2018. Evaluation of Bacillus strains for plant growth promotion and predictability of efficacy by in vitro physiological traits. *Int J Microbiol*., 1–11.

Al-shebly H. 2022. Effect of *Aspergillus flavus* on Seed Germination and Seedlings Growth of Barley and Some of Associated Weeds. *IOP Conference Series Earth and Environml Sci*., **1060(1)**: 012119; DOI: 10.1088/1755-1315/1060/1/012119.

Asriatno O, Nawangsih AA, Astuti RI and Wahyudi AT. 2023. Streptomyces–Alginate Beads Formula Promote Maize Plant Growth and Modify the Rhizosphere Microbiome. *Jordan J Biol Sci*., **16(3):**537-546; https://doi.org/10.54319/jjbs/160316

Banta N, Singh R and Singh N. 2021. Comparative protein profile analysis by SDS-PAGE of different grain cereals. *Pharma Innovation J*., **10(9)**: 104-108.

Barea JM and Richardson AE. 2015. Phosphate mobilisation by soil microorganisms. In: Lugtenberg, B. (Ed.), Principles of Plant-Microbe Interactions. Springer International Publishing, Heidelberg, Switzerland, pp. 225–234.

Berti AD, Greve NJ, Christensen QH and Thomas MG. 2007. Identification of a biosynthetic gene cluster and the six associated lipopeptides involved in swarming motility of *Pseudomonas syringae*pv. tomato DC3000. *J Bacteriol*., **189**: 6312–6323.

Blin K, Shaw S, Augustijn HE, Reitz ZL, Biermann F, Alanjary M, Fetter A, Terlouw BR, Metcalf WW, Helfrich EJN, van Wezel GP, Medema MH and Weber T. 2023. AntiSMASH 7.0: new and improved predictions for detection, regulation, chemical structures, and visualisation**.** *Nucleic Acids Res.,* doi: 10.1093/nar/gkad344 .

Boston RS, Viitanen PV andVierling E. 1996. Molecular chaperones and protein folding in plants. In: Filipowicz, W., Hohn, T. (eds) Post-Transcriptional Control of Gene Expression in Plants. Springer, Dordrecht; https://doi.org/10.1007/978-94-009-0353-1_9.

Brígido C, Glick BR andOliveira S. 2017. Survey of Plant Growth-Promoting Mechanisms in Native Portuguese *Chickpea Mesorhizobium* Isolates. *Microb Ecol*., **4**: 900–915.

Chaida A, Bensalah F, Trari B. 2022. Potential for Crude Oil and Diesel Biodegradation by the Indigenous Pseudomonas sp. Strain LGMS7 Using GC-MS and GC-FID Analyses. *Jordan J Biol Sci*., **15(3):**441- 448; https://doi.org/10.54319/jjbs/150313

Chen XH, Vater J, Piel J, Franke P, Scholz R, Schneider K, Koumoutsi A, Hitzeroth G, Grammel N, Strittmatter AW, Gottschalk G, Süssmuth RD and Borriss R. 2006. Structural and functional characterization of three polyketide synthase gene clusters in *Bacillus amyloliquefaciens* FZB 42. *J Bacteriol*., **188**: 4024–4036.

Chen XH, Koumoutsi A, Scholz R, Schneider K, Vater J, Süssmuth R, Piel J and Borriss R. 2009. Genome analysis of *Bacillus amyloliquefaciens* FZB42 reveals its potential for biocontrol of plant pathogens. *J Biotechnol*., **140**: 27–37.

Chen Y et al. 2006. Phosphate Solubilizing Bacteria from Subtropical Soil and Their Tricalcium Phosphate Solubilizing Abilities. *Appl Soil* Ecol., **1**: 33–41.

Cuddeford D.1989. Hydroponic grass. *In Practice*., **11(5)**: 211-214.

DeLong EF.1992. Archaea in coastal marine environments. *P Natl Acad* Sci., USA89:5685-5689.

Dutta S and Podile AR. 2010. Plant Growth Promoting Rhizobacteria (PGPR): the bugs to debug the root zone. *Crit Rev Microbiol*., **36(3):** 232–244.

Dworkin M and Foster J. 1958. Experiments with some microorganisms which utilize ethane and hydrogen. *J Bacteriol*., **75**: 592–603.

El-Saber M. 2021. Biochemical and molecular markers associated with salinity tolerance in bread wheat genotypes (Triticum aestivum L.) Under saline conditions. *Egyptian J Desert Res*., **71(1)**: 53-73.

Etesami H, Alikhani HA and Hosseini HM. 2015. Indole-3-acetic acid and 1-aminocyclopropane-1-carboxylate deaminase: bacterial traits required in rhizosphere, rhizoplane and/or endophytic competence by beneficial bacteria. In: Maheshwari, D.K. (Ed.), Bacterial Metabolites in Sustainable Agroecosystem. Springer International, Switzerland, pp. 183–258.

Finney P. 1983. Effect of germination on cereal and legume nutrient changes and food or feed value. Mobilization of Reserves in Germination, Springer pp. 229-305.

Fiore A, Mannina L, Sobolev AP, Salzano AM, Scaloni A, Grgurina I, Fullone MR, Gallo M, Swasey C, Fogliano V and Takemoto JY. 2008. Bioactive lipopeptides of ice-nucleating snow bacterium Pseudomonas syringae strain 31R1. *FEMS Microbiol Lett*., **286**: 158–165.

Gebremedhin WK. 2015. Nutritional benefit and economic value of feeding hydroponically grown maize and barley fodder for Konkan Kanyal goats. *J Agric Vet Sci*., **8**: 24-30.

Ghasempour HR, Anderson EM, Gaff Donald F. 2001. Effects of growth substances on the protoplasmic drought tolerance of leaf cells of the resurrection grass, Sporobolusstapfianus. *Aust J Plant Physiol*., **28**: 1115-1120.

Ghasempour HR and Kianian J. 2002. Drought stress induction of free proline, total proteins, soluble sugars and its protein profile in drought tolerant grass Sporobolus elongates. *J Sci Teacher Training Univ*., **1**: 111-118.

Ghasempour HR and Maleki MA. 2003. survey comparing desiccation tolerance in resurrection plant Nothelaenavellea and studying its protein profile during drought stress against a non-resurrection plant Nephrolepsis sp. *Iranian J Biol*., **15**: 43-48.

Gordon SA and Weber RP. 1951. Colorimetric Estimation of indoleacetic Acid. *Plant Physiol*., **26(1)**:192–195; https://doi.org/10.1104/pp.26.1.192.

Gowtham HG, Brijesh Singh S, Murali M, Shilpa N, Prasad M, Aiyaz M, Amruthesh KN and Niranjana SR. 2020. Induction of drought tolerance in tomato upon the application of ACC deaminase producing plant growth promoting rhizobacterium *Bacillus subtilis* Rhizo SF 48. *Microbiol Res*., **234**:126422; https://doi. org/10.1016/j.micres.2020.126422.

Gross H, Stockwell VO, Henkels MD, Nowak-Thompson B, Loper JE and Gerwick WH. 2007. The genomisotopic approach: a systematic method to isolate products of orphan biosynthetic gene clusters. *Chem Biol*., **14**: 53–63.

Gross H and Loper JE. 2009. Genomics of secondary metabolite production by Pseudomonas spp. *Nat Prod Rep*., **26**:1408–1446.

Hariprasad P, Chandrashekar S, Singh SB and Niranjana SR. 2014. Mechanisms of plant growth promotion and disease suppression by *Pseudomonas aeruginosa* strain 2apa. *J Basic Microbiol*., **54(8)**: 792–801.

Harper_SHT and Lynch JM. 1981. Effects of Fungi on Barley Seed Germination. *Microbiol*., **122(1)**: 55-60; https://doi.org/10.1099/00221287-122-1-55.

Honma M and Shimomura T. 1978. Matabolism of 1 - aminocyclopropane 1-carboxylate. *Agri BioI Chem*., **42**: 1825-1831.

Hussein W, Awad H and Fahim S. 2016. Systemic Resistance Induction of Tomato Plants against ToMV Virus by Surfactin Produced from *Bacillus subtilis* BMG02. *Amer J Microbiol Res*., **4(5)**: 153-158; doi: 10.12691/ajmr-4-5-5.

Hussein W, Ramadan WA and Fahim S. 2018. Isolation and characterization of *Bacillus* endophytic strains producers for non-ribosomal lipopeptides NRLPs from tomato. *Int J Res Pharma Sci*., **9**(1): 128-134.

Johansson E, Malik AH, Hussain A, Rasheed F, Newson WR, Plivelic T, Hedenqvist M, Gällstedt M and Kuktaite R. 2013. Gluten protein structures: Variation in wheat grain and for various applications. In: He, Z., Wang, D. eds., Proceeding: 11th International Gluten Workshop. Beijing, China, August 12-15, 2012, Mexico: International Maize and Wheat Improvement Center.

Kalam S, Das SN, Basu A and Podile AR. 2017a. Population densities of indigenous Acidobacteria change in the presence of plant growth promoting rhizobacteria (PGPR) in rhizosphere. *J Basic Microbiol*., **57(5)**: 376–385.

Kuiper I, Lagendijk EL, Pickford R, Derrick JP, Lamers GE, Thomas-Oates JE, Lugtenberg BJ and Bloemberg GV. 2004. Characterization of two Pseudomonas putida lipopeptide biosurfactants, putisolvin I and II, which inhibit biofilm formation and break down existing biofilms. *Mol Microbiol*., **51**: 97–113.

Kumar P, Dubey RC and Maheshwari DK. 2012. Bacillus strains isolated from rhizosphere showed plant growth promoting and antagonistic activity against phytopathogens. *Microbiol Res*., **167(8)**: 493–499.

Laemmli UK. 1970. Cleavage of structural proteins during the assembly of the head of bacteriophage T4. *Nature*., **227**: 6800685.

Ling HQ, Zhang A, Wang D, Liu D, Wang JY, Sun H, Fan HJ, Li ZS, Zhao Y, Wang DW, Zhang KP, Yang YS, Wang JJ and Dong L. 2012. Wheat A genome sequencing and its application for quality modification. In: He, Z., Wang, D. eds., Proceeding: 11th International Gluten Workshop. Beijing, China, August 12-15, 2012, Mexico: International Maize and Wheat Improvement Center.

Marahiel MA. 1997. Protein templates for the biosynthesis of peptide antibiotics. *Chem Biol*., **4**: 561-567.

Miháliková D, Galova Z, Petrovičová L and Chňapek M. 2016. Polymorphism of proteins in selected slovak winter wheat genotypes using SDS-PAGE. *J Central Europ Agricul*., **17(4)**: 970-985.

Mumtaz MZ, Ahmad M, Jamil M, Hussain T. 2017. Zinc solubilizing Bacillus spp. potential candidates for biofortification in maize. *Microbiol Res*., **202**, 51-60.

Murphy JF, Reddy MS, Ryu CM, Kloepper JW and Li R. 2003. Rhizobacteria mediated growth promotion of tomato leads to protection against cucumber mosaic virus. *Phytopathol*., **93**: 1301–1307.

Nautiyal CS. 1999. An Efficient Microbiological Growth Medium for Screening Phosphate Solubilizing Microorganisms. *FEMS Microbiol Lett*., **1**: 265–270.

Neilan BA, Dittmann E, Rouhiainen L et al. 1999. Nonribosomal peptide synthesis and toxigenicity of Cyanobacteria. *J Bacteriol*., **181**: 4089- 4097.

Olsen S, Sommers L and Page A. 1982. Methods of Soil Analysis Part 2 Chemical and microbiological properties of Phosphorus. *ASA Monogr*., **9**: 403–430.

Ongena M and Jacques P. 2008. *Bacillus* lipopeptides: versatile weapons for plant disease biocontrol. *Trends Microbiol*., **16(3)**: 115-125(2008).

Orozco-Mosqueda MC, Glick BR and Santoyo G. 2020. ACC deaminase in plant growth promoting bacteria (PGPB): an efficient mechanism to counter salt stress in crops. *Microbiol Res*., **235**: 126439.

Parray JA, Jan S, Kamili AN, Qadri RA, Egamberdieva D and Ahmad P. 2016. Current perspectives on plant growth-promoting rhizobacteria. *J Plant Growth Regul*., **35 (3)**:877–902.

Patel DK, Archana G and Kumar GN. 2008. Variation in the nature of organic acid Secretion and mineral phosphate solubilization by Citrobacter Sp. Dhrss in the Presence of Different Sugars. *Curr Microbiol*., **2**: 168–174.

Paul D and Nair S. 2008. Stress adaptations in a plant growth promoting Rhizobacterium (PGPR) with increasing salinity in the coastal agricultural soils. *J Basic Microbiol*., **48**: 1–7.

Penrose DM and Glick BR. 2001. Levels of ACC and related compounds in exudate and extracts of canola seeds treated with ACC deaminase-containing plant growth-promoting bacteria. *Can J Microbiol*., **47**: 368–372; https://doi.org/10.1139/w01- 014.

Ramadan WA and Soliman GM. 2020. Effect of different applications of bio-agent *Achromobacter xylosoxidans* against Meloidogyne incognita and gene expression in infected eggplant. *Jordan J Biologl Sci*., **13(3):** 363–370.

Rodríguez H and Fraga R. 1999. Phosphate Solubilizing Bacteria and Teir Role in Plant Growth Promotion. *Biotech Adv*., **4**: 319–339.

Rokni-Zadeh H, Mangas-Losada A and De Mot R. 2011. PCR Detection of Novel Non-ribosomal Peptide Synthetase Genes in Lipopeptide-Producing Pseudomonas. *Microb Ecol*., **62**: 941–947; DOI 10.1007/s00248-011-9885-9.

Ryu CM, Farag MA, Hu CH, Reddy MS, Kloepper JW and Pare PW. 2004. Bacterial volatiles induce systemic resistance in Arabidopsis. *Plant Physiol*., **134**: 1017–1026.

Saha M, Sarkar S, Sarkar B, Sharma BK, Bhattacharjee S and Tribedi P. 2016. Microbial siderophores and their potential applications: a review. *Environ. Sci Pollut Res*., **23**: 3984–3999.

Sansinenea, E. 2019. Bacillus spp. as plant growth-promoting bacteria. In: Singh HB, et al. (Eds.), Secondary Metabolites of Plant Growth Promoting Rhizo-microorganisms. Springer, Singapore, pp. 225–237.

Singh RK, Kumar DP, Singh P, Solanki MK, Srivastava S, Kashyap PL, Kumar SAK, Singhal PK and Arora DK. 2014. Multifarious plant growth promoting characteristics of chickpea rhizosphere associated Bacilli help to suppress soil-borne pathogens. *Plant Growth Regul.*, **73**: 91–101.

Singh SB, Gowtham HG, Murali M, Hariprasad P, Lakshmeesha TR, Murthy KN, Amruthesh KN and Niranjana SR. 2019. Plant growth promoting ability of ACC deaminase producing rhizobacteria native to Sunflower (*Helianthus annuus*L.). *Biocatal Agric Biotechnol*., **18**: 101089; https://doi.org/10.1016/j. bcab.2019.101089.

Stegmann H. 1979. Electrophoresis and focusing in slabs using the Pantaphor apparatus for analytical and preparative separations in gel (Polyacrylamide, Agarose, Starch, Sephadex). Messeweg 11, D03300, Braunschweig Institute of Biochemistry, West Germany pp: **1029**.

Süssmuth RD and Mainz A. 2017. Non-ribosomal peptide synthesis principles and prospects. *Angew Chem Int*., **E56**: 3770–3821.

Tapi A, Chollet-Imbert M, Scherens B, Jacques P. 2010. New approach for the detection of non-ribosomal peptide synthetase genes in *Bacillus* strains by polymerase chain reaction. *Appl Microbiol Biotechnol*., **85**: 1521-1531.

Tiwari G, Duraivadivel P, Sharma S and Hariprasad P. 2018. 1-Aminocyclopropane-1- carboxylic acid deaminase producing beneficial rhizobacteria ameliorate the biomass characters of *Panicum maximum* Jacq. by mitigating drought and salt stress. *Sci Rep*., **8**:17513; https://doi.org/10.1038/s41598-018-35565-3.

Vallet-Gely I, Novikov A, Augusto L, Liehl P, Bolbach G, Pechy-Tarr M, Cosson P, Keel C, Caroff M and Lemaitre B. 2010. Association of hemolytic activity of Pseudomonas entomophila, a versatile soil bacterium, with cyclic lipopeptide production. *Appl Environ Microbiol*., **76**: 910–921.

Vizcaino JA, Sanz L, Cardoza RE, Monte E and Gutierrez S. 2005. Detective of putative peptide synthetase genes in Trichoderma species: application of this method to the cloning of a gene from T. haarzianum CECT 2413. *FEMS Microbiol Lett*., **24:** 139-148.

Vyomesh SP and Pitambara Shukla YM. 2018. Proteomics study during root knot nematode (Meloidogyne incognita) infection in tomato (Solanum lycopersicum L.). *J Pharmacognosy Phytochem*., **7(3)**: 1740-1747.

Walsh CT, O'Brien RV and Khosla C. 2013. Non-proteinogenic amino acid building blocks for nonribosomal peptide and hybrid polyketide scaffolds. *Angew Chem Int*., **Ed 52**: 7098–7124.

Zhou D, Huang XF, Chaparro JM, Badri DV, Manter DK, Vivanco JM and Guo J. 2016. Root and bacterial secretions regulate the interaction between plants and PGPR leading to distinct plant growth promotion effects. *Plant Soil*., **401**: 259–272.

JJBS

Volume 17, Number 4,December 2024
ISSN 1995-6673
Pages 681 – 691
https://doi.org/10.54319/jjbs/170411

Jordan Journal of Biological Sciences

Investigation of Antioxidant and anti-melanogenic Activities from Secondary Metabolites of Endophytic Fungi Isolated from *Centella asiatica* and *Syzygium polyanthum*

Silva Abraham[1,*], Helen Octa Lentaya[2] Muhson Isroni[2], Rizka Gitami Sativa[3], Dicky Adihayyu Monconegoro[2], Teguh Baruji[4], Winda Tasia[5], Agus Supriyono[6], Sjaikhurrizal El Muttaqien[7,#], Asep Riswoko[8]

[1]Directorate of Laboratory Management, Research Facilities, and Science and Technology Park, National Research and Innovation Agency (BRIN), PUSPIPTEK, Tangerang Selatan,15314, Indonesia; [2]Research Center for Applied Microbiology, National Research and Innovation Agency (BRIN), PUSPIPTEK, Tangerang Selatan, 15314, Indonesia;[3]Research Center for Agroindustry, National Research and Innovation Agency (BRIN), PUSPIPTEK, Tangerang Selatan, 15314, Indonesia; [4]Research Center for Process and Manufacturing Industry Technology, National Research and Innovation Agency (BRIN), PUSPIPTEK, Tangerang Selatan, 15314, Indonesia; [5]Research Center for Genetic Engineering, National Research and Innovation Agency (BRIN), Jl. Raya Bogor Km. 46, Cibinong 16911, Indonesia; [6]Research Center for Pharmaceutical Ingredients and Traditional Medicine, National Research and Innovation Agency (BRIN), PUSPIPTEK, Tangerang Selatan, 15314, Indonesia; [7]Research Center for Vaccine and Drugs, National Research and Innovation Agency (BRIN), PUSPIPTEK, Tangerang Selatan, 15314, Indonesia; [8]Research Center for Polymer Technology, National Research and Innovation Agency (BRIN), PUSPIPTEK, Tangerang Selatan, 15314, Indonesia

Received: March 22, 2024; Revised: July 16, 2024; Accepted: July 18, 2024

Abstract

This study explores the potential of natural-based and environmentally friendly ingredients for functional cosmetics by investigating the antioxidant and anti-melanogenic activities of endophytic fungi associated with *Centella asiatica* (CA) and *Syzygium polyanthum* (SP). Three endophytic fungi were isolated from leaves and stems of CA and SP collected from Bogor and Serpong, Indonesia using Rose Bengal agar medium. The fungal isolates were cultivated through submerged fermentation in malt extract broth medium. After separating the mycelial biomass with Whatman filter paper, the supernatant was extracted using ethyl acetate. The ethyl acetate fraction of the mycelial biomass extract from these three fungal isolates was screened for antioxidant and anti-tyrosinase activities. In the preliminary screening using the DPPH method by thin-layer chromatography (TLC) with a mobile phase of ethyl acetate-methanol (9:1, *v/v*) and toluene-ethyl acetate (9:1, *v/v*), strong yellow spots indicating antioxidant activity were observed from each isolate after being sprayed with DPPH reagent. Screening for anti-tyrosinase activity was conducted using a colorimetric assay with button mushroom tyrosinase, kojic acid as a positive control and 3,4-dihydroxyphenylalanine (L-DOPA) as a substrate. One isolate with higher antioxidant and anti-tyrosinase activities was further identified based on sequence data of the internal transcribed spacer (ITS) rDNA (including ITS1, 5.8S rDNA, and ITS2). The identification of the selected isolate showed 99.45% similarities with *Colletotrichum sojae*.

Keywords: Endophytic fungi, *Centella asiatica*, *Syzygium polyanthum*, Secondary metabolite, Antioxidant, Anti-tyrosinase, *Colletotrichum sojae*

1. Introduction

Endophytic fungi living symbiotically within their plant host have been known as sources of various types of biologically active compounds secreted as an adaptive response to environmental stresses (Aly et al., 2013). These compounds exhibit diverse biological activities such as antioxidant, cytotoxic, antimicrobial, anti-inflammatory, anticancer, herbicidal, and anti-leishmanial properties (Anand et al., 2023). One particular interest in recent times is the evaluation of endophytic fungi for their antioxidant and anti-melanogenic activities in the cosmetic industry. This interest stems from the growing demand for natural and eco-friendly ingredients in functional cosmetics, including anti-aging, skin-lightening, and sunscreen products (Burger et al., 2016). Concerns regarding the safety of synthetic raw materials commonly used in cosmeceuticals, such as hydroquinone and retinoids, have also contributed to this shift toward natural alternatives (Barbaud, Lafforgue, 2021).

Despite the potential benefits, research on cosmetic ingredients derived from endophytic fungi remains limited. A previous study examined the skin-whitening characteristics of comoclathrin, a chemical generated by endophytic Comoclathris strains, and proved its efficacy using a tyrosinase inhibitory assay (Georgousaki et al., 2022). While metabolites' antioxidant properties are often considered as the primary mechanism for anti-aging effects, another approach for screening new skin-

* Corresponding author. e-mail: silv003@brin.go.id (SA) & sjai001@brin.go.id (SEM).

lightening agents is to inhibit the tyrosinase enzyme. Tyrosinase is crucial in the initial steps of melanin biosynthesis, and its dysregulated expression or hyperactivity can lead to pigmentation disorders (Pillaiyar et al., 2017; Slominski et al., 2004).

Antioxidants play a vital role in cellular homeostasis by neutralizing reactive oxygen species (ROS), which contribute to oxidative stress and various health disorders (Al-Ghamdi et al., 2020). Melanogenesis, the process of skin pigmentation, is influenced by oxidative stress, and excessive melanin production can result in hyperpigmentation disorders such as melasma and age spots (Lee et al., 2021; Liu et al., 2018). Two ethnomedicinal plants, *Centella asiatica* (L.) Urban. (CA) and *Syzygium polyanthum* (SP), have long been used in South and Southeast Asia to treat various ailments. CA is known for its anti-inflammatory and wound-healing properties, while SP is used traditionally to treat diabetes, hypertension, gastritis, ulcers, and skin diseases (Abdulrahman, 2022). The high antioxidant activity of bioactive compounds from CA and SP may contribute to their therapeutic effects (Gohil et al., 2010; Hartanti et al., 2019).

Previous studies have shown that the interaction between endophytic fungi and their host plants significantly influences the production of bioactive compounds and their biological activities (Jia et al., 2016). For example, endophytic fungi associated with *Nerium oleander L*. (Apocynaceae) increased the production of phenolic compounds in the host plant with potent antioxidant activity (Huang et al., 2007). Therefore, investigating endophytic fungi within medicinal plants presents a novel approach to discovering bioactive substances with enhanced characteristics and potential therapeutic applications. This study aims to evaluate the potential of endophytic fungi from CA and SP as new skin-lightening agents through screening for antioxidant and anti-tyrosinase activities. Four isolates from CA leaves and SP stems with optimal biological activities were further identified using sequence data from internal transcribed spacer (ITS) rDNA (including ITS1, 5.8S rDNA, and ITS2) and 18S.

2. Materials and methods

2.1. Materials

The study utilized the following materials: 1,1-diphenyl-2-picryl hydrazyl (DPPH), methanol, HPLC-grade methanol, Triton X-100, and ammonium sulphate, purchased from Merck (Darmstadt, Germany), ascorbic acid (vitamin C) from Kalbe Farma (Jakarta, Indonesia), fresh button mushrooms (*Agaricus bisporus*) from local market, L-DOPA from Sigma-Aldrich (Steinheim, Germany), thin-layer chromatography plates Silica gel 60 F_{254}, from Merck (Darmstadt, Germany), kojic acid from Sigma-Aldrich (Steinheim, Germany), C_{18} column chromatography XBridge 5 µm (4.6x150 mm) from Waters (Milford, Massachusetts, Amerika) equipped with a PDA detector and HPLC apparatus.

2.2. Isolation of endophytic fungi

Samples of CA and SP were collected from Serpong and Bogor, West Java, Indonesia, on March 21st, 2022. Healthy mature living leaves and twigs from randomly selected mature plants were obtained and transported to the laboratory in sterile plastic bags. Processing of the samples commenced within a few hours after the collection. The surface of the leaves and twigs was sterilized by washing with 70% ethanol followed by sterile distilled water. Subsequently, all plant samples were air-dried in a laminar airflow cabinet on sterile tissue paper for an hour (Abraham et al., 2015). The effectiveness of the sterilization procedure was evaluated following the method developed by Schulz et al (Schulz et al., 1993).

The sterilized plant tissue samples with a size approximation of 1 cm^2, were pressed onto the surface of the Rose Bengal agar medium (Himedia, Mumbai, Maharashtra, India) supplemented with chloramphenicol antibiotic. The absence of mycelia growth on the surface of the medium confirmed that the sterilization procedure was effective in removing the surface fungi from the plant tissue (Abraham et al., 2015). The combination of direct plating using Rose Bengal agar medium supplemented with chloramphenicol and a moist chamber method was applied to isolate endophytic fungi from plant samples (Ananda, Sridhar, 2002). For the direct plating method, the fragment of plant samples, approximately 0.5 cm x 0.5 cm, were placed on the surface of agar media and incubated in the incubator at 28°C. The plant samples were placed on the moist sterile towel tissue in the sterile plastic container. The growth observation of fungal mycelia in the plant sample's internal tissue was conducted daily (Polishook et al., 1996). The growth mycelial were then isolated aseptically in potato dextrose agar medium (Himedia, Mumbai, Maharashtra, India), purified and preserved in a 2 mL CryoTube containing 1 mL of 10% glycerol solution (*v/v*) and 5% lactose monohydrate (Merck, Darmstadt, Germany) (*w/v*) at −80°C (Abraham et al., 2015).

2.3. Fermentation and extraction of fungal secondary metabolites

The submerged fermentation process was conducted in a 1 L flask containing 500 mL of malt extract medium (30 g of malt extract, 5 g of peptone in 1 L of distillate water) for 14 days in a shaker incubator at 110 rpm and 28°C (Abraham et al., 2015). The mycelial biomass from each fermentation flask was separated by filtration using Whatman filter paper (no. 1), and the obtained supernatant was collected. Each filtrate was extracted by ethyl acetate (1/1, *v/v*) in the separation funnel. The water fraction on the upper layer was collected and then re-extracted three times with ethyl acetate. The ethyl acetate fraction on the bottom layer was eventually collected and concentrated using a rotary evaporator.

2.4. Screening for anti-oxidant activity

The evaluation of anti-oxidant activity was performed by using a radical scavenging assay of 2-diphenyl-1-picrylhydrazyl (DPPH). The DPPH solution (0.1 mM) was first dissolved in methanol. A series concentration of vitamin C solution (1.25; 2.50; 5; 25; 50; and 100 ppm) was then prepared in methanol as a standard solution. Each extract sample was prepared by dissolving it in methanol at the concentration of 10 mg/mL. 20 µL of the sample volume was mixed with 100 µL DPPH solution in each well of the 96-well plate and was further incubated for 15 minutes in the dark. Following the incubation, the

absorbance of the mixture was measured at 520 nm in triplicate against a blank methanol without DPPH radical (as control). The antioxidant activity was determined as an inhibition percentage of DPPH radical discoloration, and calculated using the following Eq. (1) (Guil-Guerrero et al., 2006):

$$\%\ Inhibition = \frac{A_{control} - A_{sample}}{A_{control}}\ x\ 100$$

(1) (Nurzaman et al., 2022)

where, $A_{control}$ is the absorbance of control and A_{sample} is the absorbance of the extract. To indicate the antioxidant capacity, the IC_{50} value of each extract was measured using linear regression analysis of the standard solution.

2.5. Screening for anti-tyrosinase activity

The evaluation of anti-melanogenic activity was conducted using the tyrosinase colorimetric method (Hsu et al., 2018). The tyrosinase enzyme used in this bioassay was previously extracted from fresh button mushrooms (*Agaricus bisporus*), which was purchased from a local supermarket. To extract the enzyme, 200 grams of mushroom slices were mixed with 300 mL of chilled phosphate buffer (pH 5.8) and homogenized for 10 minutes at 19,500 rpm using an Ultra Turrax homogenizer (IKA, T50 digital, Selangor, Malaysia) in an ice bath. Subsequently, the mushroom slurry was centrifuged (Hitachi, Himac CR 22N, Ibaraki, Japan) for 20 minutes at 4°C and 9,000 rpm. For enzyme precipitation, firstly the supernatant was collected, and then 80 grams of ammonium sulphate (was added. The mixture was further stirred in an ice bath using a magnetic stirrer (Thermo Fisher Scientific, Singapore) for 15 minutes to dissolve the components, which was then followed by centrifugation for 20 minutes at 4°C and 9,000 rpm to separate the tyrosinase enzyme.

The anti-melanogenic screening was done using the tyrosinase-based thin layer chromatography (TLC) assay similar to the method previously explained with some minor changes (Almeda et al., 2015). In this protocol, 3,4-dihydroxyphenylalanine (L-DOPA) was used as a reaction substrate by dissolving 2 mM L-DOPA in phosphate buffer (50 mM, pH 6.5) and followed by the addition of 1% Triton X-100. Tyrosinase (3 mg) was dissolved in 10 mL phosphate buffer. Kojic acid was used as a positive control in this assay by preparing 10 mg/mL kojic acid solution in phosphate buffer. The tested extract (10 mg/mL) was dissolved in the mixture of DMSO and phosphate buffer (1:9, *v/v*). Each extract solution was then spotted in the TLC plate and eluted with ethyl acetate and methanol (9:1, *v/v*) for separating its corresponding components. L-DOPA solution was sprayed onto the TLC surface followed by incubation of the plat at 25°C for 10 minutes. In addition, tyrosinase solution was also sprayed on the same TLC surface and further incubated at 30°C for 30 minutes. Eventually, the presence of brownish-purple spots on the plate indicates the tyrosinase inhibition activity of the extract. The inhibitory activity of the sample was expressed as the percentage of tyrosinase inhibition using the following Eq. (2) (Casañola-Martín et al., 2007):

$$\%\ Tyrosinase\ inhibition = \frac{A_{control} - A_{sample}}{A_{control}}\ x\ 100$$

(2) (Govindappa et al., 2016)

where, $A_{control}$ is the absorbance of control and A_{sample} is the absorbance of the extract.

A sample with high tyrosinase inhibition activity was further analyzed to determine its IC_{50} value using colorimetry technique. The extract solution was prepared in phosphate buffer at concentrations ranging from 7 to 1000 ng/mL. The positive control solution of kojic acid was also prepared with the concentration range of 0.39 – 50 ng/mL (Hamed, El-Sharkawy, 2020). The assay was started by mixing 70 µL sample solution with 70 µL tyrosinase solution in each well of the 96-well plate. L-DOPA solution (110 µL) was subsequently added into the mixture and followed by incubation of the well plate at 37°C for 30 minutes. The absorbance intensity of the color change after the incubation due to the formation of the DOPA chrome was measured at 450 nm using a microplate reader.

2.6. Detection of kojic acid by HPLC analysis

Sample with high anti-oxidant and anti-tyrosinase activity was further assessed to measure the kojic acid content (as a positive control) by HPLC analysis. The HPLC protocol used in this study followed a previously validated method by Rovira and coworkers (Galimany-Rovira et al., 2016). Briefly, kojic acid and ascorbic acid were separately dissolved in a mixture of methanol:water (15:85, v/v). These two standard solutions and used eluent (methanol:water, 15:85, v/v) were filtered using PTFE filter with a pore size of 0.45 µm. Both sample and standard solution (10 µL) were injected into the HPLC (C18 column) under isocratic condition at a flow rate of 1.0 ml/minute. Detection was performed using a PDA detector at 260 nm. Kojic acid was quantified using calibration curve obtained from kojic acid measurement.

2.7. Fungal identification

The rDNA of the selected fungal isolate was extracted and purified using Genomic DNA extraction with Quick-DNA Magbead Plus Kit (Zymo Research, California, USA). The fungi rDNA was amplified with primers ITS1 (5'-TCCGTAGGTGAACCTGCGG-3') and ITS4 (5'-TCCTCCGCTTATTGATATGC-3'). Each 50 µL reaction mixture consisted of 25 MyTaq™ HS Red Mix (Meredian Bioscience, Ohio, USA), 1 µL for each primer, 1 µL DNA template, and 22 µL nuclease-free water. Amplification was performed in T100 Thermal Cycler (Bio-Rad Laboratories Inc, Foster City, USA). PCR thermal cycle using ITS primers was conducted with the following parameters: initial denaturation at 94°C for 1 minute, denaturation at 95°C for 15 seconds, annealing at 52°C for 15 seconds, extension at 72°C for 45 seconds, and final extension at 75°C for 5 minutes. The total number of cycles was 35 (Wirya et al., 2020). The expected size of the PCR products was verified on a 1% TBE agarose gel using an electrophoresis apparatus (Mupid-exU, Tokyo, Japan). The DNA of the sample that exhibited higher anti-oxidant and anti-tyrosinase activity was analyzed using 3130 AB1 Applied Biosystem sequencer.

Purified PCR products were sequenced using an automated DNA sequencer (Applied Biosystems 3130 Genetic Analyzers, California, USA). The sequence data

of ITS rDNA of the fungal strains were deposited in GenBank at NCBI. The fungal isolates were identified based on sequence homology with fungal sequences obtained from the GenBank DNA database hosted by NCBI (http://blast.ncbi.nlm.nih.gov) using the BLAST search tool. The isolates were identified based on the sequence similarity cut-off point for fungal species delimitation of at least ≥ 97%, according to Brock et al. and with an E value cut-off of 0.01 (Brock et al., 2009). The sequences of ITS rDNA of fungal isolates were aligned with other sequences retrieved from GenBank using ClustalX (Thompson et al., 1997). The fungal ITS sequences were analyzed for phylogenetic evolutionary relationships using the Molecular Evolutionary Genetic Analysis program (MEGA X). A phylogenetic tree was constructed using the neighbor-joining method with bootstrap values based on 1,000 replications (Felsenstein, 1985; Saitou, Nei, 1987). The evolutionary distances were computed using the Kimura 2-parameter method (Kimura, 1980).

3. Results

3.1. Isolation of endophytic fungi

As shown in Table 1, 12 endophytic fungi isolates were obtained from CA and SP plant samples cultivated in 2 different cities in Indonesia (Serpong and Bogor). In this study, 7 endophytic fungi were successfully isolated from plant stems, and 5 isolates were obtained from plant leaves. Ten fungal isolates were obtained from direct planting method, and the other two isolates were obtained from moist chamber method. For easier discussion, specific sample denotations will be used here onwards for every isolated endophytic fungus based on their place of origin, plant source as well as its corresponding isolation method, such as Spg for Serpong, Bgr for Bogor, L for leaves, S for stem, Dp for direct planting and Mc for moist chamber.

Table 1. Fungal isolates obtained from the plant samples and the corresponding information.

No.	Plant samples	Sampling location	Source of isolate and isolation method	Sample code	Biomass yield from fermentation (gram)
1.	CA	Serpong	5 isolates from leave by direct planting; 1 isolate from stem by direct planting	CA-Spg-LDp 1.2.2	5.18
				CA-Spg-LDp 2	4.34
				CA-Spg-LDp 3.1	3.61
				CA-Spg-LDp 3.2	2.19
				CA-Spg-LDp 3.3	3.77
				CA-Spg-SDp 2.1	1.86
		Bogor	4 isolates from leave by direct planting; 2 isolates from stem by direct planting	CA-Bgr-LDp 1.1	5.46
				CA-Bgr-LDp 2.1	5.88
				CA-Bgr-LDp 2.2.2	4.83
				CA-Bgr-LDp 3.1	3.68
				CA-Bgr-SDp 3.1	2.70
				CA-Bgr-SDp 3.1	0.40
2.	SP	Serpong	1 isolate from leave by direct planting; 5 isolates from stem (3 isolates by direct planting, 2 isolates by moist chamber)	SP-Spg-LDp 3.1	2.50
				SP-Spg-SDp 1.2	3.91
				SP-Spg-SDp 3.1	1.28
				SP-Spg-SDp 3.3	4.57
				SP-Spg-SMc 1.4	4.61
				SP-Spg-SMc 2.2	2.32
		Bogor	2 isolates from leave by direct planting; 4 isolates from stem (3 isolates by direct planting, 1 isolate by moist chamber)	SP-Bgr-LDp 1.1	3.59
				SP-Bgr-LDp 2.1	4.81
				SP-Bgr-SDp 1.3	1.38
				SP-Bgr-SDp 3.1	0.31
				SP-Bgr-SDp 3.2	3.18
				SP-Bgr-SMc 1.1	5.06

The morphological characteristics of each isolate, including colony color, elevation, and texture, were observed. The representative images of the isolated fungi are shown in Figure 1. Six distinct endophytic fungi from CA were identified, and Figure 1a illustrates the range of their morphological features. These features included colony color (black, grey, and brownish with white border), colony elevation (umbonate and rugose), and colony texture (powdery and velvety). On the other hand, the endophytic fungi from SP showed different morphological characteristics compared to those from CA, including colony color (brownish white, white, blackish white, and yellowish brown), colony elevation (umbonate and rugose), and colony texture (velvety and cottony) (Figure 1b).

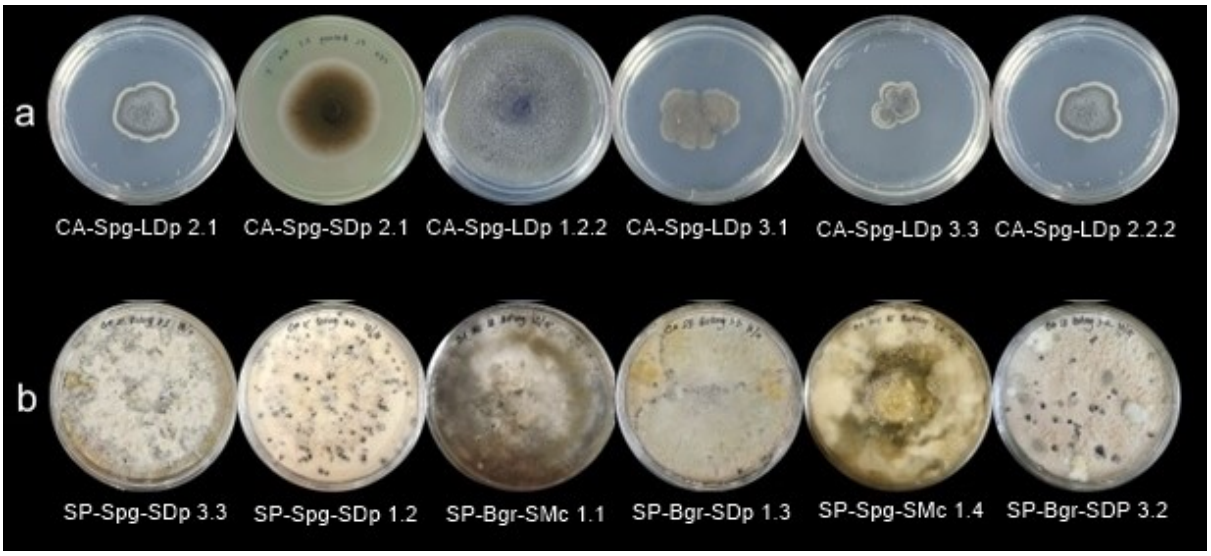

Figure 1. Colonies of endophytic fungi isolate from CA (a) on Potato Dextrose Agar Medium and SP (b) on Oatmeal Agar Medium.

3.2. Fermentation and extraction of fungal secondary metabolites

A fermentation shaker was used to ferment liquids at 110 rpm for 14 hours (28°C). Table 1 shows that fungal fermentation yield biomass range from 2.84 gr (CA-Spg-SDp 2.1) to 5.67 gr (CA-Spg-LDp 2.1).

3.3. Screening for anti-oxidant activity

The results of the screening for anti-oxidant activity are presented in Table 2. The anti-oxidant values vary widely, ranging from 29.32% (A: CA-Bgr-LDp 2.1) to 83.96% (C: CA-Spg-LDp 1.2.2). Notably, the extract with the highest inhibition value exhibits anti-oxidant activity which is comparable to that of vitamin C as a positive control (85.17%). Additionally, 70.83% of the total isolates display more than 50% DPPH radical inhibition, indicating the potential of the fungal endophytes isolated from CA and SP as anti-oxidant resources. Table 2 also reveals that most fungi obtained from CA exhibit higher anti-oxidant activity compared to those isolated from SP. To determine the concentration of extract required for 50% free radical scavenging activity, three isolates with the highest DPPH radical inhibition, isolated from the stem and leaf of CA, were tested for IC_{50} measurement. As shown in Table 3, isolate C (CA-Spg-LDp 1.2.2) exhibits an IC_{50} value of 590.19 ppm for anti-oxidant activity, whereas vitamin C has an IC_{50} value of 23.84 ppm.

Table 2. Anti-oxidant activity of the extracts.

No.	Sample code	Inhibition %
1	A (CA-Bgr-LDp 2.1)	29.32 ± 1.40
2	B (CA-Bgr-SDp 2.1)	54.55 ± 1.91
3	C (CA-Spg-LDp 1.2.2)	83.96 ± 1.08
4	D (SP-Spg-SDp 3.3)	43.94 ± 1.44
5	E (SP-Spg-SDp 1.2)	56.48 ± 0.79
6	F (SP-Bgr-SMc 1.1)	39.52 ± 4.22
7	G (SP-Bgr-SDp 1.3)	53.22 ± 5.46
8	H (CA-Spg-LDp 3.1)	73.35 ± 7.79
9	I (CA-Spg-LDp 3.3)	78.03 ± 2.60
10	J (SP-Spg-SMc 1.4)	61.82 ± 6.96
11	K (CA-Bgr-LDp 2.2.2)	79.62 ± 1.27
12	L (SP-Bgr-SDp 3.2)	60.07 ± 0.87
13	M (CA-Spg-LDp 3.2)	79.10 ± 0.76
14	N (SP-Spg-SDp 3.1)	73.58 ± 0.61
15	O (CA-Spg-SDp 2.1)	45.68 ± 8.42
16	P (SP-Bgr-SDp 3.1)	68.05 ± 1.54
17	Q (CA-Bgr-LDp 1.1)	43.01 ± 3.35
18	R (CA-Spg-LDp 2)	44.30 ± 7.09
19	S (SP-Spg-LDp 3.1)	77.81 ± 1.02
20	T (SP-Bgr-LDp 1.1)	48.10 ± 6.86
21	U (CA-Bgr-LDp 3.1)	67.36 ± 4.02
22	V (SP-Spg-SMc 2.2)	59.84 ± 4.39
23	W (CA-Bgr-SDp 3.1)	79.53 ± 0.56
24	X (SP-Bgr-LDp 2.1)	68.65± 6.28
25	Vitamin C	85.17 ± 3.80

Results are expressed as the mean ± RSD (n = 3). Vitamin C was used as positive control. The IC_{50} of the selected samples (no. 3, 11, and 23) were further analyzed.

Table 3. The IC_{50} value of the antioxidant capacity from the three selected extracts.

No.	Sample code	IC_{50} value (ppm)
1	C (CA-Spg-LDp 1.2.2)	590.19 ± 1.91
2	K (CA-Spg-LDp 2.2.2)	2943.00 ± 5.20
3	W (CA-Spg-SDp 3.1)	2143.18 ± 8.16
4	Vitamin C	23.84 ± 47.34

Results are expressed as the mean ± RSD (n = 3). Vitamin C was used as positive control.

3.4. Screening for anti-tyrosinase activity

The screening result of anti-tyrosinase activity by TLC method is shown in Figure 2. The positive result was indicated by the presence of a white zone on the black background of the TLC plate. It can be seen from the TLC result that there are two samples of C (CA-Spg-LDp 1.2.2) and R (CA-Spg-LDp 2) that actively inhibit tyrosinase activity. The active compound in sample C appears at a retention time of 5.5, while sample R appears at a retention time of 6.5. Kojic acid as a positive control in this test also appears at a retention time of 5.5. Therefore, the active compound in sample C could likely be kojic acid. Both samples C and R were then further analyzed to determine their IC_{50} values, which were 341.02 and 570.40 ppm, respectively (Table 4). This result suggests that both samples may be exploited as whitening agents.

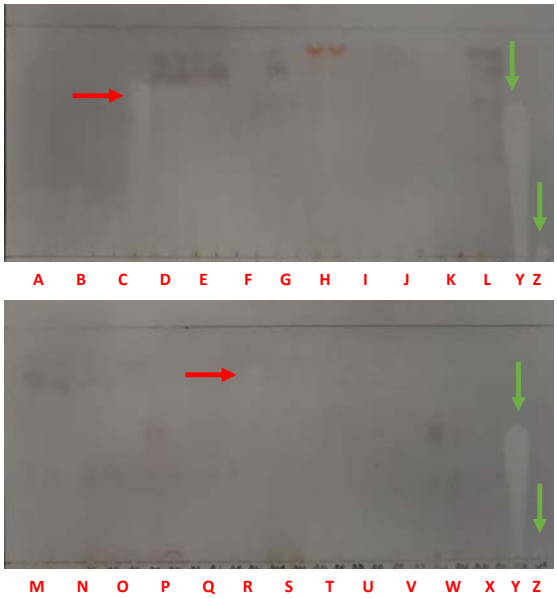

Figure 2. Tyrosinase-based TLC bioautography of the extracts. A (CA-Spg-LDp 2.1); B (CA-Spg-SDp 2.1); C (CA-Spg-LDp 1.2.2); D (SP-SPg-SDp 3.3); E (SP-Spg-SDp 1.2); F (SP-Bgr-SMc 1.1); G (SP-Bgr-SDp 1.3); H (CA-Spg-LDp 3.1); I (CA-Spg-LDp 3.3); J (SP-Spg-SMc 1.4); K (CA-Spg-LDp 2.2.2); L (SP-Bgr-SDp 3.2); M (CA-Bgr-LDp 3.2); N (SP-Spg-SDp 3.1); O (CA-Spd-SDp 2.1); P (SP-Bgr-SDp 3.1); Q (CA-Spg-LDp 1.1); R (CA-Spg-LDp 2); S (SP-Spg-LDp 3.1); T (SP-Bgr-LDp 1.1); U (CA-Spg-LDp 3.1); V (SP-Spg-SMc 2.2); W (CA-Spg-SDp 3.1); X (SP-Bgr-LDp 2.1); Y (Kojic acid); Z (Vitamin C). The red arrow indicated the expected samples with tyrosinase inhibition activity and the green arrow indicated positive control.

Table 4. The IC_{50} value of the tyrosinase inhibition activity from the selected extracts.

No.	Sample code	IC_{50} value (ppm)
1	C (CA-Spg-LDp 1.2.2)	341.02
2	R (CA-Spg-LDp 2)	570.40
3	Kojic acid	5.36

Results are expressed as the mean (n = 3). Kojic acid was used as positive control.

3.5. Detection of kojic acid by HPLC analysis

Detection of kojic acid by HPLC analysis involves extracting kojic acid from the sample exhibiting high antioxidant and anti-tyrosinase activity using an appropriate solvent. Before injecting the sample, a series of standard solutions of kojic acid and ascorbic acid at known concentrations in the mobile phase is prepared. The HPLC analysis generates retention time data for each analyte; for example, ascorbic acid and kojic acid were detected at 1.53 and 2.19 minutes, respectively. The obtained R^2 values for the standard curves are 0.9779 for ascorbic acid and 0.9945 for kojic acid (data are not shown), indicating a good linear regression. Importantly, the chromatogram of sample C (CA-Spg-LDp 1.2.2) in Figure 3 shows a significant peak at approximately 2.2 minutes, which closely resembles the kojic acid peak in the

standard solution. This data verifies the presence of kojic acid in the sample with a concentration of 9.61 ppm.

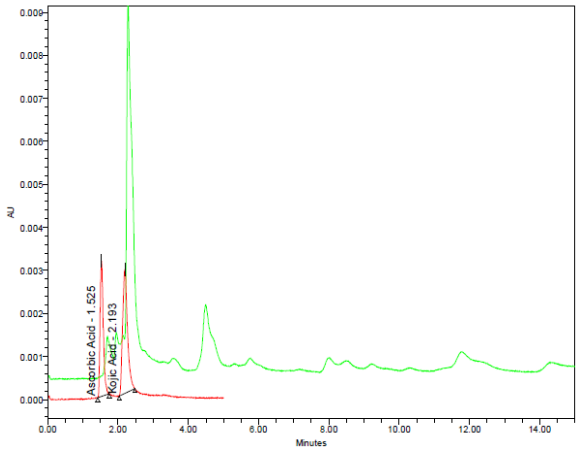

Figure 3. HPLC chromatogram of the sample C (CA-Spg-LDp 1.2.2) (green line) and positive controls (red line) of ascorbic (retention time of 1.53 minutes) acid and kojic acid (retention time of 2.19 minutes).

3.6. Fungal identification

The DNA isolated from selected fungal isolates was amplified using Internal Transcribed Spacer (ITS) primers. Figure 4 depicts the PCR results of the ITS region, indicating successful amplification of DNA samples by the appearance of DNA bands with expected gene sizes of approximately 550 bp.

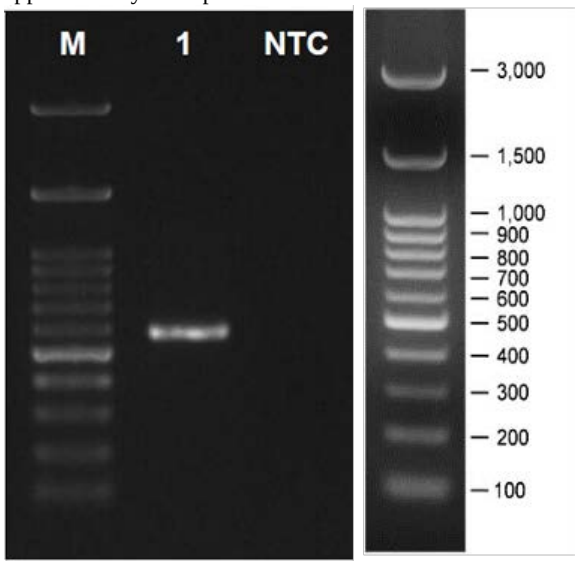

Figure 4. Electropherograms of the amplified ITS sequence of CA-Spg-LDp 1.2.2. Isolates assessed by electrophoresis with 1 % TBE agarose

Table 5. The BLAST search result of CA-Spg-LDp 1.2.2 isolates from NCBI Database.

No.	Species	Query cover	Percent identification (%)	Length (bp)	Accession number
1	*C. sojae* Strain ATCC 62257	98%	99.45	548	KC110794.1
2	*C. plurivorum* CBS 125474	96%	99.81	539	NR_160828.1
3	*C. syngoniicola* strain LC8894	100%	98.75	567	MZ595863.1
4	*C. cliviicola* CBS 125375	96%	99.63	539	NR_137097.1
5	*C. cattleyicola* CBS 170.49	96%	99.44	539	NR_160832.1
6	*C. sojae* ATCC 62257	96%	99.44	539	NR_158358.1
7	*C. musicola* CBS 132885	96%	98.89	539	NR_160830.1
8	*C. brevisporum* BCC 38876	100%	97.85	578	NR_111637.1
9	*C. brevisporum* strain LC0600	99%	97.85	592	KC790943.1
10	*C. orchidearum* CBS 135131	96%	98.70	538	NR_160831.1

The amplified sequence of CA-Spg-LDp 1.2.2 isolates was submitted to Genebank at NCBI under the accession number of PP345512.1, and BLAST analysis was performed to compare the sequence to numerous references in the NCBI database. The result showed higher homology with Colletotrichum sojae strain ATCC 62257 with a percent identification of 99.45% and gene length of 548 bp (Table 5). This finding is consistent with the electropherogram of the CR product, which indicates that the sequence is approximately 550 bp in length.

Following the analysis of the BLAST results, a phylogenetic tree was constructed to compare the isolate sequences with the reference sequences retrieved from the NCBI database. The phylogenetic analysis involved comparing one isolate from this study with ten Colletotrichum reference isolates from the Gene Bank and two fungal strains used as an outgroup. The phylogenetic tree (Figure 5) indicated that CA-Spg-LDp 1.2.2 belongs to the Colletotrichum genus and is closely related to Colletotrichum sojae strain ATCC 62257, with a bootstrap value of 73%. A bootstrap proportion of >70% often indicates a likelihood of >95%, highlighting that the clade is real.

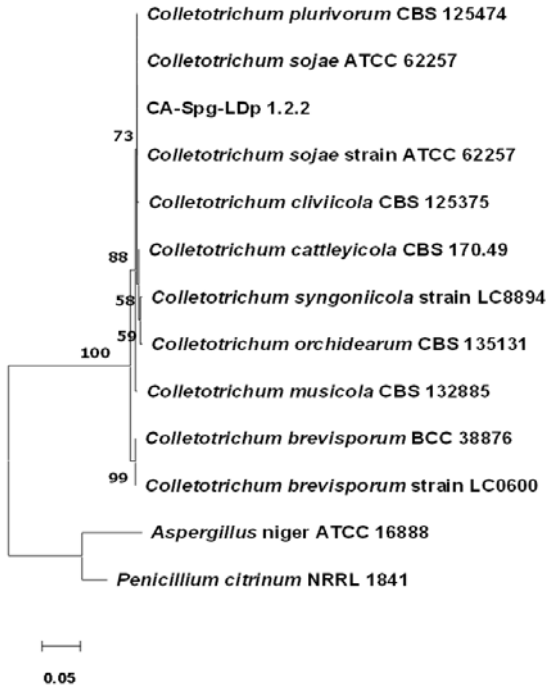

Figure 5. Phylogenetic tree of CA-Spg-LDp 1.2.2 isolates based on ITS.

4. Discussion

In this study, the number of fungi isolates obtained from the direct planting method was higher than those of direct moist chamber method. This result indicated that direct planting is more suitable for obtaining endophytic fungi from plant samples. This data is indeed consistent with the previous research groups that used direct planting techniques to isolate 85 and 18 endophytic fungi from CA and SP plants, respectively (Radiastuti et al., 2019; Widjajanti et al., 2023). The obtained endophytic fungi from CA are similar to those of other studies, displaying a variety of morphological characteristics, including colony color (ranging from black, white, brownish white, yellow, and yellowish white) and colony texture (either cottony or velvety) (Radiastuti et al., 2019). Similar morphological traits of fungi from the SP's stem are also shown by the endophytic fungi from SP, demonstrating similarity in surface colony color (yellowish brown, white yellow, white, and pale brown), colony elevation (umbonate and rugose), and colony texture (powdery and cottony) (Widjajanti et al., 2023). The distribution of the obtained fungi was influenced by the exact location of plant tissues. Most fungi were found in leaves of CA, likely due to the proximity of the leaves to the ground and soil, which supports the penetration and colonization of endophytes. Conversely, in SP, most fungi were obtained from stems. This distribution may be attributed to the varying abilities of each endophyte species to utilize substrates or tissues to acquire resources from different parts of the plant.

Based on the previous report, the fermentation method adopted in this study was used for effectively extracting secondary metabolites with antioxidants and anti-melanogenic activity (Kim et al., 2021). According to Boukaew and coworkers, the preferred medium for biomass production is malt extract medium, particularly malt extract broth (MEB) which contains carbon and nitrogen sources, minimal salts, trace elements, and vitamins, with a suitable pH (Boukaew, Prasertsan, 2014). The obtained fungal biomass correlates with the mycelial morphology, the fermentation substrate, and the species of the fungal itself, while the type of fermentation might affect fungal morphology. For instance, in submerged fermentation, filamentous fungi may exhibit freely dispersed hyphae or form spherical agglomerates of hyphae known as pellets (Quintanilla et al., 2015).

The mechanism of DPPH antioxidant screening is linked to the ability of anti-oxidants to transfer hydrogen. The odd electrons from the nitrogen atom on DPPH are reduced by accepting hydrogen atoms from anti-oxidant agents, forming 2,2-diphenyl-1-picrylhydrazine (Kedare, Singh, 2011; Liu et al., 2015). The disappearance of the deep purple color indicates the presence of anti-oxidants, as they dampen DPPH free radicals (Nath et al., 2014). Furthermore, the anti-oxidant activity is affected by methods, polarity of the solvent, extraction procedure, and purity of extracted compounds (Waisundara, Watawana, 2014). The IC_{50} value of CA-Spg-LDp 1.2.2 is quite similar to the IC_{50} value of those obtained from the extract of CA plant as a host (Waisundara, Watawana, 2014). It indicates that this isolated endophytic fungal strain could be a potential agent in scavenging free radicals (Wang et al., 2023). The anti-oxidant activity of CA endophytic fungi is attributed to their secondary metabolites, such as flavonoids, tannins, coumarins, alkaloids, and steroids (Bhavana et al., 2020). These secondary metabolites donate electrons due to the presence of a chemical structure (β-ring conjugated) with several hydroxyl groups, facilitating the hydrogenation mechanism and reacting with oxidative free radicals. Consequently, these secondary metabolites are exploited by the host plant of CA to prevent oxidative stress and to protect biochemical functions from natural oxidants (Choudhary et al., 2011).

The anti-tyrosinase activity screening finding is consistent with other study that optimized the extraction of kojic acid from fermentation of different species of fungi isolated from California, including *Penicillium* and *Aspergillus* (Couteau, Coiffard, 2016). Previous studies have shown that CA contains some significant components, including asiatic acid, asiaticoside, madecassic acid, and madecassoside which belong to the pentacyclic triterpenoids known as centelloids (Bylka et al., 2014; Kwon et al., 2014; Kwon et al., 2012). These substances have been recognized as effective skin moisturizers, antioxidants, whitening, agent, wound healers, anti-inflammation, anti-psoriatic, and anti-aging. Previous studies revealed that the water and ethanol (95%) extract of CA displayed tyrosinase inhibitory activity with inhibition values of 53.22% and 31.25%, respectively (Seo, Kim, 2019; Sungthong, Phadungkit, 2015). The active compound of asiaticoside in CA may be responsible in lowering the amount of melanin during the melanocyte formation by blocking the expression of tyrosinase mRNA (Kwon et al., 2014).

The fungal identification result is consistent with prior publications that successfully amplified the ITS region using primers ITS1 and ITS4, with an expected size of 542 bp (Wirya et al., 2020). Several researches showed endophytic fungi from *Colletotrichum* group produced bioactive compounds with anti-microbial, anti-oxidant (Gurgel et al., 2023), antidepressant, anti-inflammatory,

antioxidative, and anticancer activities (Chithra et al., 2014). In addition to some of the activities mentioned previously, *Colletotrichum* sp. AP12 has been reported to promote growth andrographolide biosynthesis of medicinal plant *Andrographis paniculata* (Burm. f.) Nees (Xu et al., 2023). Another species of *Colletotrichum gloeosporioides* isolated from *Sonneratia apetala* can produced secondary metabolites such as kojic acid which exhibited anti-microbial properties (Nurunnabi et al., 2018) and also anti-melanogenic activity (Happi et al., 2015).

5. Conclusion

We successfully isolated four endophytic fungi from CA and SP with high anti-oxidant and anti-tyrosinase activity from this result. Furthermore, one isolated with high anti-oxidant and anti-tyrosinase activity was molecularly identified using ITS rDNA, and the result showed that the selected isolate belonged to genus *Colletotrichum* and species *Colletotrichum sojae*.

6. Conflicting interests

The authors declare that they have no known competing financial interests or personal relationships that could have appeared to influence the work reported in this paper.

7. Funding

This research was funded by the grants from Indonesia Endowment Fund for Education Agency/ Lembaga Pengelola Dana Pendidikan (LPDP) through Research and Innovation Funding for Advanced Indonesia/ Riset dan Inovasi untuk Indonesia Maju (RIIM) 2022 (No. pm-0110388). The funding was assigned to Silva Abraham as the coordinator of the research project.

References

Abdulrahman, MD. 2022. Review of Ethnopharmacology, Morpho-Anatomy, Biological Evaluation and Chemical Composition of Syzygium polyanthum (Wight) Walp. *Plant Sci. Today*, **9(1)**: 167-177. https://doi.org/10.14719/pst.1386

Abraham, S, Basukriadi, A, Pawiroharsono, S, Sjamsuridzal, W. 2015. Insecticidal activity of ethyl acetate extracts from culture filtrates of mangrove fungal endophytes. *Mycobiology*, **43(2)**: 137-149. https://doi.org/10.5941/MYCO.2015.43.2.137

Al-Ghamdi, AY, Fadlelmula, AA, Abdalla, MO. 2020. Total phenolic content, antioxidant and antimicrobial activity of Ruta chalepensis L. leaf Extract in Al-Baha area, Saudi Arabia. *Jordan J Biol Sci*, **13(6)**: 675-680.

Almeda, F, Astorga, L, Orellana, A, Sampuel, L, Sierra, P, Gaitán, I, Cáceres, A. 2015. Piper genus: source of natural products with anti-tyrosinase activity favored in phytocosmetics. *Int J Phytocos Nat Ingred.*, **2(1)**: 6-6. https://doi.org/10.15171/ijpni.2015.06

Aly, A, Debbab, A, Proksch, P. 2013. Fungal endophytes–secret producers of bioactive plant metabolites. *Pharmazie*, **68(7)**: 499-505. https://doi.org/10.1691/ph.2013.6517

Anand, K, Kumar, V, Prasher, IB, Sethi, M, Raj, H, Ranjan, H, Chand, S, Pandey, GK. 2023. Bioactive molecules from fungal endophytes and their applications in pharmaceutical industries: challenges and future scope. *J. Basic Microbiol.*, **63(7)**: 690-708. https://doi.org/10.1002/jobm.202200696

Ananda, K, Sridhar, K. 2002. Diversity of endophytic fungi in the roots of mangrove species on the west coast of India. *Can. J. Microbiol.*, **48(10)**: 871-878. https://doi.org/10.1139/w02-080

Barbaud, A, Lafforgue, C. Risks associated with cosmetic ingredients. Presented at the Annales de Dermatologie et de Vénéréologie, 148 (2021) 77-93, https://doi.org/10.1016/j.annder.2020.04.027

Bhavana, NS, Prakash, HS, Nalini, MS. 2020. Fungal Endophytes from Tabernaemontana heyneana Wall.(Apocynaceae), their Molecular Characterization, L-asparaginase and Antioxidant Activities. *Jordan J. Biol. Sci.*, **13(4)**: 805-812. https://doi.org/10.54319/jjbs/140422

Boukaew, S, Prasertsan, P. 2014. Factors affecting antifungal activity of Streptomyces philanthi RM-1-138 against Rhizoctonia solani. *World J. Microbiol. Biotechnol.*, **30**: 323-329. https://doi.org/10.1007/s11274-013-1424-z

Brock, PM, Döring, H, Bidartondo, MI. 2009. How to know unknown fungi: the role of a herbarium. *New Phytol.*, **181(3)**: 719-724. https://doi.org/10.1111/j.1469-8137.2008.02703.x

Burger, P, Landreau, A, Azoulay, S, Michel, T, Fernandez, X. 2016. Skin whitening cosmetics: Feedback and challenges in the development of natural skin lighteners. *Cosmetics*, **3(4)**: 36. https://doi.org/10.3390/cosmetics3040036

Bylka, W, Znajdek-Awiżeń, P, Studzińska-Sroka, E, Dańczak-Pazdrowska, A, Brzezińska, M. 2014. Centella asiatica in dermatology: an overview. *Phytother. Res.*, **28(8)**: 1117-1124. https://doi.org/10.1002/ptr.5110

Casañola-Martín, GM, Marrero-Ponce, Y, Khan, MTH, Ather, A, Khan, KM, Torrens, F, Rotondo, R. 2007. Dragon method for finding novel tyrosinase inhibitors: Biosilico identification and experimental in vitro assays. *European journal of medicinal chemistry*, **42(11-12)**: 1370-1381. https://doi.org/10.1016/j.ejmech.2007.01.026

Chithra, S, Jasim, B, Sachidanandan, P, Jyothis, M, Radhakrishnan, E. 2014. Piperine production by endophytic fungus Colletotrichum gloeosporioides isolated from Piper nigrum. *Phytomedicine*, **21(4)**: 534-540. https://doi.org/10.1016/j.phymed.2013.10.020

Choudhary, N, Bijjem, KRV, Kalia, AN. 2011. Antiepileptic potential of flavonoids fraction from the leaves of Anisomeles malabarica. *J. Ethnopharmacol.*, **135(2)**: 238-242. https://doi.org/10.1016/j.jep.2011.02.019

Couteau, C, Coiffard, L. 2016. Overview of skin whitening agents: Drugs and cosmetic products. *Cosmetics*, **3(3)**: 27. https://doi.org/10.3390/cosmetics3030027

Felsenstein, J. 1985. Confidence limits on phylogenies: an approach using the bootstrap. *Evolution*, **39(4)**: 783-791. https://doi.org/10.1111/j.1558-5646.1985.tb00420.x

Galimany-Rovira, F, Pérez-Lozano, P, Suñé-Negre, JM, García-Montoya, E, Miñarro, M, Ticó, JR. 2016. Development and validation of a new RP-HPLC method for the simultaneous determination of hydroquinone, kojic acid, octinoxate, avobenzone, BHA and BHT in skin-whitening cream. *Anal. Methods*, **8(5)**: 1170-1180. https://doi.org/10.1039/C5AY02207J

Georgousaki, K, González-Menéndez, V, Tormo, JR, Tsafantakis, N, Mackenzie, TA, Martín, J, Gumeni, S, Trougakos, IP, Reyes, F, Fokialakis, N. 2022. Comoclathrin, a novel potent skin-whitening agent produced by endophytic Comoclathris strains associated with Andalusia desert plants. *Sci. Rep.*, **12(1)**: 1649. https://doi.org/10.1038/s41598-022-05448-9

Gohil, KJ, Patel, JA, Gajjar, AK. 2010. Pharmacological review on Centella asiatica: a potential herbal cure-all. *Indian J. Pharm. Sci.*, **72(5)**: 546. https://doi.org/10.4103/0250-474X.78519

Govindappa, M, Farheen, H, Chandrappa, C, Rai, RV, Raghavendra, VB. 2016. Mycosynthesis of silver nanoparticles using extract of endophytic fungi, Penicillium species of Glycosmis mauritiana, and its antioxidant, antimicrobial, anti-inflammatory and tyrokinase inhibitory activity. *Advances in Natural Sciences: Nanoscience and Nanotechnology*, **7(3)**: 035014. https://doi.org/10.1088/2043-6262/7/3/035014

Guil-Guerrero, J, Martínez-Guirado, C, del Mar Rebolloso-Fuentes, M, Carrique-Pérez, A. 2006. Nutrient composition and antioxidant activity of 10 pepper (Capsicum annuun) varieties. *Eur. Food Res. Technol.*, **224**: 1-9. https://doi.org/10.1007/s00217-006-0281-5

Gurgel, RS, de Melo Pereira, DÍ, Garcia, AVF, Fernandes de Souza, AT, Mendes da Silva, T, de Andrade, CP, Lima da Silva, W, Nunez, CV, Fantin, C, de Lima Procópio, RE. 2023. Antimicrobial and antioxidant activities of endophytic fungi associated with Arrabidaea chica (Bignoniaceae). *J. Fungus*, **9(8)**: 864. https://doi.org/10.3390/jof9080864

Hamed, M, El-Sharkawy, RM. 2020. Evaluation of Putative Inducers and Inhibitors toward Tyrosinase from two Trichoderma species. *Jordan J. Biol. Sci.*, **13(1)**: 7-12.

Happi, GM, Kouam, SF, Talontsi, FM, Nkenfou, CN, Longo, F, Zühlke, S, Douanla-Meli, C, Spiteller, M. 2015. A new dimeric naphtho-γ-pyrone from an endophytic fungus Aspergillus niger AKRN associated with the roots of Entandrophragma congoënse collected in Cameroon. *Z. Naturforsch. B*, **70(9)**: 625-630. https://doi.org/10.1515/znb-2015-0036

Hartanti, L, Yonas, SMK, Mustamu, JJ, Wijaya, S, Setiawan, HK, Soegianto, L. 2019. Influence of extraction methods of bay leaves (Syzygium polyanthum) on antioxidant and HMG-CoA Reductase inhibitory activity. *Heliyon*, **5(4)**: e01485. https://doi.org/10.1016/j.heliyon.2019.e01485

Hsu, K-D, Chan, Y-H, Chen, H-J, Lin, S-P, Cheng, K-C. 2018. Tyrosinase-based TLC Autography for anti-melanogenic drug screening. *Sci. Rep.*, **8(1)**: 1-10. https://doi.org/10.1038/s41598-017-18720-0

Huang, W-Y, Cai, Y-Z, Hyde, KD, Corke, H, Sun, M. 2007. Endophytic fungi from Nerium oleander L (Apocynaceae): main constituents and antioxidant activity. *World J. Microbiol. Biotechnol.*, **23**: 1253-1263. https://doi.org/10.1007/s11274-007-9357-z

Jia, M, Chen, L, Xin, H-L, Zheng, C-J, Rahman, K, Han, T, Qin, L-P. 2016. A friendly relationship between endophytic fungi and medicinal plants: a systematic review. *Front. Microbiol*, **7**: 906. https://doi.org/10.3389/fmicb.2016.00906

Kedare, SB, Singh, R. 2011. Genesis and development of DPPH method of antioxidant assay. *J Food Sci Technol*, **48**: 412-422. https://doi.org/10.1007/s13197-011-0251-1

Kim, K, Jeong, H-I, Yang, I, Nam, S-J, Lim, K-M. 2021. Acremonidin E produced by Penicillium sp. SNF123, a fungal endophyte of Panax ginseng, has antimelanogenic activities. *J. Ginseng Res.*, **45(1)**: 98-107. https://doi.org/10.1016/j.jgr.2019.11.007

Kimura, M. 1980. A simple method for estimating evolutionary rates of base substitutions through comparative studies of nucleotide sequences. *J. Mol. Evol.*, **16**: 111-120. https://doi.org/10.1007/BF01731581

Kwon, KJ, Bae, S, Kim, K, An, IS, Ahn, KJ, An, S, Cha, HJ. 2014. Asiaticoside, a component of Centella asiatica, inhibits melanogenesis in B16F10 mouse melanoma. *Mol. Med. Rep.*, **10(1)**: 503-507. https://doi.org/10.3892/mmr.2014.2159

Kwon, MC, Choi, WY, Seo, YC, Kim, JS, Yoon, CS, Lim, HW, Kim, HS, hee Ahn, J, Lee, HY. 2012. Enhancement of the skin-protective activities of Centella asiatica L. Urban by a nano-encapsulation process. *J. Biotechnol.*, **157(1)**: 100-106. https://doi.org/10.1016/j.jbiotec.2011.08.025

Lee, J-I, Seo, JH, Ko, E-S, Cho, S-M, Kang, J-R, Jeong, J-H, Jeong, YJ, Kim, CY, Cha, J-D, Kim, WS. 2021. Inhibition of melanogenesis by Aster yomena callus pellet extract in melanoma cells and patients with skin pigmentation. *Int. J. Med. Sci.*, **18(14)**: 3299. https://doi.org/10.7150%2Fijms.62530

Liu, H, Cao, J, Jiang, W. 2015. Evaluation and comparison of vitamin C, phenolic compounds, antioxidant properties and metal chelating activity of pulp and peel from selected peach cultivars. *LWT - Food Sci. Technol.*, **63(2)**: 1042-1048. https://doi.org/10.1016/j.lwt.2015.04.052

Liu, Z, Ren, Z, Zhang, J, Chuang, C-C, Kandaswamy, E, Zhou, T, Zuo, L. 2018. Role of ROS and nutritional antioxidants in human diseases. *Front. physiol.*, **9**: 477. https://doi.org/10.3389/fphys.2018.00477

Nath, A, Pathak, J, Joshi, S. 2014. Bioactivity assessment of endophytic fungi associated with Centella asiatica and Murraya koengii. *J. appl. biol. biotechnol.*, **2(5)**: 006-011. https://doi.org/10.7324/JABB.2014.2502

Nurunnabi, TR, Al-Majmaie, S, Nakouti, I, Nahar, L, Rahman, SM, Sohrab, MH, Billah, MM, Ismail, FM, Sharples, GP, Sarker, SD. 2018. Antimicrobial activity of kojic acid from endophytic fungus Colletotrichum gloeosporioides isolated from Sonneratia apetala, a mangrove plant of the Sundarbans. *Asian Pac. J. Trop. Med.*, **11(5)**: 350-354. https://doi.org/10.4103/1995-7645.233183

Nurzaman, M, Permadi, N, Setiawati, T, Hasan, R, Irawati, Y, Julaeha, E, Herlina, T. 2022. DPPH Free Radical Scavenging Activity of Citrus aurantifolia Swingle Peel Extracts and their Impact in Inhibiting the Browning of Musa Paradisiaca L. Var. Kepok Tanjung Explants. *Jordan J. Biol. Sci.*, **15(5)**: 771-777. http://dx.doi.org/10.54319/jjbs/150505

Pillaiyar, T, Manickam, M, Namasivayam, V. 2017. Skin whitening agents: Medicinal chemistry perspective of tyrosinase inhibitors. *J. Enzyme Inhib. Med. Chem.*, **32(1)**: 403-425. https://doi.org/10.1080/14756366.2016.1256882

Polishook, J, Bills, G, Lodge, D. 1996. Microfungi from decaying leaves of two rain forest trees in Puerto Rico. *J. Ind. Microbiol. Biotechnol.*, **17(3-4)**: 284-294. https://doi.org/10.1007/BF01574703

Quintanilla, D, Hagemann, T, Hansen, K, Gernaey, KV. 2015. Fungal morphology in industrial enzyme production—modelling and monitoring. *Filaments in bioprocesses*, **149**: 29-54. https://doi.org/10.1007/10_2015_309

Radiastuti, N, Susilowati, DN, Bahalwan, HA. 2019. Phylogenetic study of endophytic fungi associated with Centella asiatica from Bengkulu and Malaysian accessions based on the ITS rDNA sequence. *Biodiversitas*, **20(5)**: 1248-1258. https://doi.org/10.13057/biodiv/d200503

Saitou, N, Nei, M. 1987. The neighbor-joining method: a new method for reconstructing phylogenetic trees. *Mol. Biol. Evol.*, **4(4)**: 406-425. https://doi.org/10.1093/oxfordjournals.molbev.a040454

Schulz, B, Wanke, U, Draeger, S, Aust, H-J. 1993. Endophytes from herbaceous plants and shrubs: effectiveness of surface sterilization methods. *Mycol. Res.*, **97(12)**: 1447-1450.

Seo, S, Kim, Y. 2019. Improving cosmetic activity by optimizing Centella asiatica extraction process. *Nat. Prod. Commun.*, **14(7)**: 1-4. https://doi.org/10.1177/1934578X19867188

Slominski, A, Tobin, DJ, Shibahara, S, Wortsman, J. 2004. Melanin pigmentation in mammalian skin and its hormonal regulation. *Physiol. Rev.*, **84(4)**: 1155-1228. https://doi.org/10.1152/physrev.00044.2003

Sungthong, B, Phadungkit, M. 2015. Anti-tyrosinase and DPPH radical scavenging activities of selected Thai herbal extracts traditionally used as skin toner. *Pharmacogn. J*, **7(2)**: 97-101. https://doi.org/10.5530/pj.2015.2.3

Thompson, JD, Gibson, TJ, Plewniak, F, Jeanmougin, F, Higgins, DG. 1997. The CLUSTAL_X windows interface: flexible strategies for multiple sequence alignment aided by quality analysis tools. *Nucleic Acids Res.*, **25(24)**: 4876-4882. https://doi.org/10.1093/nar/25.24.4876

Waisundara, VY, Watawana, MI. 2014. The classification of Sri Lankan medicinal herbs: An extensive comparison of the antioxidant activities. *J. tradit. complement. med.*, **4(3)**: 196-202. https://doi.org/10.4103/2225-4110.126175

Wang, Z, Wang, L, Pan, Y, Zheng, X, Liang, X, Sheng, L, Zhang, D, Sun, Q, Wang, Q. 2023. Research advances on endophytic fungi and their bioactive metabolites. *Bioprocess Biosystems Eng*., **46(2)**: 165-170. https://doi.org/10.1007/s00449-022-02840-7

Widjajanti, H, Elfita, E, Sari, MT, Hidayati, N, Hariani, PL, Setiawan, A. 2023. Diversity and antioxidant activity of endophytic fungi isolated from salam (Syzygium polyanthum). *Biodiversitas*, **24(5)**: 3051-3062. https://doi.org/10.13057/biodiv/d240561

Wirya, G, Gargita, I, Sudiarta, I. 2020. Molecular identification of fungi the causal agent of strawberry wilt disease ball. *Int J Biosci Biotechnol*, **7**: 64-73. https://doi.org/10.24843/IJBB.2020.v07.i02.p02

Xu, D, Li, N, Gu, Y, Huang, J, Hu, B, Zheng, J, Hu, J, Du, Q. 2023. Endophytic Fungus Colletotrichum sp. AP12 Promotes Growth Physiology and Andrographolide Biosynthesis in Andrographis paniculata (Burm. f.) Nees. *Front. Plant Sci*., **14**: 1166803. https://doi.org/10.3389/fpls.2023.1166803

JJBS

Volume 17, Number 4,December 2024
ISSN 1995-6673
Pages 693 – 703
https://doi.org/10.54319/jjbs/170412

Jordan Journal of Biological Sciences

Evaluation of Antifungal, Antibacterial and Anti-insecticidal Activities of Three *Bacillus* Strains Produced by Protoplast Fusion from *Bacillus thuringensis.*

Shereen A H Mohamed[1], Hayam Fouad Ibrahim[2,*], Walaa Hussein[2], Hanaa E. Sadek[3]. and Huda H. Elbehery [3]

[1]*Department of Microbial Genetics, Biotechnology Research Institute, National Research Centre, 33 El Buhouth St, Cairo 12622, Dokki, Egypt;* [2]*Department of Genetics and Cytology Department, Biotechnology Research Institute, National Research Centre, 33 El Buhouth St, Cairo 12622, Dokki, Egypt;* [3]*Department of Pests and Plant Protection, Agricultural and Biological Research Institute, National Research Centre, Cairo 12622, Egypt.*

Received: May 9, 2024; Revised: June 23, 2024; Accepted: July 19, 2024

Abstract

In this work, the protoplast fusion technique was evaluated for its efficiency in transferring various biological products from parental strains to fusion produced ones. *Bacillus thuringiensis* was the principal parent in three different protoplast fusion processes. Three new bacterial strains were produced previously from protoplast fusion; B18 [*Bacillus thuringiensis (Bt)* x *Bacillus subtilis 168* (*Bs*1)], C80 [*Bacillus thuringiensis* (*Bt*) x *Bacillus lichiniformis* (*Bl*)] and D27 [*Bacillus thuringiensis* (*Bt*) x *Bacillus subtilis subsp. Spizizinii* (*Bs*2)]. In this work, we aim to detect the non-ribosomal peptides (NRPS) encoding genes as important secondary metabolites involved in the biocontrol of several pathogenic diseases in plants in addition to protease, and chitinase known for their broad range of industrial applications. It was observed from the results that both fusions B18 and D27 revealed the highest number of products (two NRPs; surfactin and fengycin, protease and chitinase and two NRPs; surfactin and kurstakin, protease and chitinase) followed by C80 (two NRPs; lichenysin and kurstakin and protease), respectively. The produced strains showed moderate antagonism activity against *Aspergillus aflatoxinformans* and against *Erwinia carotovora*. Anti-insecticidal activity for the three Bacillus produced strains was evaluated against *Agrotis ipsilon*, whereas B18, D27 and B18 revealed a considerable toxic effect at higher tested concentrations (10%, 5%, and 2.5%), causing 60%, 30% and 23% larvae mortality respectively. Also, D27 showed 56.67%, 26.67% and 20% larval mortality with the same concentrations, while C80 showed lower mortality at higher concentration (10%, 5%, and 2.5%), causing 40%, 20% and 16.67% larvae mortality.

Keywords: Antifungal, Chitinase, Lepidopterous, NRPS, Protease, Protoplast fusion**.**

1. Introduction

Lepidopterous is one of the most harmful pests in agriculture. It is known by the black cutworm *Agrotis ipsilon* (Hufnagel), (Lep., Noctuidae) which has a wide host range. This species can feed on nearly all vegetables, such as alfalfa, clover, cotton, rice, sorghum, strawberries, sugar beet, tobacco, and occasionally grains and grasses. It can also feed on almost any fruit. Black cutworm often has a clear predilection for weeds, and it will not attack crops until the weeds have been eaten. Adults use floral nectar for nutrition. Moths are particularly drawn to deciduous trees and shrubs, including linden, wild plum, crabapple, and lilac. Since most of its feeding occurs below soil level, the black cutworm is not thought of as a climbing cutworm. However, until roughly their fourth instar, larvae will feed aboveground. During their development, larvae can eat more than 400 sq cm of leaves, but more than 80% of this occurs during the terminal instar, and only about 10% occurs in the instar just before the last (Boughton *et al*., 2001). Chemical pesticides are the major method for controlling *A. ipsilon*. There are significant issues with using synthetic insecticides to control agricultural pests in field crops, such as pesticide residues and insect pest resistance. Therefore, the search for chemical-free crops using environmentally friendly pest control techniques is critically required. The protoplast fusion is considered one of the most important genetic engineering techniques, which proved its efficiency in transferring some important biological microbial products (Mohamed *et al*., 2021).

Bacillus thuringiensis is widely used as a pesticide to produce toxins of specific insecticidal activity kills insects by binding to and creating pores in the midgut membranes of insects. (Zhang *et al*., 2020). *Bacillus spp*. like (*B. thuringiensis*, *B. subtilis*, *B. licheniformis*, etc,.) produce diversity of lytic enzymes, such as chitinases, glucanases, lipases, proteases and various antibiotics (Bhagwat *et al*., 2019). Proteases are biological macro-molecules known as simple destructive enzymes because of their broad range of catalytic, analytic, and applications in industry Neurath and Walsh, (2011). There are different types of proteases,

* Corresponding author. e-mail: hayamfouad24@gmail.com.

such as Alkaline serine protease (Yang *et al*., 2020) and metalloprotease (Zhang *et al*., 2023). Proteases target the defense molecules of the insect (Mukherjee and Vilcinskas, 2018). In addition to the promising mechanism of non-ribosomal peptide synthesis which considers a source of alternatives to chemical substances for different plant pathogens. This NRPS mechanism is responsible for producing a wide spectrum of NRPs using a multi-enzyme function system (synthetases) (Marahiel, 1997). Among these NRPs products are lipopeptide families produced by Bacillus strains, one of which is the surfactin that is considered an extraordinarily powerful biosurfactant due to its capability to decrease the water surface tension in addition to its role as a biological membrane detergent (Carrillo *et al*., 2003). It has a wonderful activity as antiviral, anti-mycoplasma, emulsifying and foaming (Peypoux *et al*., 1999). Surfactin has an amazing number of applications in different fields; biocontrol of plant diseases (Ongena and Jacques, 2008), medicine (Kowall *et al*., 1998), food preservation (Bie *et al*., 2005), cosmetics (Kanlayavattanakul *et al*., 2010), enhanced oil recovery (Schaller *et al*., 2004) and the bioremediation (Mulligan *et al*., 2001). Also, the iturin role was proven as antifungal against various plant pathogens, so it is widely used in plant diseases biocontrol (Leclere *et al*., 2005). Kurstakin is also one of the lipopeptide families (Jacques, 2011) which was discovered recently in 2000 from *Bacillus thuringinesis* and showed antifungal activity against *Stachybotrys charatum* (Hathout *et al*., 2000). Kurstakins are found accompanying bacterial cells, especially on spores, and the kurstakin production was evaluated to 15-20 µg.mg^{-1} (Hathout *et al*., 2000; Abderrahmani *et al*., 2011; Béchet *et al*., 2012). Generally, Bacillus spp. lipopeptides are well known for their role in plant-pathogens biocontrol (Ongena and Jacques, 2008; Jacques, 2011). Also, (Yu *et al*., 2023) confirmed that kurstakin contributes to the control of the plant-pathogenic fungi; *Rhizoctonia solani*, *Ascochyta citrulline*, *fusarium graminearum* and *F. oxysporum*. The fengycin family shows antifungal activity and has induction defense specific to certain pathogen systems or plant species; for example, fengycin does not induce defence system in grapevine (Farace *et al*., 2015; Li *et al*., 2019; Deleu *et al*., 2008) but induces defense system in rice against *Rhizoctonia solani* (Chandler *et al*., 2015). This research aims to evaluate some biological products from three Bacillus strains produced by protoplast fusion to be used as alternatives to chemical substances in bicontrol.

2. Materials and methods

2.1. Bacterial strains

Four wild type parental strains and three fusions were used in this study; *Bacillus thurinigensis*, *Bacillus subtilis* 168, *Bacillus lichineformis* and *Bacillus subtilis* subsp. *spizizinii* (parental strains) and B18, C80, and D27 as fusions (Mohamed *et al*., 2016 and 2023) (Table 1).

Table 1. Parental strains and protoplast fusion produced strains

Parental strains	Produced strains by protoplast fusion	Reference
B. thurinigensis :: *B. subtilis* 168	B18	Mohamed *et al*., 2016 and 2023
B. thurinigensis :: *B. lichiniformis*	C80	
B. thurinigensis :: *B. subtilis* subsp. *spizizinii*	D27	

2.2. Bacterial culture

A single colony of each bacterium was cultured in 20 ml of LB in a 100 ml conical flask (Pyrex, United States of America) by shaking in an orbital shaker (Thermo Fisher Scientific, United States of America) at 120 rpm for 18 h at 30°C.

2.3. DNA isolation and PCR conditions

DNAs were prepared using GeneJET Genomic DNA Purification Kit (Thermo scientific, USA). Degenerate primers used in this study were previously designed according to (Tapi *et al*., 2010; Abdelrahmani *et al*., 2012) and all used primers are listed in Table (2). NRPS degenerate primers were designed by the alignment of conserved motifs of the nucleic acid sequences identified in the adenylation domain (A) and the thiolation domain (T). PCR conditions were performed by initial step of denaturation at 94 °C for 3 min, followed by 35 cycles of three steps; denaturation at 94 °C for 30 sec, annealing step at 43 °C, 44.4 °C and at 58 °C with surfactins, kurstakins and plipastatins, respectively. There was an extension step at 72 °C for 2 min with plipastatins and kurstakins except with surfactins for 45 seconds, in addition to the final extension step at 72 °C for 5 min. Protease detection PCR conditions are 95°C for 3 min; 35 cycles of 95°C for 30sec, 50°C for 30 sec, and 72°C for 1 min and a final extension of 72°C for 10 min. Detection of chitinase gene PCR conditions; 94°C for 3 min; 35 cycles of 94°C for 30sec, 48°C for 30 sec, and 72°C for 1 min and a final extension of 72°C for 10 min. PCR products were separated on a 1.2% agarose gel compared to Thermo Scientific Gene Ruler 100 bp DNA Ladder and photographed under Gel Doc™ XR+ Gel Documentation System.

Table 2. Degenerate primers used for non-ribosomal lipopeptides, protease and chitinase genes detection from fusion strains

Name	Sequence	Expected fragment size (bp)	NRLPs identified	References
AP1-F	AGMCAGCKSGCMASATCMCC	959, 929, 893	Plipastatin	Tapi *et al*., 2010
TP1-R	GCKATWWTGAARRCCGGCGG			
AS1-F	CGCGGMTACCGVATYGAGC	419, 422, 424, 431	Surfactin	Tapi *et al*., 2010
TS1-R	ATBCCTTTBTWDGAATGTCCGCC			
AKs-F	TCHACWGGRAATCCAAAGGG	1125, 1152, 1161, 1167, 1173	Kurstakin	Abderrahmani *et al*., 2011
TKs-R	CCACCDKTCAAAKAARKWATC			
Bspro-F	ATGGTGGATTACGAACGTG	1203 bp	Bacillus Protease	This study
Bspro-R	TTAACTGCCTAATTGGTCTG			
Bs ch-F	GAATTCATGCGCAAATTTAATAAACCGCT	1100 bp	chitinase	Berini *et al*., 2018
Bs ch-R	AAGCTTTTATTGAACGCCGGCGCT			

2.4. Fungi preparation

For the two fungi (*Aspergillus aflatoxiforman* and *Aspergillus flavus*), PDA liquid media was used and incubated 7 days at 30 ºC. The fungi were spread on PDA solid media using swab, and the discs supplemented with fusion bacteria were put on the petri dishes using three replicates. All plates were incubated for 3 days at 30 ºC.

2.5. Insect rearing

Agrotis ipsilon (Hufnagel) (Insecta: Lepidoptera: Noctuidae) was raised in a lab without the use of any insecticides for multiple generations. Hatched larvae are put in plastic jars and allowed to feed on the leaves of the caster bean plant *Ricinus communis* L. The newly emerging adult moths were moved to oviposition jars that included cotton tufts that had been wet with honey solution for the moths to feed on.

2.6. Bioassay

To evaluate the efficacy of the three bacterial strains (B18, C80 and D27), they were generated at various concentrations (10, 5, 2.5, 1.25 %) by dilution with water. The third larval instar of *A. ipsilon* was used to examine the bacterial strains' ability to eliminate insects. Using a dipping technique, the toxic effects of the tested botanicals were investigated. Caster bean plant leaf discs measuring 10 cm in diameter were dipped in various concentrations for two minutes, allowed to dry at room temperature, and then provided to selected *A. ipsilon* larvae. The experiment was carried out in 10 replicates, each containing three larvae. Every day, the number of alive and dead larvae was counted after 25 days of feeding.

2.7. Statistical analysis

The LC50 values were determined by SPSS software using (Finney, 1971) Probity analysis approach. Duncan's test and one-way ANOVA were employed to analyze the statistical variance between groups.

3. Results

3.1. Detection of NRPs genes involved in the sequenced genome of Bacillus parental strains available on GenBank

Bacillus parental strain genomes were analyzed by Anti-smash version 7.0 which allows rapid detection and analysis of biosynthesis gene clusters responsible for secondary metabolite production of bacterial and fungal genomes. *Bacillus subtilis* 168 genome analysis revealed the presence of three non-ribosomal lipopeptide gene clusters for surfactin, fengycin and bacillibactin and one polyketide-NRPs hybrid bacillaene. Other secondary products have been detected in the *Bs* 168 genome of different types: sporulation killing factor, sublancin, pulchemiminic acid, subtilosin and bacilycin (Table 3). This result agrees with (Kunst *et al*., 1997; Barbe *et al*., 2009). *Bacillus subtilis* subsp spezizinii genome analysis showed the presence of three non-ribosomal lipopeptide gene clusters for surfactin, mycosubtilin and bacillibactin and one polyketide-NRPs hybrid bacillaene. Other secondary products have been detected for different types: subtilin, subtilosin and rhizocticin (Table 3) according to (Fan *et al*., 2011). By AntiSmash, two NRPs lipopeptide gene clusters were detected in *B. thurinigensis* genome, kurstakin and bacillibactin as reported by (Abderrahmani *et al*., 2011; Béchet *et al*., 2012).

Table 3. AntiSmash results for detecting NRPs clusters involved into genomes of Bacillus parental strains

Strain	Region	Type	From	To	Most similar known cluster	Similarity
***B. subtilis* str. 168 AL009126.3**	Region 2	NRPS	358,303	421,744	surfactin	82 %
	Region 4	Polyketide+NRP	1,763,763	1,869,009	bacillaene	100 %
	Region 5	NRPS, betalactone	1,940,625	2,017,738	fengycin	100 %
	Region 9	NRP-metallophore	3,260,519	3,312,296	bacillibactin	100 %
B. licheniformis CP000002.3	Region 2	NRPS	359,133	424,266	Lichenysin	100 %
	Region 9	NRP-metallophore	3,698,288	3,750,032	Bacillibactin	100 %
***B. spizizenii* str. W23 CP002183.1**	Region 2	NRPS	345,342	408,676	surfactin	86 %
	Region 4	TransAT-PKS NRPS	1,721,226	1,826,452	Bacillaene	100 %
	Region 5	NRPS- betalactone-TransAT	1,893,143	1,969,153	Mycosubtilin	100 %
	Region 8	NRP-metallophore,	3,043,946	3,096,063	Bacillibactin	100 %
***B. thuringiensis* BMB171 CP001903.1**	Region 3	NRP-metallophore,	2,184,326	2,236,074	Bacillibactin	100 %
	Region 5	NRPS	2,326,120	2,392,028		
	Region 6	NRPS- betalactone	2,409,777	2,435,015	Kurstakin	100 %

3.2. NRPs synthetase genes detection in Bacillus parental and fusion strains by degenerated primers

The detection of NRPs genes responsible for lipopeptides biosynthesis in the previously sequenced genome strains available on GenBank was expected. Kurstakin biosynthesis was detected in *B. thuringiensis* strain with an expected fragment size of 1167 bp, while plipastatin and surfactin biosynthesis genes were identified in *B. subtilis* 168 with expected fragment size of 958 and 424 bp respectively. The detection of lichenysin synthetase gene by both plipastatin and surfactin primers in *B. licheniformis* agrees with (Tapi *et al*., 2010; Abderrahmani *et al*., 2011) who established the kurstakin synthetase genes detection in *B. thuringiensis* using kurstakin AKs-F/TKs-R primers and the efficiency of using surfactin degenerate As1-F/Ts2-R primers to detect surfactin synthetase genes in *Bacillus subtilis*. The strain *B. subtilis* subsp. Spizizinii amplified three fragments; 424 bp, 350 bp and 300 bp respectively with surfactin primers, whereas the fragment of 424 bp belongs to surfactin synthetase gene (Figure 1).

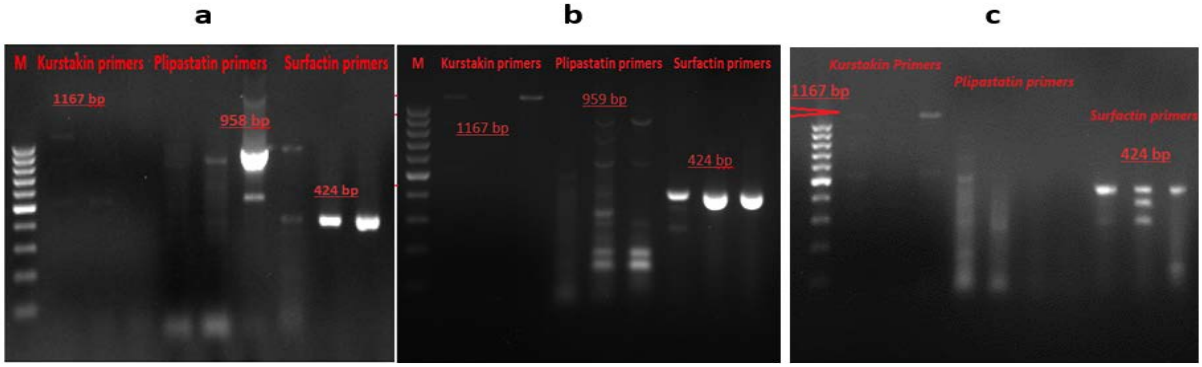

Figure 1. Degenerate primers amplification for; a. *B. thuringiensis*, *B. subtilis* 168, and B18; b. *B. thuringiensis*, *B. lichineformis*, and C80; c. *B. thuringiensis*, *B. subtilis subsp. spizizinii*, and D27 with kurstakin, plipastatin and surfactin primers respectively

The degenerate primers allowed us to detect the presence of both plipastatin and surfactin synthetase genes in B18 fusion, compared to their parental strains *B. thuringiensis* a harbouring kurstakin synthetase genes and *B. subtilis* 168 the surfactin and plipastatin harbouring synthetase genes (Figure 1. a). The fusion C80 was found to harbour the two synthetase genes of kurstakin and lichenycin (surfactin family), which have been transferred from both parental strains *B. thuringiensis* (kurstakin synthetase genes) and *B. licheniformis* (Lichenysin synthetase genes) (Figure 1. b). The fusion D27 was found to harbor kurstakin and surfactin synthetase genes which were transferred from their both parental strains *B. thuringiensis* (kurstakin synthetases genes) and *B. subtilis* subsp. Spizizinii (surfactin synthetases genes) (Figure 1c).

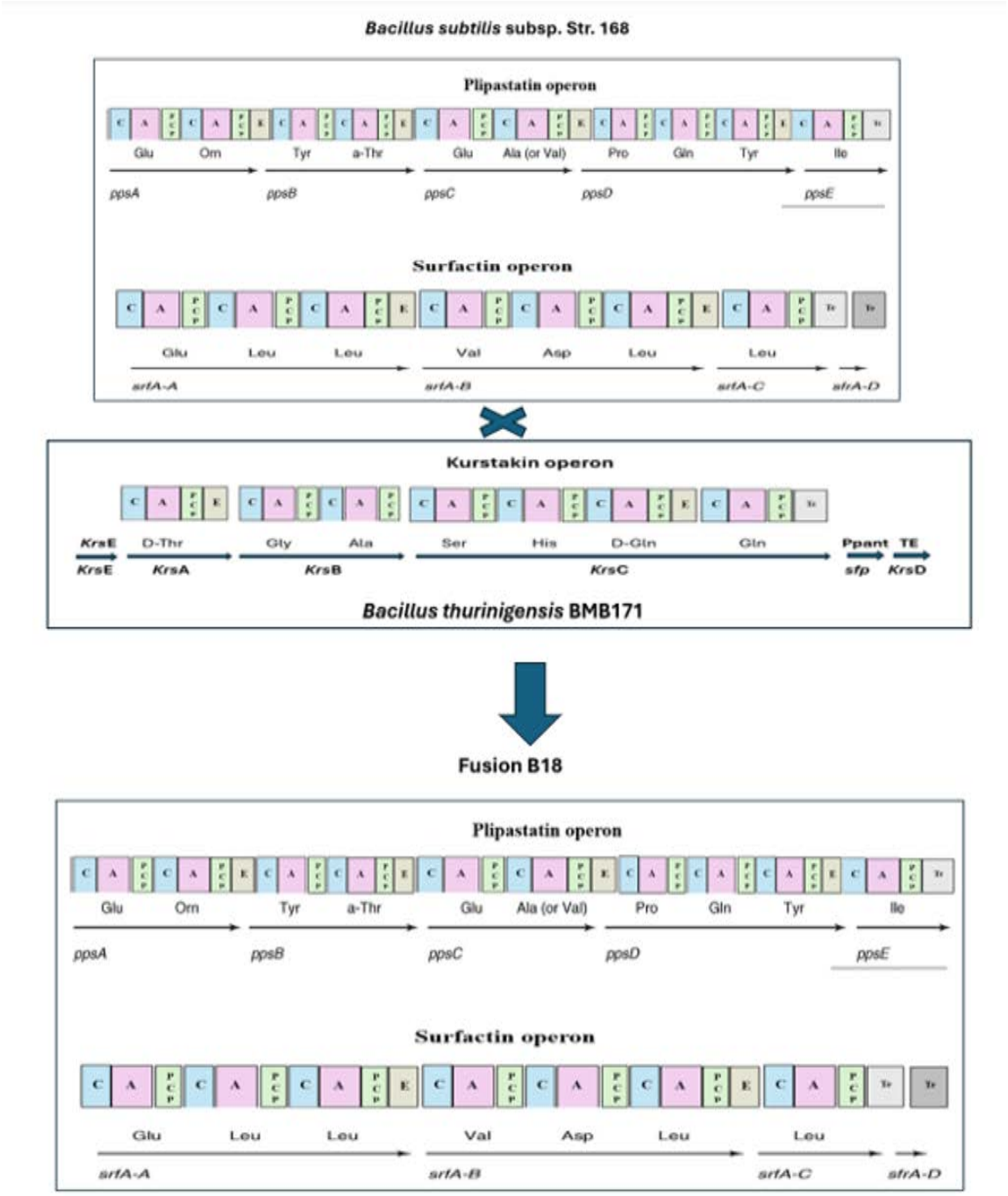

Figure 2. Schematic dendogram for NRPS synthetase clusters transferred by protoplast fusion from parental strains *B. thuringiensis* and *B. subtilis* 168 to fusion strain B18

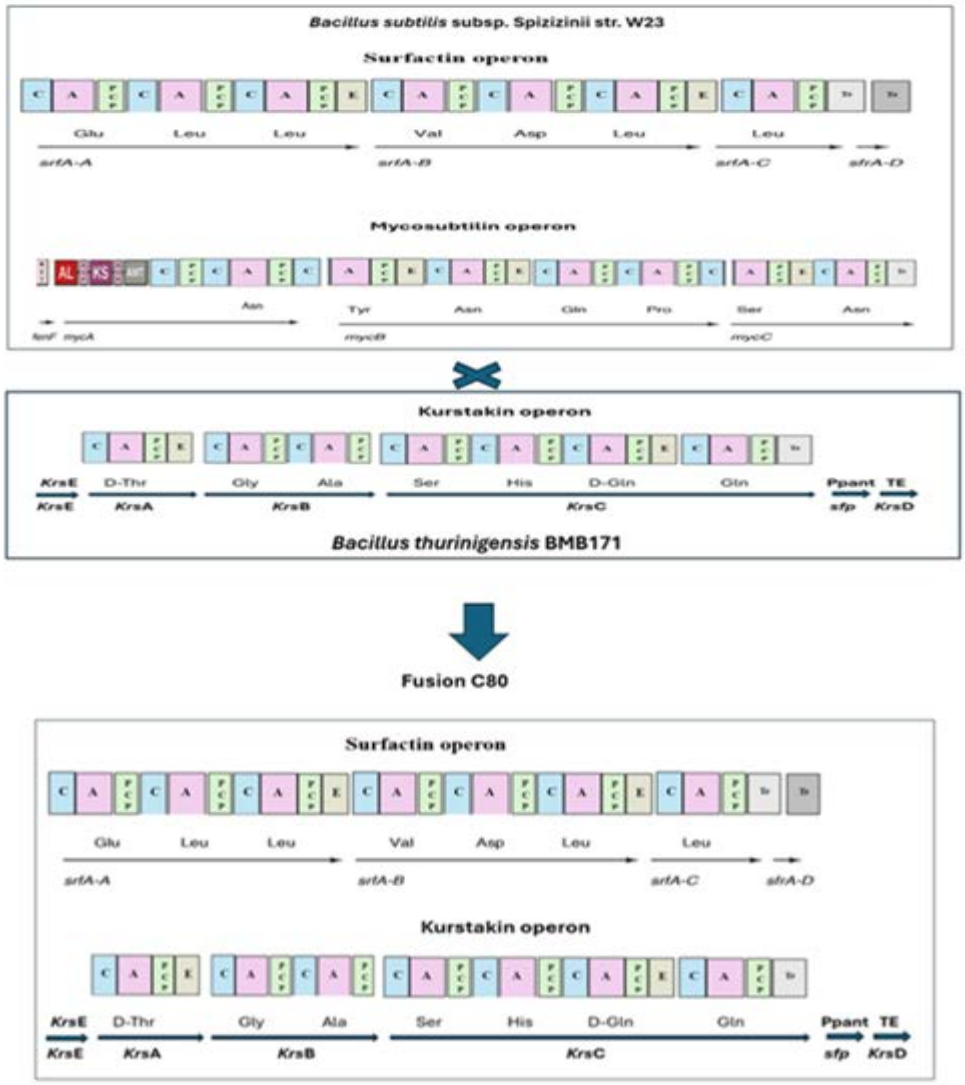

Figure 3. Schematic dendogram for NRPS synthetase clusters transferred by protoplast fusion from parental strains *B. thuringiensis* and *B. subtilis* spizizinii to fusion strain C80

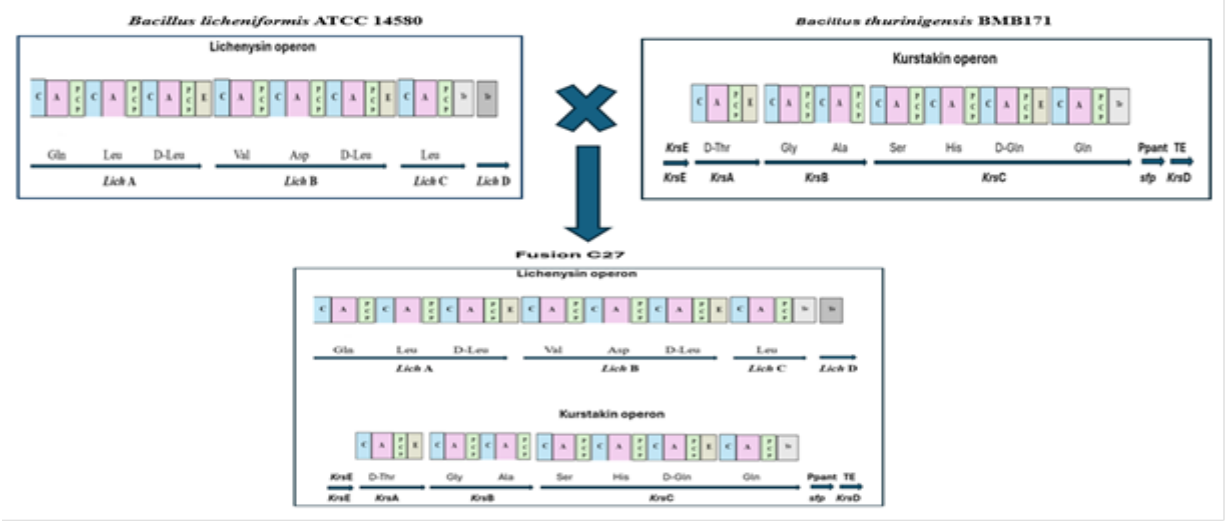

Figure 4. Schematic dendogram for NRPS synthetase clusters transferred by protoplast fusion from parental strains *B. thuringiensis* and *B. licheniformis* to fusion strain D27

3.3. PCR detection of protease gene in the modified Bacillus strains

Detection of protease gene was conducted in the parental strains *B. thuringiensis* (*Bt*), *B. subtilis* 168 (*Bs*1), *B. subtilis* subsp. Spizizinii (*Bs*2), and *B. licheniformis* (*Bl*) compared to the fusion B18 (Bt::Bs1), C80 (Bt::Bl) and D27 (Bt::Bs2). PCR has been implemented to detect the absence or presence of the protease gene in the three fusion strains and a fragment of 1203 bp of expected size was amplified. The protease gene was detected in the three fusion produced strains; B18 and parent 1(Bt::Bs1), C80 (Bt::Bl) and D27 (Bt::Bs2) (figure 5a).

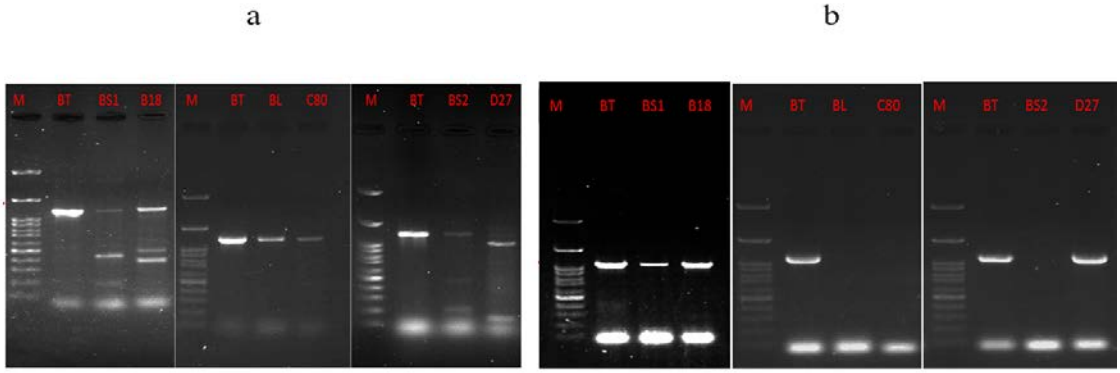

Figure 5. a. Protease; b. chitinase primers amplification for *B. thuringiensis*, *B. subtilis* 168, and B18, *B. thuringiensis*, *B. lichineformis*, and C80, *B. thuringiensis*, *B. subtilis* subsp. spizizinii, and D27.

3.4. PCR detection of chitinase gene in the modified Bacillus strains

Detection of chitinase gene in fusion strains was carried out by PCR and a fragment of 1100 bp was amplified. The chitinase gene appeared in the produced fusion strain B18 and their parents (Bt::Bs1), while it disappeared in the fusion strain C80 (Bt::Bl) and one of their parental strains (*Bl*) and appeared in the other parent Bt. Finally, chitinase gene was detected in the fusion strain D27 (Bt::Bs2) and one of their parental strains (*Bt*), while it was absent in the other parent (*Bs*) (Figure 5b).

Table 4. NRPs genes, protease and chitinase detected by PCR in Bacillus parental and fusion strains

Parental strains and fusions	***B.subtilis* 168**	***B. lichenyformis***	**B. *subtilis* subsp. *spizizinii***	**B. thuringensis**	***B.subtilis* 168+ *B. thuringensis* B18**	***B. lichenyformis* + *B. thuringensis* C80**	***B.subtilis* Spizizini+ *B. thuringensis* D27**
Surfactin	Surfactin		Surfactin		Surfactin		Surfactin
Fengycin or plipastatin	Fengycin or plipastatin				Fengycin or plipastatin		
Lichenysin		Lichenysin				Lichenysin	
Kurstakin				Kurstakin		Kurstakin	Kurstakin
Mycosubtilin			Mycosubtilin				
Protease	Protease	Protease	Protease	Protease	Protease	Protease	Protease
Chitinase	Chitinase			Chitinase	Chitinase	Chitinase	Chitinase
	4	2	3	3	4	4	4

All detected NRPs products, protease and chitinase are summarized in Table 4 for the parental and fusion produced strains. It was observed that the three fusions B18 (surfactin, fengycin, protease and chitinase), D27 (surfactin, kurstakin, protease and chitinase) and C80 (lichenysin, kurstakin and protease) revealed the same number of products.

3.5. Antifungal activity of parental and fusion produced strain against Aspergillus aflatoxinforman and Aspergillus flavus

The three fusion bacteria showed moderate antagonism activity against *A. aflatoxinforman*, the strains E (B18 and D27) and G (B18, C80 and D27) (++) followed by C (D27), and F (C80 and D27) (+), while A (B18), B (C80) and D (B18 and C80) (-) compared to control (Figure 6A).

These results may refer to a synergistic relationship between the strains (B18 and D27) and between (B18, C80 and D27) and also refer to the effective role of the strain D27 compared to the other strains. On the other hand, no anti-fungal activity was detected whether with the parental strains or the fusion produced strains against *Aspergillus flavus* (Figure 6B). The two types of fungi secrete fungal toxins (aflatoxin) cause great harm to humans. Therefore, we resort to finding a solution for combating these fungi with beneficial bacteria capable of producing various non-ribosomal peptides (NRPS) that have antifungal activity, such as (fengycin or plipastatin).

3.6. Antibacterial Activity

The three bacterial fusions (B18, C80 and D27) have revealed anti-bacterial activity against *Erwinia carotovora* whereas the highest activity was shown with A, (B18) B (C80), D (B18 and C80) and E (B18 and D27) (+++) followed by F (C80 and D27) and G (B18, C80 and D27) (++), while C (D27) (+) compared with control as shown in figure (6C).

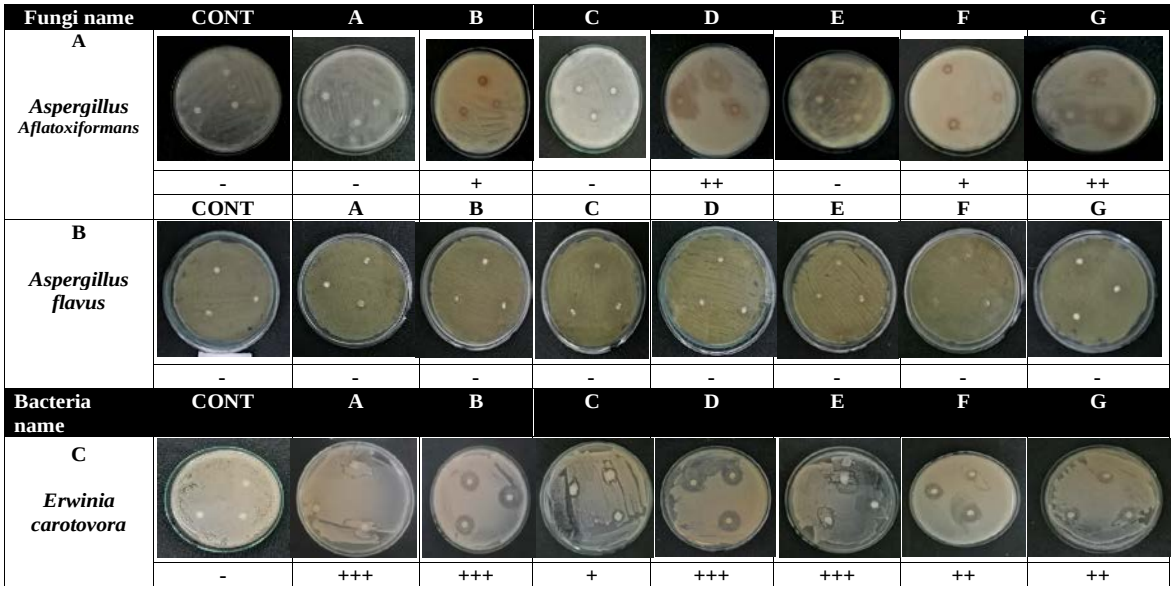

Figure 6. Antifungal activity of the three bacterial fusions against; a. *Aspergillus Aflatoxiformans* and *b*. *Aspergillus flavus* and c. Antibacterial activity against *Erwinia carotovora*, A= (B18), B=(C80), C=(D27), D= (B18+C80), E= (B18, D27), F= (C80+D27), G= (B18, C80, D27)

3.7. Anti-insecticidal activity of the three Bacillus producing strains

The data in Table 5 demonstrated the three tested bacterial strains have harmful effects on *A. ipsilon* third larval instar. B18 revealed a considerable toxic effect at higher tested concentrations (10%, 5%, and 2.5%), causing 60%, 30% and 23% larvae mortality respectively, although D27 showed 56.67%, 26.67% and 20% larval mortality with the same amount of concentration, C80 showed lower mortality at higher concentrations (10%, 5%, and 2.5%), causing 40%, 20% and 16.67% larvae mortality.

Table 5. Mortality (mean ± SE) of *A. ipsilon* 3rd larval instar after 25 days of treatment with three bacterial strains

Concentrations	B 18				C 80				D27			
10.00%	60.00	±	10.00	a	40.00	±	5.77	a	56.67	±	3.33	a
5.00%	30.00	±	5.77	b	20.00	±	5.77	b	26.67	±	3.33	b
2.50%	23.33	±	3.33	b	16.67	±	6.67	b	20.00	±	5.77	b
1.25%	6.67	±	3.33	c	3.33	±	3.33	b	6.67	±	3.33	c
control	0.00	±	0.00	c	3.33	±	3.33	b	0.00	±	0.00	c
F	22.10				8.54				36.50			
Sig.	0.00				0.00				0.00			

4. Discussion

In this work, we exhibited the effectiveness of using the degenerated primers in detecting NRPs synthetase genes, which allowed us to get a near view into bacterial genomes side by side with bioinformatics tools, such as AntiSmash and PKS-NRPS analysis websites. The degenerated primers utilization for NRPs genes detection from un-sequenced genomes became widely applied in several studies. (Marahiel, *et al*., 1997) designed primers based on the highly conserved motif A2 (KAGGAY) LV P for peptide synthetases. Another degenerate primer was designed by (Neilan *et al*., 1999; Vizcaino *et al*., 2005)

based on the adenylation domain conserved motif from various fungi and bacteria. Recently, the designation of these degenerated primers became more specific depending on bacteria genera. *Bacillus* degenerate primers for their NRPs encoding genes were designed by the alignment of the conserved nucleic acids sequence of both the adenylation and the thiolation domains (Tapi *et al*., 2010; Chen *et al*., 2006). In this work, *Bacillus* degenerate primers (Tapi *et al*., 2010; Chen *et al*., 2006) proved their effectiveness in the detection of NRLPs clusters of surfactin, (As1-F/Ts2-R primers), plipastatin (Ap1-R/Tp1-R primers) in fusion B18, lichenysin (As1-F/Ts2-R primers) and kurstakin (Aks-F/ Tks-R) from C80, surfactin (As1-F/Ts2-R primers) and kurstakin (Aks-F/ Tks-R) from strain D27. These results agree with (Tapi *et al*., 2010) who confirmed the amplification of fragments of 99% similarity with surfactin As1-F/Ts2-R primers from *B. subtilis* 168 and lichenysin from *B. licheniformis* ATCC 14580 respectively. He also confirmed the amplification of fragment with plipastatin (Ap1-R/Tp1-R) primers from *B. subtilis* 168 similarly to plipastatin (99%). (Tapi *et al*., 2010) also indicated that the Af2-F/ Tf1-R primers amplified a fragment similarly to bacillaene synthase of *B. amyloliquefaciens* FZB42 from *B. subtilis* ATCC6633, and of *B. subtilis* 168 (Chen *et al*., 2009; Al-shebly, 2022). Insect defense compounds are the focus of proteases, which break them down (Mukherjee and Vilcinskas 2018). Moreover, *B. thuringiensis* protoxin is implicated in the activation of these protoxins into dangerous forms; in this active state, the toxins bind to receptors on the intestinal epithelium in several insect groups as a result of the creation of oligomeric pores in the gut cell membrane of the larvae. Furthermore, the chitinase gene improved the behavior of the *B. thuringiensis* strain (Bravo *et al*., 2017) However, in response to *R. Speratus*, *Bacillus licheniformis* secretes hydrolytic enzymes called protease and chitinase, which break down the cuticle layers of insect pests' exoskeletons of subterranean worker termites (Moon *et al*., 2023). Notably, repurposing chitinase to restrict or eliminate pests can prevent soil contamination that could harm the ecosystem. As an example, Rostami et al. demonstrated chitinase on the spore as a possible biopesticide by fusing it with the B. subtilis spore coat protein CotG (Hosseini *et al*., 2016; Rostami *et al*., 2017). Protease used in plant defense against herbivory offers particular promise for the production of insect-resistant transgenic plants in the future. In the era of genomes and transcriptomics, a more efficient knowledge of the biology of virulence factors may facilitate the discovery of prospective proteases for application in pest control (Negi *et al*., 2023). It was discovered that the BG strains carry the genes for the ChiA and ChiB belonging to the GH18 (glycoside hydrolase) family and exert endochitinase activity (Drewnowska *et al*., 2020). Chitinases play a role in the pathophysiology of *B. thuringiensis* in insects since they break down the peritrophic membrane, which is composed of chitin and protects the insect gut from hazardous substances and toxins. In addition, chitinases are used to strengthen the defenses of genetically modified crops against pests (Berini *et al*., 2018). Therefore, the presence of genes encoding chitinolytic enzymes in BG strains increases insecticidal activity. On the other hand, Zhang *et al*., 2019, found that 558 midgut genes and 65 midgut genes are differently expressed in Vip3Aa11-M-A and Vip3Aa39-M-A respectively. *Agrotis ipsilon* midgut BBMV can be competitively bound by the Vip3Aa protein due to its trypsin sensitivity and binding specificity. However, Yan *et al*. in 2020 evaluated the effectiveness of three (C010, C009 and C008) GM maize juveniles expressing Vip3Aa19 toxins against BCW and evaluated the susceptibility of BCW neonates to 11Bt toxins, namely, Cry1Ab, Cry1Ac, Cry1Ah, Cry1F, Cry1Ie, Cry1B, Cry2Aa, Vip3_ch1, Vip3_ch4, Vip3Ca2, and Vip3Aa19. Vip3Aa19 was the most active protein against BCW (LC50 = 0.43 µg/g) according to the bioassay data of toxin diet. Less toxic chimeric proteins were Cry1F (LC50 = 83.62 µg/g), Vip3_ch1 (LC50 = 5.53 µg/g), and Cry1Ac (LC50 = 184.77 µg/g). The biological activity of six various heterologous pesticidal proteins—Cry1Aa, Cry1Ca, Cry1Ia, Cry2Ab, Cry9Ea, and Vip3Aa produced by *B. thuringiensis* have been evaluated against *A. exclamationi* histopathologically (Baranek *et al*., 2023b). Among the examined pest species, only Cry9Ea and Vip3Aa exhibited considerable mortality, with LC50 values of 950 and 140 ng/cm2 respectively. It was established how Cry9Ea and Vip3Aa affected *A. exclamationis* histopathologically. However, most currently used *B. thuringiensis*-based biocontrol agents (including the commercial strains tested in this work) primarily contain Cry1- and Cry2-type toxins as their active molecules. These toxins only cause varying degrees of growth inhibition in the target insect, not death. (Baranek *et al*., 2023a) demonstrated the presence of genetic determinants encoding the chitinolytic enzymes ChiA and ChiB in the examined entomopathogens. The examined strains exhibit insecticidal activity against two different, economically significant pest insects: *Spodoptera exigua* Hübner (Lepidoptera: Noctuidae) and *Cydia pomonella* L. (Lepidoptera: Tortricidae). When it comes to both pests, however, the BG12 and BG15 strains are noticeably more active than the BG11 strain. The strains BG12 and BG15 have the potential to be utilized in the development of novel lepidopteran-active bioinsecticides that will enhance current biocontrol approaches.

5. Conclusion

The protoplast fusion is considered one of the most important genetic engineering techniques, which proved its efficiency in transferring some important biological microbial products. In this study, we checked the transferring of various secondary metabolites, such as protease chitinase and NRPS, using bioinformatics and PCR techniques. The newly produced fusions proved their antifungal, antibacterial and anti-insecticidal activities.

References

Abderrahmani A, Tapi A, Nateche F, Chollet M, Leclère V, Wathelet B, Hacene H and Jacques P. 2011. Bioinformatics and molecular approaches to detect NRPS genes involved in the biosynthesis of kurstakin from Bacillus thuringiensis. *Appli J Microbiol Biotechnol.*, **92**: 571–581.

Al-shebly H. 2022. Effect of *Aspergillus flavus* on Seed Germination and Seedlings Growth of Barley and Some of Associated Weeds. *IOP Conference Series Earth Environm Sci.*, **1060**(1): 012119. DOI: 10.1088/1755-1315/1060/1/012119 .

Baranek J, Jakubowska M and Gabała E. 2023. Insecticidal activity of *Bacillus thuringiensis* towards Agrotis exclamationis larvae-A widespread and underestimated pest of the Palearctic zone. *PLoS One*., **16**:18(3), e0283077. Doi: 10.1371/journal.pone.0283077.

Barbe V, Cruveiller S, Kunst F, Lenoble P, Meurice G and Sekowska A, *et al*. 2009. From a consortium sequence to a unified sequence: the *Bacillus subtilis* 168 reference genome a decade later. *Microbiol*., **155**: 1758–1775. Doi: 10.1099/mic.0.027839-0.

Berini F, Katz C, Gruzdev N, Casartelli M, Tettamanti G and Marinelli F. 2018). Microbial and viral chitinases: attractive biopesticides for integrated pest management. *Biotechnol Adv*., **36**: 818–838.

Béchet M, Caradec T, Hussein W, Abderrahmani A, Chollet M, Leclère V, Dubois T, Lereclus D, Pupin M, Jacques P. Structure, biosynthesis, and properties of kurstakins, nonribosomal lipopeptides from Bacillus spp. Appl Microbiol Biotechnol. 2012 Aug;95(3):593-600. doi: 10.1007/s00253-012-4181-2. Epub 2012 Jun 9. PMID: 22678024.

Bhagwat A, Collins CH and Dordick JS. 2019. Selective antimicrobial activity of cell lytic enzymes in a bacterial consortium. *Appli Microbiol Biotechnol.*, **103**: 7041–7054.

Bie XM, Lu ZX, Lu FX and Zeng XX. 2005. Screening the main factors affecting extraction of the antimicrobial substance from Bacillus sp. fmbJ using Plackett–Burman method. *World J Microbiol Biotechnol*, **21**: 925–928.

Boughton AJ, Lewis LC and Bonning BC. 2001. Potential of nucleopolyhedrosis for suppression of the black cutworm *Agrotis ipsilon* (Lepidoptera: Noctuidae) and effect of an optical brightener on virus efficacy. *J Economic Entomol*., **94**: 1045-1052.

Bravo A, Pacheco S, Gómez I, García-Gómez BI, Onofre J and Soberón M. 2017. Insecticidal proteins from Bacillus thuringiensis and their mechanism of action. In: *Bacillus thuringiensis* and *Lysinibacillus sphaericus*, Characterization and usein the field of Biocontrol. Chapter 4, Springer.

Carrillo C, Teruel JA, Aranda FJ and Ortiz A. 2003. Molecular mechanism of membrane permeabilization by the peptide antibiotic surfactin. *Biochim Biophys Acta.*, **1611**: 91–97.

Chandler S, Van Hese N, Coutte F, Jacques P, Hofte M and De Vleesschauwer D. 2015. Role of cyclic lipopeptides produced by Bacillus subtilis in mounting induced immunity in rice (Oryza sativa L.). *Physiol Mol plant.*, **91**: 20-30.

Chen XH, Koumoutsi A, Scholz R, Schneider K, Vater J, Süssmuth R, Piel J and Borriss R. 2009. Genome analysis of *Bacillus amyloliquefaciens* FZB42 reveals its potential for biocontrol of plant pathogens. *J Biotechnol*., **140**: 27–37.

Chen XH, Vater J, Piel J, Franke P, Scholz R, Schneider K, Koumoutsi A, Hitzeroth G, Grammel N, Strittmatter AW, Gottschalk G, Süssmuth RD and Borriss R. 2006. Structural and functional characterization of three polyketide synthase gene clusters in *Bacillus amyloliquefaciens* FZB 42. *J Bacteriol*., **188**: 4024–4036.

Deleu M, Paquot M and Nylander T. 2008. Effect of fengycin, a lipopeptide produced by Bacillus subtilis, on model biomembranes. *Biophys J*., **94**: 2667-2679.

Drewnowska JM, Fiodor A, Barboza-Corona JE and Swiecicka I. 2020. Chitinolytic activity of phylogenetically diverse *Bacillus cereus sensu lato* from natural environments. *System Appl Microbiol.*, **43**: 126075.

Fan, B., Chen, X. H., Budiharjo, A., Bleiss, W., Vater, J., and Borriss, R. 2011. Efficient colonization of plant roots by the plant growth promoting bacterium Bacillus amyloliquefaciens FZB42, engineered to express green fluorescent protein. *Journal of Biotechnology*, *151*(4), 303-311.

Farace G, Fernandez O, Jacquens L, Coutte F, Krier F, Jacques P, Clément C, Barka EA, Jacquard C and Dorey S. 2015. Cyclic lipopeptides from Bacillus subtilis activate distinct patterns of defence reponses in grapevine. *Mol Plant Pathol.*, **16**:177- 187.

Finney DJ. 1971. Probit Analysis. Cambridge University Press, Cambridge, 333 p.

Hathout Y, Ho YP, Ryzhov V, Demirev P and Fenselau C. 2000. Kurstakins: a new class of lipopeptides isolated from *Bacillus thuringiensis*. *J Nat Prod.*, **63**: 1492–1496.

Hosseini-Abari A, Kim BG, Lee SH, Emtiazi G, Kim W, Kim JH. 2016. Surface display of bacterial tyrosinase on spores of Bacillus subtilis usingCotE as an anchor protein. *J Basic Microbiol*., **56**: 1331–1337. https://doi.org/10.1002/jobm.201600203.

Jacques P. 2011. Surfactin and other lipopeptides from Bacillus spp. *In Biosurfactants Microbiology Monographs*, Soberon-Chavez G, ed., Volume 20, Chapter 3, pp. 57-91, Springer.

Kanlayavattanakul M and Lourith N. 2010. Lipopeptides in cosmetics. *Inter J Cosmetic Sci.*, **32**: 1–8.

Kowall M, Vater J, Kluge B, Stein T, Franke P, Ziessow D. 1998. Separation and characterization of surfactin isoforms produced by *Bacillus subtilis* OKB 105. J Colloid Interface Sci., **204**:1–8.

Kunst F, Ogasawara N, Moszer I, Albertini AM, Alloni G, Azevedo V, Bertero MG, Bessieres P, Bolotin A, and other authors. 1997. The complete genome sequence of the Gram-positive bacterium *Bacillus subtilis*. *Nature.*, **390**: 249–256.

Leclere V, Bechet M, Adam A, Guez J-S, Wathelet B, Ongena M, Thonart P, Gancel F, Chollet-Imbert M, Jacques P (2005) Mycosubtilin overproduction by Bacillus subtilis BBG100 enhances the organism's antagonistic and biocontrol activities. Appl Envirom Microbiol 71:4577-4584

Li Y, Héloir MC, Zhang X, Geissier M, Truvelot S, Jacquens L, Henkel M, Su X, Fang X, Wang Q and Adrian M. 2019. Surfactin and fengycin contribute to the protection of a Bacillus subtilis strain against grape downey mildw by both direct and defence stimulation. *Mol Plant Pathol.*, **20(8)**: 1037-1050.

Marahiel MA. 1997. Protein templates for the biosynthesis of peptide antibiotics. *Chem Biol.*, **4**: 561-567.

Mohamed SAH, Abd-El-Aal SKh, Moawad SS and Attallah AG. 2023.Genetic improvement of some microorganisms to increase the effect of bio-control on the potato tuber moth, *Phthorimaea operculella* (Zeller) (Lepidoptera: Gelechiidae). *Egy J Biolog Pest Con*., **33(12)**: 1-10.

Mohamed SAH, Ibrahim SA, Kh, Soliman A, Abd-El-Aal S Kh, Moawad SS and Attallah AG. 2016. Genetic Improvement of Some Microorganisms That Naturally Colonize of Tomato Plants to Increase the Effect of Bio-Control on Tuta absoluta. *Res J Pharma Biolog Chemi Sci*., **7**:1502-1518.

Mohamed SAH, Ameen HH, Elkelany US, El-Wakeel MA, Hammam MM A. and Soliman GM. 2021. Genetic improvement of Pseudomonas aeruginosa and Bacillus cereus for controlling root knot nematode and two weeds under laboratory conditions. *Jordan J Biolog Sci*., 14(4) 859 – 865.

Moon JH, Ajuna HB, Won SJ, Choub V, Choi SI, Yun JY and Ahn YS. 2023. Entomopathogenic Potential of *Bacillus velezensis* CE 100 for the Biological Control of Termite Damage in Wooden Architectural Buildings of Korean Cultural Heritage. *Int J Mol Sci.*, **24(9)**: 8189.

Mukherjee K and Vilcinskas A. 2018. The entomopathogenic fungus Metarhizium robertsii communicates with the insect host Galleria mellonella during infection. *Virulence.*, **9(1)**: 402–413. https:// doi. org/ 10. 1080/ 21505 594. 2017. 14051 90.

Mulligan CN, Yong RN, Gibbs BF. 2001. Heavy metal removal from sediments by biosurfactants. *J Hazard Mater.*, **85**: 111–125.

Negi R, Sharma B, Kaur S, Kaur T, Khan SS, Kumar S and Yadav AN. 2023. Microbial antagonists: diversity, formulation and applications for management of pest–pathogens. *Egy J Biolog Pest Cont.*, **33(1)**: 105

Neilan BA, Dittmann E and Rouhiainen L. 1999. Non-ribosomal peptide synthesis and toxigenicity of Cyanobacteria. *J Bacteriol*., **181**: 4089- 4097.

Neurath H and Walsh KA. 2011. Proc. Natl. Acad. Sci. U. S. A. 73, 3825–3832. Oda, K., (2012). New families of carboxyl peptidases: serine carboxyl peptidases and glutamic peptidases. *J Biochem*., **151**: 13–25.

Ongena M and Jacques P. 2008. Bacillus lipopeptides: versatile weapons for plant disease biocontrol. *Trends in Microbiol.*, **16**: 115-125.

Peypoux F, Bonmatin JM and Wallach J. 1999. Recent trends in the biochemistry of surfactin. *Appl Microbiol Biotechnol.*, **51**: 553–563.

Rostami A, Hinc K, Goshadrou F, Shali A, Bayat M, Hassanzadeh M, Amanlou M, Eslahi N, Ahmadian G. Display of B. pumilus chitinase on the surface of B. subtilis spore as a potential biopesticide. Pestic Biochem Physiol. 2017 Aug;140:17-23. doi: 10.1016/j.pestbp.2017.05.008. Epub 2017 Jun 3. PMID: 28755689.

Schaller KD, Fox SL, Bruhn DF, Noah KS and Bala GA. 2004. Characterization of surfactin from Bacillus subtilis for application as an agent for enhanced oil recovery. *Appl Biochem Biotechnol*., Spring:113-116:827-36. doi: 10.1385/abab:115:1-3:0827. PMID: 15054235.

Tapi A, Chollet-Imbert M, Scherens B and Jacques P. 2010. New approach for the detection of non-ribosomal peptide synthetase genes in Bacillus strains by polymerase chain reaction. *Appl Microbiol Biotechnol.*, **85**,1521–1531.

Vizcaino JA, Sanz L, Cardoza RE, Monte E and Gutierrez S. 2005. Detective of putative peptide synthetase genes in Trichoderma species: application of this method to the cloning of a gene from *T. haarzianum* CECT 2413. *FEMS Microbiol Lett.*, **244**: 139-148.

Yan X, Lu J, Ren M, He Y, Wang Y, Wang Z and He K. 2020. Insecticidal Activity of 11 Bt toxins and 3 Transgenic Maize Events Expressing Vip3Aa19 to Black Cutworm, *Agrotis ipsilon* (Hufnagel). *Insects.*, **27:11(4)**: 208. doi: 10.3390/insects11040208. PMID: 32230856; PMCID: PMC7240488.PMC10019718.

Yang H, Liu Y, Ning Y, Wang C, Zhang X, Weng P and Wu Z. 2020. Characterization of an intracellular alkaline serine protease from Bacillus velezensis SW5 with fibrinolytic activity. *Current Microbiol.*, **77**: 1610-1621.

Yu YY, Zhang YY, Huang TX, Tang SY, Jin Y, Mi DD, Zheng Y, Niu DD, Guo JH and Jiang CH. 2023. Kurstakin triggers multicellular behaviors in Bacillus cereus AR156 and enhances disease control efficacy against rice sheath blight. *Plant disease.*, **107 (5)**: https://doi.org/10.1094/PDIS-01-22-0078-RE.

Zhang J, Li H, Tan J, Wei P, Yu S, Liu R and Gao J. 2019. Transcriptome profiling analysis of the intoxication response in midgut tissue of *Agrotis ipsilon* larvae to *Bacillus thuringiensis* Vip3Aa protoxin. *Pestic Biochem Physiol.*, **160**: 20–29. https://doi.org/10.1016/j.pestbp.2019.06.001

Zhang X, Al-Dossary A, Hussain M, Setlow P and Li J. 2020. Applications of Bacillus subtilis spores in biotechnology and advanced materials. *Appl Environm Microbiol*, **86(17)**: e01096-20.

Zhang Y, Hu J, Wang J, Liu C, Liu X, Sun J and Wu Y. 2023. Purification and characteristics of a novel milk-clotting metalloprotease from *Bacillus velezensis* DB219. *J Dairy Sci*, **106(10)**: 6688-6700.

JJBS

Volume 17, Number 4,December 2024
ISSN 1995-6673
Pages 705 – 713
https://doi.org/10.54319/jjbs/170413

Jordan Journal of Biological Sciences

Impact of Algal Extract on Quorum Sensing and Biofilm Formation genes of Multidrug-resistant *Staphylococcus aureus* and *Pseudomonas aeruginosa*

Abdulilah S Ismaeil[1,*]; Janan J Toma[2]; Nishtiman S Hasan[1]; Akhter A Ahmed[1]; Muhsin J Abdulwahid[1]

[1]*Department of Biology, College of Science, Salahaddin University, Erbil/ Iraq;* [2]*Department of Environmental Sciences and Health, College of Science, Salahaddin University, Erbil/ Iraq.*

Received: February 23, 2024; Revised: July 27, 2024; Accepted: August 4, 2024

Abstract

Nowadays, bacteria become resistant to different types of drugs posing a significant global health challenge; therefore, scientists are constantly searching for new alternatives to combat them. Algae have been recognized as a significant supply of biological components and have the capacity to function as valuable resources in the fight against bacterial infections. This investigation assessed the activities of two types of blue-green algae against multidrug resistant pathogenic *Pseudomonas aeruginosa* and *Staphylococcus aureus*. The efficacy of three solvents (water, diethyl ether and acetone) utilized in the extraction of two algae, *Chlorella vulgaris* and *Spirulina platensis*, was tested to show the effectiveness on both bacterial virulence and quorum sensing genes on the level of expression. Results emphasized that acetone and diethyl ether fractions of *Chlorella vulgaris* were effective at 25mg/ml. However, both tested pathogenic bacteria showed more resistance against *Spirulina platensis* fractions. Biofilm formation by *Staphylococcus aureus* was reduced significantly by diethyl ether fraction of *Chlorella vulgaris, w*hile the reduction of formation of biofilm in *Pseudomonas aeruginosa* was more efficient by *Spirulina platensis* acetone fraction. *MvfR* and *ndvF* genes of *Pseudomonas aeruginosa* downregulated when treated with diethyl ether fraction of both *Chlorella vulgaris* and *Spirulina platensis*. Interestingly, all algal extracts showed a remarkable effect on *icaC, hla* and *RNAIII* genes of *Staphylococcus aureus.* According to the findings, algal extracts can be utilized to interrupt growth and encourage the creation of biofilms and pathogenicity, downregulation of QS-related and biofilm-associated genes in MDR strains.

Key words: algal extract, antibiotic resistance, quorum sensing, virulence.

1. Introduction

Antibiotics were introduced in the last century, and they are considered as one of the most significant medical innovations ever (Ghosh *et al*., 2020). Antibiotics, which were discovered more than seventy years ago, saved countless lives by treating bacterial diseases that were previously fatal (Uddin *et al.*, 2021, Laws et al., 2019, Ventola, 2015). Antibiotic resistance has developed due to the overuse of antimicrobials for an extended period of time as well as the excessive use of these medicines, inadequate infection control measures, and a lack of innovation in pharmaceutical development research (Aslam *et al*., 2021, Ventola, 2015). In 2019, the agency World Health Organization (WHO) released a report stating that antimicrobial resistance was responsible for a minimum of at least 700,000 deaths worldwide annually. If this current situation is not addressed, it is predicted that by 2050, the number would increase to 10 million (Nji et al., 2021). The proliferation and dissemination of drug-resistant pathogens in countries with low to middle- income levels may have detrimental consequences for public health (Van Boeckel *et al*., 2019). Given that over 70% of pathogenic bacteria exhibit resistance to at least one kind of antibiotic, it is imperative to develop innovative techniques to tackle this worldwide problem (Laws *et al*., 2019 , Uddin *et al*., 2021). Reducing the harmful effects of bacteria by focusing on the quorum sensing (QS) offers a possible alternative for inhibiting or suppressing the proliferation of disease-causing bacteria (Tang *et al*., 2020). QS is a mechanism by which microorganisms communicate with each other through the activation of multiple genes, primarily those that are involved in biofilm formation and virulence factors synthesis. The control of this process relies on the formation and detection auto-inducers, which are signals that depend on population density. Further, as a possible new treatment approach for bacterial infections, "quorum quenching" is being studied. This term describes the interruption of signaling in several biological processes (Fleitas Martínez *et al*., 2019). Several plants exhibited a quorum quencher behaviors against pathogenic bacteria, for instance thyme and cinnamon (Ahmed *et al.* , 2023). Furthermore, recently nanoparticles have also been

* Corresponding author. e-mail: abdulilah.ismaeil@su.edu.krd.

reported to work as anti -bacterial QS agents as conveyed by Hasan and Ahmed (2023).

Microbial biofilm development, swarming, and maturity are all dependent on the QS system. During the formation of a biofilm, cellular communication initiates as chemical signaling reaches a particular concentration threshold. The chemical signals stimulate the production of substances outside the polymer, which triggers the activation of genes responsible for virulence and infectiousness. Biofilms consist of a wide range of bacteria that adhere to surfaces, generate an extracellular matrix using polymeric substances, and become embedded within it. The QS behavior of biofilm-linked bacteria contributes to multidrug resistance (Boominathan *et al*., 2022). Algae are nonvascular, photosynthetic plants that inhabit a variety of aquatic environments, their bioactive compounds possess antimicrobial activity (Toma and Aziz, 2023). Both *Chlorella vulgaris* and *Spirulina platensi*s are unicellular, freshwater organisms that contain bioactive substances like proteins, vitamins, sterols, pigments, long-chain polyunsaturated fatty acids, and other substances (Hussein *et al*., 2018). Methicillin-resistant *Staphylococcus aureus* (MRSA) is the most prevalent pathogen in humans. It forms biofilms which significantly increase the risk of morbidity and mortality from infections acquired in hospitals and communities. *S. aureus*, an opportunistic pathogen, might potentially lead to a variety of diseases, such as endocarditis, acute respiratory infection, septicemia, osteomyelitis, and skin and soft tissue lesions. The majority of the pathogenicity-related gene regulation in *S. aureus* occurs via the action of small RNA and RNAIII, which are part of the agr quorum-sensing system (Huntzinger *et al*., 2005). RNAIII is a significant small regulatory RNAs (sRNAs) which regulates the expression of genes by binding to target mRNAs in an antisense manner (Gupta *et al*., 2015). *S. aureus* produces additional virulence factors, including exotoxins like alpha-hemolysin (also referred to as α-toxin) that is directed by *hyl* gene (Chen *et al*., 2015). The establishment of biofilm by pathogens is the primary determinant in the long-lasting nature of chronic infection (Guilhen *et al.*, 2017). The major obstacle to effectively treating *S aureus* infections is the formation of biofilm, which highlights the bacteria's resistance (Lee *et al*., 2020). The production of polysaccharide intercellular adhesin (PIA) and an export protein, known as *IcaC*, regulate biofilm development in *S. aureus*. The production of PIA is facilitated by proteins that are encoded by the ica ADBC operon, which is located within the ica locus *(Cramton et al*., 1999). *Pseudomonas aeruginosa*, an opportunistic pathogen, can grow biofilms on a wide range of substrates, allowing bacteria to adhere to and proliferate on medical equipment. The high rate of morbidity and mortality among hospitalized patients is attributed to this factor (Lalancette *et al.*, 2017, Maurice *et al*., 2018). The generation of biofilms is influenced by multiple genetic mechanisms, but not in the growth of planktonic cells during the exponential phase paraphrase the second part after the comma with linking it with this paraphrased first part, though these same mechanisms do not affect the growth of planktonic cells during the exponential phase. The rise of biofilm resistance in *P. aeruginosa* is facilitated by these mechanisms as well. The gene ndvB is essential for one of these pathways through an unidentified mechanism (Beaudoin *et al*., 2012). The virulence factor transcriptional regulator MvfR, encoded by *mvfR*, is essential for full virulence in *P. aeruginosa*. It facilitates the production of 4-hydroxy-2-alkylquinolines (HAQs), including the quinolone signal, PQS (pseudomonas quinolone signal), and regulates several QS-controlled virulence factors (Déziel *et al*., 2005, Xiao *et al*., 2006). *MvfR* represents a valuable target for treating the majority of infections associated with *P. aeruginosa*. This is because it regulates the virulence functions that are crucial for both acute and long-term infections (Kitao *et al*., 2018, Cao *et al*., 2001). On top of that, it produces phenazines, which are redox-active pigments that have the ability to change antibiotic susceptibility through their effects on metabolic flux, redox balancing, and gene expression (Price-Whelan *et al*., 2007). The research aims to assess the influence of algal extracts on the expression of QS, virulence and biofilm-related genes in pathogenic bacteria that are resistant to multiple drugs.

2. Materials and techniques

2.1. Algal gathering and identification

In the current study, samples taken from springs in the Shaqlawa district (Aquban and Sarkand villages), which are positioned 32 kilometers to the northwest of Erbil city, were found to contain *Spirulina platensis* and *Chlorella vulgaris*. The taxonomic determination of both algal species was established by analyzing their morphological characteristics using several scientific keys for algal identification (Brook *et al*., 2011, Wehr *et al*., 2015).

2.2. Algae species isolation

The necrotic sections of algae samples were excised. The algae samples were separated and purified using the plate technique method. This method involves placing a tiny bit of the diluted microbial mixture into the middle pf a petri dish. While the petri dish is being spun, a sterile L-shaped bent glass rod is used to spread it evenly over the surface. As the procedure progresses, the curved glass rod deposits individual cells onto the agar surface. After that, a glass container was used to incubate the algae sample. Algal growth was achieved using BG-11(HI Media Laboratories, PvtLtd-India) medium in a glass container with the medium volume of 5 liters. Subsequently, the specimens were subjected to a 14-day incubation period at a temperature of 25 ± 2°C. During this period, they were exposed to a light intensity ranging from 3000 to 5000 lux for 16 hours in the light and 8 hours in the dark. The pH level during the incubation was maintained at 8.2. In order to obtain algae species that are free from impurities, this procedure was carried out more than once. After that, the resultant product was placed in an incubator with 25 ml of BG-11 medium and left to incubate for 14 days under identical conditions in order to generate an algal inoculum. The moss was isolated using streak plating method (Hussein *et al*., 2018).

2.3. Preparation of biomass and harvesting

A 100 ml beaker containing BG-11 medium was supplemented with 25 ml of isolated algae, which were then incubated for 14 days under the same conditions as previously. Following that, the culture medium was moved to a 500 ml glass beaker containing 100 ml of BG-11

medium. After that, it was kept for an additional 14 days during incubation. These procedures were repeated until the algae growth in the container, which was covered with cotton swabs, reached a volume of 4 liters. At this stage, rubber was utilized to provide air (Richmond, 2008). The algae mass was collected on day 20 by centrifuging it for ten minutes at 4000 rpm (Elnabris *et al*., 2013). Afterward, the algae samples were cleaned in sterile water and dried in an oven maintained at a temperature range of 38 to 40°C. Weighed samples of algae were then stored in a refrigerator (Hassan *et al*., 2020).

2.4. Bacterial isolates and sources

A total of 20 clinical strains of *P. aeruginosa* and *S. aureus* were gathered from various microbiology laboratories in the hospitals of Erbil city, located in Kurdistan, Iraq. The clinical isolates of *S. aureus* were re-cultivated on Mannitol salt agar and Blood agar (Merck, Germany), while *P. aeruginosa* was cultured on Cetrimide agar (acumedia, Germany). Plates were incubated aerobically overnight at 37ºC. In order to identify the individual colonies, a variety of biochemical and conventional diagnostic assays were conducted using previously established standard methods: catalase, coagulase, DNase and hemolysin tests on blood agar for identifying *S. aureus* and oxidase, catalase, motility and pigment production assays for identifying *P. aeruginosa* (Tille, 2021), The bacterial isolates were verified using the automated Vitek 2 system (BioMérieux, France) and kept at 4°C and 70°C in nutrient broth with 25% glycerol for future research purposes. The method of disc diffusion was utilized to determine the antibiotic sensitivity of strains of bacteria, this method was uesd in accordance with established guidelines set by the Laboratory and Clinical Sciences Institute (CLSI) (CLSI, 2022). Ciprofloxacin (5µg), ceftaroline (30µg), chloramphenicol (30µg), clindamycin (10µg), gentamicin (10µg), linezolid (10µg), oxacillin (30µg), penicillin (10µg), rifampicin (15µg) and trimethoprim/sulfamethoxazole (20µg) from Oxoid/UK company were used for *S. aureus*. Amikacin (30µg), cefepime (10µg), ceftazidime (10µg), ciprofloxacin (5µg), colistin (15µg), imipenem (30µg), meropenem (30µg), piperacillin (10µg) and tobramycin (30µg) from Oxoid/UK company were used for *P. aeruginosa*. The isolates with the highest resistance were chosen to evaluate inhibitory capacity of the algal extracts. Two independent samples were examined at various time points.

2.5. Algal extracts preparation

An 8-hour soxhlet extraction was performed using 300 ml each of water, diethyl ether and acetone to extract approximately 30 grams of finely ground powder. A duration of approximately three days of incubation at a temperature of 37°C is required to facilitate the evaporation of the extracted products. The extracts were dissolved in dimethyl sulfoxide (DMSO). A volume of 5 ml of DMSO was used to dissolve 1 g of each extract, resulting in a stock solution with a concentration of 200 mg/ml. The samples were then stored at -4°C until they were used (Pina-Pérez *et al.* , 2017).

2.6. Minimum inhibitory and sub-inhibitory concentrations

The algal extracts were tested against the clinical specimens of *P. aeruginosa* and *S. aureus* using broth microdilution method to determine the minimum inhibitory concentration (MIC) of the algal extracts (Wiegand *et al*., 2008). A 96-well polystyrene microtiter plate (MTP) was filled with 100 µL of nutrient broth (NB) containing extracts at concentrations ranging from 0 to 50 mg/ml, and 10 µl of stationary phase cells with an OD550 of 0.5. At 37°C, the aerobic cultures were incubated for one day. The MIC was established as the minimum detectable concentration. The MIC was established as the minimum detectable concentration. The evaluation of anti-biofilm and anti-virulence characteristics within bacterial isolates involved considering concentrations below the minimum inhibitory concentrations (MICs), known as sub-inhibitory concentrations (SICs). Three biological samples were analyzed at different occasions.

2.7. Sub-MIC impact of algae extracts on bacterial strains' biofilm

The impact of algal extract on the production of biofilm was evaluated using polyvinyl chloride biofilm formation assay. Briefly, 24-hour cultures of the isolates of *P.aeruginosa* and *S. aureus* were re-suspended in new and fresh NB medium and cultivated at 37 °C for a full day in a static environment, both with and without SICs of the algal extract. After removing the liquid cultures from the plate wells, PBS was used three times to rinse the wells. A solution of 1% crystal violet dye was added to the biofilm, and then the extra dye was washed away with distilled water. The dye was subsequently dissolved with ethanol. The binding affinity to an abiotic surface was measured using an Elisa reader (Epson, Biotek, UK) at a wavelength of 490 nm (Ismaeil & Saleh, 2019). The standard error was calculated after three biological specimens were subjected to separate analysis.

2.8. Extracting the RNA and quantifying of QS and biofilm-associated genes

Algal extracts at SIC values were assessed using real-time polymerase chain reaction (PCR) for their impact on the expression levels of the *icaC, hla,* and *RNAIII* genes of *S. aureus*, and the *ndvr, phzf,* and *mvfr* genes of *P. aeruginosa.* The manufacturer's instructions were followed to extract total RNA from bacteria exposed to the plant extract as well as from untreated bacteria that were utilized as a control (Total RNA Kit, Favorgen Biotech, Taiwan). The AddScript cDNA synthesis kit was used to reverse transcribe the isolated RNA into cDNA in accordance with the manufacturer's instructions. RealQ Plus 2x Master Mix Green (Ampliqon, Denmark) was used to produce RT-PCR reactions in the PCRmax Eco 48 RT-PCR device. Candidate genes were analyzed by qPCR using the primer sequences listed in table (1), and the results were estimated using ΔCt technique (Livak and Schmittgen, 2001).

Table 1. A list containing the genes and the corresponding primer sequences

Gene	Primer Sequence (5′–3′)		
	Frontward	Reversal	Ref.
ndvr	GGCCTGAACATCTTCTTCACC	GATCTTGCCGACCTTGAAGAC	(Ismail and Altaai, 2021)
Phzf	AACTCCTCGCCGTAGAAC	ATAATTCGAATCTTGCTGCT	(Nowroozi *et al*., 2012)
mvfr	GTTTCGACGAATGCTCGGTTG	GACAAGGTGCTCTTCGTGGA	(Faisal *et al*., 2020)
RNAIII	TTTATCTTAATTAAGGAAGGAGTGA	TGAATTTGTTCACTGTGTCG	(Bezar *et al.*, 2019)
hla	GTACAGTTGCAACTACCTGA	CCGCCAATTTTTCCTGTATC	(Bezar *et al*., 2019)
icaC	CATGAAAATATGGAGGGTGG	TCAAACTGATTTCGCCCACCG	(Gowrishankar *et al*., 2016)

2.9. Statistical Analysis

The obtained data were analysed using Graph-pad Prism 8.0 software. One-way analysis of variance (ANOVA) method was employed to conduct multiple comparisons. The data are presented as mean±SE.

3. Results

The effect of algal extracts on MDR pathogens was determined by measuring the MIC using the MTP method. The results demonstrated that the most effective fraction was *Chlorella vulgaris* extracted by acetone against *S. aureus*, *showing* an MIC of 25 mg/ml (Table 1). In contrast, the most potent extract against *P. aeruginosa* was the diethyl ether fraction of *Chlorella vulgaris*, with an MIC of 25 mg/ml (Table 2).

Table 1. Minimum Inhibitory Concentrations (MICs) and Sub-MICs of *Chlorella vulgaris* and *Spirulina platensis* extracts against *Staphylococcus aureus*

Algal extracts	MIC(mg/ml)	SIC(mg/ml)
Ch-1	40	30
Ch-2	30	20
Ch-3	25	15
S-1	40	30
S-2	30	15
S-3	35	20

Ch-1; aqueous, *Ch-2*; diethyl ether, *Ch-3*; acetone extract of *Chlorella vulgaris, S-1*; aqueous, *S-2*; diethyl ether, *S-3*; acetone extract of *Spirulina platensis*

Table 2. Minimum Inhibitory Concentrations (MICs) and Sub-MICs of Chlorella vulgaris and *Spirulina platensis* extracts against *Pseudomonas aeruginosa*

Algal extracts	MIC(mg/ml)	SIC(mg/ml)
Ch-1	45	30
Ch-2	25	15
Ch-3	30	20
S-1	45	30
S-2	35	25
S-3	40	30

Ch-1; aqueous, *Ch-2*; diethyl ether, *Ch-3*; acetone extract of *Chlorella vulgaris, S-1*; aqueous, *S-2*; diethyl ether, *S-3*; acetone extract of *Spirulina platensis*According to our data, all fractions of *Chlorella vulgaris* demonstrated a significant decrease in the amount of biofilm in both tested bacteria (*S. aureus* & *P. aeruginosa*), as shown in figures (1 & 2).

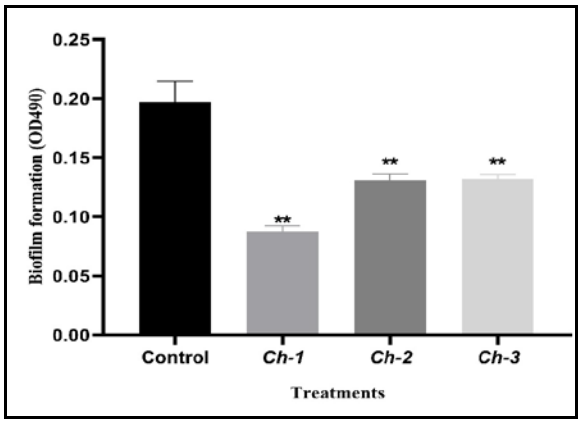

Figure 1. An enumerative analysis of the reduction in *S. aureus* biofilm caused by SICs of algal extracts, measured by absorbance at 490 nm. Data are presented as mean±SE. **Significance at P≤ 0.01. Ch-1; diethylether, Ch-2; acetone, Ch-3; aqueous extract of Chlorella vulgaris.

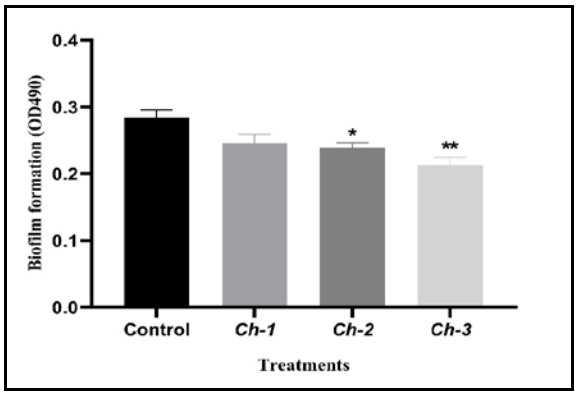

Figure 2. Quantitative assessment of *P. aeruginosa* biofilm suppression using SIC of algal extracts, measured by absorbance at 490 nm. Data are presented as mean±SE. *Significance at P≤ 0.05, **Significance at P≤ 0.01. Ch-1; diethylether, Ch-2; acetone, Ch-3; aqueous extract of Chlorella vulgaris.Furthermore, the fractions of *Spirulina platensis* exhibited a significant decrease in developing a biofilm in both tested bacteria (Figures 3 & 4).

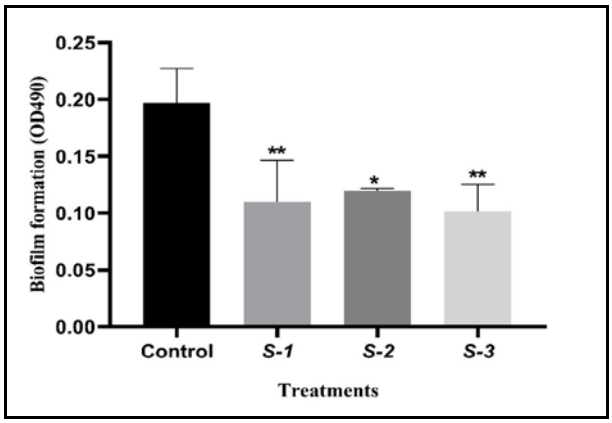

Figure 3. Quantitative assessment of *S. aureus* biofilm suppression using SIC of *algal* extracts, measured by absorbance at 490 nm. Data are presented as mean±SE. *Significance at P≤ 0.05, **Significance at *P*≤ 0.01. *S-1*; diethylether, *S-2*; acetone, *S-3*; aqueous extract of *Spirulina platensis*

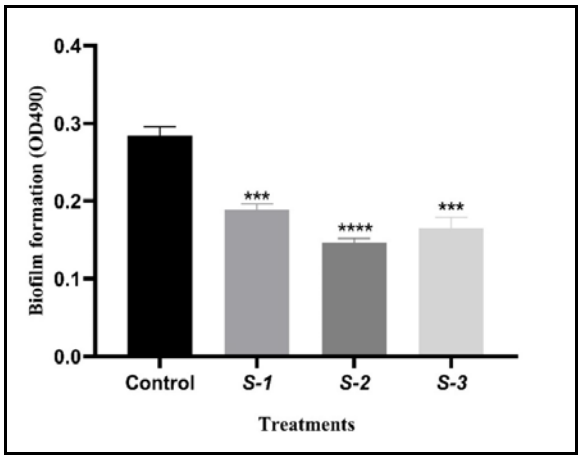

Figure 4. Quantitative assessment of *P. aeruginosa* biofilm suppression using SIC of *algal* extracts, measured by absorbance at 490 nm. Data are presented as mean±SE. ***Significance at P≤ 0.001, ****Significance at *P*≤ 0.0001. *S-1*; diethylether, *S-2*; acetone, *S-3*; aqueous extract of *Spirulina platensis*.The gene expression results showed that fractions of *Chlorella vulgaris* had different impacts on the downregulation of biofilm and QS genes in *P. aeruginosa & S. aureus.* This is illustrated in figures (5 & 6), with a particular impact observed on the *MvfR* gene in *P. aeruginosa* and *icac, hla & RNAIII* genes in *S. aureus.* Moreover, the fractions of *Spirulina platensis* suppressed the expression of genes associated with both biofilm formation and QS, specifically the *ndvF* gene in *P. aeruginosa* and the *icaC and hla* genes in *S. aureus* (Figures 7 &8).

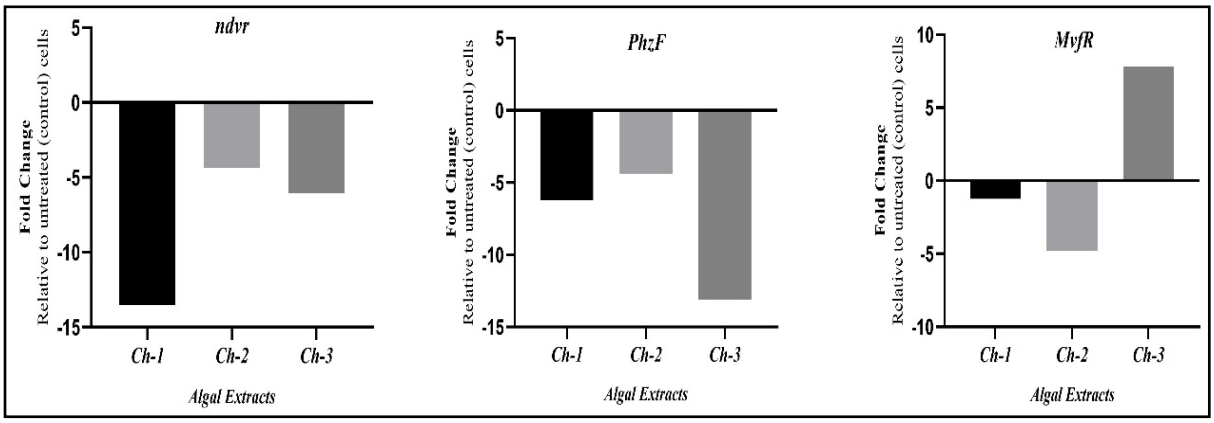

Figure 5. Transcriptional profiles of ndvF, mvfR and phzF genes in *P. aeruginosa* strains after exposure to Chlorella vulgaris SICs extracts. RT-PCR was utilized to calculate the transcriptional profiles. Ch-1; diethylether; Ch-2; acetone; Ch-3; Chlorella vulgaris aqueous extract.

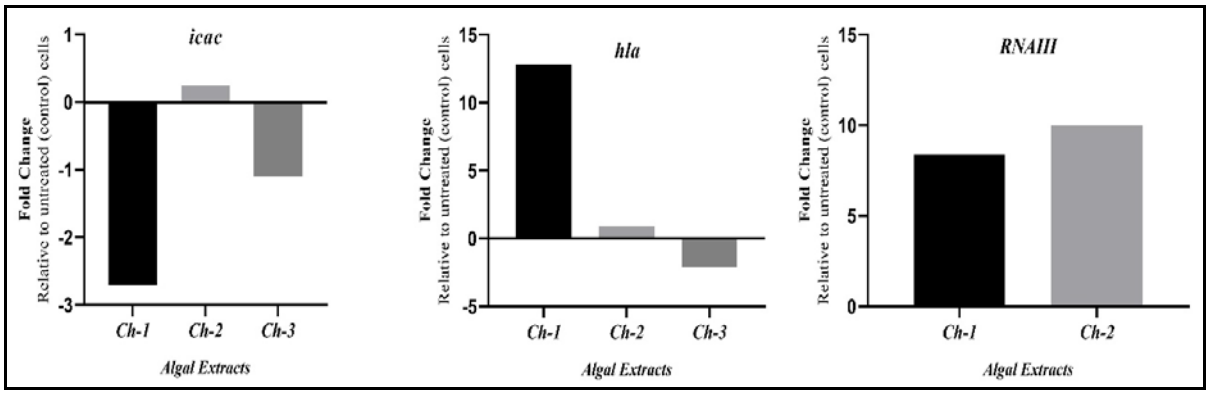

Figure 6. Transcriptional patterns of *S. aureus* isolates treated with SICs of *Chlorella vulgaris* extracts in terms of *icaC, hla*, and *RNAIII* gene expression. By using RT-PCR, transcriptional profiles were quantified. Ch-1; diethylether; Ch-2; acetone; Ch-3; *Chlorella vulgaris* aqueous
extract.

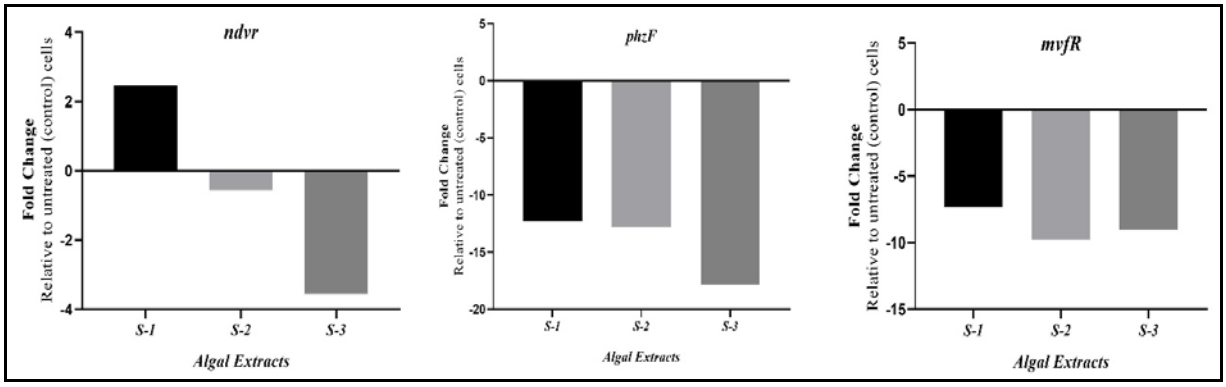

Figure 7. Transcriptional patterns of *P. aeruginosa* isolates treated with *Spirulina platensis* SICs for the *ndvF*, *mvfR*, and *phzF* genes. By using RT-PCR, transcriptional profiles were quantified. S-1; diethylether; S-2; acetone; S-3; *Spirulina platensis* aqueous extract.

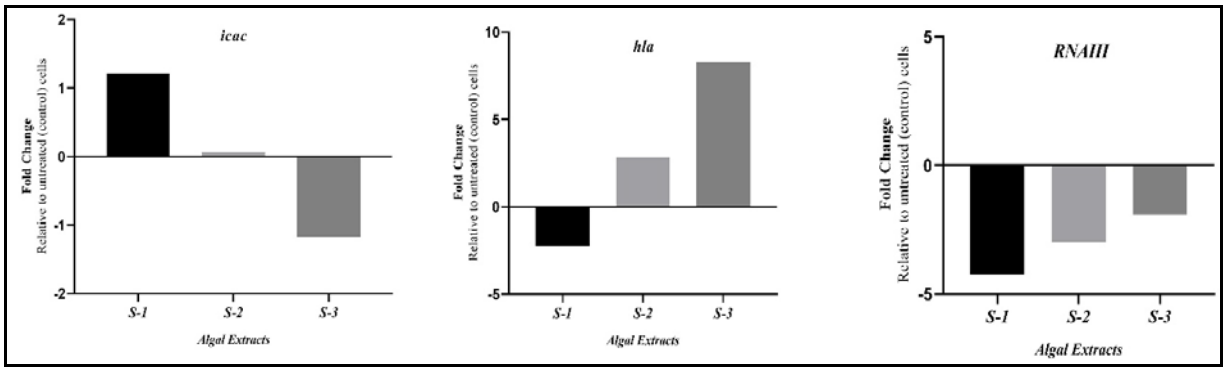

Figure 8. Transcriptional patterns of *S. aureus* isolates treated with *Spirulina platensis* extract-derived SICs for the *icaC, hla*, and *RNAIII* genes. By using RT-PCR, transcriptional profiles were quantified. S-1; diethylether; S-2; acetone; S-3; *Spirulina platensis* aqueous extract.

4. Discussion

Drug resistance is currently recognized as a serious issue that threatens not just worldwide health but food security and development as well (Nji *et al.*, 2021). *S. aureus* and *P. aeruginosa* are both antibiotic-resistant bacteria that generate concerns for human health. (Harding *et al*., 2018).

It has been proven that natural products possess a more potent effect on the pathogenicity of bacterial infections compared to traditional bacteriostatic or bactericidal medications. As a result, new methods for treating bacterial infections were developed. In order to combat diseases that do not respond to standard therapies, it is worth investigating the direct impact on the genes that control virulence activation in a more direct manner (Jiang *et al.*, 2019). Instead of focusing on bactericidal and bacteriostatic methods, researchers have begun to investigate whether QS inhibitory techniques can reduce bacterial pathogenicity in the face of multidrug-resistant bacteria (Yang *et al*., 2015).

One can effectively reduce the factors that contribute to bacterial infections by using a method that involves regulating bacterial QS signaling with QS-targeted substances. In recent times, there has been an increasing curiosity in a unique treatment that does not rely on antibiotics. This treatment has gained attention due to its capacity to prevent infection, inhibit the expression of genes linked to pathogens and reduce the likelihood of bacterial cells developing drug resistance (Jiang *et al*., 2019).

The search for remedies that are natural using innovative methods to prevent and/or treat life-threatening diseases maybe driven by the maritime environment, which is abundant in biodiversity (Guzzo *et al*., 2020). It is believed that marine organisms like algae could provide a variety of bioactive chemicals that could be used to combat the growth of antibiotic-resistant bacteria and inhibit biofilm formation.

Consequently, the objective of this study was to evaluate the antibacterial efficacy of two distinct types of algae, such as *Spirulina platensis* and *Chlorella vulgaris*, and to determine how they affect the virulence and QS-related genes at the level of expression. Results showed that the best MICs of extracts from *Chlorella vulgaris* and *Spirulina platensis* against *S. aureus* were 25 mg/ml and 30 mg/ml, respectively, for acetone and diethyl ether extracts (Table 1). The highest MICs for each of *Chlorella vulgaris* and *Spirulina platensis* extracts against *P. aeruginosa* were observed with diethyl ether (25mg/l and 35mg/l, respectively) (Table 2). The antibacterial properties of medications derived from these algae species offer some unique benefits in preventing bacterial growth, thereby enhancing vector infection control without any adverse effects (Syed *et al*., 2015). Many researchers have deduced the effective antimicrobial action of blue-green algae extracts against different pathogenic bacteria; most compounds derived from these genera are expected to be considered as antimicrobials for medical use, as they are safe for human health and the environment in which they live *(Marrez et al*., 2021). In addition, the data of this research demonstrate that the inhibitory action of *Chlorella vulgaris* extracts was much greater than that of *Spirulina platensis* extracts. This could be due to variations in the concentration and purity of the chemical substances found in each, as was demonstrated by previous research (Alghanmi and Omran, 2020).

Globally, a wide range of pathogenic bacteria present in the environment and possess the ability to form biofilms. Biofilms are physiological states where bacteria attach to a substrate by the formation of a DNA-, polysaccharide-, and protein-based extracellular matrix (Tsuneda *et al*., 2003). Hence, the development of bacterial biofilms is regarded as critical determinant in the pathogenicity of infections, since these biofilms provide comprehensive shielding from both the host immune system and the desired impact of therapeutic drugs (Vestby *et al*., 2020). The findings of reduced biofilm formation with extracts from both *Chlorella vulgaris* and *Spirulina platensis* against both bacterial strains are promising. With an 86% reduction in biofilm formation for *S. aureus* and an 81% reduction for *P. aeruginosa*, the acetone extract of *C. vulgaris* demonstrated the highest efficacy among the extracts. Consistent with previous studies that examined algal extracts against these bacteria, these results indicate that they are effective. An example of this is the 79% and 82% reduction in biofilm formation for *P. aeruginosa* and *S. aureus*, respectively, that was observed in a study using the methanol extract of *C. vulgaris* (Afzal *et al*., 2023). Another study revealed that the ethyl acetate extract derived from *Spirulina* sp. exhibited a significant reduction of 85% in biofilm formation by *S. aureus* and 80% by *P. aeruginosa* (Monteiro *et al*., 2021).

The study evaluated how algal extracts affect the expression levels of genes associated with biofilm development and QS, processes regulated by various signaling molecules in bacteria. The data showed that the extracts decreased the expression of genes associated with these processes in both bacterial species. Specifically, genes such as *MvfR* and ndvr in *P. aeruginosa*, and *icac*, *hla*, and *RNAIII* in *S. aureus*, which encode proteins responsible for regulating the production of virulence factors like exopolysaccharides, pyocyanin, rhamnolipids, intercellular adhesion, hemolysin, and toxins, were found to be downregulated by the algal extracts (Asimakis *et al.*, 2022). The downregulation of these genes suggests that the algal extracts interfere with the signaling pathways that regulates the formation of biofilm and QS in bacteria, hence diminishing their capacity to induce infections and withstand the effects of antibiotics. Previous studies have shown that the methanol extract derived from the marine algae *Asparagopsis taxiformis* had both quorum quenching and antibacterial properties against *Serratia liquefaciens* (Jha *et al*., 2013). The lichen secondary metabolite evernic acid reduces *P. aeruginosa* virulence protein production by blocking the QS system (Gökalsın and Sesal, 2016). Quorum sensing inhibitors (QSIs) from plant-derived natural remedies that affected *P. aeruginosa* included sappanol, butein, and catechin-7-xyloside (C7X). These compounds demonstrated the ability to interact with QS regulators in *P. aeruginosa* (Zhong *et al*., 2020).

According to the results of this study, the biologically active substances derived from *Chlorella vulgaris* and *Spirulina platensis* exhibited antibacterial properties against both gram- negative and gram-positive bacteria (Hussein *et al*., 2018). Syed *et al*. (2015) reported that *Chlorella vulgaris* extracts contain bioactive materials like flavonoids, tannins, terpenoids, phenolic compounds, cardiac glycosides and saponins. Our findings align with those of Hussein *et al*., (2017) and Hussein *et al*., (2018).

The mechanisms underlying the antimicrobial, anti-biofilm and gene regulation effects of algal extracts can be multifaceted. Algal extracts may include bioactive substances directly disrupt bacterial cell membranes, interfere with QS signals, or modulate the expression of virulence genes. The specific compounds responsible for these effects could include secondary metabolites, polyphenols, terpenoids, and fatty acids, which have been previously documented for their antimicrobial and anti-biofilm properties. Moreover, the mode of action by which algal extracts modulate genes expression is not clear, but it may involve binding to or inhibiting receptors or enzymes involved in these pathways.

5. Conclusion

This study demonstrates that algal extracts have inhibitory effectiveness on bacteria growth and biofilms in *S. aureus* and *P. aeruginosa* and modulate their biofilm and QS-related gene expression. These results suggest that algae may serve as a good source of natural compounds for the development of adjuvants or novel antibacterial compounds. Additional researches are required to identify the active components of algal extracts and elucidate their mode of action at the molecular level.

Acknowledgment

We would like to sincerely thank Zahraa Farazdaq Hasan for her invaluable assistance as a language editor in refining the overall quality of this article.

References

Aafzal, S., Yadav, A. K., Poonia, A. K., Choure, K., Yadav, A. N. & Pandey, A. 2023. Antimicrobial therapeutics isolated from algal source: retrospect and prospect. *Biologia*, **78(2)**, 291-305.

Ahmed, A. A. , Abdulla, P. H. , Ismaeil, A. S. & Ali, S. B. 2023. Weakening of Virulence Factors and Biofilm in Salmonella Typhi by Medicinal Plants Extracts. *Biomed. & Pharmacol. J.*, **16(3)**, 1631-1639.

Alghanmi, H. A. & Omran, A. S. 2020. Antibacterial activity of ethanol extracts of two algae species against some pathogenic bacteria isolated from hospital patients. *EurAsia J BioSci*, **14(1)**.

Asimakis, E., Shehata, A. A., Eisenreich, W., Acheuk, F., Lasram, S., Basiouni, S., Emekci, M., Ntougias, S., Taner, G., May-Simera, H., Yilmaz, M. & Tsiamis, G. 2022. Algae and Their Metabolites as Potential Bio-Pesticides. *Microorganisms*, **10(2)**, 307.

Aslam, B., Khurshid, M., Arshad, M. I., Muzammil, S., Rasool, M., Yasmeen, N., Shah, T., Chaudhry, T. H., Rasool, M. H., Shahid, A., Xueshan, X. & Baloch, Z. 2021. Antibiotic Resistance: One Health One World Outlook. *Front Cell Infect Microbiol*, **11**, 771510.

Beaudoin, T., Zhang, L., Hinz, A. J., Parr, C. J. & Mah, T.-F. 2012. The biofilm-specific antibiotic resistance gene ndvB is important for expression of ethanol oxidation genes in Pseudomonas aeruginosa biofilms. *J. bacteriol.*, **194(12)**, 3128-3136.

Bezar, I. F., Mashruwala, A. A., Boyd, J. M. & Stock, A. M. 2019. Drug-like Fragments Inhibit agr-Mediated Virulence Expression in Staphylococcus aureus. *Sci. Rep.*, **9(1)**, 6786.

Boominathan, R., Devanesan, S., Alsalhi, M. S., Balasubramanian, A., Alkhalid, I. Z., Paul, P. & Singh, A. R. 2022. Quorum quenching action of marine red alga Halemenia durvillei on biofilm forming Gram negative bacterial isolates from contact lens. *Algal Research*, **64**, 693-706.

Brook, A. J., John, D. M. & Whitton, B. A. 2011. **The freshwater algal flora of the British Isles**: an identification guide to freshwater and terrestrial algae, Cambridge University Press.

Cao, H., Krishnan, G., Goumnerov, B., Tsongalis, J., Tompkins, R. & Rahme, L. G. 2001. A quorum sensing-associated virulence gene of Pseudomonas aeruginosa encodes a LysR-like transcription regulator with a unique self-regulatory mechanism. *Proc Natl Acad Sci*, **98(25)**, 14613-14618.

Chen, Y., Yeh, A. J., Cheung, G. Y., Villaruz, A. E., Tan, V. Y., Joo, H.-S., Chatterjee, S. S., Yu, Y. & Otto, M. 2015. Basis of virulence in a Panton-Valentine leukocidin-negative community-associated methicillin-resistant Staphylococcus aureus strain. *J. Infect. Dis.*, **211(3)**, 472-480.

CLSI 2022. **Performance Standards for Antimicrobial Susceptibility Testing**. Informational Supplement. CLSI document M100Ed32E. Wayne, PA: Clinical and Laboratory Standards Institute.

Cramton, S. E., Gerke, C., Schnell, N. F., Nichols, W. W. & Götz, F. 1999. The intercellular adhesion (ica) locus is present in Staphylococcus aureus and is required for biofilm formation. *Infec. Immun.*, **67**, 5427-5433.

Déziel, E., Gopalan, S., Tampakaki, A. P., Lépine, F., Padfield, K. E., Saucier, M., Xiao, G. & Rahme, L. G. 2005. The contribution of MvfR to Pseudomonas aeruginosa pathogenesis and quorum sensing circuitry regulation: multiple quorum sensing-regulated genes are modulated without affecting lasRI, rhlRI or the production of N-acyl-l-homoserine lactones. *Mol. Microbiol.*, **55(4)**, 998-1014.

Elnabris, K., Elmanama, A. & Chihadeh, W. 2013. Antibacterial activity of four marine seaweeds collected from the coast of Gaza Strip, Palestine. *Mesopot. J. Mar. Sci*, **28(1)**, 81-92.

Faisal, A. J., Ali, M. R. & Said, L. A. 2020. Co-existence of LasI, RhI, and Pseudomonas Quinolone Signal Quorum-sensing Genes in Clinical Pseudomonas aeruginosa Isolates. *Int. J. Drug Delivery Tech*, **10(3)**, 337-343.

Fleitas Martínez, O., Rigueiras, P. O., Pires, A. D. S., Porto, W. F., Silva, O. N., De La Fuente-Nunez, C. & Franco, O. L. 2019. Interference with quorum-sensing signal biosynthesis as a promising therapeutic strategy against multidrug-resistant pathogens. *Front. Cell. Infect. Microbiol*, **8**, 444-457.

Ghosh, D., Veeraraghavan, B., Elangovan, R. & Vivekanandan, P. 2020. Antibiotic Resistance and Epigenetics: More to It than Meets the Eye. *Antimicrob Agents Chemother*, **64**(2).

Gökalsın, B. & SESAL, N. C. 2016. Lichen secondary metabolite evernic acid as potential quorum sensing inhibitor against Pseudomonas aeruginosa. *World J Microbiol Biotechnol*, **32**, 1-7.

Gowrishankar, S., Kamaladevi, A., Balamurugan, K. & Pandian, S. K. 2016. In Vitro and In Vivo Biofilm Characterization of Methicillin-Resistant Staphylococcus aureus from Patients Associated with Pharyngitis Infection. *Biomed Res Int*, 2016, 1289157.

Guilhen, C., Forestier, C. & Balestrino, D. 2017. Biofilm dispersal: multiple elaborate strategies for dissemination of bacteria with unique properties. *Mol. Microbiol.*, **105(2)**, 188-210.

Gupta, R. K., Luong, T. T. & Lee, C. Y. 2015. RNAIII of the Staphylococcus aureus agr system activates global regulator MgrA by stabilizing mRNA. *Proc Natl Acad Sci*, **112(45)**, 14036-14041.

Guzzo, F., Scognamiglio, M., Fiorentino, A., Buommino, E. & D'abrosca, B. 2020. Plant derived natural products against Pseudomonas aeruginosa and Staphylococcus aureus: Antibiofilm activity and molecular mechanisms. *Molecules*, **25**(21), 5024.

Harding, C. M., Hennon, S. W. & Feldman, M. F. 2018. Uncovering the mechanisms of Acinetobacter baumannii virulence. *Nat. Rev. Microbiol.*, **16**, 91-102.

Hasan, T. I. & Ahmed, A. A. 2023. Biogenic Silver Nanoparticles by Pseudomonas aeruginosa Reduce Expression of Biofilm and Quorum Signaling Genes in Multi-drug Resistant Acinetobacter baumannii. *JJBS*, **16(4)**, 621-632.

Hassan, I. K. A., Tuama, A. A. & Kareem, K. A. 2020. Antibacterial Activity of Crude Extracts of Spirulina Platensis Against Some Pathogenic Bacteria and Fungi Isolated from Different Sites on Human Body. *Indian J Forensic Med Toxicol*, **14**(1), 621-625.

Huntzinger, E., Boisset, S., Saveanu, C., Benito, Y., Geissmann, T., Namane, A., Lina, G., Etienne, J., Ehresmann, B. & Ehresmann, C. 2005. Staphylococcus aureus RNAIII and the endoribonuclease III coordinately regulate spa gene expression. *The EMBO journal*, **24**, 824-835.

Hussein, H. J., Al-Khafaji, N. M. S., Al-Mamoori, A. H., Juaifer, W. A. K., Al-Marzoqi, A. H. & Al-Zobiady, R. 2017. Antimicrobial effect of the crude phenolic, alkaloid and terpenoid compounds extracts of Myrtus communis L. against human gram-negative pathogenic bacteria. *JGPT*, **8(9)**, 130-133.

Hussein, H. J., Naji, S. S. & Al-Khafaji, N. M. S. 2018. Antibacterial properties of the Chlorella vulgaris isolated from polluted water in Iraq. *J. Pharm. Sci. & Res*, **10(10)**, 2457-2460.

Ismaeil, A. S. & Saleh, F. A. 2019. Sumac (Rhus coriaria L) as Quorum Sensing Inhibitors in Staphylococcus aureus. *J Pure Appl Microbiol*, **13(4)**, 2397-2404.

Ismail, S. T. & Altaai, M. I. N. 2021. Study ndvB gene expression in Pseudomonas aeruginosa producing biofilm. *Prof.(Dr) RK Sharma*, **21**, 961.

Jha, B., Kavita, K., Westphal, J., Hartmann, A. & Schmitt-Kopplin, P. 2013. Quorum sensing inhibition by Asparagopsis taxiformis, a marine macro alga: separation of the compound that interrupts bacterial communication. *Mar. Drugs*, **11(1)**, 253-265.

Jiang, Q., Chen, J., Yang, C., Yin, Y. & Yao, K. 2019. Quorum Sensing: A Prospective Therapeutic Target for Bacterial Diseases. *BioMed Res. Int.*, 2019, 1-15.

Kitao, T., Lepine, F., Babloudi, S., Walte, F., Steinbacher, S., Maskos, K., Blaesse, M., Negri, M., Pucci, M. & Zahler, B. 2018. Molecular insights into function and competitive inhibition of Pseudomonas aeruginosa multiple virulence factor regulator. *MBio*, **9(10)**.1128/mbio. 02158-17.

Lalancette, C., Charron, D., Laferrière, C., Dolcé, P., Déziel, E., Prévost, M. & Bédard, E. 2017. Hospital drains as reservoirs of Pseudomonas aeruginosa: multiple-locus variable-number of tandem repeats analysis genotypes recovered from faucets, sink surfaces and patients. *Pathogens*, **6(3)**, 36.

Laws, M., Shaaban, A. & Rahman, K. M. 2019. Antibiotic resistance breakers: current approaches and future directions. *FEMS Microbiol Rev*, **43(5)**, 490-516.

Lee, J., Zilm, P. S. & Kidd, S. P. 2020. Novel research models for Staphylococcus aureus small colony variants (SCV) development: co-pathogenesis and growth rate. *Front. Microbiol*, **11**, 321.

Livak, K. J. & Schmittgen, T. D. 2001. Analysis of Relative Gene Expression Data Using Real-Time Quantitative PCR and the 2−ΔΔCT Method. *Methods*, **25(4)**, 402-408.

Marrez, D. A., Sultan, Y. Y., Naguib, M. M. & Higazy, A. M. 2021. Antimicrobial Activity, Cytotoxicity and Chemical Constituents of the Freshwater Microalga Oscillatoria princeps. *Biointerface Res App Chem*, **12(1)**, 961-977.

Maurice, N. M., Bedi, B. & Sadikot, R. T. 2018. Pseudomonas aeruginosa biofilms: host response and clinical implications in lung infections. *Am J Respir Cell Mol Biol*, **58(4)**, 428-439.

Monteiro, M., Lavrador, A. S., Santos, R., Rangel, F., Iglesias, P., Tárraga, M., Couto, A., Serra, C. R., Tafalla, C., Da Costa, E., Domingues, M. R., Oliva-Teles, A., Carvalho, A. P., Enes, P. & Díaz-Rosales, P. 2021. Evaluation of the Potential of Marine Algae Extracts as a Source of Functional Ingredients Using Zebrafish as Animal Model for Aquaculture. *Mar. Biotechnol.*, **23**, 529-545.

Nji, E., Kazibwe, J., Hambridge, T., Joko, C. A., Larbi, A. A., Damptey, L. A. O., Nkansa-Gyamfi, N. A., Stålsby Lundborg, C. & Lien, L. T. Q. 2021. High prevalence of antibiotic resistance in commensal Escherichia coli from healthy human sources in community settings. *Sci Rep*, **11**, 3372.

Nowroozi, J., Abbas Akhavan Sepahi & Rashnonejad, A. 2012. Pyocyanine Biosynthetic Genes in Clinical and Environmental Isolates of Pseudomonas aeruginosa and Detection of Pyocyanine's Antimicrobial Effects with or without Colloidal Silver Nanoparticles. *Cell J*, **14(1)**, 7-18.

Pina-Pérez MC, Rivas A, Martínez A, Rodrigo D. 2017. Antimicrobial potential of macro and microalgae against pathogenic and spoilage microorganisms in food. *Food Chem*, **235**:34-44

Price-Whelan, A., Dietrich, L. E. & Newman, D. K. 2007. Pyocyanin alters redox homeostasis and carbon flux through central metabolic pathways in Pseudomonas aeruginosa PA14. *J Bacteriol*, **189(17)**, 6372-6381.

Richmond, A. 2008. **Handbook of microalgal culture**: biotechnology and applied phycology, John Wiley & Sons, Blackwell .

Syed, S., Arasu, A. & Ponnuswamy, I. 2015. The uses of Chlorella vulgaris as antimicrobial agent and as a diet: the presence of bio-active compounds which caters the vitamins, minerals in general. *IJBSBT*, 7**(1)**, 185-190.

Tang, J., Wang, W. & Chu, W. 2020. Antimicrobial and anti-quorum sensing activities of phlorotannins from seaweed (Hizikia fusiforme). *Front. Cell. Infect. Microbio*l, **10**, 586750-586764.

Tille, P. M. 2021. **Bailey & Scott's Diagnostic Microbiology**, 15th edition. Elsevier/Mosby, China.

Toma, J. J. & Aziz, F. H. 2023. Antibacterial Activity of Three Algal Genera against some Pathogenic Bacteria. *Baghdad Sci. J*, **20(1)**, 32-40.

Tsuneda, S., Aikawa, H., Hayashi, H., Yuasa, A. & Hirata, A. 2003. Extracellular polymeric substances responsible for bacterial adhesion onto solid surface. *FEMS microbiology letters*, **223(2)**, 287-292.

Uddin, T. M., Chakraborty, A. J., Khusro, A., Zidan, B. M. R. M., Mitra, S., Emran, T. B., Dhama, K., Ripon, M. K. H., Gajdács, M., Sahibzada, M. U. K., Hossain, M. J. & Koirala, N. 2021. Antibiotic resistance in microbes: History, mechanisms, therapeutic strategies and future prospects. *J Infect Public Health*, **14(12)**, 1750-1766.

Van Boeckel, T. P., Pires, J., Silvester, R., Zhao, C., Song, J., Criscuolo, N. G., Gilbert, M., Bonhoeffer, S. & Laxminarayan, R. 2019. Global trends in antimicrobial resistance in animals in low- and middle-income countries. *Science*, **365(6459)**, 1350–1352.

Ventola, C. L. 2015. The antibiotic resistance crisis: part 1: causes and threats. P t, **40(4)**, 277-83.

Vestby, L. K., Grønseth, T., Simm, R. & Nesse, L. L. 2020. Bacterial biofilm and its role in the pathogenesis of disease. *Antibiotics*, **9(2)**, 59.

Wehr, J. D., Sheath, R. G. & Kociolek, J. P. 2015. **Freshwater algae of North America**: ecology and classification, second ed. Elsevier, London.

Wiegand, I., Hilpert, K. & Hancock, R. E. 2008. Agar and broth dilution methods to determine the minimal inhibitory concentration (MIC) of antimicrobial substances. *Nat. protoc.*, **3(2)**, 163-175.

Xiao, G., Déziel, E., He, J., Lépine, F., Lesic, B., Castonguay, M. H., Milot, S., Tampakaki, A. P., Stachel, S. E. & Rahme, L. G. 2006. MvfR, a key Pseudomonas aeruginosa pathogenicity LTTR-class regulatory protein, has dual ligands. *Mol. Microbiol.*, **62(6)**, 1689-1699.

Yang, Q., Scheie, A. A., Benneche, T. & Defoirdt, T. 2015. Specific quorum sensing-disrupting activity (A QSI) of thiophenones and their therapeutic potential. *Sci Rep*, **5**, 1-9.

Zhong, L., Ravichandran, V., Zhang, N., Wang, H., Bian, X., Zhang, Y. & Li, A. 2020. Attenuation of Pseudomonas aeruginosa quorum sensing by natural products: Virtual screening, evaluation and biomolecular interactions. *Int. j. mol. sci.*, **21(6)**, 2190.

JJBS

Volume 17, Number 4,December 2024
ISSN 1995-6673
Pages 615 – 725
https://doi.org/10.54319/jjbs/170414

Jordan Journal of Biological Sciences

The C-terminal Domain of S1 Subunit Spike Protein Enhances the Sensitivity of COVID-19 Serological Assay

Sabar Pambudi[1,4,*], Nihayatul Karimah[1], Ika Nurlaila[1], Doddy Irawan[1], Tika Widayanti[1], Jodi Suryanggono[1], Asri Sulfianti[1], Sjaikhurrizal El Muttaqien[1], Vivi Setiawaty[2], Hana Pattipeiluhu[3], Muhammad Luqman[1]

[1]*Research Center for Vaccine and Drug, National Research and Innovation Agency (BRIN), Tangerang Selatan, 15310, Indonesia;* [2]*Ministry of Health, Jakarta, 10560, Indonesia;* [3]*Moh Ridwan Meureksa Hospital, Jln Taman Mini 1, Jakarta, 13560, Indonesia;* [4]*Department of Biotechnology, Universitas Esa Unggul, Jl, Arjuna Utara no.9, Jakarta, 11510, Indonesia*

Received: May 2, 2024; Revised: July 31, 2024; Accepted: August 7, 2024

Abstract

Evaluating antibody responses against the receptor binding domain (RBD) protein will be essential for determining the antibody response's durability and defining a vaccine-induced antibody response. Consequently, it becomes crucial for the production of innovative RBD antigens to enhance the sensitivity detection of antibody anti-COVID-19. The bottleneck to achieving these targets is the availability of effective RBD antigens construct. This study evaluated the potency RS1, RBD with C-terminal domain (CTD) of Spike S1 domain, to detect antibody anti-spike SARS-CoV-2 in patient sera. Docking simulations with ClusPro have been done to determine how antigens (RBD/RS1) and antibody (Fv) models interact. The RMSD for both complexes is accordingly still in tolerable value. The constructs RBD and RS1 were expressed in *Escherichia coli* strain Origami under the pET-32b(+) expression vector. The indirect IgG-ELISA of both recombinant proteins could differentiate the presence of negative antibody anti-spike in naïve sera and positive sera collected from COVID-19 patients between 2020 and 2022. Furthermore, the degree of detecting antibodies anti-spike utilizing the RS1 protein increased significantly compared to RBD (p = 0.0033). Our results indicate additional CTD in RS1 could access more anti-spike antibodies and enhance the sensitivity detection of antibody anti-spike COVID-19.

Keywords: COVID-19, C-terminal domain, Receptor Binding Domain, Serological assay

1. Introduction

The emerging of SARS-CoV-2 in Wuhan-China initiated the COVID-19 pandemic with a notable global mortality rate (Oglat *et al.*, 2022; Rastogi *et al.*, 2020). The spike (S), membrane (M), envelope (E), and nucleocapsid (N) are the structural proteins of the SARS-CoV-2 virus. The spike protein contains 1273 amino acid residues and is composed of three subunits: S1, S2, and a transmembrane (TM) domain. The N-terminal domain (NTD), receptor binding domain (RBD), and C-terminal domain (CTD) are present within the S1 subunit (Biswas *et al.*, 2021; Shwan *et al.*, 2022). The RBD attaches to the ACE2 receptor on the cell surface, facilitates the fusion of the virus and cellular membrane, and serves as an antigen to stimulate the production of antibodies that disrupt the binding between the virus and the host (Biswas *et al.*, 2021; Tai *et al.*, 2020).

The sera of the vast majority of COVID-19 survivors exhibit a telling presence of IgM and IgG antibodies directed against the SARS-CoV-2 spike protein. In order to effectively prevent and contain the spread of the virus, it is essential to meticulously track the antibody responses in patients who have either recovered from infection or received vaccination. The neutralizing antibody titer in sera serves as a vital indicator of the immunological outcome, providing valuable insights into the efficacy of the immune system's response to SARS-CoV-2 (Peterhoff *et al.*, 2021; Yin *et al.*, 2021).

The SARS-CoV-2 RBD protein is frequently employed in serological assays, commonly in ELISA-based assay platforms. These assays serve an important role in establishing past exposure to SARS-CoV-2 and analyzing vaccination efficacy in populations. Mutations in the RBD have been found to impact antibody binding and neutralization, with some variants showing different antibody responses compared to the wild type (Fraser *et al.*, 2022). The global serological test for COVID-19 is based on the RBD SARS-CoV-2 expressed in E. *coli*. Nonetheless, a previous study reported that the detection sensitivity using RBD from E. *coli* is less sensitive compared to RBD expressed in the mammalian expression system (Ayón-Núñez *et al.*, 2022). Despite the significant advances made in recent years, the RBD's production in eukaryotic systems has been hindered by two major constraints: a limited capacity to generate sufficient quantities and an exorbitant cost. These obstacles have far-reaching implications, as they undermine the potential for RBD-based medicines and vaccines to become viable

* Corresponding author. e-mail: saba002@brin.go.id; sabar.pambudi@esaunggul.ac.id.

options for treatment and prevention. The reality is that the current production limitations and prohibitively high expenses severely curtail the prospect of leveraging RBD as a valuable resource in the development of novel therapeutic agents. As a result, it is essential to address these challenges and find innovative solutions to overcome them, thereby paving the way for the widespread application of RBD-based technologies (He *et al.*, 2021).

In an effort to optimize the performance of serological assays reliant on RBD produced in E. *coli*, we have designed a novel construct, RS1, which incorporates the C-terminal domain (CTD) of the S1 spike protein. This domain's CTD exhibits a more extensive amino acid sequence compared to its SARS-CoV counterpart, thereby expanding its surface area and enhancing the interaction between SARS-CoV-2 and the ACE-2 receptor. This structural modification is anticipated to significantly boost the sensitivity of serological assays, allowing for more accurate and reliable detection of SARS-CoV-2 antibodies (Huang *et al.*, 2020). Several studies have demonstrated that the surface area of an antigen exerts a profound impact on the human immune response. The extent to which an antigen presents itself to the immune system has been shown to influence the magnitude and quality of the response (Heida *et al.*, 2022; Zinkhan *et al.*, 2021) and possibly to enhance the detection of anti-spike antibodies corresponding to COVID-19 infection.

Our data demonstrated that recombinant RBD and RS1 can be probed by rabbit monoclonal antibodies anti-RBD/Spike. Interestingly, compared to recombinant RBD, recombinant RS1 significantly increased the sensitivity of the ELISA assay from positive serum patients of COVID-19 collected from 2020 to 2022. In parallel, a computational approach was carried out to evaluate the structural interaction between RBD and RS1 against COVA2-39 which has been reported to target the RBD of SARS-CoV-2 (Wu *et al.*, 2020). COVA2-39 is a crystal structures of IGHV3-53 antibody that frequently bind SARS-CoV-2 RBD. This antibody is derived from a convalescent donor from Amsterdam and potently neutralizes SARS-CoV-2 virus (Brouwer *et al.*, 2020). In this study, this crystal structure is used as a neutralizing antibody model and to explore its interaction with RBD or RS1.

2. Materials and Methods

2.1. Samples

All samples, such as sera and RNA, from confirmed acute COVID-19 patients, were collected from 2020 to 2022 in a cohort study after approval of the Ethical Board of the NIHRD, Ministry of Health (LB.02.01/2/KE.432/2020). The antigenicity evaluation of the SARS-CoV-2 recombinant RBD and RS1 was performed using a random selection of collected sera.

2.2. Plasmid Construction

The amplification of the RBD (amino acid 319–541) and RS1 (amino acid 319–681) fragment genes of SARS-CoV-2 was carried out by PCR using Phusion Green Hot Start II High-Fidelity PCR Master Mix (Thermo) and specific primers (Fw: 5'-TAATggtaccATGAGAGTCCAACCAACAGAATCTAT TGTTAGATTTCC-3'; Rv:5'-TAATctcgagaaGGAAATTGACACATTTGTTTTTAACC AAATTAGTAGAC-3') and cloned into the pET-32b(+) bacterial expression vector with N and C-terminal His-tag. The genes were amplified with denaturation steps at 98^{o}C for 15 seconds, annealing at 60^{o}C for 15 seconds, and extension at 72^{o}C for 30 seconds. Both gene fragments and vector pET-32b(+) were double-digested with *Kpn1* and *Xho1* restriction enzymes, followed by ligation. The E. *coli* TOP10 colonies from the transformation were extracted, and the recombinant plasmids were verified by restriction enzymes and sequencing using T7 primers.

2.3. In Silico Study

The antibody used in this molecular modelling is a IGHV3-53 neutralizing antibody, COVA2-39, that reportedly can bind to RBD SARS-CoV-2 (Wu *et al.*, 2020). The PDB file of the antibody was retrieved from RCSB PDB; PDB ID: 7JMP. The structure of this antibody in PDB was in neutralizing condition with SARS-CoV-2 RBD. The variable light chain (VL) and variable heavy chain (VH) of the fragment antigen binding (Fab) were split up from the original 3D structure as variable fragment (Fv) and saved into separate PDB file. The processes of adding hydrogen atom and solvent deletion were done using YASARA software (Krieger *et al.*, 2014). The antigen structures to be modelled are the RBD and RS1 of SARS-CoV-2 and which both are fused with TrxA fusion protein from pET32b plasmid. The fusion form of TrxA protein and the antigen structures were modelled using I-TASSER server for iterative threading assembly (J. Yang *et al.*, 2015).

To obtain molecular complex of antigen-antibody, we performed docking between VH-VL structure and antigen-TrxA fusion protein structures using ClusPro (Kozakov *et al.*, 2017). ClusPro is a fast Fourier transform (FFT) algorithm-based docking server which incorporates Decoys as the Reference State (DARS) into PIPER docking program in the server for antigen-antibody complex prediction (Brenke *et al.*, 2012). An antibody mode, which set antibody as receptor and antigen as ligand, and automatic masking of non-complement determining region were chosen. The complexes of antigen-antibody resulted from docking simulation were then analyzed for visualization using YASARA in order to choose the complex that closely resembles the structure of RBD and the VH-VL of COVA2-39 antibody in the PDB ID 7JMP. It was also done by structural comparison of multiple-chain protein complexes between two structures with MM-align program (Mukherjee *et al.*, 2009).

For each chosen complex predicted by docking simulation, molecular dynamics with GROMACS 2021.5 was performed to get the insight of the dynamic interaction between VH-VL structure and antigen-TrxA fusion protein (Liu *et al.*, 2023). The pdb2gmx generated topology file for the protein complex using CHARMM36 force field and TIP3P original water model (Lee *et al.*, 2016). A rhombic dodecahedral shape defined the unit cell of the solvent environment with the protein complex in the center of 10 Å from the edge. The system was set in neutral condition with the addition of Na+ and Cl-. The steepest descent minimization of 50000 steps was done to remove bad contact with maximum force 1000 kJ.mol^{-1}.nm^{-1}. Two phases of equilibration including isothermal-isochoric ensemble (NVT) and isothermal-isobaric ensemble (NPT)

were performed with position restraint for the protein complex and LINCS constraint algorithm for the hydrogen bonds. The system was heated from 0 to 300 K with 2-fs time step for 50 ps in each equilibration phase. The forces of Van der Waals interactions were smoothly switched to zero between 10 Å and 12 Å. Particle Mesh Ewald for long-range electrostatics was applied with fourth-order (cubic) interpolation and grid spacing for FFT of maximum 0.16 nm. The temperature coupling used velocity rescaling in both NVT and NPT with time constant of 0.1 ps and reference temperature of 300 K. The pressure coupling used Berendsen method for NPT equilibration phase with 2 ps time constant, reference pressure of 1 bar, and isothermal compressibility of $4.5x10^{-5}$ bar^{-1}. The production phase of MD simulation was carried out in 50 ns with a time step of 2 fs without position restraint. The hydrogen bonds were constrained with SHAKE algorithm. The long-range electrostatics and temperature coupling was calculated the same as in equilibration phase, while the pressure coupling used Parrinello-Rahman barostat. The root mean square deviation (RMSD) of protein backbone and the root mean square fluctuation (RMSF) of residue position were computed. Residue interaction network before and after MD simulation were defined using The RING web server (Piovesan *et al.*, 2016).

2.4. Expression

The recombinant plasmids were transformed into E. *coli* Origami strains and cultivated in Luria Bertani (LB) medium containing 70 µg/ml ampicillin, 15 µg/ml kanamycin, and 12.5 µg/ml tetracycline. The positive clones were verified by PCR using a set of T7 primers. Recombinant E. *coli* with pET-32b(+)-RBD/RS1 or wild-type pET-32b(+) were cultivated until the optical density (OD) at 600 nm reached 0.8-1.0 and induced by IPTG to the final concentration of 0.3mM. The low-temperature induction was carried out at 25^{o}C, 150 rpm for 16 hours. The induced cells were harvested by centrifugation and stored at -20^{o}C for further analysis.

2.5. Isolation of inclusion bodies

The recombinant E. *coli* pellet was resuspended in PBS pH 7.4 and sonicated for 10 minutes on ice. The lysate was separated by centrifugation at 4^{o}C, 11,000 rpm for 3 min. The supernatant was removed, and the pellet was resuspended and incubated for 1 hour at room temperature with 0.1M Tris-Cl pH 8.5 or pH 11 with a variation in urea concentration. The supernatant containing inclusion bodies of recombinant RBD and RS1 proteins were separated from the pellet by centrifugation. Confirmation of the isolation of inclusion bodies was carried out by SDS-PAGE and western blot analysis.

2.6. Western Blot

All recombinant proteins were transferred onto PVDF membranes, blocked with 5% skim milk in PBST (PBS, 0.1% Tween-20), and probed with mouse anti-His monoclonal antibody (MA1-21315, Invitrogen), rabbit anti-RBD polyclonal antibody (PA5-114451, Invitrogen), and human anti-spike monoclonal antibody (MA5-35950, Invitrogen) at 4^{o}C for overnight. After washing with PBST, the IRDye 800 CW conjugated goat anti-mouse IgG antibody (1:5000) or goat anti-rabbit IgG (1:5000) or goat anti-human IgG (1:10000) was used as the secondary antibody. The membranes were washed with PBST and the signals were captured under the near-infrared optical imaging system (Odyssey Clx, LI-COR). The data was further analyzed by Image Studio ver 5.2 software.

2.7. Purification of RBD protein

The supernatants containing inclusion bodies of recombinant RBD and RS1 in 0.1M Tris-Cl pH 11 containing 2M urea were used in the purification step. The HisTrap HP column (Cytiva) was equilibrated with two-column volumes (CVs) of 20 mM phosphate buffer pH 7.4 with 300 mM NaCl and 20 mM imidazole (buffer A). The Akta Start (Cytiva) was set at a flow rate of 0.5 ml/min for loading samples into the resin and 1 ml/min for capturing, washing, and elution steps. The resin was washed with 5 CVs of buffer A followed by elution with 2 CVs of buffer B (20 mM phosphate buffer pH 7.4 with 300 mM NaCl and 250 mM imidazole. The eluted fraction was kept at 4^{o}C until further analysis.

2.8. . Indirect IgG-ELISA and statistic analysis

The indirect IgG-ELISA protocol was adapted from (Krähling *et al.*, 2021). The coating step was performed by diluting the RBD or RS1 protein with 0.1 M sodium carbonate pH 9.0 up to 100 ng in each well of the 96-well plate overnight and blocked with PBST with 10 % skim milk. The primary antibody, a 1:50 dilution of patient sera in PBST with 10% skim milk, was added to the plates for one hour. Followed by incubation with secondary antibody HRP-conjugated goat anti-human IgG (Invitrogen, 31410) for 30 minutes. The reactivity was measured with the HTX Sinergy plate reader (BIOTEK) at 450 nm after the addition of TMB substrate to the plates. Statistical significance of the differences between triplicate mean values between RBD and RS1 was determined by using a paired t-test with the software GraphPad Prism 5 (GraphPad Software, Inc, San Diego, CA, USA). The significance is indicated by asterisk (*) symbols. A positive sample is defined as having OD450 values of three standard deviations (SD) above the mean (Ayón-Núñez *et al.*, 2022) of a panel of six negative controls from naïve pre-pandemic sera.

3. Results

3.1. Plasmid Construction

The RBD fragment (319–541aa) and RS1 fragment (319–681) were obtained using the designed primers in a polymerase chain reaction (PCR). The cDNA from RNA SARS-CoV-2 isolated from a COVID-19 patient from 2020 was used as a PCR template. SnapGene generated the schematic diagram illustrating the design of the intended recombinant plasmid (Figure 1A). Double digestion with *Kpn1* and *Xho1* was carried out to check the recombinant plasmids of pET-32b(+)-RBD and pET-32b(+)-RS1 (Figure 1B). The specific band around 5,900 bp, which corresponds to the backbone of pET-32b(+), appears clearly for both constructs. The digested recombinant plasmid clearly shows the bands for RBD with a correct size of around 670 bp and RS1 with 1090 bp. The target genes were amplified by PCR using the T7 universal primer (Figure 1C), and DNA sequencing was further employed to verify the identity of the genes (data not shown).

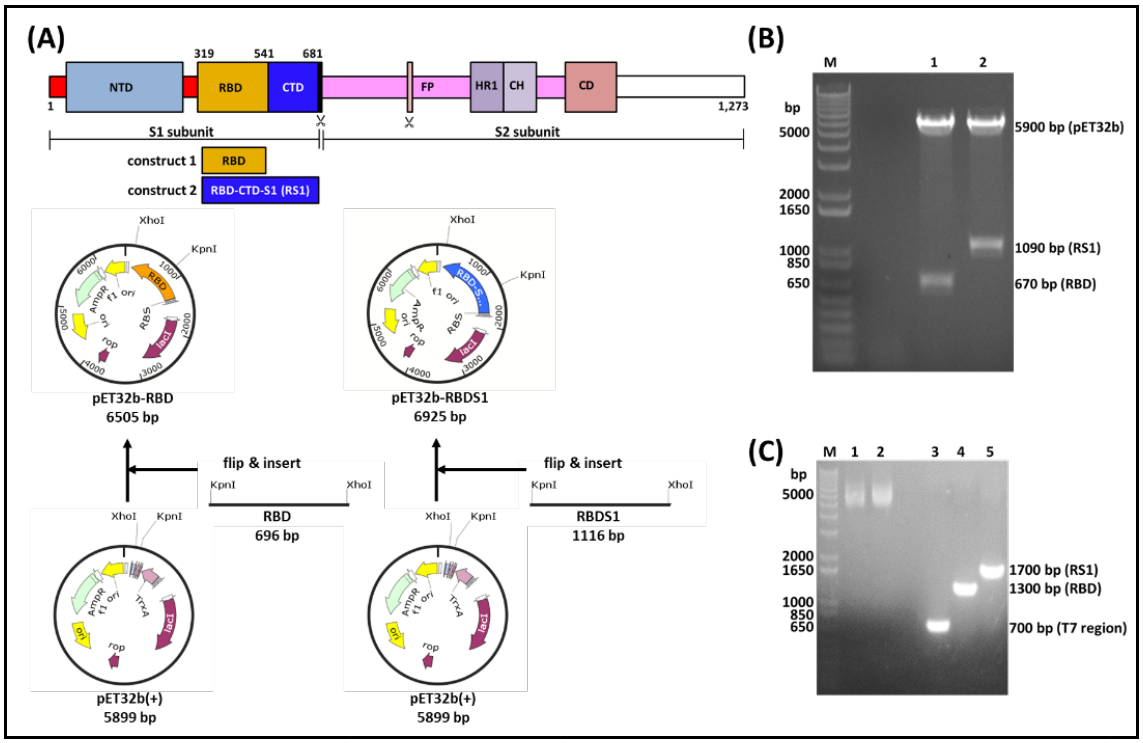

Figure 1. Recombinant plasmid verification. (A) Diagram of plasmid pET-32b(+)-RBD and pET-32b(+)-RS1. (B) Confirmation of recombinant plasmids by double digestion with *Kpn1* and *Xho1*. Both constructs showed correct fragments of insert genes and the backbone of the vector pET-32b(+) after digestion. (C) The PCR using a universal T7 primer was carried out to confirm the recombinant plasmid. Lane 1,2 are template plasmids. Lane 3 is wildtype pET-32b(+), and lane 4,5 corresponds to RBD and RS1, respectively.

3.2. In Silico Study

The fusion form of pET32b peptide "TrxA fusion protein" and the antigen structures (RBD and RS1) has been modelled. Due to the existence of TrxA fusion protein that covalently binds to the antigens, an iterative threading assembly with I-Tasser was used to build the 3D structures. The structure with the highest C-score was chosen for following simulations. C-score is the confidence score to estimate the quality of predicted structure in which the higher value indicates higher confidence of the structure quality (Yang *et al.*, 2015). The result came out that the structure of RS1 fusion form (C score = -2.39) is slightly better than the structure of RBD fusion form (C score = -3.62). No predicted structures have positive C score because the exact template for fusion form of TrxA protein and RBD/RS1 is not available. The lack of exact template also causes lower TM score (0.3 - 0.4) for each model. TM-score is a measure for assessing the topological similarity of protein structures. The value is between 0 and 1, where 1 indicates a perfect match between two structures. Correct topology can be achieved if the TM score is more than 0.5 (Xu *et al.*, 2010). Therefore, the generated topology of the models is not exactly correct but not in a random form as well.

To obtain a complex between antigen (RBD/RS1) and antibody (Fv), docking simulation with ClusPro has been performed (Figure 2). It generated 30 clusters that contain several neighboring structures within 9 Å IRMSD radius from the center structure (Kozakov *et al.*, 2017). The center structures in the five most populated clusters were then aligned with the reference complex structure (PDB ID: 7JMP) with MM-Align program to calculate sequence identity, TM-score, and RMSD. Regardless of the lowest energy in the cluster, the most populated cluster is more considered because the resulting energy indirectly relates to binding affinity (Kozakov *et al.*, 2017). The results of the docking simulation and the structural alignment were presented in the Table 1.

Table 1. The largest clusters that represent the most likely models of the complex.

Complex	Cluster	Members	The lowest energy in the cluster*	Sequence Identity**	TM-Score**	RMSD**
RBD-Fv	1	64	-304.8	0.942	0.40	1.83
	2	54	-303.5	0.842	0.43	3.63
	3	48	-305.2	0.906	0.41	2.27
	4	42	-299.9	0.855	0.42	3.40
	5	42	-274.4	0.995	0.65	1.30
RS1-Fv	1	71	-321.4	0.898	0.41	2.53
	2	71	-282.8	0.975	0.60	2.70
	3	68	-288.3	0.920	0.41	2.42
	4	65	-307.9	0.851	0.43	2.87
	5	56	-297.9	0.777	0.45	4.01

*The energy calculated by PIPER in ClusPro

**The scores calculated by MM-Align resulted from multimeric complex alignment between the model from ClusPro and the reference complex structure (PDB ID: 7JMP)

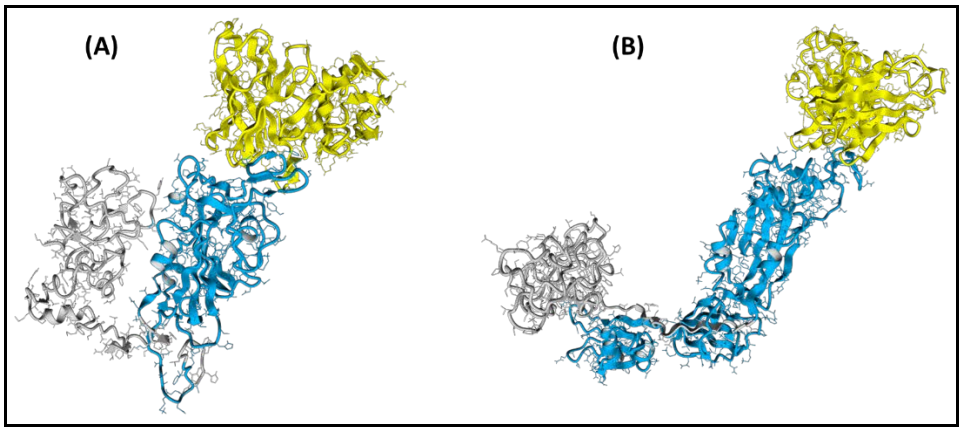

Figure 2. The structural representation of complex between antigen-TrxA fusion protein and Fv of COVA2-39 for which (A) is RBD complex and (B) is RS1 complex. The Fv is shown in yellow, the TrxA fusion protein is shown in grey, and the antigen is shown in blue.

Furthermore, the dynamic interaction between VH-VL structure and antigen-pET32b fusion was simulated in 50 ns. The complex of RBD-Fv reached its conformational stability within 3 ns with the average RMSD 10.1 Å (Figure 2A). As compared with RBD-Fv, the complex of RS1-Fv took longer time around 10 ns to maintain the stability and produced higher degree of average RMSD 13.4 Å (Figure 2B). The best complex model between antigen and antibody was chosen based on the TM-score. The complex with TM-score > 0.5 resembles the reference complex structure in terms of its global topology and chain orientation. Thus, cluster 5 with TM-score 0.65 was selected for RBD-Fv complex and cluster 2 with TM-score 0.6 was selected for RS1-Fv (Figure 2). Both selected clusters also have the highest sequence identity among other clusters, 0.995 for RBD-Fv and 0.975 for RS1-Fv. It means that the number of identical residues corresponds closely with the number of aligned residues between the model from ClusPro and the reference complex structure. The complex of RBD-Fv has lower RMSD (1.30 Å) compared to the complex of RS1-Fv (2.70 Å). Low RMSD indicates minimal local error. The RMSD or local error for both complexes is accordingly still in tolerable value.

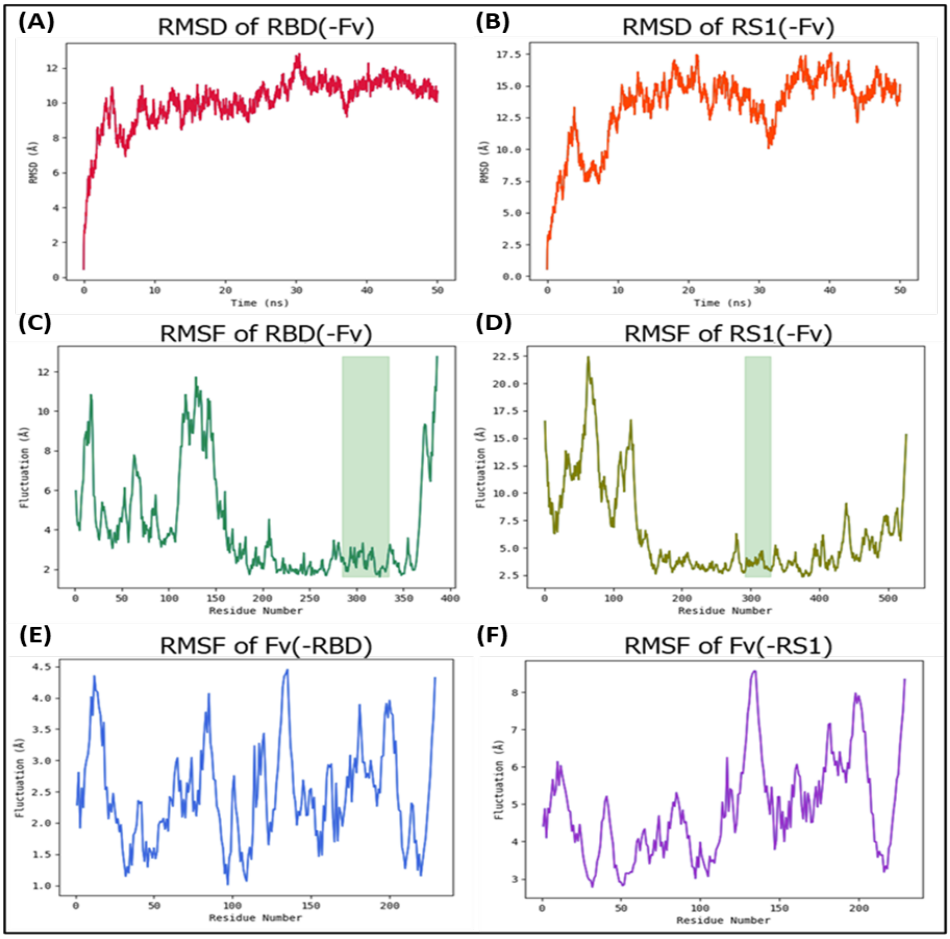

Figure 3. RMSD and RMSF analysis. RMSD of the complex: (A) RBD-Fv and (B) RS1-Fv; RMSF of the antigen: (C) RBD and (D) RS1 in complex with Fv; RMSF of the Fv in complex with antigen: (E) RBD and (F) RS1; The green boxes in (C) and (D) represent the interacting residues of the antigen with Fv.

3.3. Expression of recombinant RBD and RS1

The RBD and RS1 recombinant proteins were expressed in E. *coli* Origami strain and induced with 0.3 mM IPTG. The harvested cells were lysed and the expression of the proteins was evaluated in SDS-PAGE gels. As shown in Figure 4A, a major protein band corresponding to 45 kDa which belongs to RBD was observed in the recombinant E. *coli* after IPTG induction. Western blot was employed to evaluate the antigenicity of recombinant RBD and RS1 against antibody anti-His and polyclonal antibody anti-SARS-CoV-2 Spike RBD. Specific bands at 45 kDa and 60 kDa of RBD and RS1 recombinant protein (Figure 4B, 4C) were detected with anti-His and anti-RBD antibodies, respectively. Our results indicate that the recombinant RBD and RS1 possess the required antigenicity.

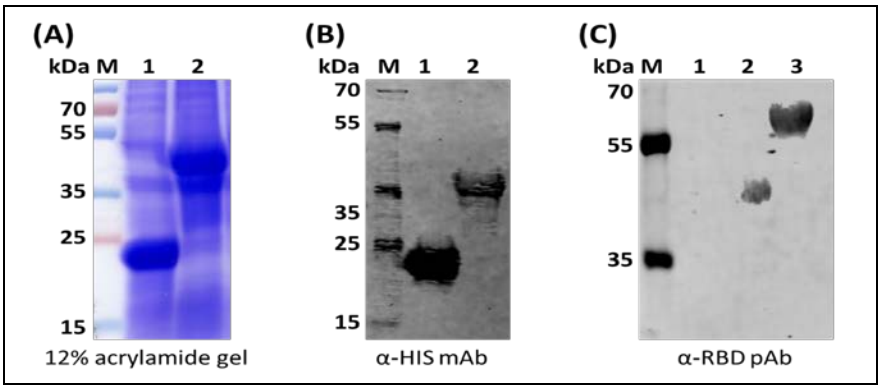

Figure 4. Expression of recombinant RBD and RS1. (a) The SDS PAGE analysis of recombinant RBD. Lane 1: induced of pET32b(+) possessing E.*coli* lysate. Lane 2: induced of pET32b(+)-RBD possessing E.*coli* lysate. (b) Reactivity of recombinant RBD probed with mouse anti-6x His tag monoclonal antibody. (c) Reactivity of recombinant RBD and RS1 with rabbit anti-SARS-CoV-2 Spike RBD pAb. Lane 1: negative control from wild-type E.*coli*. Lane 2: recombinant RBD with specific band at 45 kDa. Lane 3: recombinant RS1 with specific band at 60 kDa.

3.4. Purification of recombinant RBD and RS1 protein

To increase the production of RBD and RS1 non-classical inclusion bodies, the expression was carried out in low temperatures at 25°C, 150 rpm for 16 hours. The inclusion bodies of RBD and RS1 were solubilized using the mild denaturing buffer in 0.1 M Tris buffer 11 with a low concentration of urea 2 M, as shown in Figure 5A and 5B, respectively. Solubilization of RBD and RS1 protein from inclusion bodies was observed by increasing the pH from 8.5 to 11. Increasing urea concentration from 1 M to 2 M also improved the solubilization of the RBD and RS1 inclusion bodies. The specific band around 45 kDa and 60 kDa from RBD (blue arrow) and RS1 (red arrow) supernatant in 0.1 M tris pH 11 with 2 M urea was detected using human anti-spike monoclonal antibody in western blot analysis (Figure 5C). This result confirmed the antigenicity of solubilized RBD and RS1 with the mild buffer remains exist. Furthermore, no additional steps such as refolding were required in this study for purification. The HisTrap HP resin was employed to purify the RBD and RS1 inclusion bodies through affinity purification. As shown in Figure 5D, a major band around 45 kDa for RBD and 60 kDa for RS1 was observed upon elution with 20 mM phosphate buffer with 300 mM NaCl and 250 mM imidazole. The results indicated the recombinant RBD and RS1 were successfully produced and purified.

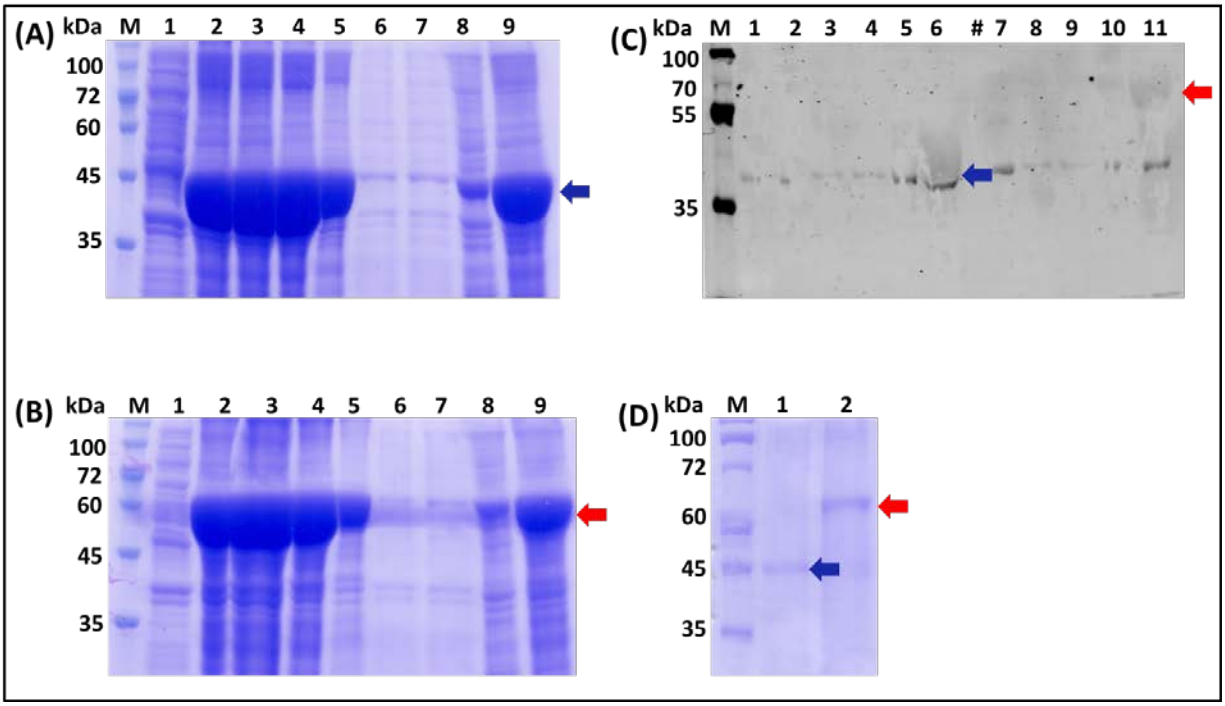

Figure 5. Isolation and purification of recombinant RBD and RS1 protein. (A,B) Effect of different lysis buffer on solubility of RBD and RS1 inclusion bodies. Lane 1: supernatant of lysed bacteria in 1X PBS buffer. Lane 2: pellet of lysed bacteria in 0.1M Tris-Cl pH 8.5 Urea 1 M. Lane 3: pellet of lysed bacteria in 0.1 M Tris-Cl pH 8.5 Urea 2 M. Lane 4: pellet of lysed bacteria in 0.1 M Tris-Cl pH 11 Urea 1 M. Lane 5: pellet of lysed bacteria in 0.1 M Tris-Cl pH 11 Urea 2 M. Lane 6: supernatant of lysed bacteria in 0.1M Tris-Cl pH 8.5 Urea 1 M. Lane 7: supernatant of lysed bacteria in 0.1 M Tris-Cl pH 8.5 Urea 2 M. Lane 8: supernatant of lysed bacteria in 0.1 M Tris-Cl pH 11 Urea 1 M. Lane 9: supernatant of lysed bacteria in 0.1 M Tris-Cl pH 11 Urea 2 M. (C) Western blot analysis of soluble inclusion bodies of RBD (lane 1-6) and RS1 (lane 7-11) detected by using human monoclonal antibody anti-spike. (D) SDS-PAGE gel of purified recombinant RBD (lane 1) and RS1 (lane 2). The recombinant RBD protein is pointed by blue arrow and the recombinant RS1 protein is pointed by red arrow.

3.5. The antigenicity evaluation of recombinant RBD and RS1 by ELISA

A total of 15 sera obtained from COVID-19 patients from different periods during the pandemic COVID-19 (2020--2022) and six naïve sera collected from pre-pandemic (2013--2015) as negative control were evaluated by indirect IgG-ELISA against recombinant RBD and RS1 (Figure 6A). No reaction was observed from all naïve pre-pandemic sera (100%) against recombinant RBD and RS1 proteins. Further, recombinant RBD reacts positively to 10 out of 15 sera (67%) according to the cut-off previously determined. Interestingly, compared to anti-RBD, recombinant RS1 protein with S1 subunit CTD appears to increase sensitivity by 80% (12 out of 15) from COVID-19 patient serum.

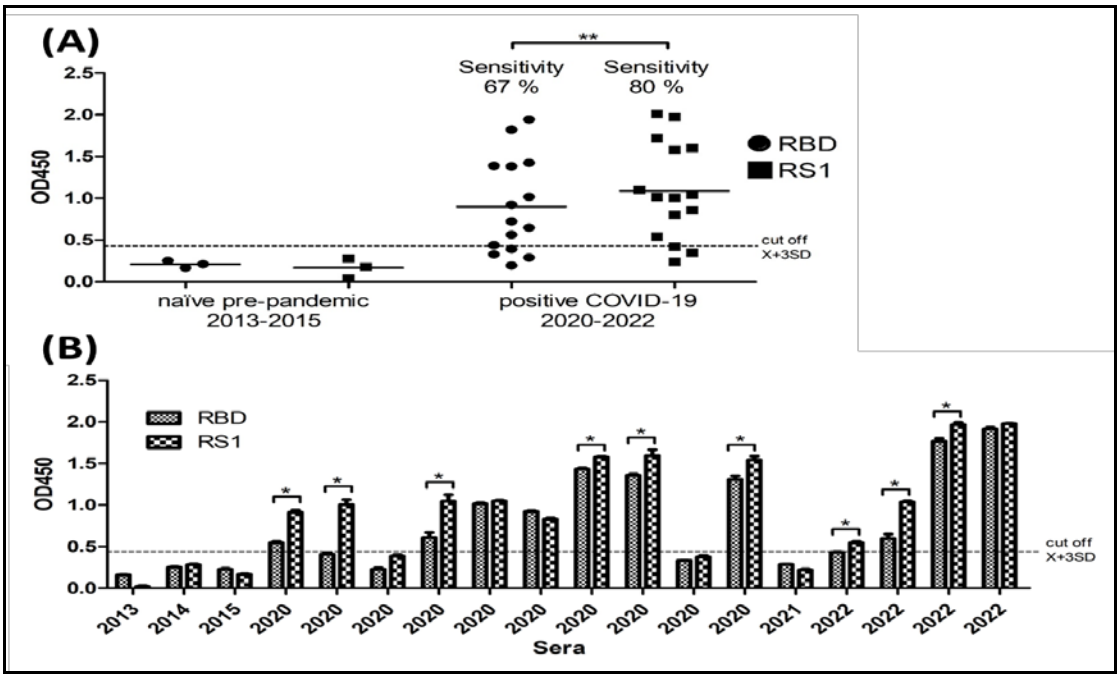

Figure 6. Evaluation of the recombinant RBD and RS1 by indirect IgG-ELISA against sera from naïve pre-pandemic and positive COVID-19. A positive sample is defined as having OD450 values of three standard deviations (SD) above the mean of a panel negative controls from naïve pre-pandemic sera. (A) The comparison sensitivity detection of RBD and RS1 was analyzed by a paired t-test. The degree of detecting antibodies anti-spike utilizing the RS1 protein increased significantly compared to RBD ($p = 0.0033$). (B) Reactivity of RBD and RS1 against antibody anti-spike from each sera is shown individually. The reactivity comparison between RBD and RS1 is statistically significant ($p<0.05$).

4. Discussion

The RBD protein is widely utilized in several applications, including serological detection and vaccine development against COVID-19 (Maffei *et al.*, 2021). Regardless of the limitation of RBD for serological detection in COVID-19, the production of the protein in the E.*coli* expression system has been reported to have several advantages over other expression systems, such as low cost and ease of handling (Ayón-Núñez *et al.*, 2022; Gao *et al.*, 2022). Additional molecules, such as streptavidin and small peptides, were exploited in E.*coli* expression system in order to enhance the solubility and functionality of RBD recombinant proteins (Brindha *et al.*, 2022; Lin *et al.*, 2023). These findings suggest that with appropriate modifications and optimizations, E.*coli*-produced RBD can achieve comparable or even improved detection sensitivity compared to mammalian expression systems. However, considering RBD mutation which affects the binding affinity and antibody escape in various "variants of concern" of SARS-CoV-2 strains (Yang *et al.*, 2021), an effort to find a new approach to increase serological detection sensitivity is needed. Evaluation of additional CTD domains in RBD recombinant to enhance the anti-spike antibody detection from COVID-19 patient sera hasn't been reported elsewhere. In this study, we constructed the recombinant plasmid encoding RBD and RBD with CTD, namely "RS1" (Figure 1A), expressed, purified, and evaluated the detection sensitivity of both constructs using a panel of COVID-19 patient sera.

In this study, several strategies were utilized in order to make our recombinant protein solubilized and refolded properly. The RBD and RS1 genes were fused with TrxA fusion protein of pET32b(+). Expression of both constructs under the TrxA fusion protein produced a larger size of recombinant RBD, as reported in the previous study (Gao *et al.*, 2022). The TrxA fusion protein promotes protein solubility and significantly reduces the formation of inclusion bodies of recombinant protein produced in E.*coli* system (Costa *et al.*, 2014). Additional strategies such as IPTG induction in low temperature and isolation with a mild denaturing buffer were utilized to enhance the solubilized inclusion bodies of RBD and RS1 protein, hence avoiding the refolding steps in purification steps.

Inclusion bodies are a common challenge encountered when using E.*coli* for recombinant protein expression (Bhatwa *et al.*, 2021). Purification of recombinant protein from inclusion bodies can be challenging. Solubilization and refolding are the critical steps to purify recombinant protein from inclusion bodies. Solubilization of inclusion bodies using a high concentration of chaotropic agent sometimes leads to protein aggregation during the refolding steps (Singh *et al.*, 2012). The expression of recombinant protein in low temperatures often results in non-classical inclusion bodies. Mild solubilization buffers could recover this type of non-classical inclusion body without losing its activity (Singh *et al.*, 2015). A certain pH of Tris buffer has been shown to make inclusion bodies of recombinant proteins produced in E.*coli* easier to dissolve (Peternel *et al.*, 2010). A previous study showed that the inclusion bodies of r-hGH were completely dissolved in a 100 mM Tris buffer with a pH of 12.5 and contained 2 M urea (Patra *et al.*, 2000).

The potency of RBD and RS1 recombinant protein to recognize anti-spike antibodies from COVID-19 patients at the acute phase was evaluated in this study. It is important to note that the construct of RBD and RS1 with CTD domain used in this study belonged to the SARS-CoV-2 Wuhan strain from the early period of COVID-19 isolated

in Indonesia. Interestingly, the RS1 recombinant protein could detect 80% (8 out of 10) and 100% (4 out of 4) antibody anti-spike from sera collected in 2020 and 2022, respectively (Figure 6B). The potency of RS1 to increase detection sensitivity is probably because of additional binding residue from CTD that could capture more anti-spike antibodies compared to RBD. The spike glycoprotein contains several epitopes directly exposed by the host immune system, making it the primary target for neutralizing antibodies (Nagesha *et al.*, 2022). A previous study documented the antibody profiles of COVID-19 patients against the full spike, NTD-S1, and CTD-S1 antigens, highlighting their dynamic nature. Over 90% of the patients recovering from COVID-19 showed immune responses, specifically IgG and IgM, that targeted the CTD-S1 antigen. These responses were similar to those observed for the full spike. Meanwhile, a mere 3.33% of the recovered patients showed IgG reactivity to NTD-S1 (Bao *et al.*, 2021). In accordance with the previous report (Bao *et al.*, 2021), the addition of CTD domain in our RBD construct (RS1) significantly increases the sensitivity of the serological assay of anti-spike antibodies compared to RBD ($p = 0.0033$). Furthermore, the SARS-CoV-2 S1 subunit CTD binding interface has more residues that directly interact with the receptor ACE2 than does SARS-S1 RBD (Huang *et al.*, 2020). The size of an antigen can affect the immune response in humans and induce more humoral immune response (Heida *et al.*, 2022; Zinkhan *et al.*, 2021). In this sense, the circulated anti-spike antibodies are not limited to RBD domain, but also another area such as CTD of S1 domain. Considering the abundance and variety of antibodies, it is conceivable to develop the ELISA assay harboring RBD with an additional CTD domain to increase the monitoring sensitivity of the spike antibody in the population.

Based on the RBD and RS1 modeling structure from the in silico study, RS1 structure (Figure 2B) showed a greater protein surface that could elicit more antigenic antibody determinants. It is correlated with the ELISA result of RS1, which had higher detection sensitivity. From the molecular dynamics result, the different topologies of RBD-Fv and RS1-Fv complexes may cause RMSD differences, especially the longer chain of the RS1 that makes the pET32b open out (Figure 2B). The extended RBD chain in RS1 seems like a linker region between RBD chain and pET32b(+) that lead to the open conformation. This open conformation gives rise to the greater fluctuation of amino acid residues during dynamic simulation and, consequently, the backbones deviate more from its original state. The first 150 residues are the pET32b part that accounts for the greatest fluctuations of the overall antigen molecule (Figure 3C and 3D). On the other hand, residue fluctuation in Fv molecule binding to RBD has almost the same pattern as Fv molecule binding to RS1 (Figure 3E and 3F). The higher fluctuations occur mostly in the loop regions, which are more flexible and undergo random motions, especially those in the surface area. The binding stability between antigen and antibody can be seen through RMSF of the interacting residues (Figure 3C and 3D). Major residues in the contact region generate Van der Waals interaction. Some others use pi-pi stacks and hydrogen bonds. These interactions increase the binding affinity and stabilize the binding between antigen and antibody, leading to low fluctuations in the interacting residues. The average RMSF of interacting residues in RBD is lower (2.0 Å) than that of RS1 (3.3 Å). Compared with RBD, RS1 produced a two-fold higher degree of fluctuation in the overall complex due to its open conformation. Due to the different topology of modeled structure between RBD and RS1, we cannot conclude that the system's lower fluctuations of RBD amino acid residues correspond to higher binding affinity with the antibody molecule. Mainly because the interacting residues with the antibody in both RBD and RS1 show relatively low fluctuation, both antigens have stable binding with the antibody. The epitope antigenicity between RBD and RS1 should be compared for further study.

5. Conclusion

Antigen size affects the immune response in humans, specifically the humoral immune response. In this sense, the circulated anti-spike antibodies are not limited to targeting the RBD domain but also targeting another area, such as the C terminal domain (CTD). Considering the abundance and variety of antibodies, developing the ELISA assay harboring RBD with an additional CTD domain is conceivable to increase the monitoring sensitivity of the relevant antibody in the population.

Acknowledgments

This research was supported by the DIPA grant 2021 Menristek/BRIN and RIIM grant (B-3451/II.7.5/FR.06.00/10/2023), BRIN.

Competing Interests

The authors declare no competing interests.

References

Ayón-Núñez, D. A., Cervantes-Torres, J., Cabello-Gutiérrez, C., Rosales-Mendoza, S., Rios-Valencia, D., Huerta, L., Bobes, R. J., Carrero, J. C., Segura-Velázquez, R., Fierro, N. A., Hernández, M., Zúñiga-Ramos, J., Gamba, G., Cárdenas, G., Frías-Jiménez, E., Herrera, L. A., Fragoso, G., Sciutto, E., Suárez-Güemes, F., & Laclette, J. P. (2022). An RBD-Based Diagnostic Method Useful for the Surveillance of Protective Immunity against SARS-CoV-2 in the Population. *Diagnostics (Basel)*, **12**. doi:10.3390/diagnostics12071629

Bao, Y., Ling, Y., Chen, Y. Y., Tian, D., Zhao, G. P., Zhang, X. H., Hang, H., Li, Y., Su, B., Lu, H. Z., Xu, J., & Wang, Y. (2021). Dynamic anti-spike protein antibody profiles in COVID-19 patients. *Int J Infect Dis*, **103**:540-548. doi:10.1016/j.ijid.2020.12.014

Bhatwa, A., Wang, W., Hassan, Y. I., Abraham, N., Li, X. Z., & Zhou, T. (2021). Challenges Associated With the Formation of Recombinant Protein Inclusion Bodies in Escherichia coli and Strategies to Address Them for Industrial Applications. *Front Bioeng Biotechnol*, **9**:630551. doi:10.3389/fbioe.2021.630551

Biswas, S., Mahmud, S., Mita, M. A., Afrose, S., Hasan, M. R., Sultana Shimu, M. S., Saleh, M. A., Mostafa-Hedeab, G., Alqarni, M., Obaidullah, A. J., & Batiha, G. E. (2021). Molecular Docking and Dynamics Studies to Explore Effective Inhibitory Peptides Against the Spike Receptor Binding Domain of SARS-CoV-2. *Front Mol Biosci*, **8**:791642. doi:10.3389/fmolb.2021.791642

Brenke, R., Hall, D. R., Chuang, G.-Y., Comeau, S. R., Bohnuud, T., Beglov, D., Schueler-Furman, O., Vajda, S., & Kozakov, D. (2012). Application of asymmetric statistical potentials to antibody–protein docking. *Bioinformatics*, **28**: 2608-2614. doi:10.1093/bioinformatics/bts493

Brindha, S., & Kuroda, Y. (2022). A Multi-Disulfide Receptor-Binding Domain (RBD) of the SARS-CoV-2 Spike Protein Expressed in E. coli Using a SEP-Tag Produces Antisera Interacting with the Mammalian Cell Expressed Spike (S1) Protein. *Int J Mol Sci*, **23**. doi:10.3390/ijms23031703

Brouwer, P. J. M., Caniels, T. G., van der Straten, K., Snitselaar, J. L., Aldon, Y., Bangaru, S., Torres, J. L., Okba, N. M. A., Claireaux, M., Kerster, G., Bentlage, A. E. H., van Haaren, M. M., Guerra, D., Burger, J. A., Schermer, E. E., Verheul, K. D., van der Velde, N., van der Kooi, A., van Schooten, J., van Breemen, M. J., Bijl, T. P. L., Sliepen, K., Aartse, A., Derking, R., Bontjer, I., Kootstra, N. A., Wiersinga, W. J., Vidarsson, G., Haagmans, B. L., Ward, A. B., de Bree, G. J., Sanders, R. W., & van Gils, M. J. (2020). Potent neutralizing antibodies from COVID-19 patients define multiple targets of vulnerability. *Science*, 369:643-650. doi:10.1126/science.abc5902

Costa, S., Almeida, A., Castro, A., & Domingues, L. (2014). Fusion tags for protein solubility, purification and immunogenicity in Escherichia coli: the novel Fh8 system. *Front Microbiol*, **5**. doi:10.3389/fmicb.2014.00063

Fraser, D. D., Miller, M. R., Martin, C. M., Slessarev, M., Hahn, P., Higgins, I., Melo, C., Pest, M. A., Rothery, N., Wang, X., Zeidler, J., & Cruz-Aguado, J. A. (2022). Cohort-Specific Serological Recognition of SARS-CoV-2 Variant RBD Antigens. *Ann Clin Lab Sci*, **52**:651-662.

Gao, X., Peng, S., Mei, S., Liang, K., Khan, M. S. I., Vong, E. G., & Zhan, J. (2022). Expression and functional identification of recombinant SARS-CoV-2 receptor binding domain (RBD) from E. coli system. *Prep Biochem Biotechnol*, **52**:318-324. doi:10.1080/10826068.2021.1941106

He, Y., Qi, J., Xiao, L., Shen, L., Yu, W., & Hu, T. (2021). Purification and characterization of the receptor-binding domain of SARS-CoV-2 spike protein from Escherichia coli. *Eng Life Sci*, **21**:453-460. doi:10.1002/elsc.202000106

Heida, R., Born, P. A., Tapia-Calle, G., Frijlink, H. W., Salvati, A., Huckriede, A. L. W., & Hinrichs, W. L. J. (2022). Assessing the Immunomodulatory Effect of Size on the Uptake and Immunogenicity of Influenza- and Hepatitis B Subunit Vaccines In Vitro. *Pharmaceuticals (Basel)*, **15**. doi:10.3390/ph15070887

Huang, Y., Yang, C., Xu, X.-f., Xu, W., & Liu, S.-w. (2020). Structural and functional properties of SARS-CoV-2 spike protein: potential antivirus drug development for COVID-19. *Acta Pharmacol. Sin.*, **41**:1141-1149. doi:10.1038/s41401-020-0485-4

Kozakov, D., Hall, D. R., Xia, B., Porter, K. A., Padhorny, D., Yueh, C., Beglov, D., & Vajda, S. (2017). The ClusPro web server for protein-protein docking. *Nat. Protoc.*, **12**:255-278. doi:10.1038/nprot.2016.169

Krähling, V., Halwe, S., Rohde, C., Becker, D., Berghöfer, S., Dahlke, C., Eickmann, M., Ercanoglu, M. S., Gieselmann, L., Herwig, A., Kupke, A., Müller, H., Neubauer-Rädel, P., Klein, F., Keller, C., & Becker, S. (2021). Development and characterization of an indirect ELISA to detect SARS-CoV-2 spike protein-specific antibodies. *J Immunol Methods*, **490**. 112958. doi:10.1016/j.jim.2021.112958

Krieger, E., & Vriend, G. (2014). YASARA View - molecular graphics for all devices - from smartphones to workstations. *Bioinformatics*, **30**:2981-2982. doi:10.1093/bioinformatics/btu426

Lee, J., Cheng, X., Swails, J. M., Yeom, M. S., Eastman, P. K., Lemkul, J. A., Wei, S., Buckner, J., Jeong, J. C., Qi, Y., Jo, S., Pande, V. S., Case, D. A., Brooks, C. L., III, MacKerell, A. D., Jr., Klauda, J. B., & Im, W. (2016). CHARMM-GUI Input Generator for NAMD, GROMACS, AMBER, OpenMM, and CHARMM/OpenMM Simulations Using the CHARMM36 Additive Force Field. *J. Chem. Theory Comput.*, **12**:405-413. doi:10.1021/acs.jctc.5b00935

Lin, W.-Z., Wang, J.-P., Ma, I. C., Hsieh, P.-C., Hung, Y.-J., Hung, C.-M., & Hou, S.-Y. (2023). Highly sensitive β-galactosidase detection using streptavidin-display E. coli and lateral flow immunoassay. *Sens. Actuators, A.*, **350**. 114114. doi:https://doi.org/10.1016/j.sna.2022.114114

Liu, L., Jiao, Y., Yang, M., Wu, L., Long, G., & Hu, W. (2023). Network Pharmacology, Molecular Docking and Molecular Dynamics to Explore the Potential Immunomodulatory Mechanisms of Deer Antler. *Int J Mol Sci*, **24**. doi:10.3390/ijms241210370

Maffei, M., Montemiglio, L. C., Vitagliano, G., Fedele, L., Sellathurai, S., Bucci, F., Compagnone, M., Chiarini, V., Exertier, C., Muzi, A., Roscilli, G., Vallone, B., & Marra, E. (2021). The Nuts and Bolts of SARS-CoV-2 Spike Receptor-Binding Domain Heterologous Expression. *Biomolecules*, **11**. doi:10.3390/biom11121812

Mukherjee, S., & Zhang, Y. (2009). MM-align: a quick algorithm for aligning multiple-chain protein complex structures using iterative dynamic programming. *Nucleic Acids Res*, **37**. e83. doi:10.1093/nar/gkp318

Nagesha, S. N., Ramesh, B. N., Pradeep, C., Shashidhara, K. S., Ramakrishnappa, T., Bagoji, M., & Chandaragi, S. S. (2022). SARS-CoV 2 spike protein S1 subunit as an ideal target for stable vaccines: A bioinformatic study. *Mater Today Proc*, **49**:904-912. doi:10.1016/j.matpr.2021.07.163

Oglat, A. A., Oqlat, M. A., Oqlat, A. A., Alanagreh, L. a., Khaniabadi, P. M., Dheyab, M. A., Khaleel, H., & Althalji, O. (2022). Imaging Aspects (Chest Radiographic and CT Scan Findings) of COVID-19 with Clinical Classifications. *Jordan J Biol Sci.*, **15**.

Patra, A. K., Mukhopadhyay, R., Mukhija, R., Krishnan, A., Garg, L. C., & Panda, A. K. (2000). Optimization of inclusion body solubilization and renaturation of recombinant human growth hormone from Escherichia coli. *Protein Expr Purif*, **18**:182-192. doi:10.1006/prep.1999.1179

Peterhoff, D., Glück, V., Vogel, M., Schuster, P., Schütz, A., Neubert, P., Albert, V., Frisch, S., Kiessling, M., Pervan, P., Werner, M., Ritter, N., Babl, L., Deichner, M., Hanses, F., Lubnow, M., Müller, T., Lunz, D., Hitzenbichler, F., Audebert, F., Hähnel, V., Offner, R., Müller, M., Schmid, S., Burkhardt, R., Glück, T., Koller, M., Niller, H. H., Graf, B., Salzberger, B., Wenzel, J. J., Jantsch, J., Gessner, A., Schmidt, B., & Wagner, R. (2021). A highly specific and sensitive serological assay detects SARS-CoV-2 antibody levels in COVID-19 patients that correlate with neutralization. *Infection*, **49**:75-82. doi:10.1007/s15010-020-01503-7

Peternel, S., & Komel, R. (2010). Isolation of biologically active nanomaterial (inclusion bodies) from bacterial cells. *Microb Cell Fact*, **9**. doi:10.1186/1475-2859-9-66

Piovesan, D., Minervini, G., & Tosatto, S. C. (2016). The RING 2.0 web server for high quality residue interaction networks. *Nucleic Acids Res*, **44**:W367-374. doi:10.1093/nar/gkw315

Rastogi, Y. R., Sharma, A., Nagraik, R., Aygün, A., & Şen, F. (2020). The novel coronavirus 2019-nCoV: Its evolution and transmission into humans causing global COVID-19 pandemic. *Int J Environ Sci Technol (Tehran)*, **17**:4381-4388. doi:10.1007/s13762-020-02781-2

Shwan, N. A., Aziz, S. S., Hamad, B. K., & Hussein, O. A. (2022). Characterizing New Genomic and Proteomic Variations among SARS-CoV-2 Strains. *Jordan J Biol Sci.*, **15**.

Singh, A., Upadhyay, V., Upadhyay, A. K., Singh, S. M., & Panda, A. K. (2015). Protein recovery from inclusion bodies of Escherichia coli using mild solubilization process. *Microb Cell Fact*, **14**. doi:10.1186/s12934-015-0222-8

Singh, S. M., Sharma, A., Upadhyay, A. K., Singh, A., Garg, L. C., & Panda, A. K. (2012). Solubilization of inclusion body proteins using n-propanol and its refolding into bioactive form. *Protein Expr Purif.*, **81**:75-82. doi:https://doi.org/10.1016/j.pep.2011.09.004

Tai, W., He, L., Zhang, X., Pu, J., Voronin, D., Jiang, S., Zhou, Y., & Du, L. (2020). Characterization of the receptor-binding domain (RBD) of 2019 novel coronavirus: implication for development of RBD protein as a viral attachment inhibitor and vaccine. *Cell. Mol. Immunol.*, **17**:613-620. doi:10.1038/s41423-020-0400-4

Wu, N. C., Yuan, M., Liu, H., Lee, C. D., Zhu, X., Bangaru, S., Torres, J. L., Caniels, T. G., Brouwer, P. J. M., van Gils, M. J., Sanders, R. W., Ward, A. B., & Wilson, I. A. (2020). An Alternative Binding Mode of IGHV3-53 Antibodies to the SARS-CoV-2 Receptor Binding Domain. *Cell Rep*, **33**.108274. doi:10.1016/j.celrep.2020.108274

Xu, J., & Zhang, Y. (2010). How significant is a protein structure similarity with TM-score = 0.5? *Bioinformatics*, **26**:889-895. doi:10.1093/bioinformatics/btq066

Yang, J., Yan, R., Roy, A., Xu, D., Poisson, J., & Zhang, Y. (2015). The I-TASSER Suite: protein structure and function prediction. *Nat. Methods*, **12**:7-8. doi:10.1038/nmeth.3213

Yang, L., Li, J., Guo, S., Hou, C., Liao, C., Shi, L., Ma, X., Jiang, S., Zheng, B., Fang, Y., Ye, L., & He, X. (2021). SARS-CoV-2 Variants, RBD Mutations, Binding Affinity, and Antibody Escape. *Int J Mol Sci*, **22**. doi:10.3390/ijms222212114

Yin, Q., Zhang, Y., Lian, L., Qu, Y., Wu, W., Chen, Z., Pei, R., Chen, T., Sun, L., Li, C., Li, A., Li, J., Li, D., Wang, S., Guan, W., & Liang, M. (2021). Chemiluminescence Immunoassay Based Serological Immunoassays for Detection of SARS-CoV-2 Neutralizing Antibodies in COVID-19 Convalescent Patients and Vaccinated Population. *Viruses*, **13**. doi:10.3390/v13081508

Zinkhan, S., Ogrina, A., Balke, I., Reseviča, G., Zeltins, A., de Brot, S., Lipp, C., Chang, X., Zha, L., Vogel, M., Bachmann, M. F., & Mohsen, M. O. (2021). The impact of size on particle drainage dynamics and antibody response. *J Control Release*, *331*, 296-308. doi:10.1016/j.jconrel.2021.01.012

JJBS

Volume 17, Number 4,December 2024
ISSN 1995-6673
Pages 727 – 735
https://doi.org/10.54319/jjbs/170415

Jordan Journal of Biological Sciences

Determination of the Genetic Variations of Chickpea (*Cicer Arietinum* L.) Genotypes Preserved in the Jordanian Seed Genbank Using ISSR and SCoT Molecular Markers

Ghina J. Al-Hmoud[1,*] and Emel Sözen[2]

[1] *Department of Biology/ Botany, Faculty of Science, University of Anatolia, Eskisehir, Turkey;* [2] *Department of Biology/Botany, Faculty of Science, Eskisehir Technical University, Eskisehir, Turkey.*

Received: April 19, 2024; Revised: July 26, 2024; Accepted: August 8, 2024

Abstract

This study was the first report on the genetic diversity among 18 local chickpea (*Cicer arietinum*) genotypes presented in the Jordanian National Agricultural Research Center (NARC) Seed Genbank collected from different Jordanian regions. Inter-Simple Sequence Repeat (ISSR) and Start Codon Target (SCoT) Polymorphism molecular markers were used to investigate their relationship. 13 different ISSR primers amplified 135 bands, among them 110 were polymorphic. In comparison, the 10 SCoT primers amplified 166 bands, among them 129 were polymorphic. The polymorphism average and the PIC values in ISSR and SCoT primers were 72%, 75%, 0.17, and 0.26, respectively. The genetic similarity values were moderate, for ISSR-PCR analyses between 0.769-0.452, while for SCoT-PCR analyses ranged from 0.744 to 0.468. The UPGMA analysis grouped the 18 *Cicer arietinum* genotypes into two main clusters divided into sub-clusters and smaller groups in both ISSR and SCoT analyses. STRUCTURE analyses produced three populations mixed within each other in ISSR and SCoT analyses. Current results indicated that SCoT molecular marker proved to be more informative in distinguishing closely related genotypes than ISSR molecular marker. The 18 *C. arietinum* genotypes are genetically related to each other, even though they were geographically distant landraces. Our findings provided significant data for characterizing the genotypes within the seed genebank.; however, there is no duplication among the stored *Cicer arietinum* genotypes.

Keywords: Genetic diversity, Chickpea, Seed Genbank, ISSR, SCoT, PIC.

1. Introductıon

Chickpea (*Cicer arietinum* L.) is a self-pollinated legume species from the family Fabaceae (2n = 16), a semi-arid region growing type (De Giovanni *et al*., 2017), containing a high nutritive content and being a cheap source of protein, in addition to improve land fertility (Saeed *et al*., 2011) and soil health through symbiotic nitrogen fixation (Thudi *et al*., 2016). Chickpeas were domesticated as a crop around 10,000 years ago in Southwest Asia (Anatolia). From there, they spread throughout the Fertile Crescent, reaching South Asia, East Africa (Ethiopia), Australia, and North America (Sani *et al*., 2018). Cultivated Chickpea (*C. arietinum*) is part of a group of annual chickpea species native to Mediterranean regions, while the majority of the remaining species in the genus are perennial species native to colder climates in Anatolia, the Caucasus, and Central Asia (Coyne *et al*., 2020). Chickpea has little genetic diversity due to obligatory self-pollination and an extensively monotonous genome (Aggarwal *et al*., 2015).

Genetic diversity assessment is important for crop improvement and efficient management and conservation of germplasm resources (Pakseresht *et al*., 2013). The concept of genetic resources frameworks breeding, and conservation involved a genocentric perspective with their erosion and the danger of losing biodiversity (Aubry, 2019). Genbank widely reflects the available sources of genetic diversity in landraces, The National Plant Germplasm System (a collaborative program that preserves the genetic diversity of plants) contains over 4000 accessions of chickpeas that originated from almost 50 countries, which made them available to scientists worldwide to support plant breeding and other research program on chickpea (Redden and Berger, 2007). The International Crops Research Institute for the Semi-Arid Tropics (ICRISAT) has the largest collection with 19,959 accessions of cultivated chickpeas and 308 accessions of 18 wild Cicer species from 60 countries (Plekhanova *et al*., 2017).

Genetic techniques and biotechnology tools enable us to leverage the information stored in genebanks more efficiently and rapidly. Thus, genotyping of the collections will allow us to identify the duplication, establish varietal limits, and estimate the population variability (Díez *et al*., 2018). ISSR markers can be targeted towards specific sequences, which are reported to be abundant in the genome and can overcome the technical difficulties of RFLP and RAPD. The previous two markers could not address the reliable genetic variation within chickpeas (Pakseresht *et al*., 2013).

* Corresponding author. e-mail: eng_ghina2009@yahoo.com.

ISSR markers were reported to be more compatible than the RAPD markers, as they were highly reproducible polymorphic DNA markers able to expose various informative loci from a single amplification and had been successfully used to study diversity and phylogenetic relationships for the last decade (Aggarwal *et al*., 2015). For a long time, genetic fingerprinting in chickpeas was inhibited by the little genome variability, which can be facilitated by highly polymorphic functional markers such as SCoT marker. ISSR and SCoT techniques were more informative than prior biochemical such as isozymes and storage proteins, in addition to other molecular methods as RAPD markers, which are used to study variation and genetic relationships in *Cicer* species (Pakseresht *et al*., 2013). The genetic variation detected by ISSR and SCoT markers within and between *Cicer* species was higher than the amount computed from RAPD and AFLP markers (Amirmoradi *et al*., 2012).

Pakseresht *et al*. (2013) mentioned in their study that 40 Chickpea landraces were collected from different geographical locations in northwest Iran and were amplified using ISSR and SCoT markers. The accessions from the same geographical regions showed more genetic similarities than those from different or isolated places. According to the observed results, SCoT marker was more informative than ISSR marker, and both of them were revealed to be better than previous markers for *Cicer* genotypes diversity assessment. Another study done on 48 Iranian chickpea genotypes was identified using 9 SCoT primers; the average PIC value was 0.45 and showed an elevated level of polymorphism and diversity (Hajibarat *et al*., 2015).

In other research, a genetic diversity study on cultivated chickpea *C. arietinum* and its wild progenitor *C. reticulatum* using RAPD and ISSR markers concluded that ISSR analysis was a more reliable reference for genetic diversity estimation than RAPD marker (Gautam et al., 2016). Ahmad and Talebi (2017) examined the genetic diversity of 35 chickpea breeding lines using 14 SCoT primers, with an average PIC value of 0.36 per primer. Cluster analysis grouped the 35 breeding lines into three major clusters.

Jordan has four distinct biogeographical regions, the cultivated areas for *C. arietinum* were found in the Mediterranean and Irano-Turanian regions. This is the first report of studying genetic variability and the relationship of *C. arietinum* genotypes at a DNA level. Therefore, this study aimed to determine the genetic variability of different *C. arietinum* genotypes, and to find any duplication presented in the National Agricultural Research Center (NARC) seed genbank using ISSR and SCoT molecular markers.

2. Methodology

2.1. Plant Material and DNA Extraction

The genetic material used in this study were seeds of 18 local genotypes of *Cicer arietinum* (Kabuli type), obtained from the seed genbank of the NATIONAL AGRICULTURAL RESEARCH CENTER (NARC), Jordan, shown in Table 1. Total genomic DNA was extracted from the young leaf tissues of 2-week-old *C. arietinum* seedlings according to the 2X CTAB protocol (Doyle and Doyle, 1990). DNA quality was assessed using electrophoresis in a 0.8% agarose gel with a 1kb DNA ladder, while DNA purity and quantification were measured using a Nanodrop Spectrophotometer.

Table 1: List of locally cultivated genotypes of *Cicer arietinum* studied, working code, original serial number, and province.

Working code	Serial No.	Taxonomic Name	Province
C1	2775	*Cicer arietinum*	Amman
C2	2777	*Cicer arietinum*	Balqa'
C3	2779	*Cicer arietinum*	Mafraq
C4	2780	*Cicer arietinum*	Amman
C5	2787	*Cicer arietinum*	Ma'an
C6	2788	*Cicer arietinum*	Unknown
C7	2791	*Cicer arietinum*	Jerash
C8	2793	*Cicer arietinum*	Ma'an
C9	2794	*Cicer arietinum*	Karak
C10	2795	*Cicer arietinum*	Zarqa
C11	2796	*Cicer arietinum*	Ma'an
C12	2798	*Cicer arietinum*	Madaba
C13	2799	*Cicer arietinum*	Irbid
C14	2801	*Cicer arietinum*	Unknown
C15	3588	*Cicer arietinum*	Unknown
C16	3590	*Cicer arietinum*	Unknown
C17	4361	*Cicer arietinum*	Ma'an
C18	4537	*Cicer arietinum*	Ma'an

2.2. ISSR-PCR Analysis

26 ISSR primers (designed by the UNIVERSITY OF BRITISH COLUMBIA BIOTECHNOLOGY LABORATORIES) were used in this study. ISSR amplifications were performed with a volume of 15 µl including 10X Taq Buffer (1.5 µl), 25 mM $MgCl_2$ (1.2 µl), 2.5 mM dNTP (1.2 µl), 2.5 µM primer (1 µl), 5 ng/ µl of templet DNA (3 µl), 1U of *Taq* Polymerase (0.15 µl) (FERMENTAS). Amplifications were performed in the thermal cycler with the following program: initial denaturation at 94 °C 4 min, 45 cycles at 94 °C 45 sec, annealing at 50-61 °C 90 sec, extension at 72 °C 2 min, and final extension at 72 °C 5 min. PCR products were electrophoresed in 1.8 % agarose gel containing 5µl Red Safe run for 1 h and 30 min at 85V in the gel tank, then the records were photographed and preserved.

2.3. SCoT-PCR Analysis

19 SCoT primers (synthesized by OLIGOMER BIOTECHNOLOGY COMPANY, ANKARA, TURKEY) were used in this study. SCoT amplifications were performed with a volume of 25 µl including 10X Taq Buffer KCL (2.5 µl), 25 mM $MgCl_2$ (2 µl), 2.5 mM dNTP (2 µl), 2.5 µM primer (5 µl), 10 ng/ µl of templet DNA (5 µl), 1U of *Taq* Polymerase (0.2 µl) (FERMENTAS). Amplifications were performed in the thermal cycler with the following program: initial denaturation at 94°C 3 min, 40 cycles at 94 °C 1 min, annealing at 50-61 °C 1 min, extension at 72 °C 2 min, and final extension at 72 °C 5 min. PCR products were electrophoresed in 1.8 % agarose gel containing 5µl Red Safe run for 1 h and 30 min at 85V in the gel tank, photographed with a UV documentation system and the records were preserved.

2.4. Data Analysis

The amplified products of each ISSR and SCoT PCR reaction were analyzed using the TOTALLAB CLIQS (1D gels) software program. A binary matrix was prepared based on the results obtained, as present (1) or absent (0). The PIC (polymorphism information content) was calculated as a formula suggested by De Riek *et al*. (2001). Genetic similarity values were calculated by the Jaccard coefficient using the DendroUPGMA program. Dendrograms were constructed using the MEGA software version 11. The population structure analysis was performed by the STRUCTURE software program v. 2.3.4 (Pritchard *et al*. 2000). STRUCTURE HARVESTER (Earl and VonHoldt, 2012) was used to calculate the K values, delta K graph and to extract the suitable bar plot graph using the binary matrix.

3. Results

3.1. Assessment of ISSR-PCR Analysis

Out of 26 ISSR primers, 13 ISSR primers produced clear and reproducible band profiles (Fig. 1) which amplified a total of 135 bands from 18 *C. arietinum* genotypes; among these bands 110 were polymorphic. The number of amplified bands varied between 2-18 with an average of 10.4 bands per primer. The band sizes ranged from 333 bp to 3919 bp. PPB% ranged from 0 to 100% with an average of 72%. The PIC values ranged from 0 to 0.3 with an average of 0.17 (Table 2).

Table 2. Primers, primer sequences, annealing temperatures, band profiles, polymorphism percentages, and PIC values of *C. arietinum* genotypes using ISSR molecular marker.

Primer	Sequences (5'-3')	An.T	Band Size (bp)	TB	PB	PPB%	PIC
ISSR 807	$(AG)_8$-T	52	566-1790	10	7	70	0.17
ISSR 810	$(GA)_8$-T	50	467-2231	8	7	87.5	0.2
ISSR 811	$(GA)_8$-C	50	333-3919	18	17	94	0.26
ISSR 812	$(GA)_8$-A	50	560-1700	9	6	67	0.23
ISSR 813	$(CT)_8$-T	50	406-1560	4	2	50	0.13
ISSR 817	$(CA)_8$-A	50	949-1320	2	0	0	0
ISSR 818	$(CA)_8$-G	53	609-2381	14	14	100	0.3
ISSR 819	$(TC)_8$-C	50	712-1423	5	3	60	0.05
ISSR 829	$(TG)_8$-C	53	510-3000	16	15	94	0.27
ISSR 834	$(AG)_8$-YT	53	364-1122	13	12	92	0.17
ISSR 847	$(CA)_8$-RC	55	582-2368	13	10	77	0.14
ISSR 853	$(TC)_8$-RT	53	400-1433	13	10	77	0.18
ISSR 855	$(AC)_8$-YT	53	470-1887	10	7	70	0.1
SUM				135	110	-	-
AVG				10.4	-	72	0.17

Where Y= (C, T), R= (A, G), An.T: annealing temp., TB: total no. of bands, PB: polymorphic bands, PPB%: The polymorphism percentage, and PIC: polymorphism information content.

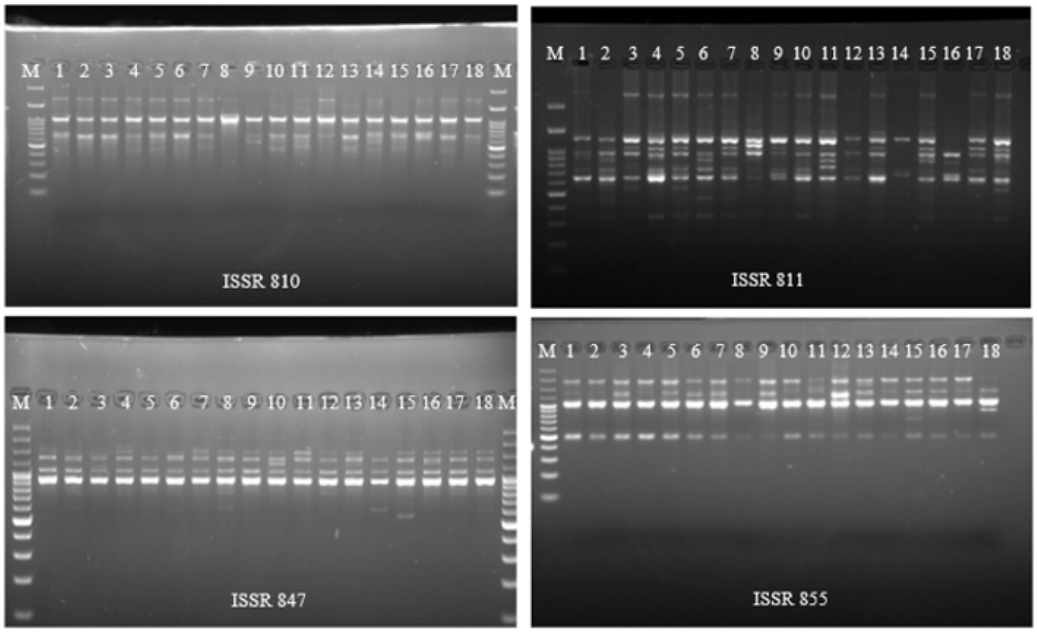

Figure 1. ISSR band profiles of *C. arietinum* genotypes with ISSR primers 810, 811, 847and 855. M: 100 bp plus DNA marker (FERMENTAS), (1:C1, 2:C2, 3:C3, 4:C4, 5:C5, 6:C6, 7:C7, 8:C8, 9:C9, 10:C10, 11:C11, 12:C12, 13:C13, 14:C14, 15:C15, 16:C16, 17:C17, and 18:C18).

The genetic similarity among the 18 *C. arietinum* genotypes ranged from 0.769 to 0.452. The highest similarity (0.769) was observed between 4537 (C18) and 4361 (C17) genotypes both from Maan, and the lowest genetic similarity (0.452) was found between 2798 from Madaba (C12) and 2795 from Zarqa (C10) (Table 3). UPGMA dendrogram grouped the 18 *C. arietinum* genotypes into two main clusters (Fig. 2). Cluster I included only one variety 2795 from Zarqa (C10), and cluster II divided into two sub-clusters; the first sub-cluster included 2801 Unknown (C14), and the second sub-cluster included all the other 16 *C. arietinum* genotypes divided into smaller groups. For more genetic examination within the 18 *C. arietinum* genotypes population structures, STRUCTURE analysis was used and according to Delta K, they were divided into three clusters (Fig. 3 and Fig. 4).

Table 3. ISSR genetic Jaccard similarity matrix between *C. arietinum* genotypes.

	C1 Amman	C4 Amman	C2 Balqa	C3 Mafraq	C5 Maan	C8 Maan	C11 Maan	C17 Maan	C18 Maan	C7 Jerash	C9 Karak	C10 Zarqa	C13 Irbid	C14 Unknown	C15 Unknown	C16 Unknown	C6 Unknown	C12 Madaba
C1 Amman	1	0.634	0.592	0.56	0.62	0.533	0.646	0.556	0.539	0.541	0.592	0.507	0.527	0.521	0.545	0.5	0.566	0.551
C4 Amman		1	0.643	0.676	0.671	0.603	0.603	0.676	0.587	0.634	0.618	0.533	0.62	0.548	0.613	0.569	0.635	0.603
C2 Balqa			1	0.634	0.629	0.629	0.631	0.657	0.657	0.638	0.6	0.514	0.623	0.571	0.662	0.618	0.662	0.656
C3 Mafraq				1	0.686	0.573	0.571	0.62	0.558	0.581	0.55	0.547	0.547	0.541	0.605	0.52	0.584	0.618
C5 Maan					1	0.681	0.662	0.766	0.639	0.643	0.671	0.562	0.606	0.556	0.69	0.556	0.714	0.688
C8 Maan						1	0.612	0.687	0.662	0.62	0.584	0.481	0.606	0.514	0.644	0.556	0.667	0.714
C11 Maan							1	0.694	0.692	0.646	0.52	0.582	0.606	0.486	0.623	0.552	0.623	0.587
C17 Maan								1	0.769	0.697	0.63	0.542	0.632	0.557	0.721	0.627	0.671	0.694
C18 Maan									1	0.603	0.55	0.506	0.568	0.52	0.649	0.629	0.605	0.618
C7 Jerash										1	0.551	0.527	0.614	0.5	0.63	0.563	0.653	0.621
C9 Karak											1	0.538	0.644	0.616	0.595	0.513	0.556	0.562
C10 Zarqa												1	0.577	0.467	0.513	0.467	0.494	0.452
C13 Irbid													1	0.549	0.639	0.507	0.573	0.559
C14 Unknown														1	0.526	0.479	0.526	0.552
C15 Unknown															1	0.589	0.653	0.672
C16 Unknown																1	0.547	0.576
C6 Unknown																	1	0.6
C12 Madaba																		1

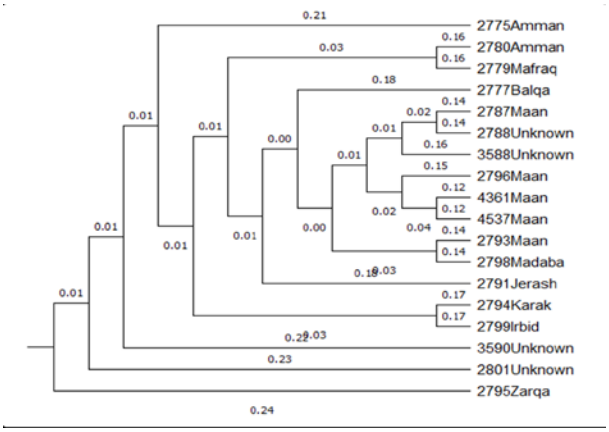

Figure 2. UPGMA clustering pattern of 18 *C. arietinum* genotypes based on the genetic similarity values of ISSR analyses.

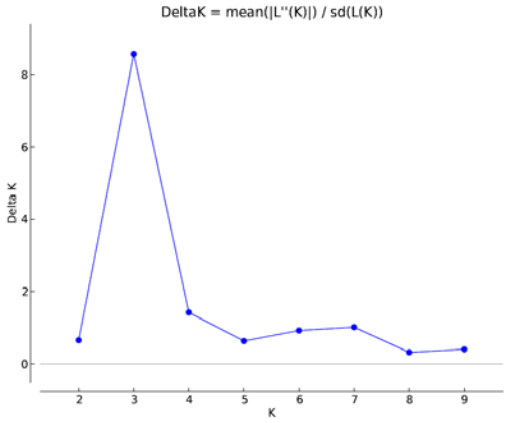

Figure 3. STRUCTURE analysis for the number of clusters (K = 3) of *C. arietinum* genotypes based on ISSR analyses.

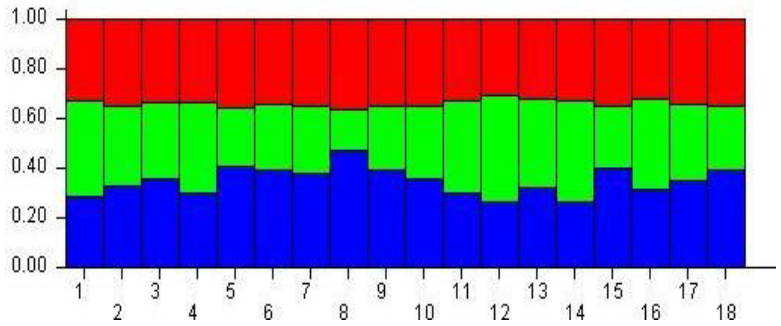

Figure 4. STRUCTURE analysis of the 18 *C. arietinum* genotypes based on ISSR analyses. The same color indicates the same group.

3.2. Assessment of SCoT-PCR Analysis

Of 19 SCoT primers, 10 primers produced clear and reproducible band profiles (Fig. 5) which amplified a total of 166 bands from 18 *C. arietinum* genotypes; among these bands, 129 were polymorphic. The number of amplified bands varied between 8-25 with an average of 16.6 bands per primer. The band sizes ranged from 185 bp to 3825 bp. PPB% ranged from 50 to 92% with an average of 75%. The PIC values ranged from 0.13 to 0.35 with an average of 0.26 (Table 4).

Table 4. Primers, primer sequences, annealing temperatures, band profiles, polymorphism percentages, and PIC values of *C. arietinum* genotypes using SCoT molecular marker.

Primer	Sequences (5'- 3')	An.T	Band Size (bp)	TB	PB	PPB%	PIC
SCoT 3	CAACAATGGCTACCACCG	52	588-2650	13	12	92	0.35
SCoT 9	CAACAATGGCTACCAGCA	54	800-2935	8	4	50	0.19
SCoT 12	ACGACATGGCGACCAACG	56	185-2729	20	16	80	0.26
SCoT 15	ACGACATGGCGACCGCGA	54	225-2911	21	18	86	0.31
SCoT 16	ACCATGGCTACCACCGAC	52	288-3404	20	18	90	0.30
SCoT 18	ACCATGGCTACCACCGCC	54	227-2927	13	7	54	0.13
SCoT 19	ACCATGGCTACCACCGGC	54	688-3825	17	15	88	0.31
SCoT 21	ACGACATGGCGACCCACA	52	230-1733	14	10	71	0.21
SCoT 28	CCATGGCTACCACCGCCA	50	295-3048	15	9	60	0.24
SCoT 32	CCATGGCTACCACCGCAC	50	240-3281	25	20	80	0.26
SUM				166	129	-	-
AVG				16.6		75	0.26

An.T: annealing temp., TB: total no. of bands, PB: polymorphic bands, PPB%: The polymorphism percentage, and PIC: polymorphism information content.

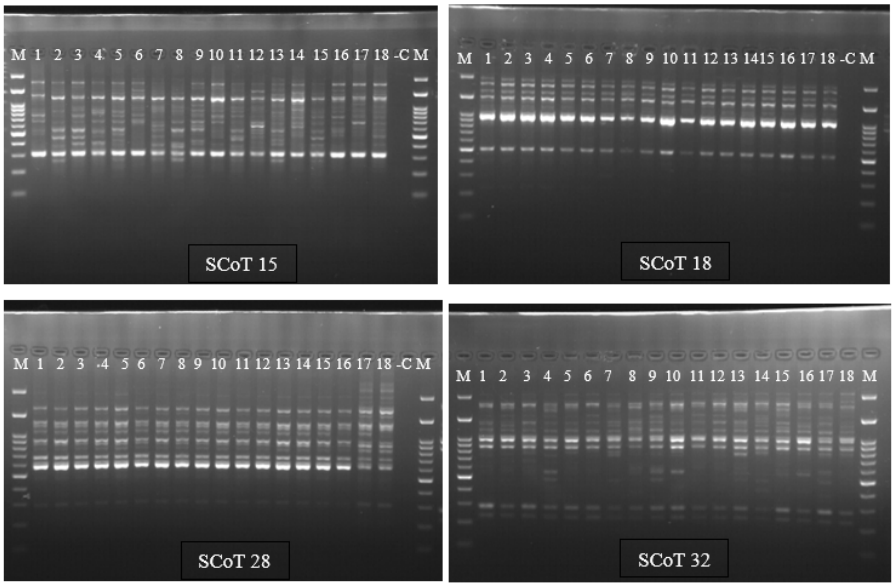

Figure 5. SCoT band profiles of *C. arietinum* genotypes with SCoT primers 15, 18, 28 and 32. M: 100 bp plus DNA marker (FERMENTAS), -C: negative control, (1:C1, 2:C2, 3:C3, 4:C4, 5:C5, 6:C6, 7:C7, 8:C8, 9:C9, 10:C10, 11:C11, 12:C12, 13:C13, 14:C14, 15:C15, 16:C16, 17:C17, and 18:C18).

The genetic similarity among the 18 *C. arietinum* genotypes ranged from 0.744 to 0.468. The highest similarity (0.744) was observed between 2779 from Mafraq (C3) and 2777 from Balqa (C2) genotypes, and the lowest genetic similarity (0.468) was found between 3590 Unknown (C16) and 2779 from Mafraq (C3) (Table 5). UPGMA dendrogram grouped the 18 *C. arietinum* genotypes into two main clusters (Fig. 6). Cluster I included genotypes 3590 Unknown (C16) and 3588 Unknown (C15), and cluster II divided into two sub-clusters; sub-cluster I included genotypes 2801 Unknown (C14), 2799 from Irbid (C14), 2798 from Madaba (C12), 2795 from Zarqa (C10), 2794 from Karak (C9), 2788 Unknown (C6), 2791 from Jerash (C7), with 2793 (C8), 4537 (C18), 4361 (C17), 2796 (C11) and 2787 (C5) from Maan divided in much smaller groups. Sub-cluster II included 2779 from Mafraq (C3), 2777 from Balqa (C2), 2780 (C4), and 2775 (C1) from Amman genotypes. For more genetic examination within the 18 *C. arietinum* genotypes population structures, STRUCTURE analysis was used and according to Delta K, they were divided into three clusters (Fig. 7 and Fig. 8).

Table 5. SCoT genetic Jaccard similarity matrix between *C. arietinum* genotypes.

	2775Amman	2780Amman	2777Balqa	2779Mafraq	2787Maan	2793Maan	2796Maan	4361Maan	4537Maan	2791Jerash	2794Karak	2795Zarqa	2798Madaba	2799Irbid	2801Unknown	3588Unknown	3590Unknown	2788Unknown
2775Amman	1	0.698	0.646	0.653	0.59	0.518	0.643	0.56	0.518	0.533	0.559	0.625	0.545	0.523	0.589	0.496	0.519	0.571
2780Amman		1	0.63	0.67	0.654	0.549	0.66	0.636	0.633	0.565	0.604	0.611	0.562	0.569	0.606	0.5	0.495	0.59
2777Balqa			1	0.744	0.59	0.518	0.66	0.518	0.491	0.505	0.504	0.565	0.532	0.551	0.56	0.565	0.519	0.54
2779Mafraq				1	0.644	0.579	0.649	0.536	0.564	0.552	0.564	0.615	0.565	0.514	0.565	0.527	0.468	0.561
2787Maan					1	0.627	0.735	0.642	0.655	0.617	0.596	0.604	0.613	0.606	0.642	0.575	0.532	0.583
2793Maan						1	0.648	0.625	0.595	0.6	0.568	0.56	0.583	0.508	0.517	0.574	0.491	0.551
2796Maan							1	0.713	0.676	0.59	0.615	0.654	0.663	0.625	0.587	0.578	0.577	0.635
4361Maan								1	0.682	0.571	0.581	0.56	0.556	0.575	0.611	0.484	0.587	0.596
4537Maan									1	0.627	0.593	0.628	0.529	0.602	0.581	0.508	0.615	0.641
2791Jerash										1	0.598	0.62	0.558	0.593	0.558	0.562	0.532	0.684
2794Karak											1	0.688	0.623	0.616	0.623	0.559	0.492	0.579
2795Zarqa												1	0.574	0.609	0.534	0.593	0.55	0.618
2798Madaba													1	0.618	0.556	0.574	0.504	0.551
2799Irbid														1	0.575	0.595	0.61	0.588
2801Unknown															1	0.56	0.545	0.596
3588Unknown																1	0.55	0.528
3590Unknown																	1	0.602
2788Unknown																		1

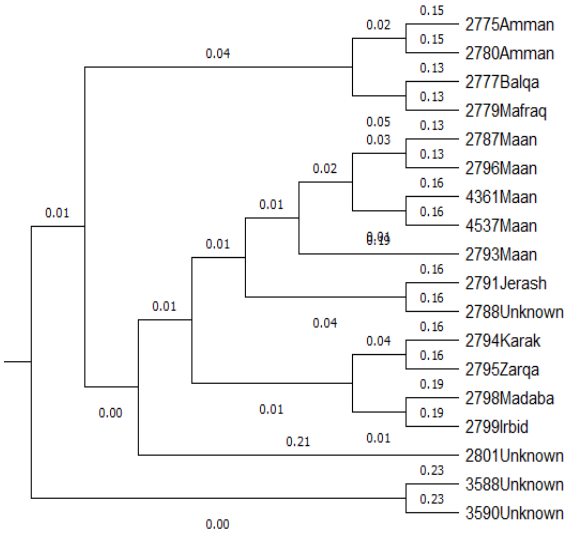

Figure 6. UPGMA clustering pattern of 18 *C. arietinum* genotypes based on the genetic similarity values of SCoT analyses.

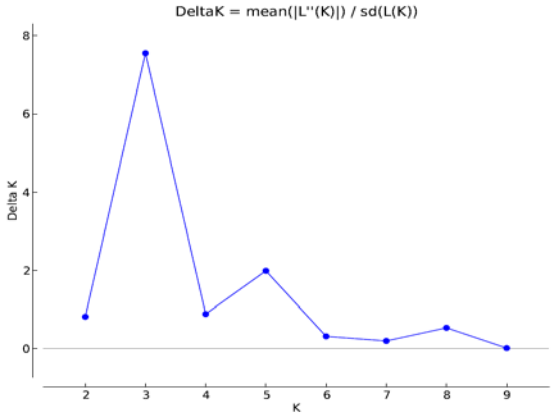

Figure 7. STRUCTURE analysis for the number of clusters (K = 3) of *C. arietinum* genotypes based on SCoT analyses.

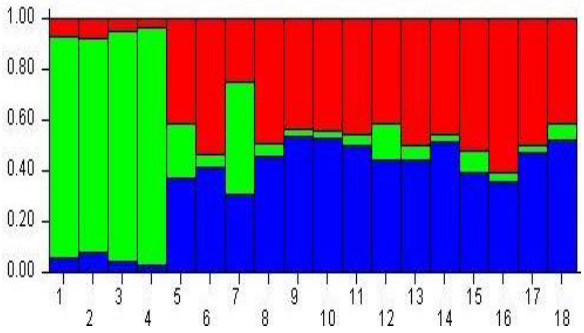

Figure 8. STRUCTURE analysis of the 18 *C. arietinum* genotypes based on SCoT analyses. The same color indicates the same group.

4. Discussion

The collection of *C. arietinum* genotypes obtained from the Jordanian seed genebank (NARC) contains 18 genotypes collected from 10 different regions of Jordan presented in Table 1. In this study, genetic diversity was assessed among 18 Jordanian genotypes of *C. arietinum* using 13 ISSR and 10 SCoT primers. The ISSR analyses yielded a total of 135 bands of which 110 were polymorphic, with an average of 72 % polymorphism. The number of amplified bands varied between 2 -18 with an average of 10.4 bands per primer. The average PIC value of ISSR primers was calculated as 0.17. On the other hand, 10 SCoT primers amplified reproducible 166 bands, among these 129 were polymorphic (PPB: 75%). The number of amplified bands varied between 8 - 25 with an average of 16.6 bands per primer. The average PIC value of SCoT primers was calculated as 0.26. The number of bands and polymorphism levels of SCoT primers were higher than ISSR.

The average PIC value of SCoT primers (0.26) was higher than that of ISSR (0.17), although the polymorphism rate for these two primers was high, their informativeness (PIC) was not the highest value for a dominant marker, which is said to be 0.5 according to De Riek *et al.* (2001). These results showed that SCoT primers were more efficient and informative than ISSR in estimating genetic diversity in studied Jordanian *C. arietinum* genotypes. *C. arietinum* is known to have a narrow genetic base and minimal polymorphism as previously demonstrated by molecular markers, including seed protein, isozyme, and RFLP analyses (Iruela *et al*., 2018). Using RAPD and ISSR markers, a molecular analysis was conducted to determine the genetic diversity and relationships among chickpea cultivars; 33 bands overall were produced by the 5 polymorphic primers with 63.6 % polymorphism (Tahir and Karim, 2011). In another study, 10 SCoT primers were used to fingerprint 10 genotypes of *Cicer arietinum*, 33 polymorphic bands out of 94 amplified bands were recorded, and the polymorphism percentage was 35 % (Serag, 2021).

On the other hand, some studies obtained higher polymorphism levels than the present study. For example, ISSR and SCoT markers were used for the analysis of genetic relationships among 38 accessions of 8 annual *Cicer* species, including the cultivated *C. arietinum* which detected an elevated level of polymorphism about 97 % (Amirmoradi *et al*., 2012). Results obtained from the same study confirmed that *C. arietinum* has the narrowest genetic base among all the annual species and the wild *C. reticulatum* genetically is the closest species to C. *arietinum.* Aggarwal *et al*. (2015) reported that 26 ISSR primers yielded a total of 232 bands representing the genetic diversity of 125 cultivars of chickpeas of Indian origin, 213 of which were polymorphic (91.8 %) with an average of 9 bands per primer.

In addition, Hajibarat *et al.* (2015) showed that 9 SCoT primers amplified a total of 145 bands from 48 Iranian chickpea accessions; among these bands 133 were polymorphic. The average PIC value was 0.45 and showed a prominent level of polymorphism and diversity. The three prior studies reported higher polymorphism levels than this study due to the use of different *Cicer* species and a greater number of genotypes. However, Pakseresht *et al.* (2013) studied 40 Iranian chickpea genotypes using 7 ISSR and 10 SCoT primers. The average PIC values were 0.216 for ISSR markers and 0.232 for the SCoT markers, which was close to the results of our study. They concluded similarly that SCoT marker was more informative than ISSR markers.

The genetic similarity matrix between *C. arietinum* genotypes was calculated based on Jaccard's similarity coefficient. For ISSR molecular marker, the genetic

similarity values were moderate (0.769 - 0.452). The genetically closest genotypes were 4537 from Maan and 4361 from Maan (0.769), and the most distant genotypes were 2798 from Madaba and 2795 from Zarqa (0.452). For SCoT molecular marker, the genetic similarity values were between 0.744 and 0.468; the genetically closest genotypes were 2779 from Mafraq and 2777 from Balqa (0.744), and genetically the lowest genotypes were 3590 Unknown and 2779 from Mafraq (0.468). The similarity coefficient values for the two molecular markers were similar, but they did not produce identical clusters in the UPGMA dendrograms. The difference between the two markers is due to the different DNA sequences presented in each primer, which tracked different readings among the PCR analyses, producing different band profiles.

According to UPGMA clustering pattern obtained from ISSR analyses, the 18 *C. arietinum* genotypes were grouped into 2 main clusters: cluster I included only one variety 2795 from Zarqa, and cluster II was divided into two sub-clusters, the first sub-cluster included 2801 Unknown, and the second sub-cluster included the rest 16 *C. arietinum* genotypes divided into smaller groups. 3590 Unknown placed closest to 2801 Unknown in the first sub-cluster, followed by 2799 from Irbid, 2794 from Karak, and 2791 from Jerash were grouped close with each other. After that, 2798 from Madaba, 2793 from Maan, 4537 from Maan, 4361 from Maan, 2796 from Maan, 3588 Unknown, 2788 Unknown, 2787 from Maan, and 2777 from Balqa were genetically grouped. 2779 from Mafraq, 2780 from Amman, and 2775 from Amman were placed close altogether.

On the other hand, the UPGMA dendrogram produced using SCoT analyses grouped the 18 *C. arietinum* into 2 main clusters: cluster I included 3590 Unknown and 3588 Unknown, and cluster II contained the remaining 16 genotypes divided into two main sub-clusters. Sub-cluster I was split into more small groups; group I with only 2801 Unknown (the closest to cluster I), group II contained 2799 from Irbid, 2798 from Madaba, 2795 from Zarqa, and 2794 from Karak. Group III had 2788 Unknown and 2791 from Jerash, while group IV included all genotypes from the same collected provinces 2793, 4537, 4361, 2796, and 2787 from Maan. Sub-cluster II included 2779 from Mafraq, 2777 from Balqa, 2780 from Amman, and 2775 from Amman. In both UPGMA dendrograms, the *C. arietinum* genotypes collected from Amman and Maan provinces were placed in the same group "genetically close to each other." The four genotypes with Unknown localities were placed differently each time. However, 2801 Unknown and 3590 Unknown lay close in both analyses.

The ISSR genetic STRUCTURE analyses grouped the 18 Jordanian *C. arietinum* genotypes into 3 clusters, which were presented and mixed in all the 18 genotypes; the red cluster presented somehow in equal balance. However, the green and blue clusters fluctuate all over the 18 genotypes. Likewise, the SCoT genetic structure grouped them also into 3 clusters, with different arrangements all over the 18 genotypes. The green cluster presented the most in 2775 from Amman, 2780 from Amman, 2779 from Mafraq, 2777 from Balqa, and 2791 from Jerash genotypes, while the red and blue clusters ranged in a balance between the remaining genotypes. SCoT molecular marker proved to be more informative in distinguishing closely related genotypes than ISSR molecular marker. These findings implied that the 3 clusters (populations) were mixed over the years as they had been cultivated throughout the country.

5. Conclusion

To our knowledge, this is the first report estimating the genetic variability of the cultivated *C. arietinum* genotypes using ISSR and SCoT molecular marker techniques. Molecular markers are stable, quick, and reliable techniques that can be applied in laboratory conditions. ISSR and SCoT molecular markers are dominant, highly reproducible, require a small amount of DNA, simple to work with, making them a valuable tool for studying plant genetic populations and diversity. In this study, we cannot prove any differences between the cultivated *C. arietinum* genotypes according to the biogeographical areas via ISSR analyses. However, SCoT analysis showed that the genotypes from Amman, Mafraq, and Balqa were the genotypes genetically closest to each other according to UPGMA dendrogram and Structure software clustering model.

Amman, Mafraq, and Balqa provinces presented in the Middle to North of Jordan and considered near each other in the same biogeographical regions mixed between the Mediterranean and the Irano-Turanian, have the same genetic structure. The genotypes from Maan province were all clustered in the same group and genetically the same. All of the 18 *C. arietinum* genotypes are genetically related to each other, even though they were geographically distant landraces. According to our ISSR-PCR and SCoT-PCR results, most of the genotypes were the same in some of the primers, but they were not identical. Therefore, there is no duplication among the stored genotypes; however, more studies can be done to ensure the previous results.

Acknowledgments

This work was part of a Doctoral thesis, funded by Eskişehir Technical University (project 21DRP101). The authors express their gratitude to the Jordanian National Agriculture Research Centre (NARC) seed genebank, particularly Dr. Khaled Abu-Laila (Director of plant biodiversity and genetic resources) and Eng. Hiba Wrikat for providing the *C. arietinum* seed samples.

References

Aggarwal H, Rao A, Kumar A, Singh J, Rana JS, Naik PK and Chhokar V. 2015. Assessment of genetic diversity among 125 cultivars of chickpea (*Cicer arietinum* L.) of Indian origin using ISSR markers. *Turk J Bot.*, **39:** 218-226.

Ahmad KM and Talebi R. 2017. Genetic Diversity Assessment in Chickpea Using Morphological Characters and Start Codon Targeted (SCoT) Molecular Markers. *Annu Res Rev Biol.*, **15 (1):**1-8.

Amirmoradi B, Talebi R and Karami E. 2012. Comparison of genetic variation and differentiation among annual Cicer species using start codon targeted (SCoT) polymorphism, DAMD-PCR, and ISSR markers. *Plant Syst Evol.*, **298 (9):** 1679-1688.

Aubry S. 2019. The future of digital sequence information for plant genetic resources for food and agriculture. *Front Plant Sci.*, **10:** 1046.

Coyne CJ, Kuma, S, von Wettberg EJ, Marques E, Berger J, Redden RJ, Ellis TN, Brus J, Zablatzká L and Smýkal, P. 2020. Potential and limits of exploitation of crop wild relatives for pea, lentil, and chickpea improvement. *Legum Sci.*, **2 (2):** 36.

De Giovanni C, Pavan S, Taranto F, Di Rienzo V, Miazzi MM, Marcotrigiano AR, Mangini G, Montemurro C, Ricciardi L and Lotti C. 2017. Genetic variation of a global germplasm collection of chickpeas (*Cicer arietinum* L.) including Italian accessions at risk of genetic erosion. *Physiol Mol Biol plants*, **23 (1):** 197-205.

De Riek J, Calsyn E, Everaert I, Van Bockstaele E and De Loose M. 2001. AFLP based alternatives for the assessment of distinctness, uniformity, and stability of sugar beet varieties. *Theor Appl Genet.*, **103 (8):** 1254-1265.

Díez MJ, De la Rosa L, Martín I, Guasch L, Cartea ME, Mallor C, Casals J, Simó J, Rivera A, Anastasio G, Prohens J. 2018. Plant genebanks: present situation and proposals for their improvement. The case of the Spanish Network. *Front Plant Sci.*, **9:** 1794.

Doyle J and Doyle J. 1990. Isolation of Plant DNA from Fresh Tissue. *Focus*, **12:** 13-15.

Earl DA and VonHoldt BM. 2012. STRUCTURE HARVESTER: a website and program for visualizing STRUCTURE output and implementing the Evanno method. *Conserv Genet Resour.*, **4 (2):** 359-361.

Gautam AK, Gupta N, Bhadkariya R, Srivastava N and Bhagyawant SS. 2016. Genetic diversity analysis in chickpea employing ISSR markers. *Agrotechnology*, **5 (2):** 2168-9881.

Hajibarat Z, Saidi A, Hajibarat Z and Talebi R. 2015. Characterization of genetic diversity in chickpea using SSR markers, start codon targeted polymorphism (SCoT) and conserved DNA-derived polymorphism (CDDP). *Physiol Mol Bio Plants*, **21 (3):** 365-373.

Iruela M, Rubio J, Cubero JI, Gil J and Millan T. 2002. Phylogenetic analysis in the genus Cicer and cultivated chickpea using RAPD and ISSR markers. *Theor Appl Genet.*, **104 (4):** 643-651.

Pakseresht F, Talebi R and Karami E. 2013. Comparative assessment of ISSR, DAMD and SCoT markers for evaluation of genetic diversity and conservation of landrace chickpea (*Cicer arietinum* L.) genotypes collected from north-west of Iran. *Physiol Mol Bio Plants*, **19 (4):** 563-574.

Plekhanova E, Vishnyakova MA, Bulyntsev S, Chang PL, Carrasquilla-Garcia N, Negash K, Wettberg EV, Noujdina N, Cook DR, Samsonova MG and Nuzhdin SV. 2017. Genomic and phenotypic analysis of Vavilov's historic landraces reveals the impact of environment and genomic islands of agronomic traits. *Sci Rep.*, **7 (1):** 4816.

Pritchard JK, Stephens M and Donnelly P. 2000. Inference of population structure using multilocus genotype data. *Genetics*, **155:** 945–959.

Redden RJ and Berger JD. 2007. **History and origin of chickpea.** *Chickpea breeding and management*, **1:** 1-13.

Saeed A, Hovsepyan H, Darvishzadeh R, Imtiaz M, Panguluri SK and Nazaryan R. 2011. Genetic diversity of Iranian accessions, improved lines of chickpea (*Cicer arietinum* L.) and their wild relatives by using simple sequence repeats. *Plant Mol Biol Rep.*, **29 (4):** 848-858.

Sani SG, Chang PL, Zubair A, Carrasquilla-Garcia N, Cordeiro M, Penmetsa, RV, Munis MF, Nuzhdin SV, Cook DR and von Wettberg EJ. 2018. Genetic diversity, population structure, and genetic correlation with climatic variation in chickpea (*Cicer arietinum*) landraces from Pakistan. *Plant Genome*, **11 (1):** 1-11.

Serag AM. 2021. Molecular Characterization of Ten *Cicer arietinum* L. Genotypes Using SCOT Marker. *JACB*, **12 (1):** 1-4.

Tahir NA and Karim HF. 2011. Determination of genetic relationship among some varieties of chickpea (*Cicer arietinum* L.) in Sulaimani by RAPD and ISSR markers. *Jordan J Biol Sci.*, **4 (2):** 77-86.

Thudi M, Chitikineni A, Liu X, He W, Roorkiwal M, Yang W, Jian J, Doddamani D, Gaur PM, Rathore A, Samineni S. 2016. Recent breeding programs enhanced genetic diversity in both desi and kabuli varieties of chickpea (*Cicer arietinum* L.). *Sci Rep.*, **6 (1):** 38636.

Subscription

Jordan Journal of Biological Sciences

An International Peer – Reviewed Research Journal

Published by the Deanship of Scientific Research, The Hashemite University, Zarqa, Jordan

Name: ..... الاسم:

Specialty: ..... التخصص:

Address: ..... العنوان:

P.O. Box: ..... صندوق البريد:

City &Postal Code:..... المدينة: الرمز البريدي:

Country: ..... الدولة:

Phone: ..... رقم الهاتف

Fax No.: ..... رقم الفاكس:

E-mail: ..... البريد الإلكتروني:

Method of payment: ..... طريقة الدفع:

Amount Enclosed: ..... المبلغ المرفق:

Signature: ..... التوقيع:

Cheque should be paid to Deanship of Research and Graduate Studies – The Hashemite University.

I would like to subscribe to the Journal

For

- ☐ One year
- ☐ Two years
- ☐ Three years

One Year Subscription Rates

	Inside Jordan	Outside Jordan
Individuals	JD10	$70
Students	JD5	$35
Institutions	JD 20	$90

Correspondence

Subscriptions and sales:

The Hashemite University
P.O. Box 330127-Zarqa 13115 – Jordan
Telephone: 00 962 5 3903333
Fax no. : 0096253903349
E. mail: jjbs@hu.edu.jo

المجلة الأردنية للعلوم الحياتية
Jordan Journal of Biological Sciences (JJBS)

http://jjbs.hu.edu.jo

المجلة الأردنية للعلوم الحياتية: مجلة علمية عالمية محكمة ومفهرسة ومصنفة، تصدرعن الجامعة الهاشمية وبدعم من صندوق دعم البحث العلمي والإبتكار – وزراة التعليم العالي والبحث العلمي.

ترسل البحوث الى العنوان التالي:

رئيس تحرير المجلة الأردنية للعلوم الحياتية
الجامعة الهاشمية
ص.ب , 330127 , الزرقاء, 13115 , الأردن
هاتف: 0096253903333
E-mail: jjbs@hu.edu.jo, Website: www.jjbs.hu.edu.jo

المملكة الأردنية الهاشمية

المجلة الأردنية

للعلوم الحياتية

مجلة علمية عالمية محكمة

تصدر بدعم من صندوق دعم البحث العلمي و الابتكار

http://jjbs.hu.edu.jo/